# TWO-PHASE METHANATION OF LACTOSE IN BIOFILM REACTORS

By

Jian Yu

B. Sc. Zhejiang Institute of Technology, 1982

M. Sc. Zhejiang University, 1985

A THESIS SUBMITTED IN PARTIAL FULFILLMENT OF

THE REQUIREMENTS FOR THE DEGREE OF

DOCTOR OF PHILOSOPHY

in

THE FACULTY OF GRADUATE STUDIES

CHEMICAL ENGINEERING

We accept this thesis as conforming

to the required standard

THE UNIVERSITY OF BRITISH COLUMBIA

April 1991

In presenting this thesis in partial fulfilment of the requirements for an advanced degree at the University of British Columbia, I agree that the Library shall make it freely available for reference and study. I further agree that permission for extensive copying of this thesis for scholarly purposes may be granted by the head of my department or by his or her representatives. It is understood that copying or publication of this thesis for financial gain shall not be allowed without my written permission.

Department of CHEMICAL ENGINEERING

The University of British Columbia
Vancouver, Canada

Date Aug 22/91

## Abstract

Anaerobic methanation of lactose, the main component of cheese whey, is an attractive alternative for the disposal of this wastewater because of its added benefit of recovering energy as methane. Two advances in this technology have been the separation of the bacteria in two reactors according to their substrates and the retention of the anaerobic bacteria in the form of bacterial biofilms on solid supports. The mass transfer rate of the substrates within the active biofilms must be known for the determination of an optimum biofilm thickness. A prerequisite for the investigation of substrate mass transfer rate in an active biofilm is the knowledge of intrinsic kinetics of the substrate utilization by the embedded bacterial cells. Start-up of symbiotic methanogenic biofilms was also investigated on inert supports.

In recycled reactors, mesophilic (35 $^{0}$C) acid-producing bacteria or methane-producing bacteria, cultured with lactose at a pH of 4.6 for the former or cultured with mixed acids (acetate, propionate and butyrate) at a pH of 7.1 for the latter , attached onto PVC sheets, forming thin acidogenic or methanogenic biofilms, respectively. After the external mass transfer resistance had been eliminated by increasing the recycle rate and the internal mass transfer resistance was minimized by using thin biofilms, the intrinsic kinetics of lactose acidogenesis and methanogenesis of organic acids were investigated in the newly formed acidogenic and methanogenic biofilms, respectively. The lactose digestion rate as well as the production of two main products, acetate and butyrate, can be described by Michaelis–Menten equations. The production of propionate, as a minor product, was depressed in the culture environment. The digestion of acetate could also be modelled by a Michaelis–Menten equation while the dissimilation of propionate

and butyrate was affected by propionate concentration, the propionate digestion being promoted but the butyrate digestion being inhibited at high propionate concentrations. Two models have been proposed for their utilization.

Substrate mass transfer in the active biofilms was investigated with a diffusion cell. After symmetric biofilms formed on the two membrane filters of the cell, the substrate concentrations on the biofilm surfaces and inside the cell were measured at steady state. The effective diffusivities of substrates in the active biofilms were estimated by numerically solving the diffusion-reaction equations using the intrinsic kinetics and the substrate concentrations as the boundary conditions. The effective diffusivity of lactose in an acidogenic biofilm was about 65.3 % of its diffusivity in water, and the diffusivities of acetate, propionate and butyrate in a methanogenic biofilm were reduced to about 30.2 % of the values in water. Comparing the fractional void volumes in the two types of biofilms showed that the methanogenic biofilm, which grew more slowly, had a more tortuous structure of channels than did the acidogenic biofilm.

Studies on the build–up of symbiotic methanogenic biofilms were conducted using supports of wood, ceramic rings, PVC and stainless steel, which gave a range of water contact angle from $0^0$ to $99.7^0$. The accumulation of acetate–, propionate– and butyrate–degrading bacteria on the supports were monitored by measuring the substrate utilization rates of each bacterial group in a standard batch culture which was seeded by the supports with the attached biofilms. The three types of bacteria had different preference to a hydrophilic support surface,

$$\text{butyrate degrader} > \text{acetate degrader} > \text{propionate degrader}$$

Based on the analysis of the process of biofilm formation, a model has been proposed. The parameters which depict the attachment of free cells onto clean surfaces were found to have a linear relationship with the water contact angles of the support surfaces.

## Acknowledgement

The author expresses here his sincere appreciation to Dr. K. L. Pinder for his advice, direction and support throughout this research project. He is also grateful to Dr. R. M. R. Branion and Dr. K. V. Lo, two members of his supervision committee, for their constructive criticisms and review of this thesis.

The author is obliged for financial support of this research to the Foundation of Pao Zhao-Long and Pao Yu-Gang Scholarship and the Natural Science and Engineering Research Council of Canada.

Special thanks go to his family and parents for their understanding and support.

## Table of Contents

## List of Tables

## List of Figures

# Chapter 1

# Introduction

Lactose, a major constituent of cheese whey, influences the technologies applied to treatment of whey. Whey is the residual watery portion of milk after removal of the curd (cheese) during the cheese–making process. It is an opaque, greenish–yellow liquid with about 6 to 6.5 percent total solids and a biological oxygen demand (BOD) of 32000 mg/l or higher [1].

Treatment of this by-product is a really challenging problem to cheese manufacturers considering that 9 kilograms of whey are produced for each kilogram of cheese and over 277 million kilograms of cheese were produced in Canada and over 3 billion kilograms in North America in 1987 [2]. In recent years, growing concern about environmental pollution has forced the manufacturers to give up the conventional disposal methods such as direct discharge into receiving waters [3], landfills [4], municipal sewage system [5] and adopt other more suitable methods. Obviously, the most satisfactory method is to re-use the organic components to reduce or eliminate the cost of treatment and disposal of whey.

## 1.1 Utilization of Lactose in Whey

As shown in Table 1.1, lactose is the principal component of whey, and consequently, utilization of whey actually becomes the utilization of lactose although processes for obtaining milk proteins by ultrafiltration techniques to allow their utilization have been developed [6].

Table 1.1: Major components of a typical whey

| Component | Composition (w/w %) |
|---|---|
| water | 93.1 |
| lactose | 4.9 |
| protein | 0.9 |
| lacto-globulin | |
| lacto-albumin | |
| lummune-globulins | |
| fat | 0.3 |
| lactic acid | 0.2 |
| ash | 0.6 |
| oxides of K Na Ca Mg Fe | |
| phsophrous pentoxide | |
| chlorine oxide | |
| sulfur trioxide | |
| total solids | 6.9 |

Source is [7].

Whey powders are produced by drying whey [8]. Also lactose can be separated from whey by the processes of concentration and crystallization. These products can be used as feed for animals or as substrate for biological processes (e.g. penicillin production) [9]. Obviously, a great amount of energy is consumed for the removal of about 93 percent water.

Use of whey as a substrate for fermentations can upgrade the raw material into useful products such as yeast, alcohol, organic acids, vitamins, alcoholic beverages and vinegar by employing microorganisms that are able to utilize lactose [1].

A variety of procedures have been suggested for the growth of yeast (*Saccharomyces fragilis*) in whey [10], producing food- and feed-grade yeast or yeast-whey products which, if properly produced, are highly nutritious, nontoxic sources of protein and vitamins and under the right circumstances can find application in human and animal

nutrition. Whey has also been used to grow microorganisms which produce useful enzymes, including $\beta - galactosidase$ [11]. Anaerobic growth of lactose utilizing yeast (*Kluyveromyces* species) in whey converts lactose into ethanol [12], but a simple fermentation of whey produces a solution containing only ca 2% of ethanol, which is uneconomic to distill. Some dried whey permeate has been added to liquid whey giving a high concentration of lactose and thus of ethanol.

It is clear that only economical reasons prevent the use of these approaches to treat whey. First of all, not all the whey produced is available for the uses mentioned above, since much cheese is made in small factories at scattered locations, making it impractical to transport the bulky whey to a centralized plant for processing. Moreover, for recovery systems the capital and operation costs are comparatively high because of the low concentration of lactose. Finally, the supply of whey for re-use often exceeds the demand. This situation has left many smaller cheese plants in an insecure position with regard to whey disposal, because economically acceptable alternatives to the re-use options have not been identified [13].

## 1.2 Anaerobic Methanation of Lactose

Anaerobic methanation is a biological digestion process in which various anaerobic bacterial species cooperate to convert organic materials (carbohydrates, fats, proteins, etc) to organic acids and finally a gaseous mixture of methane and carbon dioxide in the absence of molecular oxygen. In the past, broad scale applications of this process, à well known process in waste management area, have been largely with the treatment of municipal sewage sludge and animal residues to achieve waste stabilization and solid reduction.

Compared with the processes of whey fermentation to products such as alcohol, yeasts, as mentioned above, the most distinctive advantage of whey anaerobic methanation is

that the final product, methane, naturally separates from the liquid waste to save energy in downstream processing and is also useable in large quantities as a fuel without major modification to existing furnaces in the plants. Other advantages include no requirement for sterilization of the wastewater, low nutrient requirement etc.

Compared to the aerobic treatment, lactose utilization by anaerobic sludge also offers several distinctive advantages including:

1. lower solids/sludge production,
2. highly stabilized waste biological sludge that, as a rule, can be easily dewatered,
3. no energy requirement for aeration,
4. production of methane, a useful end product.

However, the conventional anaerobic processes suffer from a slow digestion rate and poor process stability (unstable performance, susceptibility to shock loading) and relatively long periods of time required to start up the process or recover from an unstable condition.

To overcome these problems encountered in a convertional process of anaerobic digestion, the key role of cell immobilization has been recognized and it was found that success of a biological treatment was directly related to the efficiency of cell immobilization and/or retention because of the higher cell concentration which resulted in a lower reactor volume requirement and better stability. The use of biomass immobilization has led to development of different configurations of anaerobic digesters such as anaerobic filter [14], fluidized/expanded bed reactor [15], and the upflow anaerobic sludge blanket (UASB) digester [16] as illustrated in Figure 1.1.

The bacteria attach and grow on an inert support material which is static in anaerobic filters (e.g. rocks, plastics) and movable in fluidized/expanded bed reactors (e.g.

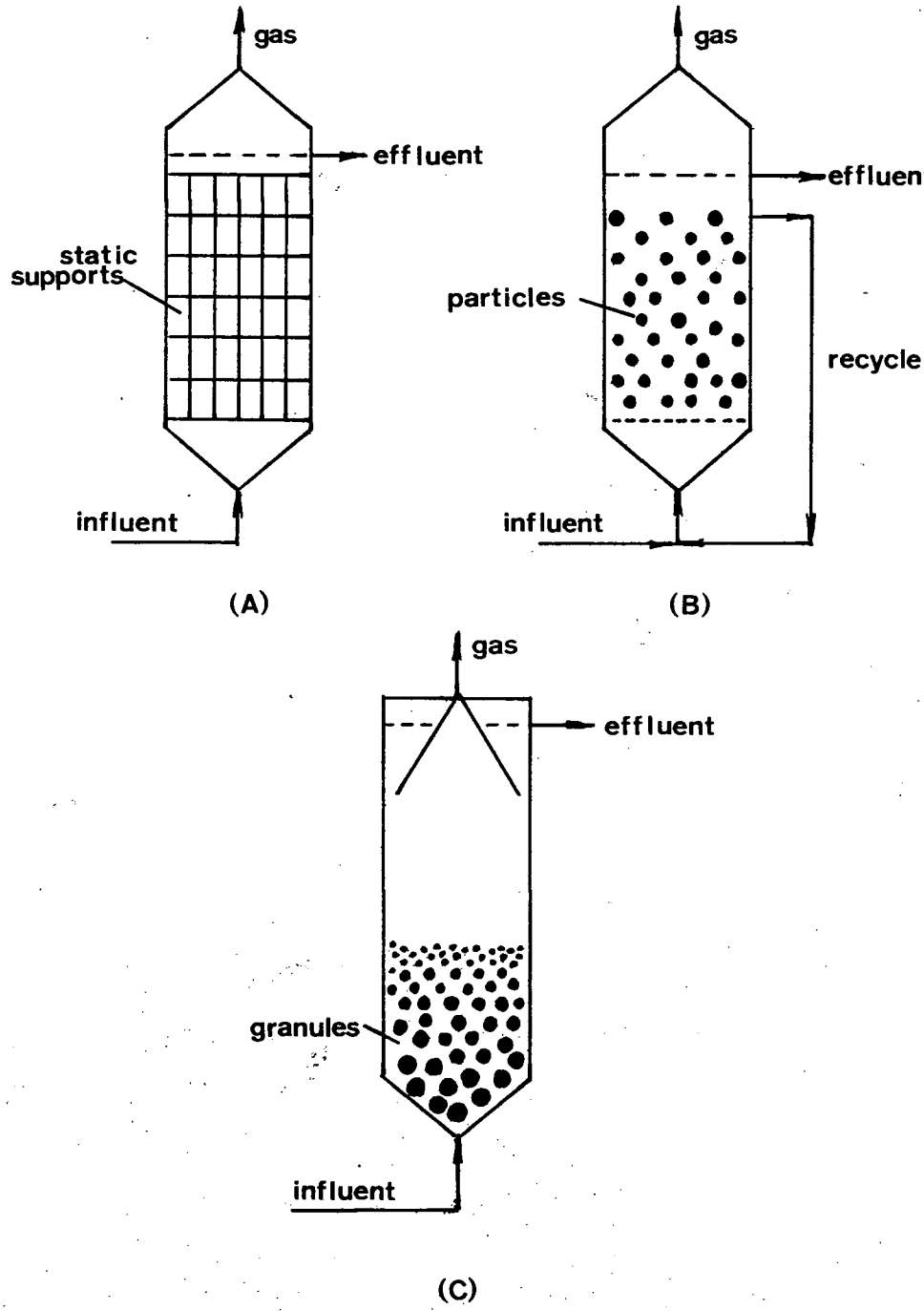


Figure 1.1: Illustration of configurations of anaerobic filter (A), fluidized/expanded bed (B) and upflow anaerobic sludge blanket (C)

sands), forming slime bacteria films on the support and resulting in a long retention time and a high concentration of bacteria in the digesters. In UASB reactors, under favorable chemical and physical conditions the bacteria flocculate to form granules with superior settling characteristics, which gives a high concentration and a long retention time of bacteria in the reactors. For anaerobic methanation of whey or lactose, Switzenbaum and Danskin [17], Boeing and Larsen [18] utilized the fluidized or expanded bed reactors. Dehaast et al [19], van den Berg and Kennedy [20], Wildenauer and Winter [21] applied upflow or downflow fixed film reactors. Reynolds and Colleran [22] used a hybrid sludge-bed/fixed-bed reactor which was actually a combination of a UASB reactor and an anaerobic filter.

Further understanding of the microbiology and biochemistry involved in the anaerobic methanation of soluble organic materials which will be discussed in the following chapter in detail has led to a two-phase process in which acid-producing bacteria and methane-producing bacteria are cultured in separated reactors because it is believed that the acidogens and methanogens have different biological properties and thus culture requirements. Also in a two-phase process, more opportunities are offered for controlling the flow of the substrates between the distinct groups of bacteria, and thus, producing a better match between them [23].

## 1.3 More Considerations on Two-phase Methanation of Lactose

In a two-phase process, the first phase reactor contains acid-forming bacteria which ferment lactose to a mixture of mainly acetic, propionic and butyric acids. They are fast-growing bacteria (minimum doubling time around 30 min). In the second phase reactor, the bacteria can be divided into two groups, acetate-forming bacteria which convert propionic and butyric acids to acetate, and methane-forming bacteria which

utilize acetate and $H_2/CO_2$ to produce methane. All of them grow very slowly, the former having minimum doubling times of 1.5–4.0 days and the latter of 2–3 days [24]. Figure 1.2 illustrates the concept of two-phase anaerobic digestion of wastes.

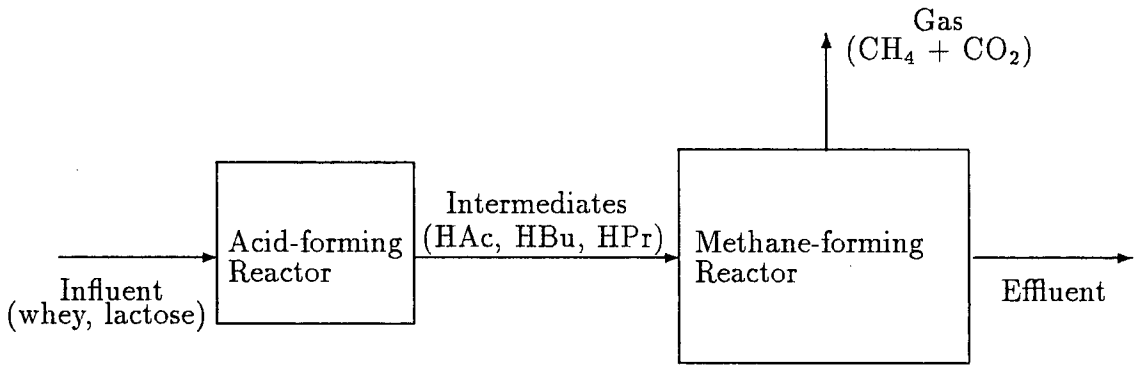


Figure 1.2: Two-phase process of anaerobic digestion of organic wastes

A number of researchers have investigated the two-phase processes. Some efforts were focused on the methods of separating methanogenic from acidogenic species and on achieving and characterizing the resulting environment in each phase. Pohland and Ghosh [23] washed the methanogens out of the first phase reactor using kinetic controls. Investigations [25,26,27,28,29] have indicated that the environmental requirements of acidogenic and methanogenic (acetogens plus methanogens) phases are quite different from each other in terms of pH and oxidation-reduction potentials (ORP). After comparing the performance of a conventional single-phase and a two-phase anaerobic digestion of soft-drink waste, Ghosh et al [30] indicated that phase separation could improve the operation stability as well as quality of product gas. Table 1.2 lists the applications of the two-phase process in the treatment of various wastewaters.

In design and operation of a two-phase biofilm process of anaerobic digestion of whey,

Table 1.2: Pilot- and full-scale plants of two-phase anaerobic treatment of wastewaters

| Year | Industry | Location | Type | Capacity (kg COD/day) |
|---|---|---|---|---|
| 1977 | Distillery (enzyme, alcohol) | Belgium | Pilot | 180 |
| 1980 | Beet sugar | West Germany | Pilot | 45 |
| 1980 | Distillery (yeast, alcohol) | Belgium | Pilot | 135 |
| 1981 | Beet sugar | Belgium | Pilot | 170 |
| 1981 | Citric acid | West Germany | Pilot | 120 |
| 1981 | Beet sugar | West Germany | Pilot | 45 |
| 1980 | Flax retting | Belgium | Full-scale | 350 |
| 1982 | Starch-to-glucose | West Germany | Full-scale | 20,000 |
| 1983 | Yeast-alcohol | Netherlands | Full-scale | 20,000 |
| 1984 | Baker's yeast | France | Full-scale | 7,000 |

Source is [13,30,31].

further consideration are needed on several points, especially, the fermentation kinetics in each phase, mass transfer of substrates in the biofilms and build-up of anaerobic biofilms.

### 1.3.1 Kinetics in Each Phase Reactor

When steady state operation in a two-phase system is established, the production of organic acids in the first phase reactor must be balanced by their consumption in the second phase reactor, otherwise, accumulation of these acids would lead to a "sour" process if the pH is uncontrolled. In this case more caustic solution will be consumed for controlling the pH of the second phase reactor in a narrow neutral range with more organic acids appearing in the effluent in the form of salts. Therefore, the knowledge of yield and consumption rates of organic acids are essential for process development. Furthermore, the effluent from a cheese plant, as is well known, has a variable flow rate and BOD strength [3]. This requires the process have an operation range over which it

can withstand the normal feed fluctuations. The response of each phase reactor to feed fluctuations may be used for the determination of this operation range.

Most of the experiments conducted to date on the anaerobic methanation of lactose or whey were designed to evaluate the performance of the process [17,18,19,20,21,22,32, 33,34,35]. Detailed biochemical kinetic information is virtually non-existent. For other substrates, some kinetic results of anaerobic methanation are available. However, most of them were obtained in single-phase processes which differ greatly from two-phase processes considering the effects of phase separation which results in a constant production of organic acids (e.g. propionic and butyric acids) in the first phase, and correspondingly, a healthy population of obligate hydrogen-producing acetogens (OHPA) and associated hydrogen-oxidizing methanogens (HOM) which ensured the rapid assimilation of those acids in the second phase reactor [36].

### 1.3.2 Mass Transfer in the Biofilms

As discussed above, the biomass must be retained in reactors to make a long solid retention time (SRT) possible even at short hydraulic retention times (HRT) and to maximize biomass concentrations in the reactors, which has been fulfilled by developing three major types of reactor configurations as shown in Figure 1.1. As biomass accumulates in the form of biofilms (anaerobic filters and fluidized/expanded beds) or granules (UASB) in a reactor of specified volume, two problems may arise. One is that the biomass will form a solid phase in which the substrates are gradually consumed as they diffuse into the biomass, and so, the bacterial cells embedded in the film see different substrate concentrations. The combination of the consumption and the diffusion rates determines a effective thickness of biofilm beyond which no substrate is available to the bacteria. Secondly, since the living bacteria are continuously growing with the consumption of substrates even though the growth rate is relatively slow in anaerobic processes, the actual HRT

may be reduced to impractically low values due to the accumulation of active biomass (within an effective thickness) and/or dead biomass which reduce the available reactor volume.

Because of these considerations, a knowledge of mass transfer within the acidogenic and methanogenic biofilms is necessary for the estimation of the most effective biofilm thickness for maximizing the biomass concentration as well as a long term stable operation.

Compared with fluidized/expanded bed and UASB, an anaerobic filter is more affected by mass transfer limitations because the biomass can be almost completely retained. This problem has been recognized by literature reports of phenomena caused by plugging and channeling in laboratory scale anaerobic filters [37,38]. In a full scale downflow anaerobic reactor which contained three layers of clay blocks with square vertical channels as supports, treating an effluent from a dairy plant (1500 to 1800 $m^3$/day, 2000–3000 kg $BOD_5$ or 4000–6000 kg COD per day), the COD removal decreased from a range of 60–80 % after the start-up period to 50 % and less at the end of 2 years when it was found that the active reactor volume had declined by 80 percent [3]. Based on observations of the long term performances of an anaerobic filter and a UASB reactor and their abilities to prevent the accumulation of excess biomass, a hybrid reactor configuration (combination of these two types of reactor) was developed in Wastewater Technology Centre, Canada, in order to minimize the excess biomass accumulation and its impact on reactor hydraulics [39].

Obviously, a growing biofilm should be controlled at its optimum thickness so as to maintain effective and long term stable operation in an anaerobic digestion process. Knowledge of mass transfer rates of substrates in anaerobic biofilms is essential to estimate this optimal biofilm thickness. The majority of the studies on mass transfer in biomass, however, has been concerned with aerobic microbial aggregates, because it was

easy to recognize that $O_2$ supply is limiting due to its low solubility in water. Few works have been conducted on anaerobic bacterial aggregates and to the author's knowledge, no report on the transport of lactose and organic acids in anaerobic microbial aggregates exists.

### 1.3.3 Start-up of Anaerobic Biofilms

One disadvantage of anaerobic digestion processes is that a relatively long time is needed for start up due to the very slow growth rate of anaerobic bacteria, especially the acetogens and methanogens. A mature reactor is characterized by a well developed, immobilized biomass (granules or biofilms). During the process of biofilm formation the first step is attachment of bacteria onto inert solid supports, which is affected by many factors such as bacterial strain, limiting nutrients, physio-chemical properties of the solid surfaces. Then the attached bacteria proliferate forming microcolonies, and a biofilm by the merging of these colonies. Start-up of an anaerobic process to a great extent nowadays still relies on industrial experience because of the complexity of the process.

In a two-phase system, the acidogens grow fast and also form a biofilm more easily. The formation of a methanogenic biofilm (including acetogens), thus, becomes the rate-limiting step. Furthermore, it would also be interesting if the properties of solid supports would affect the relative attachment rates of each type of bacteria (acetate-, propionate-, and butyrate-degrading bacteria) when the supports are immersed in the mixture of these microorganisms. Choice of a solid supporter would then in part depend on the knowledge of its effect on the ease with which each group of bacteria attach on it.

A number of studies on methanogenic film development have been conducted. Most of them were based on the total consumption rate of organic carbon [40], methane production rate [41], or total protein content of a biofilm [42], which can not answer the

question whether or not and how the surface properties influence the attachment of various bacterial types in a mixed culture. Some researchers [43] used a single substrate (acetate) to investigate the influence of solid surfaces on biofilm development. This approach can only give partial information because it neglects the symbiotic relationship between bacteria.

## 1.4 Research Objectives and Scope

The two-phase anaerobic methanation of whey has been, as indicated above, demonstrated as a potentially successful process. However, some further studies are needed, especially on the three topics discussed above, if it is to become an economic, reliable, and stable alternate for the treatment of high BOD wastewaters.

Kisaalita, Lo and Pinder [44,45] have studied the acidogenesis of lactose in a continuous stirred reactor (CSTR) in which the bacteria were suspended. They found that the dilution rate and pH would affect the acidogenic product distribution which was assumed to be caused by a shift in the bacterial population.

The present research is an extension of their effort to introduce the two–phase method for whey treatment and will be mainly focussed on immobilized acidogenic and methanogenic bacteria. Specifically, the present study includes the following major topics:

1. Intrinsic kinetics of lactose acidogenesis and methanogenesis

   Under selected conditions (temperature, pH, nutrients) which are based on the results of Kisaalita [46] and others, investigate the utilization rate of lactose and production rates of organic acids in a fixed-film acidogenic reactor, and conduct studies on the utilization rates of organic acids in a fixed-film methanogenic reactor. These results should be obtained under conditions where there is negligible effect

of external and internal mass transfer resistance. Also, some studies will be made on the responses of these two reactors to feed fluctuations.

2. Mass transfer of lactose in acidogenic biofilms and organic acids in methanogenic biofilms

   Mass transfer within active biofilms is a very complicated process because it involves both mass transfer and reactions. Some researchers have described the influence of mass transfer on reaction with macro-kinetics which included both intrinsic kinetics as well as mass transfer and gave an overall reaction of half order [47]. Some studied a simplified biofilm which was deactivated to eliminate the influence of reaction on mass transfer. The present research will use a specially designed device to measure directly the substrate concentration drop within living biofilms. The diffusivities of substrates (lactose, acetate, propionate and butyrate) in their corresponding biofilms will be found by using a reaction-diffusion model which describes the mass transfer process of these substrates in anaerobic biofilms.

3. Start-up of symbiotic methanogenic biofilms

   Considering that many factors can effect the start-up of biofilms, this research will concentrate on the effect of solid surfaces, in terms of their water contact angles (0 - $100^0$), on the attachment of acetogenic and methanogenic bacteria groups. Some efforts will be made to establish a model to describe the start-up of a symbiotic methanogenic biofilm.

# Chapter 2

# Theoretical Aspects and Previous Studies

## 2.1 Process Biochemistry and Microbiology

Anaerobic digestion is usually considered to be a two-phase process consisting of acid-formation (acidogenesis) and methane-formation (methanogenesis). It has been known that at least three large, physiologically different, bacterial populations must be present for the overall conversion of organic matter to methane and carbon dioxide to occur. In the first phase, organic matter (proteins, lipids, carbohydrates) are converted by a heterogeneous group of microorganisms into fatty acids by hydrolysis and fermentation. In the second phase, the end-products of the first phase fermentation are converted to methane and carbon dioxide by strict obligate anaerobic bacteria (methanogenic bacteria) with the assistance from another group of bacteria termed acetogenic bacteria. The latter can convert the compounds the methanogenic bacteria cannot digest into acetate, dihydrogen and carbon dioxide which can be utilized by methanogenic bacteria.

If the hydrolysis of biopolymer molecules is the slowest step (e.g. cellulose hydrolysis) in the whole process, the fatty acids produced in the first phase would not be accumulated in the culture medium due to their being digested by methanogenic bacteria. If the organic matter, however, is readily hydrolyzed (e.g. lactose which can be directly transported into microbial cells), the slowest step becomes the methanogenesis of fatty acids. It would then be possible that the fatty acids may not be digested rapidly enough by methanogenic bacteria and their accumulation in the culture medium would lead to

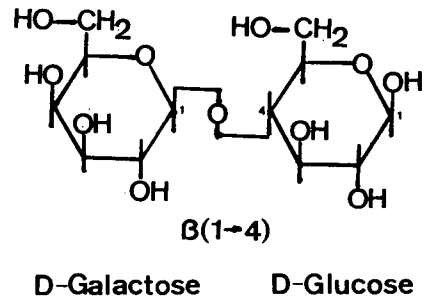


Figure 2.3: Illustration of lactose structure

an undesirable 'sour' process and no gas is produced [46].

### 2.1.1 Lactose Acidogenesis

Lactose, a reducing disaccharide, is constructed from a galactose residue and a glucose residue. The glycosidic link is $\beta(1 \rightarrow 4)$, which means that the OH group on the anomeric carbon atom of galactose is in $\beta$ position as shown in Figure 2.3.

Although the anomeric atom on galactose residue is involved in the glycosidic bond, the anomeric carbon atom (C1) on the glucose residue can still participate in forming a free aldehyde group and thus the free carbonyl oxygen can reduce a number of substances, for example, divalent copper ($Cu^{++}$) to the monovalent species ($Cu^{+}$). This reducing capacity of lactose has been used in this study to measure its concentration in a culture medium.

The $\beta(1 \rightarrow 4)$ glycosidic link may have a significant effect on the properties of lactose, which can be projected by comparing the properties of cellulose and amylose (a type of starch having straight carbon chains). Cellulose is constructed from repeating units of D-glucose held together by $\beta(1 \rightarrow 4)$ glycosidic bonds and amylose by $\alpha(1 \rightarrow 4)$ glycosidic

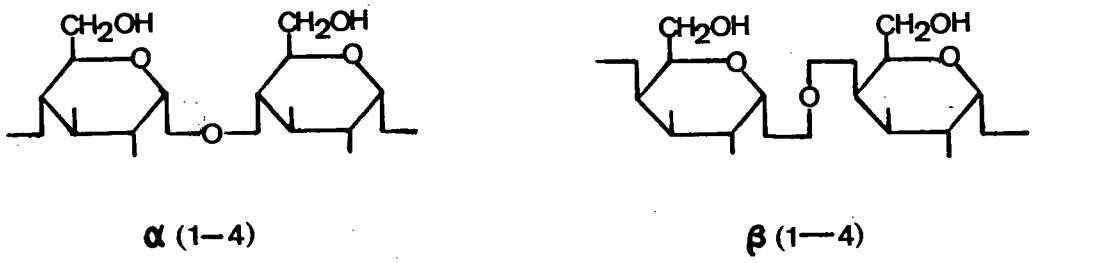


Figure 2.4: Illustration of two types of glycosidic links

bonds (Figure 2.4).

This subtle difference, however, results in a significant difference in the physical properties of the two types of polysaccharides; starch, a storage form of cellular fuel which is quite easily digested by mammals, yeasts or bacteria, and cellulose, a structural element of plant cells which cannot be hydrolyzed by most mammals, including humans. The microorganisms capable of secreting the enzyme cellulase can hydrolyze the $\beta(1 \rightarrow 4)$ link of cellulose into D–glucose.

Breakage of the lactose $\beta(1 \rightarrow 4)$ glycosidic bond involves a special enzyme, $\beta$ – galactosidase, coded and controlled by a segment of DNA in bacteria termed *lac* operon. Studies of the structure of the *lac* operon in *Escherichia coli* clearly demonstrated the whole process for producing the enzymes required for lactose transport and metabolism. A diagram of the *lac* operon is shown in Figure 2.5 [48].

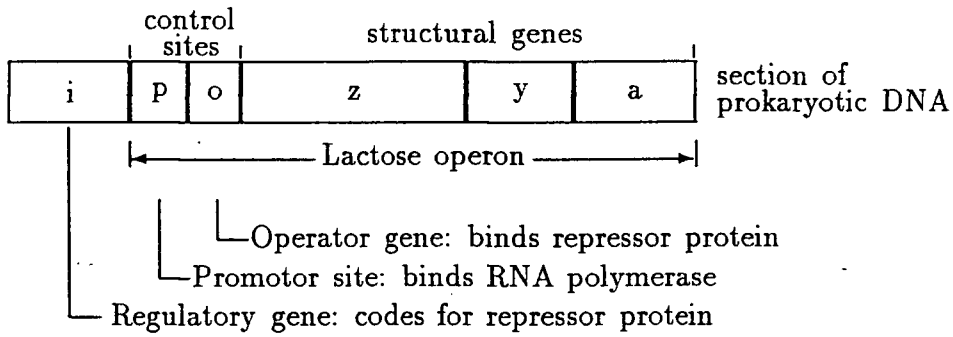


Figure 2.5: Structure of *lac* operon

The *lac* operon consists of three distinct parts: the regulatory gene (i), the operator gene (o) and the structural genes (z, y, a). The structural genes (z, y, a) code for three separate enzymes involved with lactose metabolism. The 'z' gene codes for $\beta$ – galactosidase, the enzyme that hydrolyzes lactose into glucose and galactose for further use in energy production.

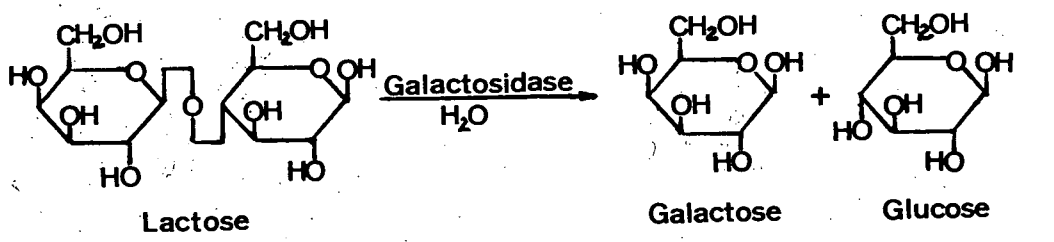


The 'y' gene codes for galactoside permease, the enzyme that mediates the transport of lactose into the cell, which means that the hydrolysis of lactose occurs in the cell's cytoplasm rather than in the culture medium. The 'a' gene codes for galacoside acetylase (function unknown). A textbook [48] should be consulted for how the *E coli* cell mediates the transport and metabolism through the regulatory and operator genes. The glucose

Table 2.3: Main genera of acid-producing bacteria implicated in first phase

| | Genus | Substrate | Products |
|---|---|---|---|
| Aerobes | *Pseudomonas* | nutritionally highly | |
| | *Micrococcus* | versatile starch | lactate |
| Facultative | *Bacillus* | starch maltose | lactate |
| Anaerobes | *Lactobacillus* | numerous sugars | acetate |
| | *Escherichia* | numerous sugars | |
| | *Clostridia* | | succinate, acetate |
| Obligate | *Ruminococcus* | cellulose, cellobiose | ethanol, hydrogen |
| Anaerobes | *Bacteroides* | hemicellulose, pectin | formate |
| | *Butyrivibrio* | starch | butyrate, lactate |
| | *Megasphera* | lactate, glucose | branched VFA, hydrogen |
| | *Selenomonas* | sugars | acetate, propionate |
| | *Desulfobibrio* | lactate, malate | acetate |
| | *Bifidobacteria* | proteins | VFA |
| | *Propionibacterium* | amino–acids | propionate |
| | *Anaerovibrio* | | |

Source is [49].

and galactose in the bacterial cells undergo further various reactions depending on the bacterial species present.

The bacteria isolated from the anaerobic digestion mixture of the first phase include a wide range of physiological groups as shown in Table 2.3.

Whether all the different isolates obtained by various workers are physiologically significant in the digestion process still remains to be determined. However, the presence of various genera in a mixed culture can supply various enzymes crucial to the hydrolysis and fermentation of various organic materials. This is especially desirable in a process for wastewater treatment which may contain many kinds of organic wastes. Moreover, whether a bacterial species can survive and dominate in a digester depends greatly on the environmental conditions (temperature, pH, nutrients, etc.) and its efficiency of extracting energy from the environment. The more energy it is able to get from the nutrients,

the faster it will grow. Presence of aerobes and facultative anaerobes in anaerobic digesters was explained by McKinney [50] by the ease of growth of the facultative bacteria which gives them an edge over the strict anaerobes and so the acid-formers are made up predominantly of facultative bacteria with a few strict anaerobes. The oxygen needed for growth of facultative anaerobic bacteria may come from the dissolved oxygen in the feed solution. After they developed a method to enumerate obligate anaerobic acidogenic bacteria in digesters, Toerien et al [51] reported $39\times10^7$ to $15\times10^9$ obligate anaerobic non-methanogenic and $8\times10^5$ to $1\times10^8$ aerobic and facultative anaerobic bacteria per ml in several digesters. The anaerobic counts were usually 100 or more times greater than the aerobic counts. Post et al [52] also reported the presence of a large obligate anaerobic bacterial population in anaerobic digester.

While so many bacterial species are present in a digester, glucose and its epimers (galactose, mannose etc.) are catabolized to pyruvate anaerobically by four currently recognized routes [53].

- Embden–Meyerhof–Parnas (EMP) pathway.
- Hexose monophosphate (HMP) pathway.
- Enter–Doudoroff (ED) pathway.
- Phosphoketolase (PK) pathway.

Through the use of $^{14}C$ tracers, McCarty et al [54] concluded that both EMP glycolysis and hexose phosphate pathways probably mainly occurred in anaerobic digesters receiving carbohydrates. Among the four pathways, the EMP pathway provides bacteria with the greatest amount of ATP under anaerobic condition [53].

$$\text{Glucose} + 2\text{ATP} + 2\text{NAD}^+ \longrightarrow 2\text{Pyruvate} + 4\text{ATP} + 2\text{NADH} + 2\text{H}^+$$

But it does not produce the important precursors for purine, pyrimidine, DNA and RNA biosynthesis. In contrast, the HMP pathway produces all the precursors necessary for these important biomolecules, giving half the amount of ATP. Microorganisms growing on simple defined media such as glucose (or lactose) plus mineral salts must use other pathways such as the HMP pathway if they are not supplied with growth factors. The ratio of usage of the EMP and HMP pathways can vary greatly depending on environmental conditions.

Biological activities of living cells involve catabolic and anabolic pathways. Catabolic pathways are the degradative reactions through which nutrient molecules are degraded into simpler molecules, releasing chemical energy. Anabolic pathways are biosynthetic processes in which various cellular constituents are synthesized from simpler precursor molecules and require the input of chemical energy. The whole process is accomplished by what are known as coupled reactions usually catalyzed by enzymes. The released chemical energy is trapped in the form of an energy–rich intermediate and used to drive a second reaction. Adenosine triphosphate (ATP) is the primary energy carrier in all life forms. As nutrients are broken down, some of the free energy contained in those molecules is conserved in the form of ATP. When cells must synthesize various molecules, free energy is required to make the new bonds; this energy is supplied by the ATP molecules. Specifically, ATP hydrolyses into adenosine diphosphate (ADP) and inorganic phosphate, releasing a significant amount of free energy.

$$\mathrm{ATP} + \mathrm{H_2O} \longrightarrow \mathrm{ADP} + \mathrm{P_i} \qquad (\Delta G^0 = -7.3 \text{ kcal/mol})$$

The standard conditions specified in this thesis are; one atmosphere for each gaseous components, all other compounds in aqueous solution at 1 M activity at pH of 7.0 and 25 $^0C$.

Details of the four routes can be found in Appendix A. The other points of importance

in the sequence of the EMP glycolysis are emphasized here because its product, pyruvate, is the key component for further reactions in acidogenesis.

- Glucose has first to be activated and converted to a phosphated fructose by consuming two ATP molecules.
- After the fructose is split into two triosephosphates, the oxidation of the trioses is coupled to the reduction of a electron/hydrogen carrier, nicotinamide adenine dinucleotide (NAD)
- In the subsequent steps to pyruvate, a total of 4 moles of ATP are formed. The reduced $NAD^+$ must be regenerated by some mechanism, which to a great extent determines the final fermentation product distribution.

In addition to 2 moles of pyruvate and ATP, the glycolysis gives 2 moles of reduced $NAD^+$ (NADH) which must be reoxidized under anaerobic conditions for repeated use.

$$NAD^+ + H_2 \rightleftharpoons NADH + H^+$$

Depending on the mechanisms by which they oxidize the reduced NAD, the acidogenic bacteria give rise to a diversity of products by further metabolism of pyruvate (see Figure 2.6). These reactions permit an overall oxidation–reduction balance to be preserved under anaerobic conditions.

The change in free energy during the reoxidation of NADH into $NAD^+$ and $H_2$ becomes negative only when the partial pressure of hydrogen drops below $10^{-3}$ atmospheres [180]. Thus a low hydrogen partial pressure can pull the overall metabolism towards the formation of $H_2$, $CO_2$ and acetate. On the other hand, higher values of hydrogen partial pressure will inhibit the oxidation of NADH and then it must be reoxidized by the reduction of pyruvate or acetyl–CoA, forming reduced products such as lactate, ethanol,

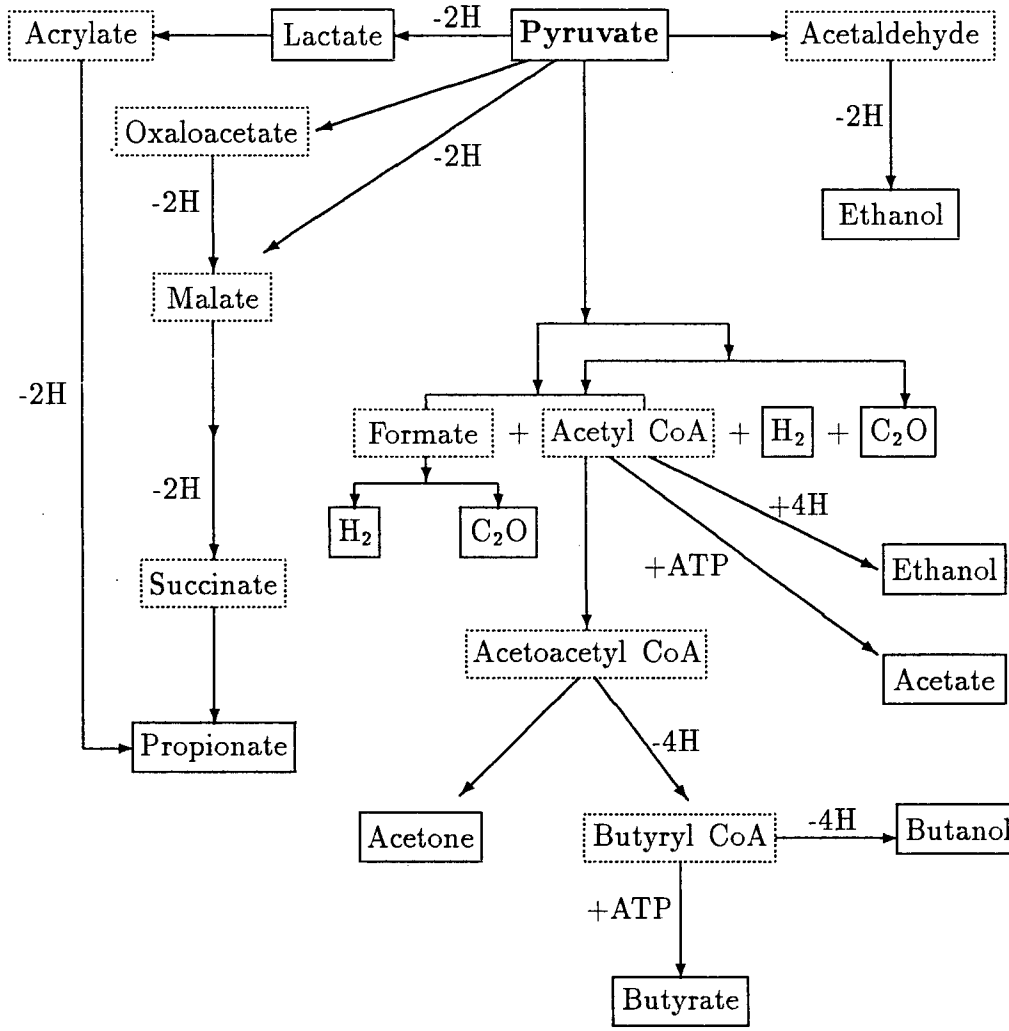


Figure 2.6: Bacterial fermentation products of pyruvate. Pyruvate formed by the catabolism of glucose is further metabolized by pathways which are characteristic of particular organisms. End products of fermentations are shown in boxes and intermediates in dash boxes. "-" refers to consumption and "+" to production.

propionate and butyrate. Among them, some products (acetate, butyrate) give rise to additional energy by substrate–level phosphorylations, e.g. the conversion of an acetyl–CoA derivative to free acid,

$$CH_3CO\text{–}SCoA + ADP + P_i \longrightarrow CH_3COOH + ATP + SCoA$$

$$CH_3CH_2CH_2CO\text{-}SCoA + ADP + P_i \longrightarrow CH_3CH_2CH_2COOH + ATP + SCoA$$

Some reactions (formation of lactate, ethanol, etc), however, can not produce extra ATP and only keep oxidation–reduction in balance by oxidizing the reduced $NAD^+$.

$$CH_3COCOOH + NADH + H^+ \longrightarrow CH_3CHOHCOOH + NAD^+$$

The effect of environments (pH, temperature, etc.) on the distribution of fermentation products is also quite significant. As the culture pH drops, it becomes more and more difficult to reoxidize NADH from the point of view of energetics. Therefore, the production of acetate as sole end product would not be satisfied, and bacteria will utilize pyruvate not only to form acetate but also butyrate, a weaker acid than acetate. If the pH drops below 4, some neutral compounds are produced such as butanol and acetone. If the environmental conditions are not favorable to a bacterial species, its characteristic product from the fermentation of pyruvate apparently would not occur.

Hungate [56] first expressed the idea that hydrogen production and utilization could profoundly influence the course of a fermentation in anaerobic ecosystems. The regulatory role of hydrogen in the course of anaerobic fermentations is effected by interspecies hydrogen transfer, induced by hydrogen–trophic organisms (methanogenic bacteria), to pull the reactions toward the direction in which more hydrogen is produced. In a two-phase process, the acid-formation and methane-formation phases are physically separated and the hydrogentrophic methanogens are not present in the first phase reactor because of some

Table 2.4: Classification of seven genera of methanogenic bacteria

| Order | Genus | Morphology | Gram | Substrate |
|---|---|---|---|---|
| I | *Methanobacterium* | long rods to filaments | + | $H_2/CO_2$, formate |
| | *Methanobrevibcter* | short rod to lancet cocci | + | $H_2/CO_2$, formate |
| II | *Methanococcus* | irregular and small | - | $H_2/CO_2$, formate |
| III | *Methanomicrobium* | short rods | - | $H_2/CO_2$, formate |
| | *Methanogenium* | irregular small cocci | - | $H_2/CO_2$, formate |
| | *Methanospirillum* | short to long wavy spirilla | - | $H_2/CO_2$, formate |
| | *Methanosarcina* | pseudosarcina | + | $H_2/CO_2$, methanol acetate, methylamine |

Source is [57].

deliberately chosen conditions (low pH, low hydraulic residence time etc.). Therefore, it is essential to investigate the rate and product distribution of lactose fermentation in a separated acidogenic biofilm reactor without effects from hydrogentrophic methanogens.

### 2.1.2 Methanogenesis of Fatty Acids

Methanogenic bacteria are members of a very distinct group of bacteria with respect to their physiology and ecology. They are present in extremely anaerobic environments like the rumens, sewage sludge digesters and anoxic muds and sediments. They are the terminal organisms in the anaerobic transformation of the substrates available in such environments. A taxonomy, to replace an old one based on bacterial morphology, has been recently adopted which is based on the structure of their 16S ribosomal RNA (see Table 2.4). This molecule has changed very slowly during evolution, so any significant differences that are observed must indicate a very long evolution history.

Table 2.4 indicates that, based on the structure of 16S rRNA, there is a very great diversity among the methanogens. They are not a homogeneous and closely related group of bacteria. The unifying characteristic of this bacterial group is that all members are able to reduce carbon dioxide into methane as final product of their energetic metabolism. Growth on $CO_2$ as carbon source is autotrophy, but the autotrophic growth of the methanogens is totally different from that of virtually all phototrophs and chemoautotrophs because it does not involve the ribolase bisphosphate (Calvin) cycle. As a consequence, they have been classified into a group of bacteria called archbacteria which is distinct from the "Classical" procaryotes. In this group, extreme halophiles (*Halobacteriaceae* ) and thermoacidophiles (*Sulfolobus* ) have also been placed [58].

The methanogens are strict obligate anaerobes, but they are capable of existing well in close association with other classes of bacteria which are capable of removing oxygen. Kiener and Leisinger investigated the sensitivity of five methanogenic bacteria (belonging to four genera) to oxygen [59]. The death curves of *Methanobacterium thermoautotrophicum* , *Methanobrevibacter arboriphilus* and *Methanosarcina barkeri* were biphasic. For these strains, exposure to air for 10 to 30 hours was without effect on their survival. Up to a critical time of contact, oxygen apparently caused no or only reversible damage on these organisms. For the two methanococci species (*M. voltae* and *M. vannielii*), however, the number of surviving cells upon exposure to air dropped exponentially without lag. The three comparatively robust strains were originally isolated from sludge digesters, i.e. ecosystems which are periodically subjected to oxygen stress and therefore may favour the development of air-tolerant methanogenic bacteria. In contrast to them, the two *Methanococci* strains were highly sensitive to oxygen. Sea and lake sediments, the natural habitats of *Methanococci* , are not exposed to oxygen thereby providing a safe environment for these highly oxygen sensitive methanogens. This information is very useful for judging the extent to which strictly anaerobic conditions should

be kept in handling methanogens.

All methanogenic bacteria are capable of extracting energy from the oxidation of dihydrogen under anaerobic conditions using carbon dioxide as electron acceptor.

$$4H_2 + HCO_3^- + H^+ \longrightarrow CH_4 + 3H_2O \qquad (\Delta G^0 = -138.9 \text{ kJ}) \qquad (2.1)$$

The initial reduction of carbon dioxide to the level of formaldehyde is thermodynamically unfavorable whereas further reduction of formaldehyde to methane is very favorable, and the standard free energy change of the reaction would theoretically support the formation of two molecules of ATP. The dihydrogen–dependent reduction of $CO_2$ requires an anaerobic electron transport pathway. The exact nature of the electron carriers involved in this pathway has not yet been determined. A methyl carrier, coenzyme M, has been detected in all methanogenic bacteria and appears to be unique to this group of organisms [60]. An early labelled reduction product of $^{14}CO_2$ that can be detected in whole cells or in the extract of methanogenic bacteria is methyl–coenzyme M. It is believed that this compound is the substrate for the final step in methane production catalyzed by methyl–CoM reductase [61].

$$CH_3\text{–}SCoM + H_2 \longrightarrow CH_4 + HSCoM$$

Methanogens differ from other autotrophs (organisms that proliferate with $CO_2$ as the sole carbon source) in that their $CO_2$ metabolism involves both fixation to cell carbon and reduction to methane. At present, little is known about the initial reactions involved in $CO_2$ reduction to methane and fixation into cellular intermediates.

The biochemical mechanism of methane formation from organic acids (the major products of the acid-formation phase) and its coupling to ATP synthesis is virtually unknown. Recently, a fluorescent electron transfer coenzyme (coenzyme $F_{420}$) has been found in all methanogens but has not been detected elsewhere. $F_{420}$ participates as an electron carrier in the nicotinamide adenine dinucleotide phosphate (NADP) linked

hydrogenase and formate dehydrogenase systems in methanogens [62]. Thus, formate and hydrogen are essentially equivalent sources of electrons for the reduction of carbon dioxide to methane.

In anaerobic digesters, the major source of methane appears to be acetate rather than carbon dioxide or formate even though only a few methanogenic species are able to use acetate as their energy and carbon source. Estimations based on carbon isotope labelling indicate that 67 to 75 per cent of the methane is derived from acetate [63,64]. *Methanosarcina barkeri*, one of a few species having a wider substrate spectrum, has shown its ability to use acetate, methanol and methylated amines as sole carbon and energy source instead of $H_2/CO_2$. It has been confirmed by labelling acetate that its methyl group during the fermentation is transferred intact into methane; there is no evidence of the acetate being oxidized first to $CO_2$ [65,66].

$$C^*H_3COOH \longrightarrow C^*H_4 + CO_2 \qquad (\Delta G^0 = -32 \text{ kJ/mol}) \qquad (2.2)$$

Conservation of the protons in the methyl moiety strongly suggests that methane production from acetate was attained via a single reduction step by a single organism. Under standard conditions, the acetate conversion to methane can only offer limited energy. Therefore, acetate–fermenting methanogens would be inherently slow growing, and it would be questionable if fermentation of acetate alone would sustain the energy requirements for growth. Values reported for the free energy of ATP hydrolysis have been estimated to range from -34.4 to -52.4 kJ/mol at physiological conditions. Normal efficiencies of energy transfer in bacteria are 30 to 50 per cent. Thus, the reactions that yield less than -49 kJ/mol at standard conditions makes the formation of an energy-rich compound via substrate level phosphorylation unlikely and is insufficient for cell growth [67]. "Highly purified" cultures of *Methanosarcina barkeri* and *Methanococcus* species showed a very slow acetate fermentation [68]. Isotopic tracer studies by Zeikus et al [69] indicated that hydrogen was required for the metabolism of acetate to methane by

several pure cultures. Comparing the energy formed per mole of methane produced from reactions 2.1 and 2.2 shows that approximately four times as much energy is available from respiration of hydrogen than that from acetate fermentation. Adding hydrogen to pure acetate fermentation cultures not only raises the actual free energy released from the acetate fermentation due to decreased $CO_2$ concentration but also supplies more free energy for bacterial growth from the reduction of carbon dioxide. Alternatively, The methanogenic species which are capable of utilizing acetate may possess a mechanism through which sufficient free energy can be accumulated from the fermentations of more than one acetate molecule and then the energy is used to produce ATP. As a result, up to 70 per cent methane is produced from the reaction of acetate fermentation. In mixed cultures, more complexly, the acetate utilization was affected by many factors such as ions strength, redox potential of the culture [71] and even the presence of sulfate–reducing species [70]

### 2.1.3 Acetogenesis of Fatty Acids

As discussed above, the substrate spectra of methanogenic bacteria are very narrow, only including $H_2/CO_2$, formate, methanol, methylamide and acetate, while the end products from the first phase (acids-formation) include a large number of organic acids containing more than two carbon atoms (propionate, butyrate, etc.) which can not be directly utilized by methanogenic bacteria. A third group of bacteria must exist as a bridge between the acidogenic and the methanogenic microbes. These obligate hydrogen-producing bacteria, acetogens, are able to convert the chemical compounds (ethanol, propionate, butyrate, etc.) that the methanogens cannot utilize to acetate, $CO_2$ and $H_2$.

$$CH_3CH_2OH + H_2O \longrightarrow CH_3COO^- + H^+ + 2H_2 \qquad (\Delta G^0 = +9.6 \text{ kJ})$$

$$CH_3CH_2COO^- + 3H_2O \longrightarrow CH_3COO^- + H^+ + 3H_2 + HCO_3^- \qquad (\Delta G^0 = +76.1 \text{ kJ})$$

$$CH_3CH_2CH_2COO^- + 2H_2O \longrightarrow 2CH_3COO^- + H^+ + 2H_2 \qquad (\Delta G^0 = +48.1 \text{ kJ})$$

Thermodynamically, however, these reactions are unfavorable under standard conditions ($\Delta G^0 > 0$) and move towards the right only under a very low partial pressure of hydrogen (below $10^{-4}$ atmospheres) [72]. This can be accomplished by the action of hydrogentrophic bacteria such as methanogens or sulfate-reducing bacteria. Thus, the acetogens and methanogens constitute a symbiotic association; the former needs the latter to remove $H_2$ to create a favorable environment and the latter can obtain their substrates (acetate, $H_2/CO_2$) from the metabolic products of the former. This advance in the knowledge of anaerobic digestion goes back to the classical studies of Bryant, Wolin and Wolfe [73] who reported in 1967 that "*Methanobacillus omelianskii*", a species capable of producing methane from ethanol, was actually a symbiotic association of two different species. Microscopic observations suggested that *M. omelianskii* consisted of two organisms of different shape. When the organisms were separated, one, a methanogen later named *Methanobacterium bryantii*, grew on hydrogen and carbon dioxide but no other substrates. The other species, *S* organism oxidized ethanol to acetate and hydrogen. The electrons generated from this oxidation were transferred to a pyridine nucleotide carrier ($NAD^+$) and ultimately used to reduce protons to molecular hydrogen. The significance of this study is their speculation that alcohols other than methanol and fatty acids other than acetate and formate are not catabolized by methanogens, but by another group of nonmethanogenic bacteria. Later, McInerney et al (1981) [75] obtained *Syntrophomonas wolfei*, an anaerobic butyrate-oxidizing bacterium in co-culture with either a hydrogenotrophic sulfate reducer or a hydrogenotrophic methanogen. A syntrophic association of an anaerobic propionate oxidizer in co-culture with a hydrogentrophic organism was reported by Boone and Bryant (1981) [76]. Table 2.5 lists the currently known mesophilic acetogens.

Table 2.5: Currently known mesophilic obligate proton-reducing bacteria

| Organisms | Co-culture with | Habitat | Substrate |
|---|---|---|---|
| *Syntrophobacter wolinii* | *Desulfovibrio G11* or *M. hungatei + D. G11* | digester | propionic acid |
| *Syntrophomonas wolfei* | *Desulfovibrio G11*, *M. hungatei* | digester, sediments | monocarboxylic saturated fatty acids (14–8 C) |
| *Syntrophus buwellii* | *Desulfovibrio G11*, *M. hungatei + D. G11* | digester, sediments | Benzoic acid |
| *Clostridium bryantii* | *Desulfovibri E70*, *M. hungatei M1H* | digester, sediments | monocarboxylic fatty acids (to 11 C) |
| *Strain Gra I val* | *Desulfovibrio E70* | marine sediment | isovaleric acid |
| *Strain Go I val* | *Desulfovibrio* | digester | isovaleric acid |
| *Strain SF-1, NSF-2* | *M. hungatei* or *Desulfovibrio sp.* | digester | monocarboxylic saturated fatty acids (4–6 C) |
| *Strain BZ-2* | *Desulfovibrio PS-1 Methanosporillum sp.* | digester | benzoic acid |

Source is [74].

A direct cell count of co-cultures of *Syntrophomonas wolfei* with *Methanospirillum hungatei* fed with butyrate indicated that the former made up 30 per cent of the population versus the latter 70 per cent [78]. The growth rate of acetogens is very low as shown in Table 2.6 with or without sulfate-reducing bacteria (SRB) as co-culture.

Table 2.6: Growth rate of obligate $H_2$–producing actogens

| Organism | Substrate | $\mu$ (day$^{-1}$) with SRB | $\mu$ (day$^{-1}$) without SRB | Reference |
|---|---|---|---|---|
| *Syntrophobacter wolinii* | propionate | 0.192 | 0.103 | [76] |
| *Syntrophomonas wolfei* | butyrate | 0.307 | 0.185 | [75] |
| *Syntrophus buswillii* | benzoate | 0.127 | 0.101 | [77] |

Obviously, the sulfate-reducing bacteria can promote the growth of obligate $H_2$–producing acetogens because of a much faster removal of the hydrogen released at the expense of some energy and carbon source ($H_2$, acetate, etc.) consumed by sulfate-reducing bacteria.

Hardly any information is presently available on the biochemical pathways in acetogens, as pure cultures are not yet available. Tracer studies with enrichment cultures that converted propionate to methane and acetate [79] showed that the $^{14}C$–labeled carboxyl group exclusively appeared in carbon dioxide whereas the accumulated acetate was practically free of labeled carbon. Both [2–$^{14}C$] and [3–$^{14}C$]–propionate lead to the production of radioactive acetate. The methyl group and the carboxyl group of the acetate produced were equally labeled, regardless of whether [2–$^{14}C$] or [3–$^{14}C$]–propionate had been used. These observations suggested that propionate was degraded through a randomizing pathway. Of the three reactions mentioned above, propionate oxidation is thermodynamically the most unfavorable, and so, propionate is not easily digested in the methanogenesis phase and occurs in the effluent in quite high concentrations, especially when the acidogenesis phase is producing a large amount of propionate due to some disturbance caused by changes in load, pH, temperature etc..

The anaerobic oxidation of butyrate in *S. wolfei* has been postulated to go via $\beta$–oxidation [75], but detailed labeling studies are lacking. However, the observation that the conversion of normal monocarboxylic saturated four to eight carbon fatty acids yields $H_2$ and acetate, or $H_2$ and acetate plus propionate is consistent with a $\beta$–oxidation mechanism for the degradation of fatty acids by *Syntrophomonas wolfei*. Selective lysing of cells of *Syntrophomonas wolfei* recently allowed McInerney and co-workers [78] to demonstrate the presence of enzyme activities consistent with a $\beta$–oxidation pathway for butyrate degradation.

## 2.2 Start-up of Anaerobic Biofilms

The operational principle of anaerobic biofilm reactors is based on the fact that attachment of anaerobic bacteria which grow very slowly, to support surfaces prevents them from being washed out of the reactor. The startup of anaerobic biofilm reactors, however, is generally time consuming and often difficult partly because of the low growth rate of anaerobes, especially the methanogenic and acetogenic bacteria, and also due to the lack of understanding of the mechanisms underlying the process and the factors affecting the attachment of bacteria onto support surfaces. The present status of the understanding of the start-up of an anaerobic biofilm reactor is more experimental than theoretical [80].

### 2.2.1 Mechanism of Build-up of Bacterial Biofilms

Biofilm formation is the net result of depositional, metabolic and removal processes [81], including:

1. Cellular particles transport from bulk liquid to support surfaces.

   Bacteria, as particles (d = 1 $\mu$m) suspended in culture medium, can be transported to a surface by any one, or a combination of, the following mechanisms: motility and chemotaxis; gravity; molecular diffusion (in laminar flow); and eddy diffusion (in turbulent flow). It is doubtful, in a nutrient-rich fermenter, that chemotaxis and gravity would play a significant role in transport of bacterial cells which have a density (1.05–1.1 g/cm$^3$) very close to that of the medium. And so, molecular diffusion and/or eddy diffusion may be the dominating mechanisms for cell particles transport in a laminar or turbulent flow situation [82,83]. The fluid flow velocity has two principal effects on the formation of biofilms; the shear stress which increases with increased velocity and a change in the flux of cells/nutrients across the boundary layer or viscous sub-layer which is compressed as the velocity increases.

Moreover, the concentration of cells in the bulk aqueous phase may also play a role to some extent. Bryers and Characklis [86] reported that under turbulent flow the deposition rate increased by a factor of 4.5 for a 5 times increase in cell mass concentration.

2. Microbial adhesion.

   Once bacterial cells are close to or on the surface, they adhere reversibly and then irreversibly. Zobell (1943) [84] observed that bacterial attachment was often reversible–that bacteria which appeared to have settled on a substratum could be washed off by a stream of water, and that firm attachment appeared to occur only after a bacterium had remained settled for several hours. The investigations of Marshall et al (1971) [85] supported this two-stage attachment theory, called 'reversible' and 'irreversible sorption' respectively. Reversible sorption is the initial stage of bacterial attachment when the bacterium, exhibiting Brownian motion, is only weakly held at the surface while irreversible sorption was a time- dependent stage, which is due to the synthesis of exocellular polymers bridging the bacterial and substratum surfaces. The fixed bacterial cell does not exhibit Brownian motion and is not removed by washing.

3. Colonization of the surface by growth of the organism and formation of a biofilm.

   After becoming firmly attached, the cells multiply and are joined by additional attaching cells, which leads to the formation of microcolonies. These isolated points of growth eventually unite to form a continuous layer of microbial mass, i.e. a biofilm.

4. Detachment of the microbial film due to shear force and sloughing.

Generally, sloughing and/or biomass decay more likely occur in a thick biofilm due to lack of nutrients in deeper layers while in the period of startup of biofilm or of a thin biofilm, the removal caused by shear force may predominate [87]. A dynamic equilibrium is maintained when steps 3 and 4 are occurring at the same rate.

The attachment of bacteria to solid surfaces in aqueous solution is affected by many factors since it involves three components: the bacterial surface, the solid substratum, and the surrounding liquid phase. A factor which can directly or indirectly affect one of them would play a significant role in the process of attachment. The influence of bacterial cell surface on attachment, for example, is reflected in the fact that the attachment depends upon the growth conditions of the cells, such as the medium components [85], the limiting nutrients [88], the dilution rate in a continuous culture [89] and growth phase in batch culture [90]. Some factors can influence more than one component, such as electrolyte concentration [85], presence of dissolved substances which are adsorbed onto the surfaces modifying the surface properties [91], pH of the medium [92] as well as temperature [90]. Obviously, the intrinsic properties of the substratum and the bacterial surface have significant influence on attachment. The physicochemical properties (surface charge, surface free energy) of a potential substratum have been implicated in influencing attachment [93]. Recently, the hydrophobicity of bacterial cell surfaces has been studied [95,96] as an overall parameter for the measurement of the adhesion potential to solid surfaces, because in low-ion-strength environments the microbial surface hydrophobicity and charges are of greater importance [97] while most previous studies on bacterial attachment were conducted in a marine environment [98].

Initial attempts were made to model the adhesion phenomenon on the basis of colloid stability theory (DELVO theory) since the small size, low density and net negative charge of bacterial cells are similar to those of colloidal particles. This approach has achieved

some success in the explanation of general features and 'long range' interactions between cells and surfaces [99]. An alternative phenomenological approach involving the study of free energies employs an analysis of the thermodynamic potential for cell adhesion on the basis of known interfacial tensions [100] and has also been in some measure successful in modeling cell–surface contact events in terms of decreases in surface free energies resulting from adhesion [102]. The weakness of the physico-chemical models lies in their failure to take account of biological reactions since the cells are treated as solid inert particles rather than as living systems. Marshall [101] proposed a two-stage model based on experimental observations. The first stage involves cell deposition in which the bacterial cell is held a small but finite distance from the solid surface, and this situation is maintained by the existence of an energy barrier. The second stage occurs when the energy barrier is breached allowing intimate surface contact and permanent adhesion.

Three bridging mechanisms have been suggested: short-range physico-chemical forces such as chemical bonds or hydrophobic bonding [100]; specialized bacterial holdfasts, such as pili, fimbriae; and 'polymer bridging' through the mediation of bacterial extracellular polymers. Since most bacteria have no obvious structures for attachment, it is widely believed that the existence or 'in situ' synthesis of extracellular adhesives is required for permanent adhesion, the polymer occurring as an acidic polysaccharide [103], glycoproteins [104] etc. Polymer bridging was the mechanism proposed by Marshall for the time dependent second stage in which irreversible sorption awaits polymer synthesis. However, it has been observed that some bacteria have the ability to bind rapidly to surfaces — this spontaneous binding suggests that bridging may depend on the compatibility of biopolymers (exuded prior to reversible adsorption) with the solid surface. It is further observed that the initial, rapid attachment of a marine pseudomonad was mediated by a compact acidic polysaccharide followed by synthesis of a 'second' fibrous polysaccharide responsible for biofilm consolidation [103].

Many bacteria (Gram–positive and Gram–negative) can produce layers of polysaccharide outside their cell wall (capsules or slimes). The degree of capsulation and the production of extracellular polysaccharides by a particular organism can be markedly influenced by the growth conditions. The nature of the linkage to the underlying wall structures remains unknown. However, the biosynthesis of several capsular polysaccharides is known to require the participation of lipid intermediates [105]. In terms of structure, capsules and slime layers are in general highly hydrated. Capsules of *Klebsiella aerogenes* strains A1 and A3 were reported to give a viscous solution containing only 1 to 2 per cent polysaccharide material [106]. Therefore, a bacterial cell can be imagined as a small ball around which a layer of hydrated adhesive exists.

### 2.2.2 Startup of Methanogenic Biofilms

In the anaerobic treatment of cheese whey, the methanogenic and acetogenic bacteria grow much more slowly than do acidogens. Therefore, the start-up of the methanogenic biofilm is more time consuming than that of acidogenic biofilm. Moreover, in the methanogenic phase a symbiotic community is involved which includes methanogens and acetogens. It is essential to know whether the properties of support surfaces would affect the attachment of each bacterial type — that is whether or not the attached biomass would have the same bacterial composition as that in the bulk culture medium.

Shapiro and Switzenbaum [107] investigated the initial anaerobic biofilm development in a mixed culture fed with sucrose. The methanogen accumulation was monitored by $F_{420}$ fluorescence content of the biofilm material. The ratio of methanogens to total anaerobic biomass was found to remain constant throughout 25 days for high organic space loadings. Longer solid residence time (SRT), higher concentrations of anaerobic microorganisms and higher organic space loadings were beneficial to the startup of anaerobic biofilms.

Many investigations have been conducted on the effect of support surface on startup

of methanogenic biofilms. Murray and van den Berg [43] studied the development of methanogenic fixed films on pieces of polyvinyl chloride (PVC) plastic, etched glass and baked clay and the results showed that support material markedly affected the rate of attachment and growth of bacteria converting acetic acid to methane. Scanning electron micrographs showed that the film of bacteria attached to clay was thick and uniform, while the bacterial film attached to PVC plastic was thin but still uniform. Attachment to etched glass was spotty. That the clay was superior was attributed to its rough porous surface and the presence of minerals in it, particularly iron which is known to stimulate methanogenesis and growth. More supports were tested by van den Berg and co-workers [109]. Comparing methane production rates of anaerobic biofilms on four supports, needle punched polyester, red draintile clay, gray potters clay and PVC, they found that needle punched polyester was one of the most effective in developing an active biomass film even though it could not offer the microbes extra nutrients like clay.

A series of packing materials, non porous and porous, were compared by Huysman et al [110] in a mixed anaerobic biofilm reactor in order to elucidate the most important factors for biofilm formation. Their results indicate that surface roughness and total porosity plus pore size have the largest effect on the colonization velocity, and a reticulated polyurethane foam appeared an excellent colonization matrix. However, the study of attachment of methanogenic bacteria to solid supports with various porosities performed by Kuroda et al [40] revealed that methanogens adhered to moderately rough surfaces that had pores measuring a few tenths of a micron in diameter more than to polished and rough surfaces, and also preferably adhered to solid supports made of carbon material. Obviously, the roughness of a support surface is playing a significant role in the development of biofilms because a rough surface either offers more area for microbes to attack or entrap the fixed biomass by preventing them from being detached by shear stress of fluid flow. In this sense, the porosity of a surface is a common factor to all

bacterial attachment (not only beneficial to methanogens and acetogens). Furthermore, it should be controlled because in thick biomass entrapped in the channels of supports (e.g. foam) the resistance to mass transfer would become significant, resulting in more dead volume in digesters.

A fundamental study was conducted by Verrier and Albagnac [111] to investigate adhesion of methanogenic bacteria onto inert solid surfaces, PVC and glass slides. Again the experiments showed that bacterial attachment on glass slides was very spotty, and remained always low, while it was higher and increased constantly with time on PVC slides. It was calculated that $7\times10^3$ bacteria adhered per $mm^2$ of PVC per day. The predominant bacteria were filaments with septa and irregular surfaces tentatively identified to be Methanothrix soehngenii. A strong influence of calcium concentration on bacterial adhesion was observed with an optimal effect at about 2 mM of $Ca^{++}$. Above this concentration a negative effect appeared due to bacterial aggregation. Sodium addition was less effective. Verrier and co-workers conducted more research on the adhesion of methanogens onto surfaces [112]. This time, 4 pure methanogenic cultures were used to investigate their initial adhesion on polymeric surfaces with different hydrophobicities. *Methanothrix soehngenii* adhered preferentially to hydrophobic polymers while *Methanospirillum hungatei* preferred hydrophilic surfaces and *Methanobrevibacter arboriphilicus* adhered onto all the supports. These results suggest that initial adhesion may influence the start-up rate of anaerobic fixed film reactors and is a function of the support hydrophobicity. It is interesting that *Methanosarcina mazei*, an acetate-degrading species, did not adhere to any support even though *Methanosarcina spp* can always be found in large amounts in methanogenic biofilms, which may imply that some symbiotic function is involved when a mixed bacterial population attaches onto support surfaces. The importance of support materials on anaerobic biofilm formation was also pointed out by Switzenbaum et al [113], but their effort to enhance the rate of initial anaerobic

biofilm accumulation by precoating support media with denitrifying bacteria biofilms (biological precoating) and various polymers (chemical precoating), failed.

Recently, Wollersheim [42] investigated the adhesion and biofilm development of methanogenic biofilms on glass. The experiments carried out with an undefined culture as well as with a propionate-degrading anaerobic culture revealed that the primary adhesion was a passive process while the following biofilm development was an active one, which was accompanied by excretion of polysaccharides. The primary adhesion of bacteria may be controlled by the hydrophobicity and the surface charge of the supporting material. The adsorption of acetogenic and methanogenic bacteria to wood chips, studied by Moo-Young and co-workers [114], has been assessed in terms of adsorbed particulate organic nitrogen (PON) representing a total amount of symbiotic biomass. It was found that the adsorbed PON/$m^2$ of support could be related to the cell concentration in solution by a Freundlich-type isotherm.

It seems that the installation of the first bacterial layer may be of major importance for further biofilm growth and stability. To this author's knowledge, however, no study has been conducted on the effect of support materials on the bacterial composition of an attached microbial biomass in a symbiotic bacterial community (methanogens plus acetogens) because of the difficulty in differentiating the specific substrate-degrading bacterial type from a mixed culture.

## 2.3 Mass Transfer in Anaerobic Biofilms

Once an anaerobic biofilm forms on a support surface, two major phases exist in the fermenter, an aqueous medium phase and a concentrated biomass phase. The sequence of steps occurring during substrate utilization by the biofilm can be simplified into two important steps: (1) substrates are transported from the bulk medium solution to the

interface between the liquid and the biofilm (external mass transfer), (2) diffusion and consumption of substrates within the biological slime (internal mass transfer plus reaction). These two steps are in series, and so the slower one becomes the rate-limiting step of the overall process. The transport rate of substrates from the bulk solution to the film-fluid interface can be represented by the equation below

$$N = k_L(S_b - S_s) \tag{2.1}$$

where $N$ is the rate (flux) of mass transfer (mg/sec/cm$^2$), $k_L$ is the mass transfer coefficient (cm/sec), $S_b$ and $S_s$ are the substrate concentrations in the bulk solution and at the biofilm surface (mg/cm$^3$), respectively. If the mass transfer coefficient is so large that the external mass transfer rate is much faster than the rate of internal mass transfer plus reaction, at any particular value of $S_b$, the overall rate will depend only on the kinetics of internal mass transfer plus reaction. This limiting regime has been termed kinetic regime, or reaction-controlled regime [115]. It is the only case in which the actual reaction kinetics of the biological film can be directly measured, provided the internal diffusional effects are reduced to negligible level.

Frequently, the external mass transfer coefficient, $k_L$ is incorporated in the dimensionless Sherwood number, $Sh$, which is predicted as a function of Reynolds number, $Re$, and Schmidt number, $Sc$, characterizing hydrodynamic conditions and molecular diffusion, respectively,

$$Sh = f(Re, Sc) \tag{2.2}$$

where $Sh = k_L d/D_L$; $Re = ud/\nu$; and $Sc = \nu/D_L$. For creeping flow ($Re < 1$), the theory developed by Levich [116] shows that:

$$Sh = 0.99 Re^{1/3} Sc^{1/3} \tag{2.3}$$

In the range $10 < Re < 10^4$,

$$Sh = 0.95 Re^{1/2} Sc^{1/3} \tag{2.4}$$

More empirical or semi-empirical equations can be found for other fluid patterns [117]. Use of stagnant film theory, i.e., estimation of a liquid/solid mass transfer coefficient as the quotient of a diffusivity and diffusion layer thickness ($k_L = D_w/\delta_w$) is an alternative method which gives a lower bound for $k_L$ when Re number is less than 0.01 [118]. The stagnant diffusion layer can be taken, for example, to be the ratio of the liquid volume to media surface area. Obviously, the external mass transfer coefficient is markedly affected by fluid flow pattern in a fermenter. Experimentally, the external mass transfer resistance can be minimized or eliminated by increasing the fluid velocity over the biofilm [119].

### 2.3.1 Structure of Anaerobic Biofilms

By using light, UV, scanning and transmission electron microscopy, Robinson et al [120] examined the structure of anaerobic biofilms sampled from eight anaerobic fixed-film digesters fed with swine waste which had been in operation for 12 months at the University of Florida Swine Research Unit. Although the biofilm samples were collected from various support materials (different shapes of plastics and blocks of pine, cypress, oak), the biofilms did not differ significantly in microbial or overall appearance. The overall surface of the biofilms was rough and uneven. Protuberances resembling volcanoes were observed with openings of 100 to 500 $\mu$m in diameter with a smooth microbial lining. Cross-sections of biofilms revealed a high density of material containing a heterogeneous bacterial population toward the base of the biofilms. Various cell types were found in small, loosely packed congregates or microcolonies. Some microcolonies contain only one morphological type of coccus, but most microcolonies contained several different types of cells (perhaps symbiotic communities). Large aggregations of sarcina-containing cysts

were the most prevalent microbe found in thin sections cut from the biofilms. Individual cells were enclosed by a dark-staining wall closely associated with an amorphous matrix material 180 nm thick that extended throughout the cyst. Cells on the periphery of the cyst were covered by a capsule–like material or by a honeycombed netword of dead cells.

Transmission electron micrographs of thin sectioned biofilm samples fixed with ruthenium red, an electron dense marker which can stain the extracellular polysaccharides, revealed that at least three types of matrix material or glycocalyx existed in biofilms [121]. Around individual cells is glycocalyx type II which is a flexible integral microcapsule and glycocalyx III envelopes microcolonies containing morphologically similar sister cells. The type I, rigid peripheral glycocalyx, appears to be spatially extensive and possesses interstices which have different cross sectional size. A clear demarcation was seen between the interstices and their boundary walls; suggesting that the interstices may be channels within the type I glycocalyx. Large vacant areas in some of the interstices were observed and it was attributed to dead cells which once occupied these areas and left their 'foot print' in the rigid matrix [98].

The glycocalyx also contain mineral precipitates containing Ca, P and a small amount of Mg [120]. In a methanogenic biofilm on a needle–punched polyester support, the concentrations of Ca and P in the extracellular matrix were 92 and 28 times higher, respectively, than in the cells [122]. In the sense of internal mass transfer, a biofilm may be described as an assemblage of bacterial cells, biological catalytic centers, that are distributed in an extracellular fibrous polysaccharide–containing matrix and connected by tortuous channels of various size as shown in Figure 2.7.

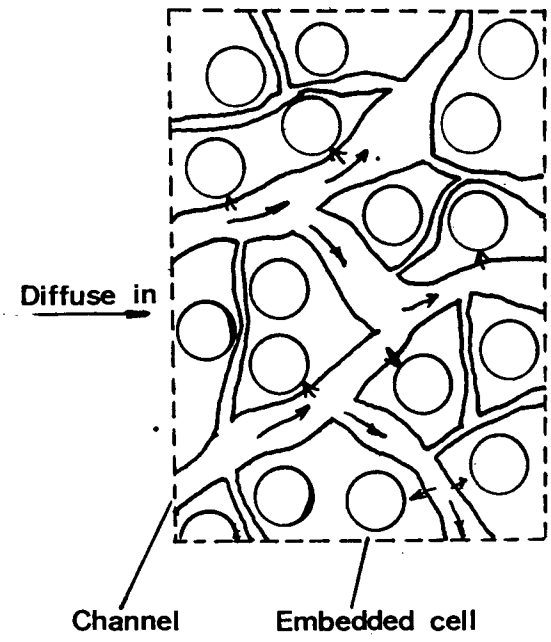


Figure 2.7: Structure of biofilms

### 2.3.2 Mass Transfer within Biofilms

Because of the gelatinous character of biofilm matrix it is thought that convective transport contributes little to the movement of reactive constituents within biofilms and substrate molecules transport towards the inner layers of biofilms along the tortuous channels by a mechanism of diffusion. Simultaneously, they also transport, by some mechanisms (passive and/or active transfer etc.), into the embedded microbes (see Figure 2.7) where utilization reactions occur. It should be pointed out here that this latter mass transfer is a part of the intrinsic kinetics of substrate utilization by microorganisms because it involves some characteristic enzymes of the bacteria even though immobilization of living cells may produce a layer of exocellular polymers (glycocalyx type II) around the cells which affects the mass transfer rate. It is almost impossible to determine the actual transfer mechanism and rate of diffusion within the tortuous pores of the biofilms, and therefore, some workers have defined an effective diffusivity $D_e$ in such a way that the

substrate molecules may be thought of as diffusing through an equivalent homogeneous medium as is done in the study of porous catalysts.

$$N = -D_e(dS/dx) \tag{2.5}$$

Unlike in homogeneous systems such as water solutions where the major diffusional resistance comes from the collision of solute molecules with water molecules, the diffusion of substrate molecules in biofilms will be further retarded because they must move through the gelatinous matrix. In addition to the factors which influence the diffusivity in pure water, D, such as temperature, molecule size and viscosity, the effective diffusivity, by its definition, must be influenced by the structures of biofilms. Therefore, investigation of internal mass transfer within a biofilm comes to be the measurement of the effective diffusivity, $D_e$, of substrate molecules in the biofilm.

Effective diffusion coefficients of some substrates have been measured in aerobic microbial aggregates (films, blocs) because the supply of oxygen to aerobes embedded in microbial aggregates is believed to be the rate-limiting step. These are reported in several papers which have been reviewed by Libicki and coworkers (1988) [123]. In contrast, no report has been found by this writer on the internal mass transfer in fermentative biofilms. Actually, as discussed in Chapter 1, the knowledge of effective diffusion coefficients in fermentative biofilms and then, an optimum biofilm thickness, becomes essential when the anaerobic technology is applied to industry where a long term stable and optimal operation is required.

To evaluate the internal mass transfer parameter under a negligible external transfer resistance, three approaches have been taken: (1) evaluation of intrinsic reaction rates from a separate experimental study or literature and the internal transfer rate by fitting them simultaneously to the reactor breakthrough data (indirect method) [124], (2)

evaluation of internal mass transfer rate by measuring a concentration gradient through an active biofilm and coupling it with the flux of material into the biofilm [125], (3) evaluation of internal mass transfer rate from the flux across an inactive biofilm in a two chamber device (direct method) [127]. The biofilm is often killed by chemicals (mercuric chloride) or radiation (ultraviolet) [128]. In the first method by which most diffusivities in active microbial aggregates have been measured, the effective diffusivities have been used as fitting parameters in substrate utilization models and it is likely that error would be introduced into their results if the reactor hydrodynamics was not exactly the same as predicted by their model. The second method is a direct method to measure effective diffusivities in active biofilms, but measuring a concentration profile within an active biofilm needs special probes which should be very small in size and able to detect the target molecules. This method has been used by Bungay and co-workers for oxygen diffusion into laboratory-grown [125] and actual trickling filter films [126]. The third method may be able to avoid the effects of non-ideal reactor deviations on the measurement of effective diffusivities because it focuses on the two sides of the target biofilm. But it usually uses an 'inactive' biofilm to avoid the uncertainty caused by the kinetics of substrate utilization. The measurements involve the concentration changes in the chambers with time after a pulse input is given to one chamber. Not only must it be certain that the biofilm is completely killed and so no reaction will occur [128] but also some factors of importance in a living biofilm like gaseous products released in small bubbles, symbiotic relationship and interaction between active bacterial species are neglected. Furthermore, the process of deactivating a biofilm may introduce some changes in the structure of the biofilms. Table 2.7 summarizes some experimentally determined diffusivities in inactive biomass.

Variability in these results is substantial even in this narrow sample of experiments.

Table 2.7: Ratios of effective diffusivities measured in inactive biomass to diffusivities in water

| $D_e/D_w$ | | | | | | Biofilm | Reference |
|---|---|---|---|---|---|---|---|
| Oxygen | Glucose | $NH_4^+$ | $NO_2^-$ | $NO_3^-$ | $Na^+$ | preparation | |
| 0.85 | - | 0.8–0.87 | 0.86 | 0.93–1.0 | - | filtered | [127] |
| 0.2–1.0 | 0.3–0.5 | - | - | - | - | centrifuged, pressed | [128] |
| 1.2 | 0.15-1.2 | 0.7 | - | - | - | settled, filtered | [129] |
| - | 0.6 | - | - | - | 0.6 | grown in place | [130] |
| 0.3 | - | - | - | - | - | centrifuged | [131] |

This may be due in part to the differences in biomass growth conditions but it is probably also due to the different techniques that have been used to prepare the biofilms. For example, Onuma and Omura [129] have reported variance in film diffusivities with carbon to nitrogen ratio in the media in which the biomass was grown. Matson and Characklis [128] grew mixed cultures of bacteria on glucose in completely mixed reactors, concentrated them by centrifugation, and formed them into films by spreading them onto a template with a spatula. The biofilm was then sandwiched between two membrane filters prior to its placement in the diffusion apparatus. It is possible that some artificial effects may be introduced by the process of preparing such a biofilm because the major difference in diffusivities in water and in hydrated biofilms is caused by the matrix made of exocellular polymers. In order to avoid the possible effects introduced by artificially treating biofilms, a nonreactive solute has been used to measure its effective diffusive permeability in intact microbial cell aggregates [123].

Because of the difficulties associated with the direct measurement of the effective diffusivity, most studies on the modeling of fixed-film reactors have used assumed values. Based on their previous work on prepared biofilms of aerobic, autotrophic, nitrifying bacteria [127], subsequent studies by Williamson, McCarty and their co-workers [132,133]

have assumed effective diffusivities of 80 percent of the free values for a larger number of substances in various biofilms. The effective diffusivity of acetate in a methanogenic biofilm was also taken as 80 percent of the value in free water, based on that same work [134]. Harris and Hansford [135] assumed that the effective diffusivity of glucose was equal to the value in water because of the results of Atkinson and Daoud [136].

It is one purpose of the present study to measure the effective diffusivities of lactose in active acidogenic biofilms, and organic acids in active symbiotic methanogenic biofilms in a two-chamber device which can offer a more direct measurement. However, in situ measurement of effective diffusivities in an active biofilm needs firstly the knowledge of intrinsic kinetics of substrate utilization by the biofilm.

## 2.4 Intrinsic Kinetics of Substrate Utilization in Anaerobic Biofilms

The so–called intrinsic kinetics describe the relationship between the utilization rates and substrate concentrations in biofilms without interference from external and internal mass transfer resistances. Thus, the focus is on the process by which the substrate molecules are transported into microbial cells and dissimilated in the cytoplasm of the cells rather than on the transport of substrates from bulk solution to individual cells. As discussed in Section 1, this process involves various enzymes, and each of them is responsible for the catalysis of a specific chemical reaction. Generally, the slowest reaction catalyzed by a key enzyme becomes the rate-limiting step and determines the overall rate of substrate utilization.

### 2.4.1 Expression of Intrinsic Kinetics

Michaelis and Menten proposed a theory of enzyme action. Enzyme $E$ can bind to substrate $S$, forming an enzyme-substrate complex ($ES$ complex).

$$E + S \underset{k_{-1}}{\overset{k_1}{\rightleftharpoons}} ES \xrightarrow{k_2} P + E$$

This ES complex breaks down to yield free enzyme and product (P). The $k_1$, $k_{-1}$ and $k_2$ are rate constants that define how fast the individual steps proceed. They further assumed that the $ES$ complex does not easily reform from free enzyme and products, and more importantly, that the rate of formation of the $ES$ complex was equal to its rate of degradation – that is, that the formation of the $ES$ complex has reached a steady state. In this case, the concentration of the $ES$ complex will be constant. Using these assumptions, Michaelis and Menten derived Equation 2.6,

$$r = \frac{r_{max} S}{K_s + S} \tag{2.6}$$

$K_s = (k_2 + k_{-1})/k_1$, indicating the affinity of the substrate for the enzyme active site. This classical equation is identical to the empirical Monod equation which depicts microbial growth and has been used as a theoretical basis for the Monod equation since growth is the result of a number of enzymatically catalyzed biosynthetic steps. Another advantage of this mechanistic model is that modifying the reaction pathways can give rate equations describing some unusual phenomena such as substrate inhibition [137].

Cell growth and substrate utilization are generally considered to be coupled reactions, i.e., substrate removal occurs because of cell growth. The proportionality constant is the true growth yield, $Y_g$. Intrinsic rates of biological reactions are generally expressed on the basis of a unit of biomass, e.g. the intrinsic rate of substrate removal is expressed as the mass of substrate removed per unit time per unit of biomass. The unit can be based on some biomass volumetric property, such as dry weight, carbon content, protein

content. The substrate removal rate is related to the specific growth rate of microbes by

$$r = \mu / Y_g \tag{2.7}$$

The Monod expression for the specific growth rate is

$$\mu = \frac{\mu_{max} S}{K_s + S} \tag{2.8}$$

and so, $r_{max} = \mu_{max} / Y_g$.

These definitions assume that all substrate utilization is channeled into cell synthesis and that cell maintenance needs are met by decay. Another approach would be to assume that a portion of the substrate was channeled directly into cell maintenance. Although there are differences in the fundamental mechanisms employed by the two models both yield the same result and can be considered to be equivalent [138].

### 2.4.2 Elimination of External and Internal Mass Transfer Resistances

In an active biofilm, reaction and diffusion are occurring at the same time, which creates various substrate concentration profiles within the film as illustrated in Figure 2.8. Figure 2.8 also illustrates that external mass transfer resistance, which is modeled with a diffusion layer, effects the substrate concentration at the biofilm surface. Having lower concentrations entering into the biofilm means that the reaction rate per unit biomass may decline as the biomass is located further away from the outer biofilm surface.

Indirect evidence for the importance of external mass transfer resistance has been obtained by observing changes in the reaction rate when the fluid velocity past a biofilm is changed. As introduced in the last section, the external mass transfer resistance can be minimized or eliminated by increasing the fluid velocity over the biofilm. By using a rotating annular reactor, LaMotta [119] found that the reaction rate increased until the velocity past the biofilm was around 0.8 m/s, but that thereafter it was constant.

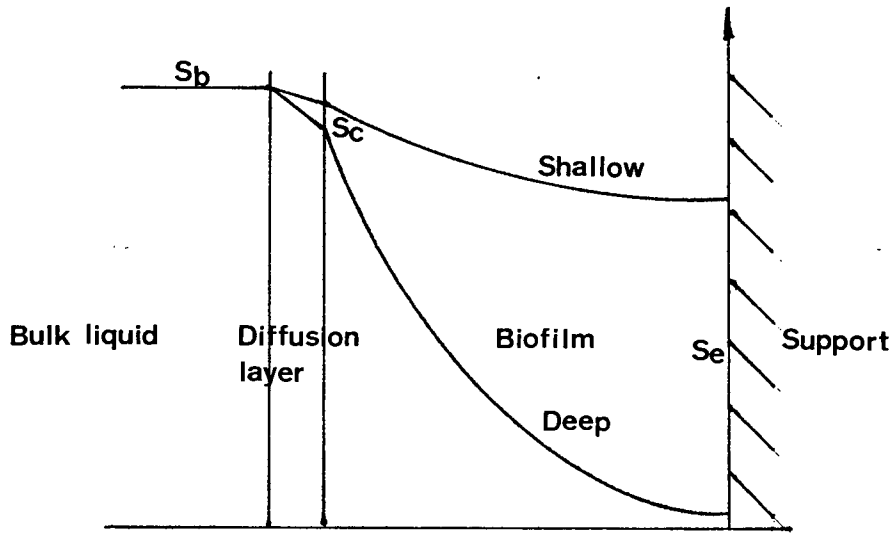


Figure 2.8: Illustration of substrate concentration profiles in biofilms

Since the external mass transfer is in series with the diffusion plus reaction, whether the external mass transfer resistance is important and what velocity past the biofilm can eliminate the external mass transfer resistance depend upon the potential (intrinsic) reaction rates in the biofilm. The slower the intrinsic reaction rates, the more easily the external mass transfer resistance is minimized.

In contrast to external mass transfer resistance, the internal mass transfer resistance is more difficult to eliminate because it occurs simultaneously with reaction. The distribution of substrate concentration within the biofilm, as shown in Figure 2.8, depends on the relative rates of diffusion and intrinsic reaction. Fast diffusion with slow reaction gives a shallow substrate concentration profile while slow diffusion with fast consumption causes a deep profile where substrate concentration reaches zero at or before the support surface. A strategy, widely applied in reaction engineering to minimize the internal mass transfer resistance of porous catalysts, is to reduce the thickness of the biofilm so that

the concentration drop in the biofilm is not substantial and can be represented by the concentration at the surface. Experimentally, this has been achieved by LaMotta [124] in aerobic utilization of glucose and by Shieh and Mulcahy [139] in biological denitrification with methanol as the organic carbon source. It should be noted that much faster intrinsic reactions were involved in these studies than in lactose and organic acid fermentations. Shieh and Mulcahy observed that for each feed concentration, a critical biofilm thickness existed, beyond which the observed denitrification rate, on a per unit biomass basis, decreased sharply. And then, the denitrification rates obtained from experimental runs in which the biofilm thickness was less than the critical value were used to determine the intrinsic kinetic parameters. To what extent a biofilm thickness should be reduced, obviously, depends upon the relative rates of diffusion and intrinsic reaction, and can only be determined by experiments. Therefore, an ideal support surface should give a uniform, thin biofilm for a relatively long period of time. Considering the effects of support materials on the thickness of biofilms, as discussed in Section 2, smooth polyvinyl chloride (PVC) sheet may be a good support material for the studies of intrinsic kinetics of lactose and organic acid fermentations in anaerobic biofilms.

### 2.4.3 Kinetics of Acidogenesis and Methanogenesis

Many laboratory experiments have been performed on the anaerobic methanation of whey or lactose to evaluate the performance of reactors using immobilized bacteria [35,140,19, 18,17,33,32], but kinetic data of the process are virtually non-existent. Kisaalita [46] investigated mainly the reaction pathways of lactose acidogenesis as well as the effects of dilution rate and pH on the pathways in a suspended culture. But the growth rate expression for acidogenic bacteria was not satisfied due to considerable wall growth which would cause a more serious problem at high dilution rates.

In contrast to lactose acidogenesis, more kinetic studies have been conducted on

Table 2.8: Growth constants of anaerobic cultures at 35 $^0C$

| Culture | $\mu_{max}$ $day^{-1}$ | $Y_{max}$ gVSS/gCOD | $r_{max} = \mu_{max}/Y_{max}$ gCOD/gVSS/day | $K_s$ gCOD/l |
|---|---|---|---|---|
| Acetic acid producing bacteria | 2.0 | 0.15 | 13 | 0.2 |
| Methane producing bacteria | 0.4 | 0.03 | 13 | 0.05 |
| Combined culture | 0.4 | 0.18 | 2 | - |

Source is [144].

methanogenesis of organic acids. Lawrence and McCarty investigated the kinetics of methane production in cultures enriched by acetate, propionate and butyrate [142]. After a calculation was made that the specific utilization rate of one acid was based only on the fraction of biomass which was responsible for the bioconversion of that acid, their results showed that the three bacterial groups responsible for degradation of three organic acids had the same specific growth rate, 0.37–0.4 ($day^{-1}$). In a suspended methanogenic culture stirred by bubbling of recycled gas, Lin et al [143] studied the kinetics of the methanogenesis of mixtures of organic acids, and expressed the Michaelis-Menten model as a function of the COD concentration of total organic acids.

Many results on the anaerobic treatment of wastewater in fixed film reactors can be found in a comprehensive review by Henze and Harremoes [144]. After reviewing the results of theoretical and experimental studies on various anaerobic systems, they proposed growth constants of anaerobic cultures as listed in Table 2.8.

However, this author has found no report on intrinsic kinetics of lactose acidogenesis and methanogenesis of organic acids. In most of the kinetic studies, the researchers had made no effort to eliminate external and/or internal mass transfer resistance nor

have they described clearly in their reports their handling of this problem even though microbial aggregates (biofilms, blocs) were involved in their investigations. If the possible effects of bacterial immobilization on the metabolic behavior of the attached microbes are considered, such as the exocellular glycocalyx around the wall of individual cells, it will further reduce the available information on intrinsic kinetics of lactose methanation by immobilized bacteria.

From the discussions on these topics; attachment of symbiotic communities of acetogens and methanogens onto inert solid supports; effective diffusivities of lactose in acidogenic biofilms and organic acids in methanogenic biofilms; intrinsic fermentation kinetics of lactose and organic acids by anaerobic biofilms, it can be seen that related information is available but no previous work has been conducted specifically on these topics. This study will concentrate on these topics and some fundamental investigations will be made which may be valuable for a better understanding of the complex process of lactose anaerobic methanation in fixed biofilms.

# Chapter 3

## Experimental Conditions and Setup

It has been indicated in Chapter 1 that this study, as an extension of studies of lactose acidogenesis in suspended cultures conducted by Kisaalita [46], will concentrate on lactose utilization in two-phase anaerobic biofilms. Although a great deal of research has been carried out on anaerobic digestion of organic substrates, some problems still need more investigations which are crucial for an optimal design and operation of a process in which lactose is utilized in two–phase anaerobic biofilm reactors. Among these, five have been selected as the present research objects: intrinsic kinetics of lactose utilization and organic acids production in acidogenic biofilms, attachment and build-up of symbiotic methanogenic biofilms, intrinsic kinetics of organic acids dissimilation in methanogenic biofilms, lactose transfer in the acidogenic biofilms and organic acids transfer in the methanogenic biofilms.

Mass transfer data are prerequisites for estimating and controlling the optimum biofilm thickness so that a stable operation can be achieved in a fermenter with growing biofilms. The intrinsic kinetics of substrate utilization by anaerobic biofilms not only give fundamental knowledge on how fast the sugar and the acids can be digested by the responsible microbes embedded in the biofilms but also are needed to estimate the diffusion properties of substrates in living biofilms.

All the five research subtitles will involve different microbial species, substrates, culture conditions and biofilm supports, which will be detailed in each of the following chapters. However, some common conditions and setups which will be used in all these

investigations are described in this chapter.

## 3.1 Experimental Conditions

Experimental conditions mainly include culture temperature, culture pH, composition and concentration of growth nutrients.

### 3.1.1 Culture Temperature

Microbial growth rate, and thus substrate utilization rate caused by the biological activities of microorganisms, as with all chemical reactions, are a function of temperature. It has been found that in nature microorganisms can grow at temperatures below 0 $^0C$ and above 93 $^0C$ — the primary requirement is for liquid water. According to their biological activities in different temperature ranges, bacteria can be classified into three groups, psychrophiles, mesophiles and thermophiles. There are three generalizations that can be made concerning the effect of temperature on growth rate as shown in Figure 3.9 [210].

First, growth only occurs over a 30 $^0C$ range for any group of microorganisms; second, growth rate increases slowly with raising temperature until the maximum growth rate is reached; and third, at temperatures above the maximum, growth rate falls rapidly. In general, the maximum growth rate of each group of microorganisms increases with temperature. It can be seen in Figure 3.9 that the maximum substrate utilization rates occur over a very narrow temperature range. Psychrophiles are able to grow at lower temperatures, but few of them are found in industrial practice due to their low biological activity, especially anaerobic microbes which have very low intrinsic growth rates. Thermophiles have attracted research interests recently in anaerobic treatment of wastewater because of their faster growth rates. Compared with mesophiles, however, they have two disadvantages, worse process stability and more energy is needed to maintain the

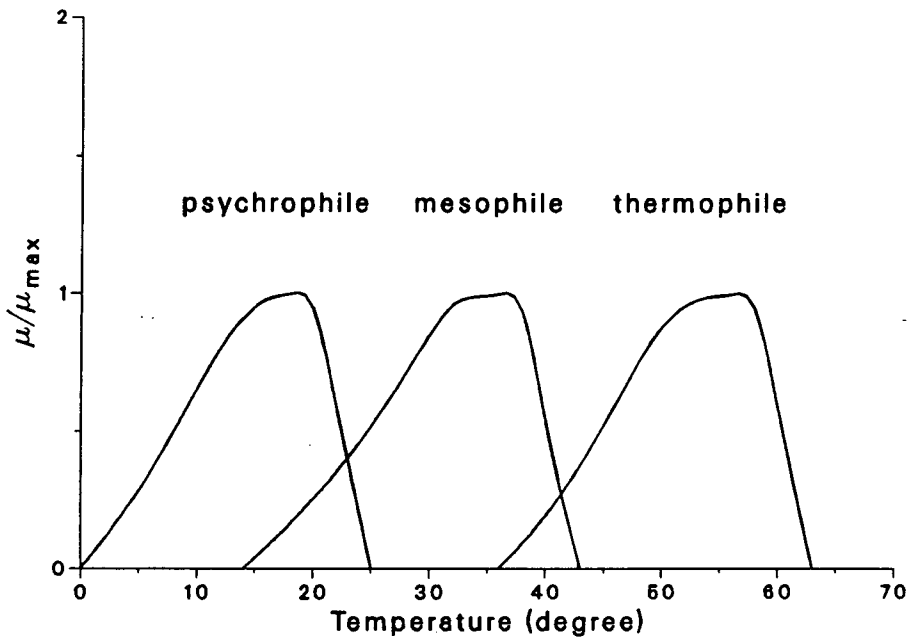


Figure 3.9: Illustration of temperature influence on growth rate of microbes.

culture at a higher temperature. Cheese whey, when it is discharged from the plant, has a temperature which is suitable for mesophilic bacterial growth and little or no energy is needed to heat the culture. Moreover, in the temperature range of 32–38 $^0C$, the mesophiles behave actively [144].

This study will adapt and use mesophilic bacteria at $35 \pm 2\ ^0C$ to investigate the fermentation kinetics, mass transfer of lactose and organic acids in biofilms and build-up of methanogenic biofilms.

### 3.1.2 Culture pH

The pH, a measure of the hydrogen ion ($H^+$) activity, is particularly important as a parameter of microbial growth. Most microorganisms grow over a pH range of 3–4 units; this represents a 1000 to 10000 fold range of hydrogen ion concentration. However, they have an optimum biological activity around pH 6.5–7.5.

The acidogens responsible for lactose fermentation grow in a quite wide pH range of 4–8. The studies conducted by Kisaalita et al [44] on the influence of culture pH on lactose acidogenesis revealed that the utilization rate of lactose was not significantly affected by pH in the pH range of 4–7 and the pH had a great influence on the distribution of the acids producted by the fermentation. A low pH value can not only depress the production of propionic acid which is the product most difficultly digested in the following methanogenic phase [145] but can also save caustic solution which is needed for maintaining the culture pH at a higher value due to the accumulation of acid products of lactose acidogenesis.

Although the methane-producing bacteria have been found in alkaline (pH 9.7) lake sediments [146] and in acidic peat (pH 3.6) [147] , the favorable pH range of methanogenic bacteria in a digester is narrow, 6–8, as proposed by Zehnder et al [148]. In their investigations on methane production from organic acids in immobilized cell bioreactors, Scharer and co-workers [114] found a narrower optimum pH range of 6.5–7.5 over which no significant differences in the rate of methane production occurred.

In this study, the pH value of lactose acidogenesis will be controlled at $4.6 \pm 0.2$ and the pH value for methanogenesis of organic acids at $7.1 \pm 0.2$ .

### 3.1.3 Growth Nutrients

In this study, the utilization of lactose and organic acids in anaerobic biofilms were investigated separately. Two types of medium were used which contained lactose or organic acids respectively. It is desirable that only the carbon source, lactose or organic acids, is the growth limiting component in the culture medium.

In addition to the carbon source, lactose or organic acids, the bacteria also need N, P, S, as well as trace elements for their growth. Ammonium is the preferred nitrogen source for methanogenic bacteria [149], although for one species of Methanobacterium it could be replaced by glutamine [150]. Nitrate is not a suitable nitrogen source for methanogens.

In addition, it increases the redox potential of the media and may result in overgrowth of enrichment cultures by nitrate-reducing bacteria. van den Berg and Lentz [151] found a suitable COD/N (or C/N) ratio to be 420/7 (or 158/7) and a good N/P ratio can be considered to be 7 [152]. Sulfide has often been used as both sulphur source and reducing agent since the redox potential of the media for methanogenesis should be reduced to Eh < -200 mv, but in high concentrations sulfide may inhibit growth [153]. Theoretically, it is believed that enrichment media must usually be free of sulfate because methanogens may otherwise be outcompeted by sulfate reducing bacteria at least for the most common substrates $H_2$ and acetate. However, assimilatory sulfate reduction was also described for methanogens by Daniels et al [154]. And the concentration of sulfide produced from the reduction of sulfate would not be high enough to inhibit bacterial growth. Sulfates of Mg, Fe, Zn and Cu added to the medium supply both the metal ions and sulphur.

For mixed cultures used for acidogenic and methanogenic bacteria, a ratio of C:N:P (158:7:1) was required for balanced biological growth [152,155,156]. But little work has been done on the growth requirements for single phase systems. Into the lactose acidogenesis medium having the same C:N:P ratio as mentioned above, Kisaalita [46] added, as growth nutrients for the acidogens, the same inorganic salts which were used by McCarty [157] and Speece et al [158] in their mixed cultures. Concentrations of calcium and sodium were kept at 100 – 200 mg/l while potassium and magnesium concentrations were at 200-250 mg/l. It was believed that under such concentrations of growth nutrients the carbon source (lactose) was the only growth limiting component. It would be expected that the inorganic salts which satisfy the growth requirements of mixed cultures of acidogenesis and methanogenesis should also supply enough nutrients to a separated culture, acidogenesis or methanogenesis. Table 3.9 lists the chemical components and their concentrations used in this study which are similar to those used by Kisaalita.

The concentrations of inorganic salts are based on a lactose concentration of 12 g/l

Table 3.9: Chemical components and concentrations in culture medium

| Component | Concentration (g/l) |
|---|---|
| Substrates | |
| Lactose | 12 |
| HAc : HPr : HBu | 6 : 3 : 3 |
| Macro elements | |
| $NH_4Cl$ | 0.42 |
| $(NH_4)_2HPO_4$ | 0.8 |
| $MgSO_4.7H_2O$ | 0.35 |
| KCl | 0.7 |
| $CaCl_2.2H_2O$ | 0.5 |
| Micro elements | |
| $Fe(NH_4)_2SO_4$ | 0.2 |
| $ZnSO_4.7H_2O$ | 0.005 |
| $MnCl_2.4H_2O$ | 0.005 |
| $CuSO_4.5H_2O$ | 0.002 |
| $NaB_4O_2.10H_2O$ | 0.002 |
| $NaMoO_4.2H_2O$ | 0.002 |

for lactose acidogenesis or a mixed solution of organic acids for organic acid methanogenesis where acetic acid is 6 g/l, propionic acid 3 g/l and butyric acid 3 g/l. If the substrate concentrations were changed, the concentrations of the nutrients were also adjusted correspondingly. No growth factors (vitamins, yeast extract etc.) were added to this chemically defined medium. All the chemicals were reagent grade and supplied by BDH unless otherwise indicated.

Table 3.10 summerizes the experimental conditions used in each type of fermentation.

## 3.2 Experimental Setups

Experimental setups include the general experimental setup, the configuration and operation properties of the reactor, and the biofilm supports used in three types of experiments.

Table 3.10: Comparison of experimental conditions for each phase

| Phase | Substrate | pH | Temp. | pH adj. soln. | experiments |
|---|---|---|---|---|---|
| Acidogenesis | Lactose | 4.6 | 35 $^0C$ | KOH+NaOH | kinetics |
| | | | | | mass transfer |
| Methanogenesis | HAc,HPr,HBu | 7.1 | 35 $^0C$ | HCl | kinetics |
| | | | | | mass transfer |
| | | | | | build-up of biofilms |

### 3.2.1 General Setup

A reactor and some auxiliary facilities are needed to keep the bacteria, acidogens or methanogens, in a defined environment and to investigate their biological behavior in the environment. Figure 3.10 illustrates the general setup which allowed the control of culture temperature, pH, feed, recycle rate etc. needed for this study.

Lactose (or salts of organic acids) was mixed with the inorganic nutrient solutions (see Table 3.9) and diluted to a desired concentration with tap water. The feed was stored in the feed tank and cooled to 1–4 $^0C$ by a refrigerated circulating bath (NESLAB). Nitrogen was bubbling through the feed to maintain a positive oxygen-free atmosphere in the tank, which is necessary for anaerobic microbes, especially for the strict anaerobic methanogens. A Masterflex pump (COLE PARMER) recycled the feed between the feed tank and the head tank, mixing the feed and maintaining a constant liquid head over the reactor to give a stable feed flow rate. The feed flow rates were controlled with a micro-valve and monitored with a rotameter at high flow rates or with a break tube at low flow rates by counting the feed drops over a period of time. The break tube also prevented contamination of the feed in the tanks by the microbes in the fermenter.

The desired pH values of the cultures were controlled by a pH/pump system (Cole Parmer Series 7142). As pH adjusting solutions, an equimolar KOH and NaOH solution

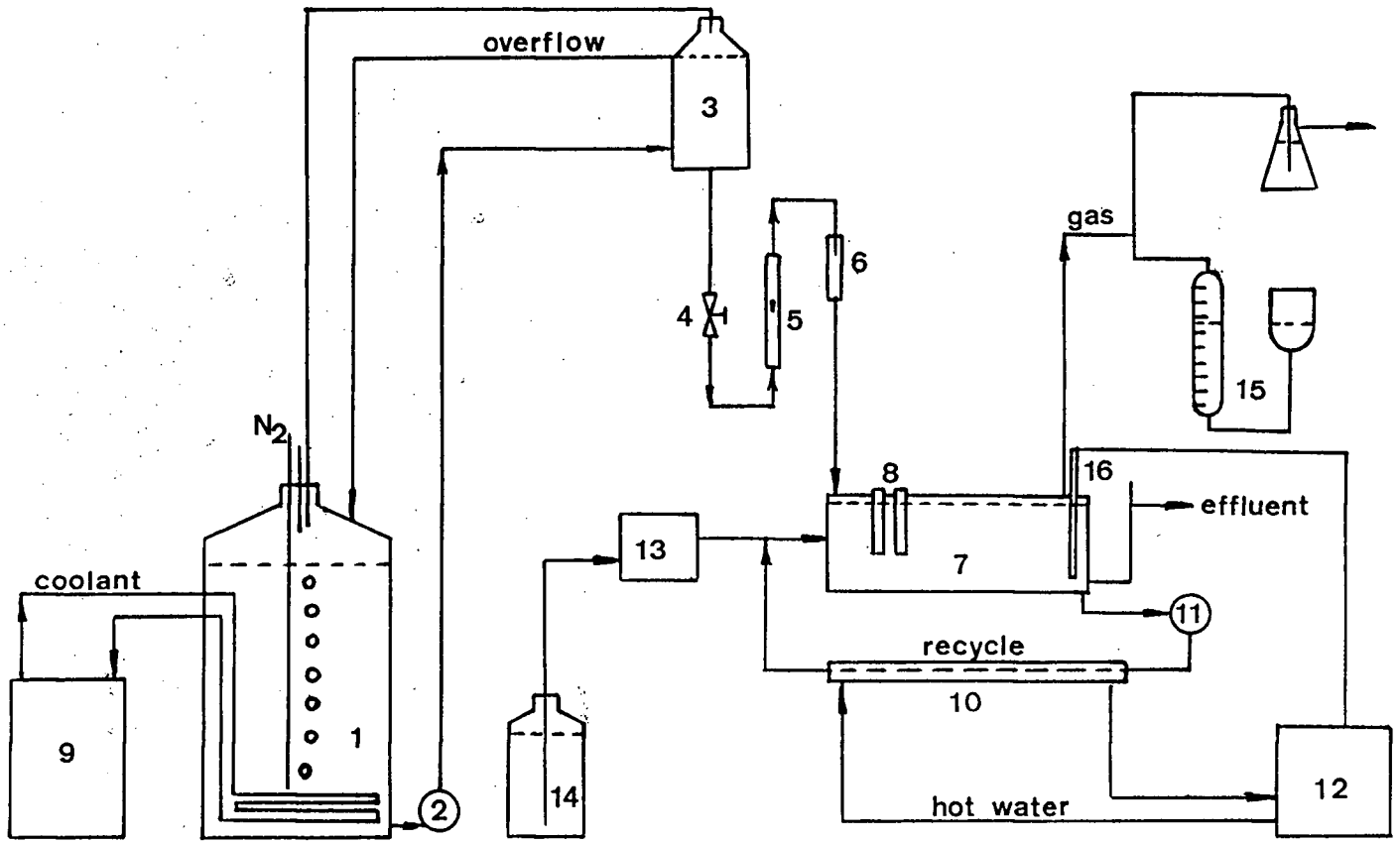


Figure 3.10: Illustration of general experimental setup. 1–feed tank, 2–pump, 3–head tank, 4–microvalve, 5–rotameter, 6–break tube, 7–reactor, 8–biofilm support, 9–refrigerated bath, 10–heat exchanger, 11–pump, 12–thermostat bath, 13–pH controller, 14–pH adjusting solution, 15–gas collector, 16–thermoregulator

(total concentrations 0.5–2 N) was used for lactose fermentation and a HCl solution (concentrations 0.3–1 N) for organic acids fermentation. The culture temperature was maintained at $35\pm2\ ^0C$ by heating the recycled culture medium with hot water from a ultra thermostat (COLORA). The temperature of the thermostat was in turn adjusted according to the culture temperature by the thermoregulator inserted in the reactor.

The production rates (volume/time) of gaseous products from lactose fermentation ($CO_2$, $H_2$ etc.) and from organic acids fermentation ($CH_4$, $CO_2$ etc.) were measured with the gas collector. The two liquid surfaces in the collector were kept at almost the same level when the gas was collected. A layer of oil was added on the liquid surface in the scaled tube to prevent the soluble gaseous components (e.g. $CO_2$) from absorbing into the water.

### 3.2.2 Reactor

For studies on anaerobic biofilms, the properties of biofilms must be known during the experiments. A common practice is to measure a biofilm on a removable support slide which is identical to the biofilm supports immersed in a reactor. Unlike investigations on aerobic biofilms where a reactor is open to air and a biofilm which is attached to a removable slide can be repeatedly measured, anaerobic biofilms on a slide can not be put back into the reactor after it has been exposed to the atmosphere for a long time. Therefore it is required that the reactor can hold enough sampling slides for multiple measurements. The reactor is made of a half Plexiglass tube as shown in Figure 3.11.

35 sampling ports could be arranged on the large surface area of the top and the curved bottom minimized the accumulation of bacterial sludge in the reactor. The removable slides were fixed in slots cut in rubber stoppers which in turn were fixed in the sampling ports in the reactor cover as shown in Figure 3.12.

Recycling the culture medium by a Masterflex pump (COLE PARMER) is another

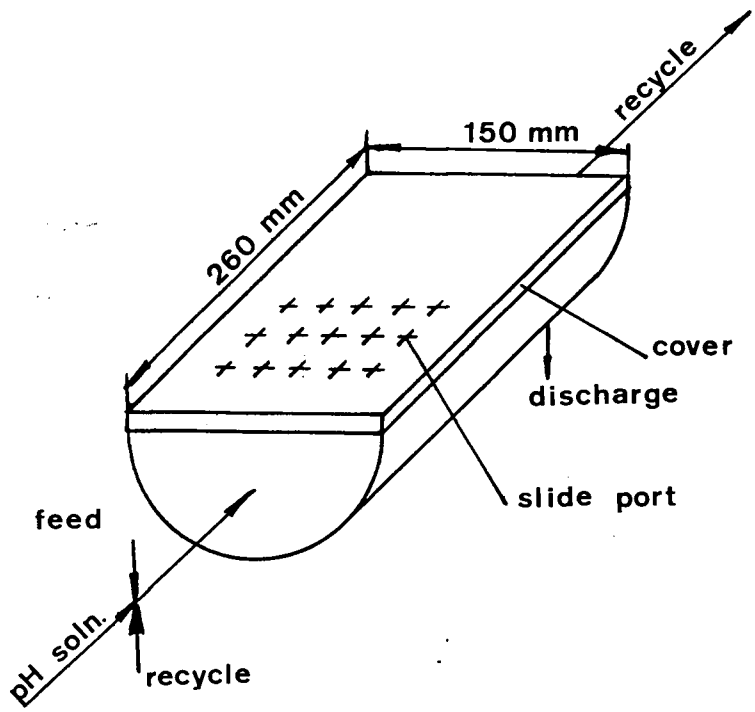


Figure 3.11: Illustration of reactor configuration

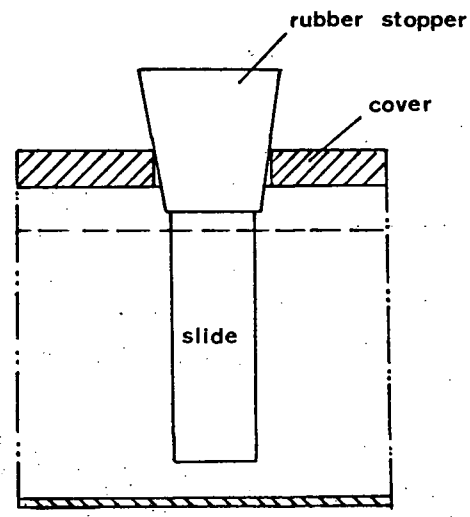


Figure 3.12: A removable sampling slide

significant characteristic of this reactor, which offers a means for controlling the culture temperature by heating the recycled medium. More importantly, it was possible to reduce and even eliminate the influence of external mass transfer on the substrate utilization rates by increasing the recycling rate, i.e. increasing the linear velocity over the biofilms without changing the feed rate. This is a critical requirement for the investigation of the intrinsic kinetics of substrate digestion in biofilms and will be explained in detail in following chapters which describe the experiments. Another important advantage of the recycle flow is that the reactor behavior approaches, and can be modelled as, a continuous stirred tank reactor (CSTR). For the ideal CSTR reactor model, the concentration of substrate (temperature etc.) in the reactor is uniform and is equal to the concentration in the effluent, which greatly reduces the complexity of modeling the reactor. Generally, when the ratio of recycle rate to the fresh feed rate is above 10, the reactor can be approximated as a CSTR. A pulse test was used to confirm this behavior. In a continuous completely mixed reactor, the concentration change of tracer in the effluent with the time after a pulse input of the tracer can be described as follows:

$$C = C_0 e^{-t/(V/F)} \tag{3.9}$$

where $C_0$ is the concentration at the beginning of measurement, $V$ the reactor volume and $F$ the constant flow rate. Equation 3.9 can be rewritten as,

$$-\log C = (V/F)(\log e)t - \log C_0 \tag{3.10}$$

HCl solution was used as the tracer in a flow of tap water and the pH change in the effluent should have a linear relationship with time if the reactor could be taken as a CSTR at a high enough recycle ratio.

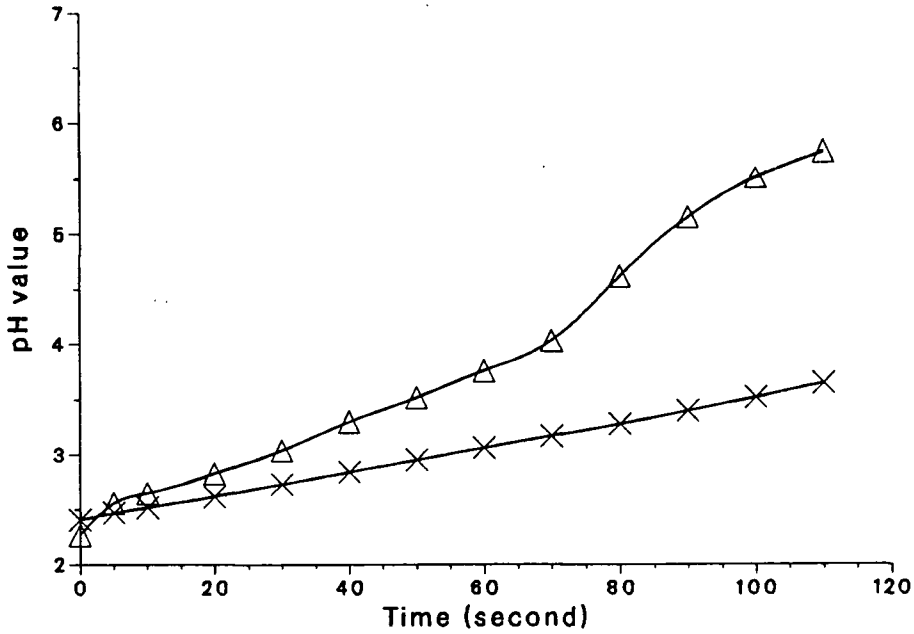


Figure 3.13: Effect of recycle ratio on reactor's behavior. △–recycle ratio 3.8, ×–recycle ratio 7.6

$$-\log[H^+] = (V/F)(\log e)t - \log[H^+]_0 \tag{3.11}$$

and,

$$pH = At - B \tag{3.12}$$

where $A$, $B$ are constants. At a fixed recycle rate, the flow rate of tap water was changed to test the influence of the recycle ratio on mixing behavior in the reactor. Figure 3.13 indicates that as long as the recycle ratio was kept above 8, the reactor behaved like a CSTR.

It was found in the kinetic tests (see Chapters 4 and 6) that the recycle rate had to be kept above 14 l/hr to minimize the effect of external mass transfer resistance on substrate utilization in biofilms, therefore, the feed flow rate had to be kept below 1.7

l/hr. This requirement was satisfied in all experiments.

## 3.3 Biofilm Supports

In addition to a controlled environment, the microbes must also be given a solid support on which to form biofilms, only then can the biofilms be investigated in detail; fermentation kinetics of substrates in biofilms, mass transfer in biofilms and build-up of biofilms. Each of these themes requires a special biofilm support because of its different focus. Three kinds of supports were designed and used in this study.

### 3.3.1 Supports for Kinetic Studies

The investigation of the intrinsic kinetics of lactose utilization in acidogenic biofilms or methanogenesis of organic acids in methanogenic biofilms needs as much biofilm as possible so that the biofilms contain most of the biomass in the reactor and the contribution from suspended microbes may be neglected. Intrinsic kinetic data can be obtained only after both the external and internal mass transfer resistance have been greatly reduced. Generally, the internal mass transfer resistance can be minimized by using a thin biofilm. Kennedy and Droste [159] used several materials as anaerobic biofilm supports, including needle-punched polyester, polyvinyl chloride sheet (PVC), glass and two types of clay, and found that PVC supported biofilms gave a relatively low methane production rate due to small mass of the biofilm (a thin biofilm) and this low methane production rate was stable and could last up to 80 days. Obviously, it is desirable for a thin biofilm to be able to last a long time during the experiments. The biofilm supports used in kinetic studies of lactose or organic acids fermentation, therefore, were made of PVC sheets as shown in Figure 3.14. The material has other advantages as well such as no physiological effect on the bacteria [43] and ease of fabrication. The total support surface had an area

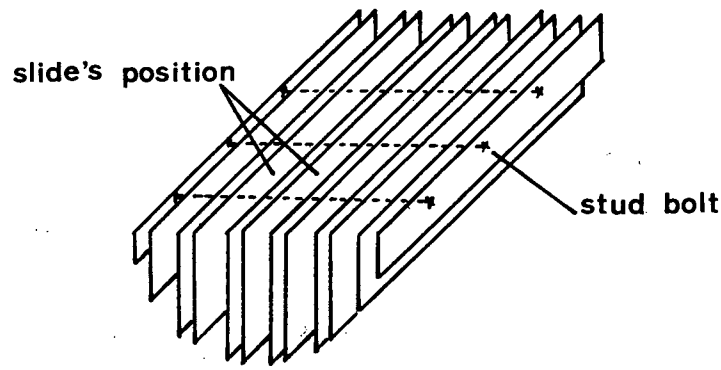


Figure 3.14: PVC biofilm support for kinetic studies of lactose or organic acids fermentation

of 1280 $cm^2$. The picture (Figure 3.15) shows a section of a thin and uniform biofilm on the PVC support as seen under a microscope (NIKON).

### 3.3.2 Supports for Mass Transfer Studies

In the investigation of substrate mass transfer in biofilms, attention was focussed on a part of a biofilm in the reactor and the measurement of substrate concentration difference on the two sides of the biofilm. The configuration of the biofilm support is shown in Figure 3.16. The reasons for this design will be given in Chapter 7 on mass transfer in biofilms.

Since it was made from a section of Plexiglass tube, the device had a symmetrical structure. On each side a nitrocellulose membrane filter, which has no biological effect on the bacterial growth, was sandwiched by rubber gaskets and fixed by two stainless steel flanges, forming a closed volume of 30 ml. The porosity of the filters (d=0.45 $\mu$m) kept the microbes (generally, d = 1 $\mu$m) from entering the device while the substrate molecules

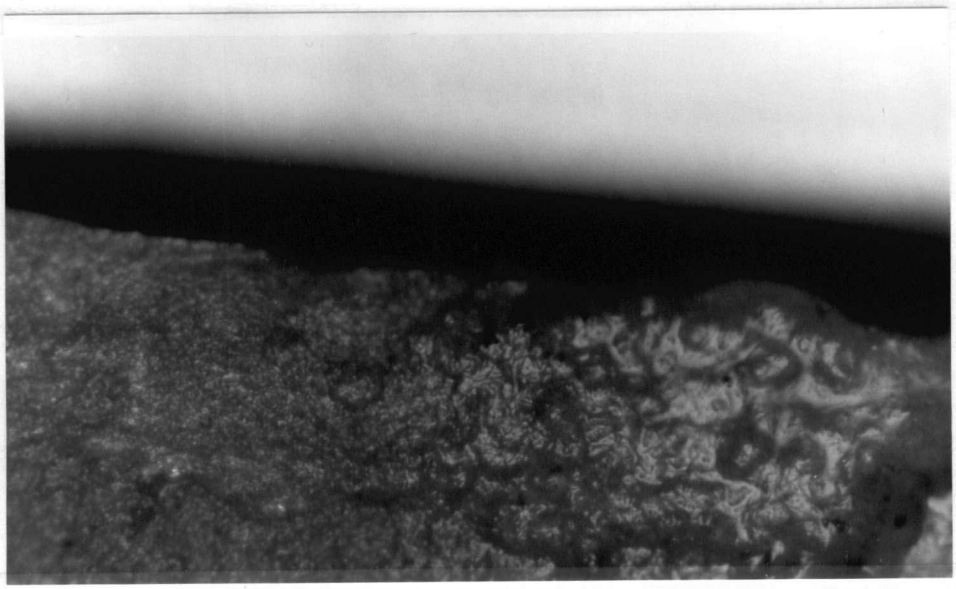

Figure 3.15: A thin biofilm (the black up-layer) on a PVC support, magnified by 100 times.

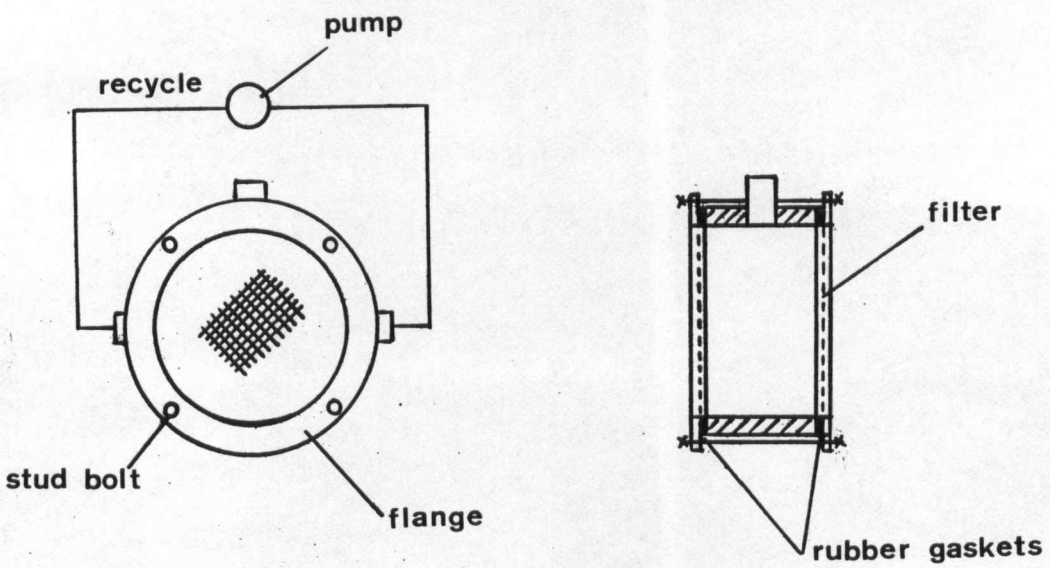


Figure 3.16: A biofilm support device for mass transfer studies of lactose or organic acids in biofilms

could enter it freely. When the device was immersed in a culture medium, some biofilm formed on its two membrane filters. A higher substrate concentration outside the device than inside the device caused a substrate transfer into the device by the mechanism of molecular diffusion through the biofilms and filters. The medium inside the device was recycled with a Masterflex pump (COLE PARMER) to promote establishment of a uniform concentration inside it. At steady state, the concentrations of substrates outside and inside the device were measured and used to estimate the mass transfer properties of the substrates within the biofilms. In order to avoid convective mass transfer through the biofilms, the pressure as well as the liquid levels outside and inside the cell were kept the same. The hole on the top of the cell was not only to maintain a zero pressure difference but also to eliminate any mechanical disturbance to the filters caused by the recycle.

### 3.3.3 Supports for Studies of Biofilm Start-up

Attachment and build-up of symbiotic methanogenic biofilms were investigated on 4 types of solid materials; wood, ceramic Rasching rings, PVC and stainless steel. These materials have a wide range of surface wettability as can be seen in Table 3.11 and also are widely used in industry. Except for the ceramic rings, which are often used as packing material in separation towers and reactors to give a large surface area, the other three materials have the same shape, like microscope slides, and so, they could be fixed on rubber stoppers as mentioned before. Suspending a ceramic ring in the culture medium as a removable support was done by hanging the ring on a hook which was made from a thin steel wire and fixed on a rubber stopper.

After the surfaces were immersed in a culture medium, the accumulation of biologically active materials on these inert solid supports was measured and used to follow the build-up of biofilms.

Table 3.11: Properties of biofilm supports for studies of biofilm formation

| Substratum | Size $mm \times mm \times mm$ | Water contact angle Degrees |
|---|---|---|
| Wood (fir) | $15 \times 35 \times 2$ | 0.0 |
| Ceramic ring | $(\phi 10 - \phi 6) \times 9$ | 56.6 |
| PVC | $15 \times 35 \times 1.5$ | 88.0 |
| Stainless steel | $15 \times 35 \times 1$ | 99.7 |

## 3.4 Experimental Analysis

Many samples were collected during the experiments for analysis. The samples can be classified into three groups; solid, liquid and gas, and hence different methods of analysis were needed, which are briefly described here while the details are given in Appendix B.

### 3.4.1 Solid Sample Analysis

Solid samples were taken of acidogenic or methanogenic biofilms. For the studies on substrate fermentation and mass transfer in anaerobic biofilms, the properties of the biofilms such as dry weight, total organic carbon content, density and thickness of the biofilms were needed.

- Dry weight of a biofilm sample:

  A sample of biofilm attached on a PVC slide as described in Figure 3.12 or taken from a support was dried at 70 $^0C$ to a constant weight. The low temperature was used to avoid any disturbance from the plastic material. After the dried biomass with the slide or in a container was weighed, it was dissolved away in distilled water which had been acidified with sulfuric acid to pH 1. The cleaned and dried slide or container was weighed again. The difference of two weights was taken as the dry weight of the biofilm sample.

- Total organic carbon of a biofilm sample:

  The total organic carbon of the dissolved biomass, the dry weight of which had been measured, was analyzed with a carbon analyzer (ASTRO). Thus, the total organic carbon content in the biofilm sample was known directly.

- Density of a biofilm:

  The density of a biofilm refers to the dry weight (or carbon content) of biomass in a unit volume of the biofilm. An intact biofilm was scraped from a support surface and put into a glass tube (d=6 mm), and then, was centrifuged at 4000 rpm to have a constant total volume (height) consisting of a solid volume at the bottom and a clean water volume above. After the total volume, $V$, was measured, the solid biomass was dried for dry weight ($W_d$) analysis and the TOC content ($W_{toc}$) of this biofilm sample was measured.

$$\rho_d = W_d/V \tag{3.13}$$

$$\rho_{toc} = W_{toc}/V \tag{3.14}$$

- Thickness of a biofilm:

  This measurement is crucial to the measurement of diffusion properties of substrates (lactose and organic acids) in biofilms. The total biomass attached on a membrane filter of the device as shown in Figure 7.65 was carefully scraped into a container and dried to measure the dry weight and TOC content. Based on the area of the filter from which the biomass was collected and the density of the biofilm, the

biofilm thickness could be estimated as following:

$$L = \frac{W_d}{\rho_d A} = \frac{W_{toc}}{\rho_{toc} A} \tag{3.15}$$

where

$W_d$ = total dry weight of a biofilm,

$\rho_d$ = biofilm density based on dry weight of biomass,

$W_{toc}$ = total organic carbon content of a biofilm,

$\rho_{toc}$ = biofilm density based on organic carbon content of biomass,

$A$ = filter area

Obviously, this thickness is an average value over the whole surface.

### 3.4.2 Liquid Sample Analysis

Liquid samples were collected in all three parts of the study (kinetics, mass transfer and biofilm build-up). Analysis of these samples was done with a spectrophotometer and a gas chromatograph (GC). The components analyzed by the spectrophotometer included lactose and lactate and those by the GC were acetic, propionic, butyric acids and ethanol.

- Lactose and lactate analysis:

  Lactose contains a reduced group which can give an orange-yellow color when treated with phenol and concentrated sulfuric acid. Lactate in a very diluted solution can be converted to acetaldehyde when heated in the presence of sulfuric acid. The acetaldehyde acting with p–hydroxydiphenyl gives a purple color. At a characteristic wave length, absorption of a monochromatic light is proportional to the color strength of a solution which is placed between the light source and a light receiver. The more lactose (lactate) in a sample solution, the stronger the color produced, and thus the more light that is absorbed. The concentration was

found from a standard curve which was obtained by analyzing several samples with known concentrations.

- Organic acids and ethanol analysis:

  The organic acids in their free form and ethanol are easily vaporized and can be analyzed with a GC (CARLE) equipped with a flame-ion detector (FID). The samples were acidified to below pH 2.5 with a $H_3PO_4$ solution since acetic acid, the strongest acid compound, is in free form below this pH value.

- Solid carbon content in a liquid sample:

  The solid carbon content in a liquid sample is needed to determine the mass of free microbes in the culture medium. Half the volume of a liquid sample was analyzed with a carbon analyzer to find the original carbon content of the sample. The rest of the sample was filtered through a membrane filter (d = 0.45 $\mu$m) to remove the suspended microbes in the medium, and then the total carbon content of the filtrate was measured under the same instrument conditions. The difference in total carbon content of these two parts reflected the free microbe content in the liquid sample.

### 3.4.3 Gaseous sample analysis

Gaseous samples were mainly collected during the studies of the methanogenesis of organic acids ($CH_4$, $CO_2$ etc.) while much less gas was produced from lactose acidogenesis ($CO_2$ etc.). The concentrations of the gas components are needed when a carbon balance around the reactor is made. Therefore, only methane and carbon dioxide were analyzed by using a GC (CARLE) equipped with a thermal conductivity detector (TCD).

# Chapter 4

## Intrinsic Kinetics of Lactose Utilization

Anaerobic digestion of lactose in a two-phase process consists of acidogenesis and methanogenesis which are carried out in series reactors. In the acids-forming reactor, lactose is utilized by acidogens with the main products of acetates, propionates and butyrates. Then, these intermediates are converted to methane and $CO_2$ by the methanogens in the following methanogenic reactor. This chapter describes the intrinsic kinetics of lactose utilization in acidogenic biofilms.

### 4.1 Experiments on Lactose Acidogenesis

The general experimental setup is as shown in Figure 3.10. The feed consisted of lactose as the limiting organic substrate and inorganic salts as the stimulating nutrients which are listed in Table 3.9. The lactose concentration of the feed ranged from 5 to 10 g/l in order to control its level in the fermenter with the experimental dilution rates used. This range of lactose and nutrient concentrations made lactose the only possible limiting substrate [46]. The methods used to keep the feed from fermenting in the storage tank include:

- Low temperature, the medium was maintained in 1 to 4 $^0C$ in the tank;
- Low oxygen partial pressure, nitrogen was slowly bubbled through the medium;
- Small amount of feed was stored at one time, enough for only 4 to 5 days operation.

The feed concentration was determined from the first and final day sample analyses during the storage of 4 to 5 days.

The fermenter had a working volume of 1,000 ml. The flow rate of feed, measured from the effluent collected over a period of time (3–8 hours), was controlled at above 150 ml/hr (D = 0.15 $hr^{-1}$) so that the suspended bacteria were washed from the reactor and this part of the biomass, compared with the fixed bacteria, could be neglected. Henze and Harremoes reviewed the literature on anaerobic processes and reported a maximum specific growth rate of acetic acid producing bacteria at 35 $^0C$ of 2 $day^{-1}$ (or D = 0.083 $hr^{-1}$) [144]. The carbon content of the solids in the effluent under these conditions was found to be negligible when the carbon contents of both the effluent and their filtrate from a membrane filter (d = 0.45$\mu$m) were analyzed and compared by using a TOC analyzer (ASTRO). This indicated that no significant amount of biomass was suspended in the reactor.

The pH of the culture was controlled at 4.6±0.2 with 0.5 to 2 N equimolar NaOH and KOH solutions. The caustic concentration was adjusted on the basis of lactose utilization rates to produce a negligible influence on the dilution rates. The inoculum was obtained from the first phase reactor of a two-phase mini-plant which had been fed with cheese whey for two years.

The experiment can be divided into four stages.

1. Adaptation; The fermenter was filled with a diluted lactose solution (2 g/l) and $N_2$ was continuously introduced to strip the dissolved oxygen. When the temperature reached 35 $^0C$, the fermenter was seeded (200 ml inoculum) and then operated in batch mode. After lactose had been used up, < 0.01 g/l, half the volume of the culture (500 ml) was replaced by fresh feed (4 g/l lactose) and this was repeated five times.

2. Build-up of biofilm; The operation, then, was shifted to continuous mode while the flow rate was controlled at less than 50 ml/hr to prevent the suspended bacteria from washout. It was observed that a white slimy biofilm gradually started to form on the grey PVC supports.

3. Steady state operation; After the build-up of biofilms, the flow rate was gradually increased to greater than 150 ml/hr. The temperature was maintained at 35 $^0C$, and the pH of the medium at 4.6. To investigate the influence of lactose concentration on the rates of lactose utilization and organic acid production, the lactose concentration in the reactor was controlled by adjusting either the feed flow rate (residence time) or the feed concentration, sometimes both of them. These two control modes had the same effect in a reactor in which the bacteria were immobilized. A dynamic response caused by a change in flow rate is described and discussed in Section 4.5. At each desired concentration level, a steady state during which there was no significant lactose concentration change ($< 10$ %) in the effluent, was maintained more than 2 days to collect experimental data. The concentration was adjusted from a low to a high level , and after a set of desired levels had been investigated, the tests on the same set of levels were repeated. Since the biofilm thickness increased with time, the lactose utilization rate at each of the concentration levels was obtained with acidogenic biofilms having different thickness. Therefore, by comparing the data, the influence of internal mass transfer resistance on lactose digestion rate could be estimated.

4. Influence of pH change; After the kinetic experiments had been completed, the culture pH was gradually increased from 4.6 to 6.5 while the flowrate and temperature were maintained at 220 ml/hr and 35 $^0$C, respectively.

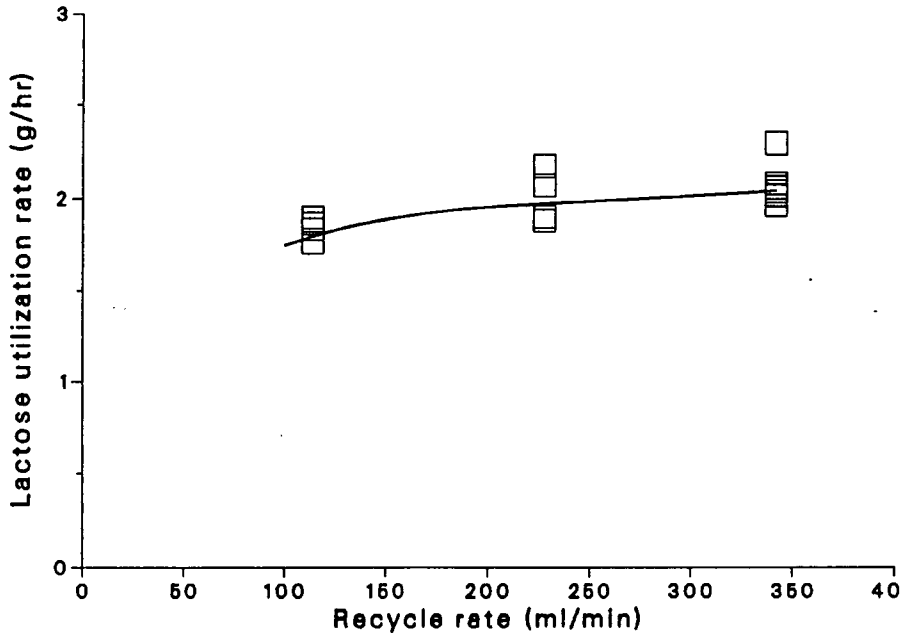


Figure 4.17: External mass transfer resistance on lactose utilization in biofilms is tested by changing recycle rate.

Before the intrinsic kinetic data could be collected, the influence of external mass transfer was tested by varying the recycle rate. Figure 4.17 shows that the lactose utilization rate would not be affected by the external mass transfer resistance as long as the recycle rate was kept above 228 ml/min, corresponding to a linear velocity over the biofilm of 3.3 cm/min.

The influence of internal mass transfer is often reduced by using a thin biofilm which is available in the early stage of biofilm development. To extend the experimental time during which the effect of internal mass transfer resistance could be minimized even though the biofilms were getting thicker, the experiments were arranged in such a way that the concentration levels were adjusted from low to high for a test recycle. At higher bulk concentrations the internal concentrations were also relatively high, which would give all the bacterial cells embedded in a thick biofilm the maximum utilization rate,

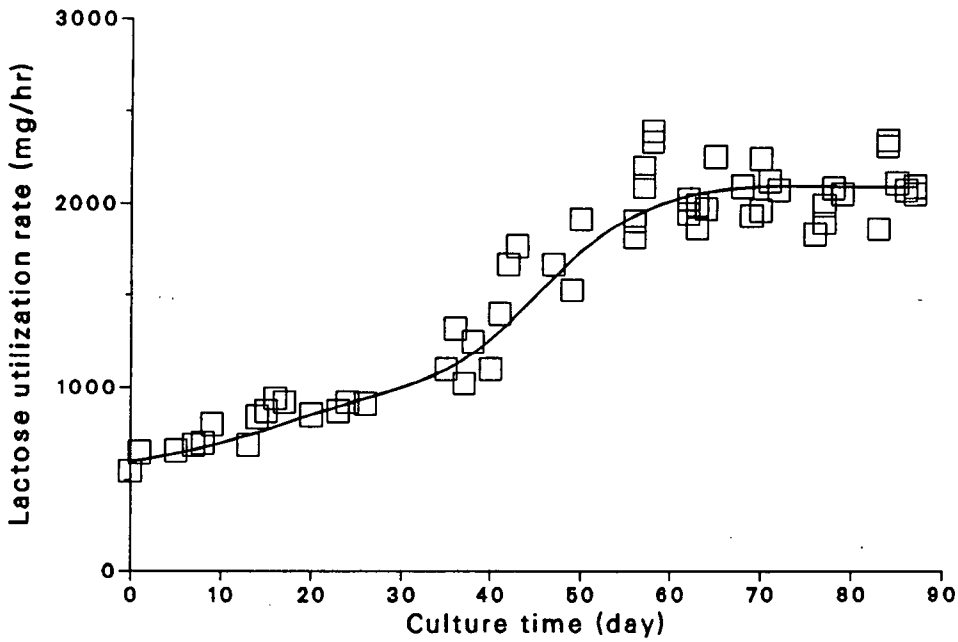


Figure 4.18: Lactose digestion rate of whole reactor changes with time

thereby, the influence of concentration distribution could be reduced.

Figure 4.18 indicates that the lactose digestion rate based on the whole reactor gradually increased and then leveled off because of the gradually thickening biofilm, which means that more bacteria saw lower substrate concentration. Since the experiments were repeated at several concentration levels from low to high, it can be assumed that the kinetic data obtained on days 0 to 55 were not markedly affected by the internal mass transfer resistance. This becomes clear if the lactose digestion rates based on unit weight of biomass (mgCarbon) are plotted versus biofilm thickness (Figure 4.19).

The experimental conditions are summarized in the Table 4.12.

## 4.2 Development of an Acidogenic Biofilm

As discussed in the previous chapters, the presence of solid supports helps the retention of biomass in a reactor, and so the total amount of biomass in the reactor will increase

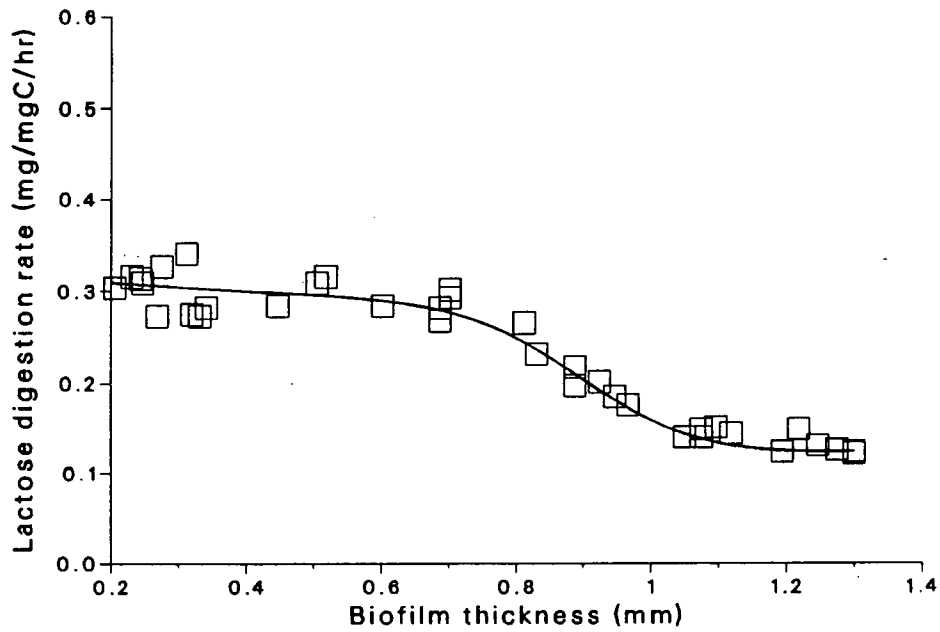


Figure 4.19: Specific lactose digestion rate changes with biofilm thickness

Table 4.12: Experimental conditions of lactose acidogenesis

| Parameter | Condition |
|---|---|
| Temperature | $35 \pm 2\ ^0C$ |
| pH | $4.6 \pm 0.2$ |
| Lactose feed | 5–10 g/l |
| Flow rate | $> 150$ ml/hr (2.5 ml/min) |
| Dilution rate | $> 0.15\ hr^{-1}$ |
| Biomass | acidogens |
| Recycle rate | $> 230$ ml/min |

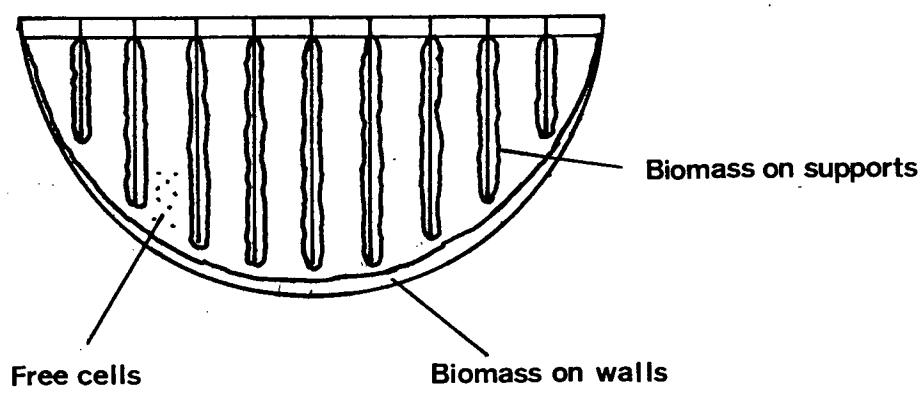


Figure 4.20: Biomass distribution in the fermenter

slowly with the digestion of substrates. To estimate the lactose utilization rate based on unit mass of biomass, it is essential to know the total mass of biomass retained in the reactor during the experimental time. Three types of biomass existed in the reactor as shown in Figure 4.20;

- suspended bacteria,
- attached bacteria on the supports,
- sludge.

The suspended bacteria, compared with the fixed ones, were negligible as mentioned above. The biomass in the biofilms was the major part of the total biomass retained in the fermenter, and measured during the experiments by analyzing the biomass on the removable slides at given time intervals. The time when the first kinetic data were

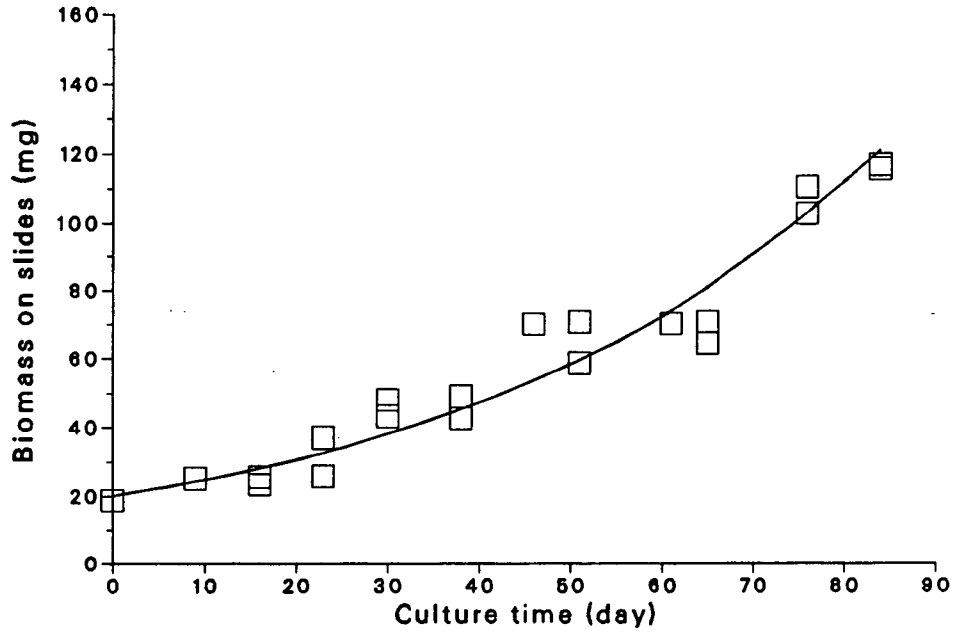


Figure 4.21: Biomass on removable slides increases with time

collected was recorded as zero time, and then, after each time interval (5 to 8 days) one or two slides which had been immersed at different positions in the reactor were removed and analyzed. It was found that the two slides immersed at different positions in the reactor had very close biomass accumulations and hence, the distribution of biofilms was quite uniform in the fermenter. Figure 4.21 shows that the biomass on the slides increased gradually with time.

The carbon content and the dry biomass weight had a very good linear relationship as shown in Figure 4.22 and the slope was 0.382, which means that the dry biomass of the biofilm contained 38.2 per cent organic carbon. In general, the carbon content in a single cell ranges from 45 to 50 percent. The decrease in carbon content of the biofilm is probably due to the considerable amount of inorganic salts trapped in the films. Turakhia and Characklis [161] reported that a major portion of calcium was immobilized in the extracellular components of the biofilm matrix.

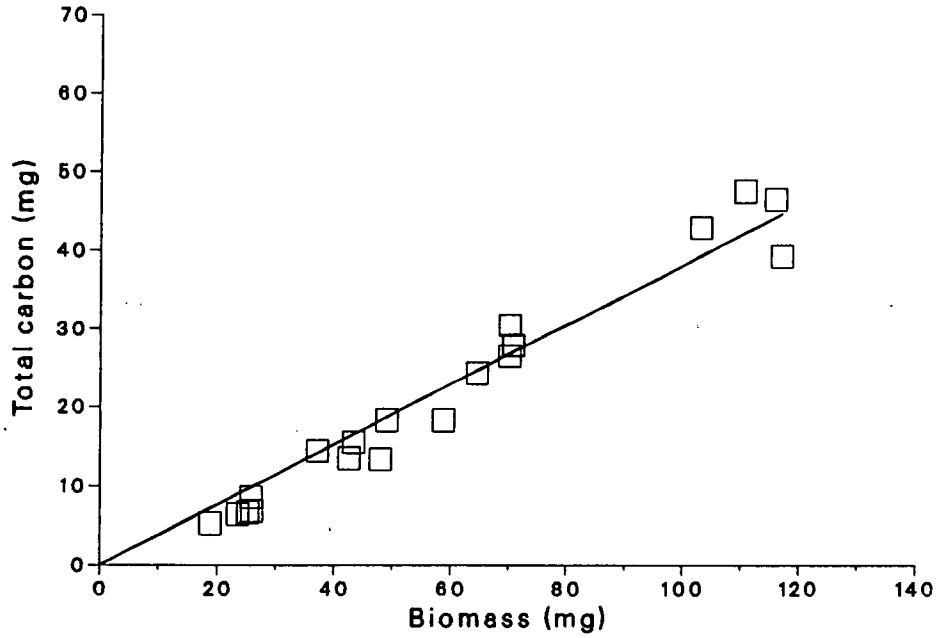


Figure 4.22: Carbon content in the biomass

The total carbon (TC) content of biofilms retained in the fermenter was obtained by multiplying the carbon content on a slide by the area ratio of the total supports to the slide, and its development with time is shown in Figure 4.23.

A good correlation of total carbon with time is given by an exponential expression as follows and shown in Figure 4.23.

$$TC = 5.697e^{0.0259t}A/a = 1813.8e^{0.0259t} \tag{4.16}$$

Where '$t$' was the time, '$A$' the total support area and '$a$' the slide area. An exponential function was used since in a thin biofilm the bacteria could get enough food from the environment and so grow exponentially.

The biomass deposited on the reactor walls was estimated based on three assumptions. Firstly, the experimental period was in the early stage of biofilm development and so no significant sloughing occurred because sloughing is believed to be due to lack of nutrients

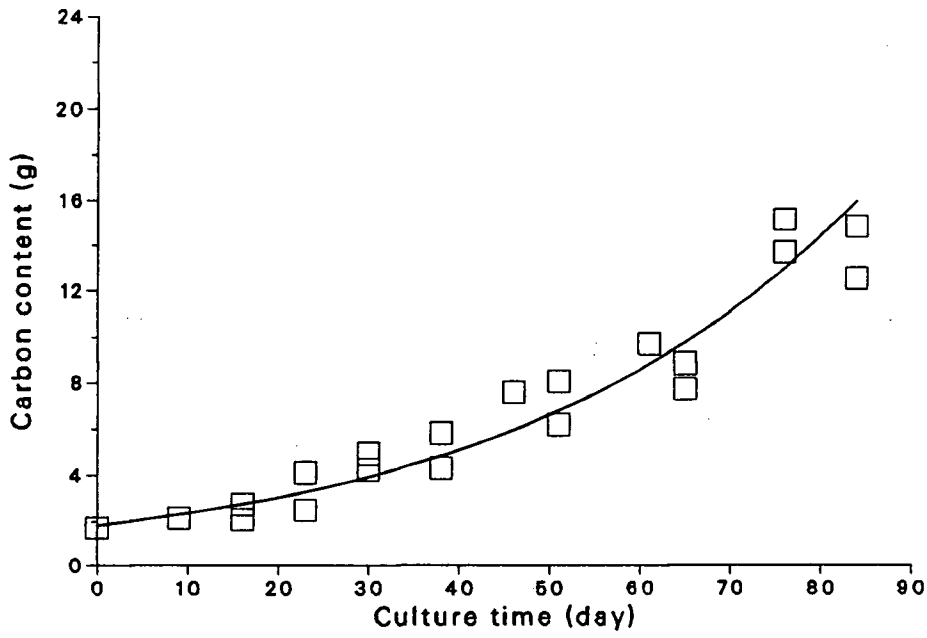


Figure 4.23: Total carbon content developed on the supports. The line was calculated from Equation 4.16

in a thick biofilm [160]. Secondly, the biomass detached by fluid stress was continuously washed out by the high dilution rates. Hence, the sludge was attributed to the biofilm formed on the reactor walls. Finally, this part of the biofilm had the same growth rate as that on the supports. Experimentally, before the first kinetic data were collected, all the sludge which formed in the first two stages of adaptation and biofilm start-up as mentioned above were removed by discharging the medium in the reactor. At the end of experiments the biomass on the reactor wall was collected and measured. It contained only 1.5 g of carbon compared with 15.0 grams in the biomass on the supports. Including this part of biomass Equation 4.16 becomes

$$TC = (1813.8 + 175)e^{0.0259t} \tag{4.17}$$

This correlation predicted the final biomass in the reactor at 86 days within 7 percent.

## 4.3 Utilization Rate of Lactose

The lactose concentration in the fermenter, which the bacteria actually saw, was the same as that in the effluent since the reactor was operated in a completely mixed mode. At a steady state, the amount of lactose in the reactor was balanced as following;

$$\text{Flow in} = \text{Flow out} + \text{Consumption due to reaction}$$

that is,

$$FS_{in} = FS_{out} + Wr \tag{4.18}$$

or,

$$r = F(S_{in} - S_{out})/W \tag{4.19}$$

Where $r$ is the lactose utilization rate based on unit weight of carbon content (mgC) of biomass (mg S/mgC/hr), $F$ the feed flow rate (ml/hr), $S_{in}$ and $S_{out}$ the lactose concentrations in the feed and the effluent respectively (mg/ml), $W$ is the total amount of biomass carbon content retained in the reactor at that time and is estimated from Equation 4.17. The right side of Equation 4.19 can be experimentally measured and thus, the lactose utilization rate, $r$, at the lactose concentration of $S_{out}$ can be found.

Figure 4.24 indicates that the lactose digestion rate at various lactose concentrations can be correlated very well with the lactose concentration by a Michaelis-Menten type equation as

$$r = \frac{r_{max} S}{K_s + S} \tag{4.20}$$

For a non-linear model like Equation 4.20, it is better in general to estimate the parameters ($r_{max}$, $K_s$) by using a direct search method since the fit errors of the model with the experimental data are not then affected by the methods used to linearize the

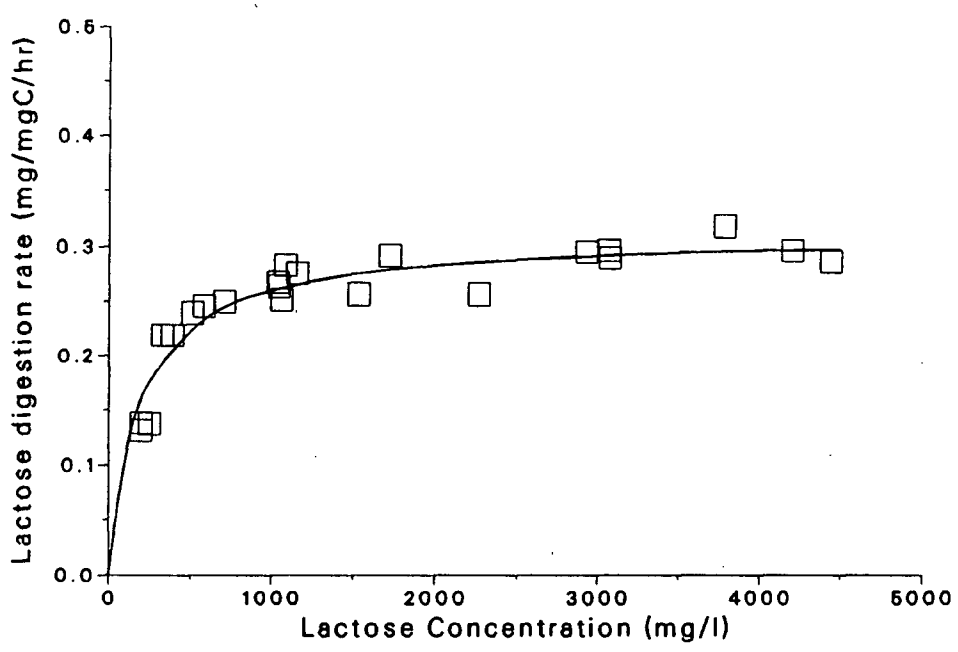


Figure 4.24: Effect of lactose concentration on lactose digestion rate. The line is calculated from Equation 4.20

model. However, a direct search method is very sensitive to the selection of the initial search points which often give local optimal points. Therefore, many more calculations are needed by a direct search method to determine a 'real' optimal point from many initial search points. In the present work, if an initial point could be estimated by linearizing a non-linear model, the direct search, then, was started from that initial point to get a set of optimal parameters. Otherwise, the parameters could only be determined by searching from various initial points.

The initial estimation of the two parameters in Equation 4.20, $r_{max}$ and $K_s$, was made by a linear least-square method after a transformation of Equation 4.20 to,

$$\frac{S}{r} = \frac{K_s}{r_{max}} + \frac{S}{r_{max}} \tag{4.21}$$

and then, a direct search (see Appendix G) was carried out to optimize the fit of Equation 4.20 to the experimental data. The results were

$$r_{max} = 0.3144 \qquad \text{mg lactose/mgC/hr}$$

$$K_s = 201 \qquad \text{mg lactose/l.}$$

To compare these data with the literature data which are summarized in Table 4.13, the units were converted to kgCOD/kgVSS/hr and kgCOD/$m^3$, respectively, assuming 1 kg lactose equivalent to 1.067 kg COD for complete oxidation of lactose and 1 kg biomass carbon equivalent to 2.61 kg VSS.

$$C_{12}H_{22}O_{11} + 12O_2 \longrightarrow 12CO_2 + 11H_2O$$

Compared with Kisaalita's data, the second set in Table 4.13 which were obtained in suspended cultures, the maximum lactose utilization rate was much lower and the half velocity constant higher. Kisaalita noticed that bacteria attached and grew on the walls of his reactor and auxiliary internal parts and this might have caused errors if the fixed biomass had not been included, especially under high dilution rates with fewer free cells [46].

Another possible reason was that the immobilized bacteiral cells excreted more extracellular polymers than the free cells. Therefore, the lactose utilization rate based on unit weight of immobilized biomass (carbon or suspended solids) was lower than that based on unit weight of free cells.

The difference may also be attributed to the fact that immobilization of bacteria has a large influence on the substrate digestion rate. It has been found that, in nature where the substrate concentration was relatively low, attached bacteria are often more active than free cells due to the concentrating function of the supports [167,168,169]. In a fermenter where substrate level is quite high, however, this kind of concentrating function plays no significant role. Very recently, Van Loosdrecht and coworkers [170] reviewed the

Table 4.13: Maximum lactose digestion rate and half velocity concentration

| $r_{max}$ kgCOD/kgVSS/hr | $K_s$ kgCOD/m$^3$ | Temp/pH $^0C$ | Culture/Substrate | Reference |
|---|---|---|---|---|
| 2.63 | $\rightarrow 0$ | 30/6 | suspended anaerobic /glucose | [145] |
| 2.28 | 0.022 | 35/4.5 | suspended anaerobic /lactose | [46] |
| 2.14 | 0.37 | 35/6.6-7.3 | mixed anaerobic /glucose | [162] |
| 1.52 | 0.0053-0.008 | 35/6 | suspended anaerobic /lactose | [46] |
| 0.564 | 18.3 | 35/6.6-7.3 | mixed anaerobic /sewage sludge | [162] |
| 0.545 | 30.9 | 35/6.6-7.3 | mixed anaerobic /cellulose | [162] |
| 0.395 | 37 | 36/5.8 | mixed anaerobic /activated sludge | [26] |
| 0.313 | 0.192 | 35/7.0 | theoretical model /glucose | [163] |
| 0.145 | 0.214 | 35/4.5 | fixed anaerobic /lactose | This study |
| $> 0.103$ | | 38/5.6-7.2 | anaerobic sludge /dextrose, tryptone | [164] |
| 0.0917 | 2.0 | 35/6.3-8.1 | fixed films /dextrose, protein | [165] |
| 0.0417 | 0.15 | 35/6.3-8.1 | fixed films /dextrose | [165] |
| 0.0367 | 0.25 | 20-35/$> 6$ | anaerobic filter /starch | [166] |

literature on the influence of immobilization on the bacterial activity and concluded that so far neither experimental nor theoretical evidence exists that immobilization of cells directly affects their metabolism.

For the phenomena of decreased substrate utilization, growth rate, assimilation etc. in a community of immobilized bacteria, various explanations existed such as less cell surface available for substrate uptake [171,172], higher maintenance coefficient [172], substrate transport limitation [173], and desorption limitation [174,175]. Around fixed cells quite a lot of extracellular polysaccharides have been found under the microscope, which connects the cells forming a network of channels as described in Chapter 2 while on free cells there is less extracellular polysaccharides (only a thin capsule if any). Therefore, the mass transfer from outside to inside of cells, which is a part of intrinsic kinetic process, has more resistance due to the extra polysaccharides on the cell wall which is excreted by the bacteria during the immobilization of the free cells. Moreover, part of a cell surface may be unavailable for the mass transfer due to very close proximity between some cells.

On the basis of activity measurements on attached and free living *Vibriosp.*, Jeffrey and Paul [171] suggested that not only the maximum substrate consumption rate but also the apparent substrate affinity of attached cells are different from suspended cells. A decrease in substrate affinity or an increase in the half saturation constant, $K_s$, for adhered cells has often been reported [173,176,177]. According to Bright and Fletcher [176], there are two possible explanations: (1) the difference is due to changes in the environment of the cell, or (2) the higher $K_s$ values for surface-associated cells is a reflection of a real difference in assimilation behavior.

Independent experimental evidence that the results of the present study are more reliable can be obtained from the experimental data of lactose transport through active acidogenic biofilms (see Chapter 7). By using Kisaalita's kinetic data and assuming that the diffusivity of lactose in free solution is its effective diffusivity within the biofilms, the

lactose concentration found from the reaction-diffusion model very quickly dropped to less than $10^{-3}$ at a biofilm thickness 0.5 mm while the measured lactose concentration was about 50 mg/l at a biofilm thickness 1.3 mm (Table 7.26). If Kisaalita's kinetic data and the measured lactose concentrations on the two sides of a biofilm were used to estimate the effective diffusivity of lactose in the biofilm, the lactose effective diffusivity was found to be in a range of 15 to 25 times higher than its value in free solution. However, the estimated lactose diffusivity by the kinetic data of the present study was quite reasonable, $De/D < 1$.

## 4.4 Production of Organic Acids

At the same time the lactose digestion rate was measured, the products were also analyzed and measured. The detectable products included acetate, propionate, butyrate, ethanol and lactate, the major ones being acetate and butyrate (see Appendix C). Some organic acids with carbon number more than 4 ($C_6$, $C_8$) were also detected in transient processes (change in dilution rate, feed concentration etc. ), but at steady state they disappeared. Table 4.14 lists the reactions of lactose being converted to those products and their standard free energy. Although the standard free energy of the reaction for butyrate formation is the least, butyrates were produced in large amounts in this experiment. This must have been affected by the experimental conditions.

A carbon balance on conversion of lactose to these products ranged from 52.1 to 67.7 percent as shown in Appendix C, a reasonable range considering the fact that the carbon converted to $CO_2$ and to biomass had not been included in the balance. If carbon leaving the reactor in gaseous bubbles, or dissolved in the effluent was estimated according to the reactions in Table 4.14 (e.g. 1 mole of acetate accompanied with 1 mole of $HCO_3^-$), the carbon balance was between 85 and 102 percent.

Table 4.14: Reactions of Lactose Conversion

| Reactions | $\Delta G^0$ (kJ) |
|---|---|
| $C_{12}H_{22}O_{11} + 9H_2O \rightarrow 4CH_3COO^- + 4HCO_3^- + 8H^+ + 8H_2$ | -412.6 |
| $C_{12}H_{22}O_{11} + 4H_2 \rightarrow 4CH_3CH_2COO^- + 3H_2O + 4H^+$ | -716.2 |
| $C_{12}H_{22}O_{11} + 5H_2O \rightarrow 2CH_3CH_2CH_2COO^- + 4HCO_3^- + 6H^+ + 4H_2$ | -50.92 |
| $C_{12}H_{22}O_{11} + 5H_2O \rightarrow 4C_2H_5OH + 4HCO_3^- + 4H^+$ | -451.8 |
| $C_{12}H_{22}O_{11} + H_2O \rightarrow 4CH_3CHOHCOO^- + 4H^+$ | -396.6 |

Source is [156].

Similar to the utilization of lactose, each of the products was balanced around the reactor at a steady state.

Produced from the reactions + Flow in = Flow out

The 'flow in' amount was zero because no digestion of lactose occurred in the feed tank under the measures mentioned before. So, for the ith component, at steady state,

Production rate = Flow out

that is,

$$r_i W = FC_i \tag{4.22}$$

or,

$$r_i = FC_i/W \tag{4.23}$$

Where $r_i$ is the production rate of the ith component based on the unit weight of carbon content of biomass (mg i/mgC/hr), $F$ the feed flow rate (ml/hr), $C_i$ the concentration of the component in the effluent (mg i/l) and $W$ the total amount of biomass carbon content within the reactor at that time. The right side of Equation 4.23 can be calculated from the experimental data of $F$, $C_i$ and $W$, and thus the production rate of the ith product can be found.

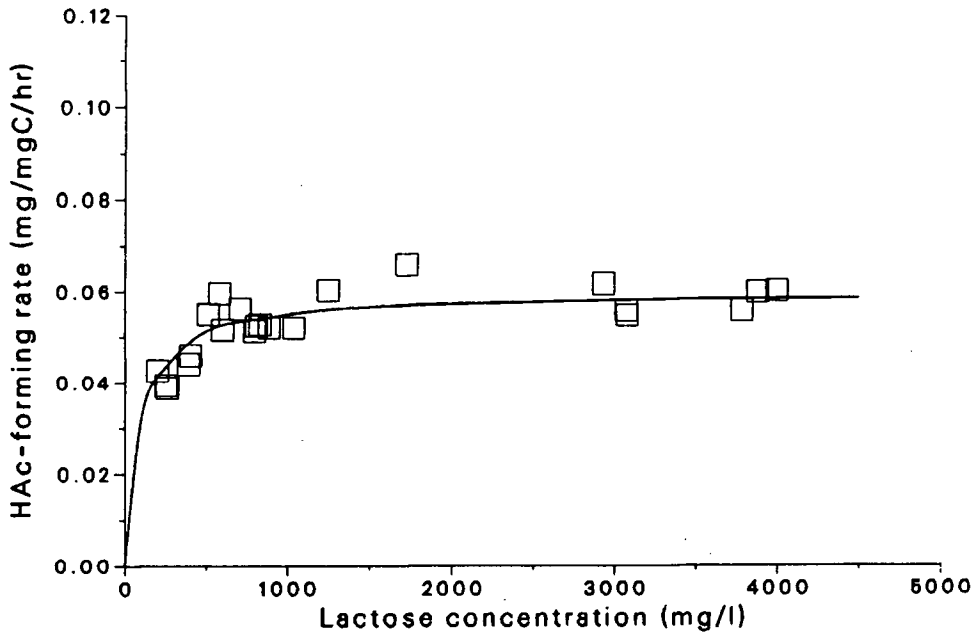


Figure 4.25: Influence of lactose concentration on acetate production rate. The line is calculated from Equation 4.24 and the parameter values in Table 4.15

As discussed in Chapter 2, lactose fermentation proceeds via the Embden-Meyerhof pathway and pyruvate is the key intermediate from which other products are formed. The rates of these parallel reactions were dependent on the concentration of pyruvate and thus lactose concentration. The dependence of the production rate of each product on lactose concentration is shown in Figures 4.25,4.26,4.27, 4.28,4.29.

The products can be divided into two groups according to the pattern of influence of lactose concentration on their production rates; acetate, butyrate and ethanol one group (Figures 4.25, 4.26, 4.27), lactate and propionate another (Figures 4.28, 4.29). The first group can be described with a Michaelis-Menten type equation;

$$r_i = \frac{r_{max,i} S}{K_{s,i} + S} \tag{4.24}$$

Where $r_{max,i}$ is the maximum production rate of the ith component (acetate, butyrate and

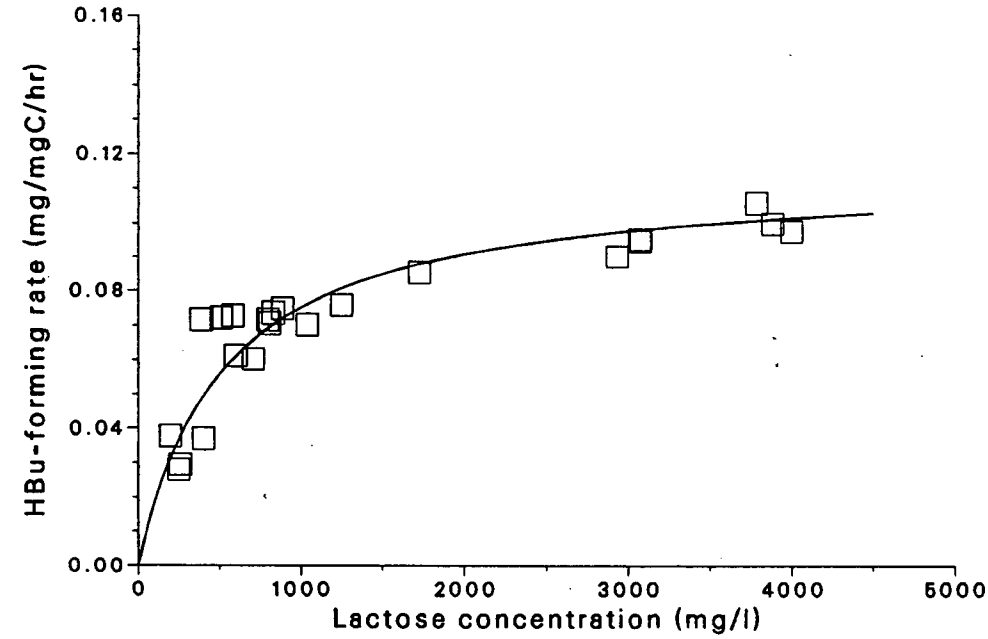


Figure 4.26: Influence of lactose concentration on butyrate production rate. The line is calculated from Equation 4.24 and the parameter values in Table 4.15

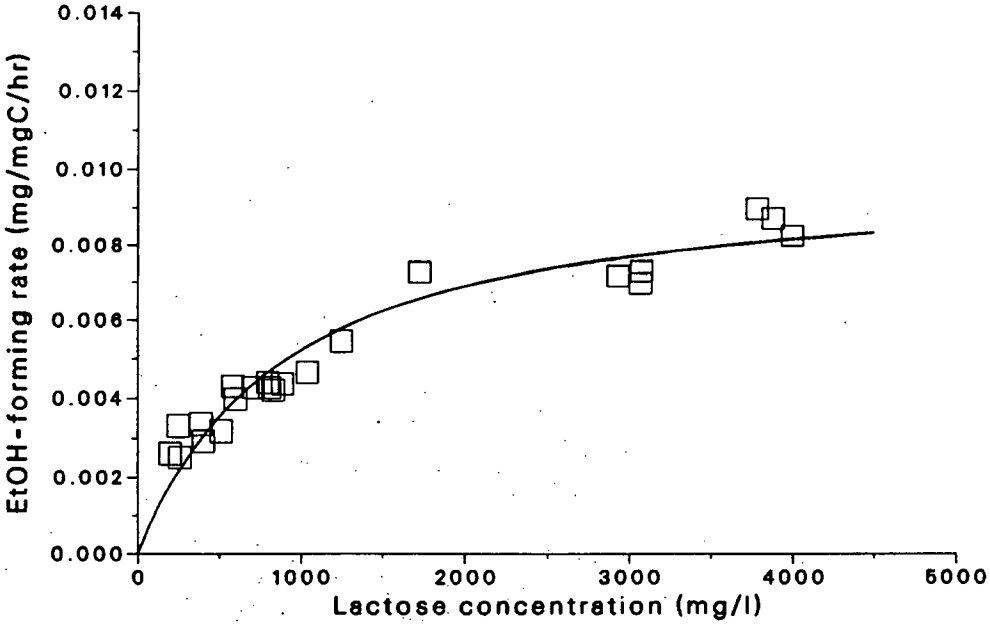


Figure 4.27: Influence of lactose concentration on ethanol production rate. The line is calculated from Equation 4.24 and the parameter values in Table 4.15

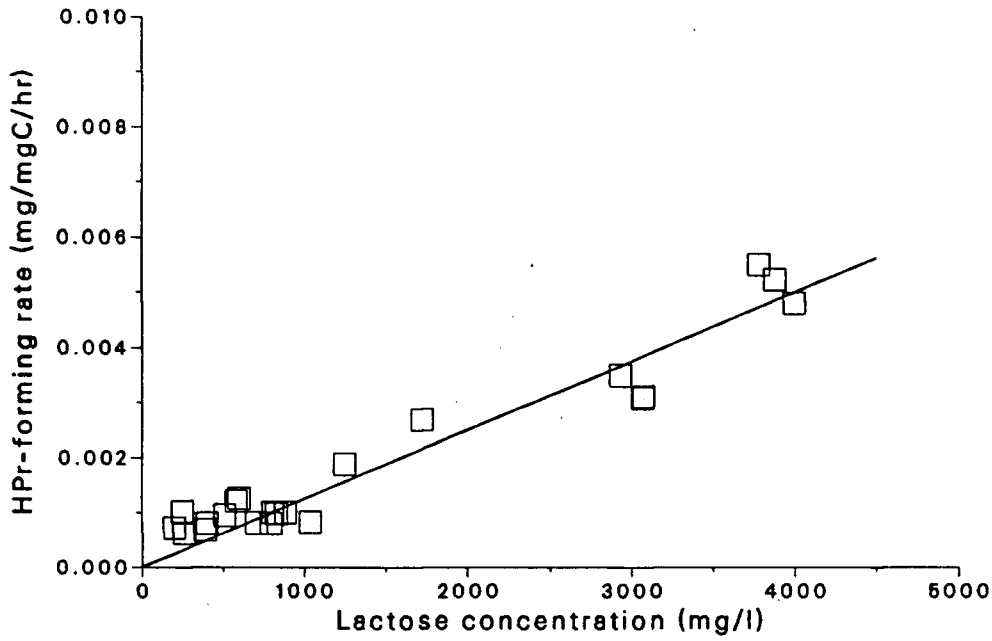


Figure 4.28: Influence of lactose concentration on propionate production rate. The line is calculated from Equation 4.25 and the parameter value in Table 4.15

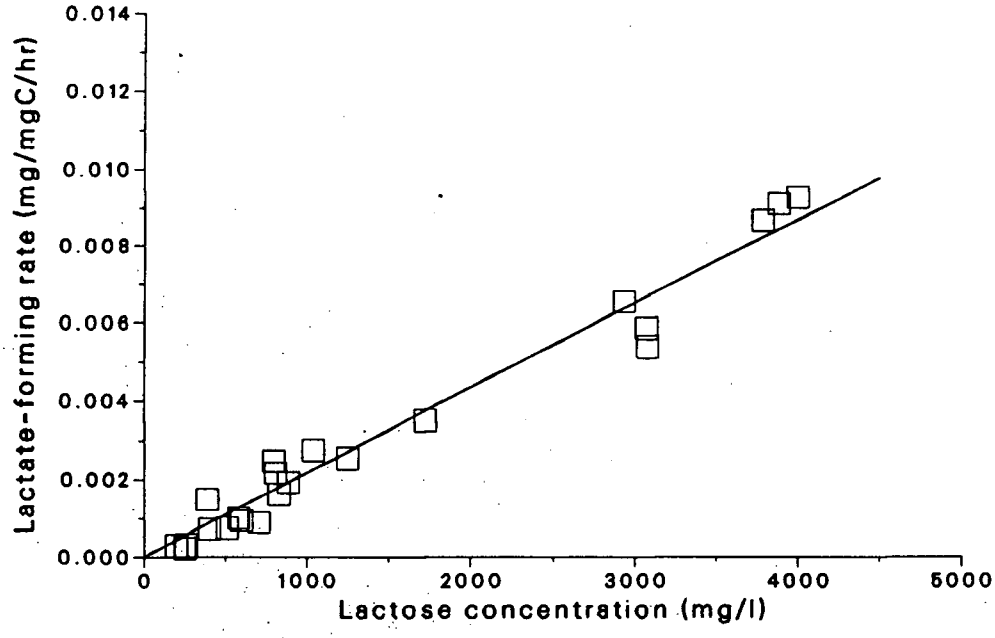


Figure 4.29: Influence of lactose concentration on lactate production rate. The line is calculated from Equation 4.25 and the parameter value in Table 4.15

Table 4.15: Rate parameters of the products in lactose fermentation

| | $r_{max,i}$ (mg i/mgC/hr) | $K_{s,i}$ (mg s/l) | $k_i$ $\frac{mgi/mgC/hr}{mgs/l}10^{-6}$ | F test | $F_{0.95}$ |
|---|---|---|---|---|---|
| Acetate | 0.0599 | 89 | | 3129 | 2.1 |
| Butyrate | 0.115 | 532 | | 1246 | 2.1 |
| Ethanol | 0.0101 | 929 | | 556 | 2.1 |
| Lactate | | | 2.18 | 1383 | 2.1 |
| Propionate | | | 1.25 | 705 | 2.1 |

ethanol) (mg i/mgC/hr), $S$ the lactose concentration (mg/l) and $K_{s,i}$ the half velocity concentration (mg/l). The two parameters, $r_{max,i}$ and $K_{s,i}$, were estimated with the same method as for lactose utilization rate, i.e. by a linear least-square method after a transformation of Equation 4.24 to a linear expression like Equation 4.21, and then by the direct search method to optimize the fit of Equation 4.24 to the experimental data. The estimated values of parameters are listed in Table 4.15

The production rates of the second group, including propionate and lactate, has a linear relationship with the lactose concentration.

$$r_i = k_i S \tag{4.25}$$

Where $k_i$ is the specific reaction rate (mg i/mgC/hr)$(mg/l)^{-1}$ which is the production rate when lactose concentration is 1 mg/l. The estimated values of $k_i$ are also listed in Table 4.15. The statistical tests (F test) indicate that the influence of lactose concentration is significant on the yield rates of these 5 products.

Cohen and co-workers [178] investigated acidogenesis of glucose in a suspended culture and found that propionate and butyrate were formed by at least two different species, and thus two types of fermentation occurred under different environments:

- butyrate type fermentation; production of mainly butyrate, acetate, $CO_2$, $H_2$ and

low Eh values,

- propionate type fermentation; mainly propionate and acetate, minor amounts of valerate, low or no gas production consisting solely of $CO_2$, relatively high Eh values.

Under the present experimental conditions as summarized in Table 4.12, the butyrate type fermentation predominated.

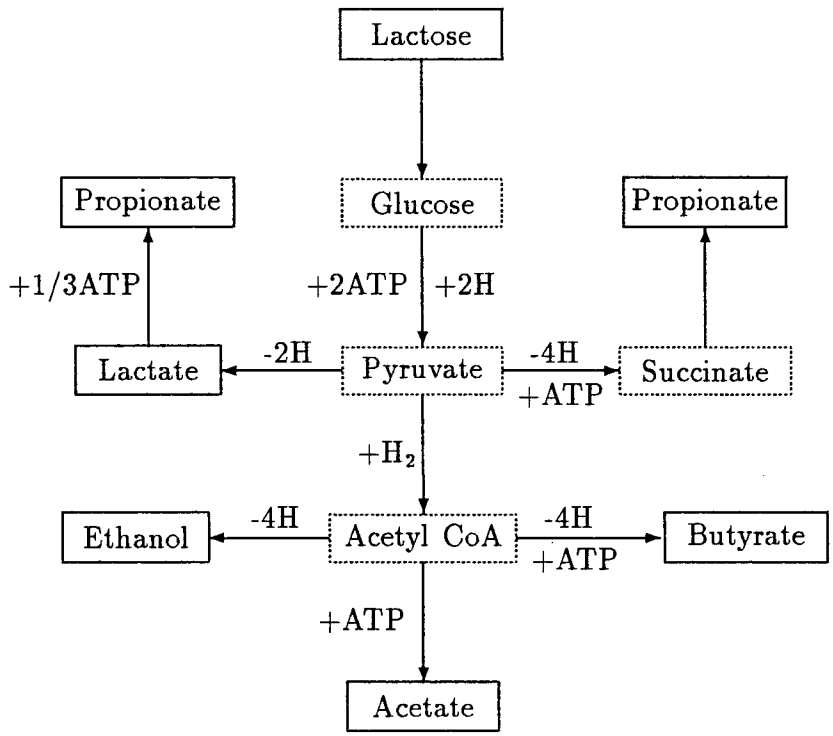


Figure 4.30: Pathways of acidogenesis of lactose. Sign (-) refers to consumption, and (+) refers to production. The intermediates are in dash boxes and products in solid boxes.

Many reaction pathways are known which lead to a great variety of fermentation products for carbohydrate anaerobic digestion as reviewed in Chapter 2. Figure 4.30 gives a simple relationship between the substrate and the products as well as production of ATP and transfer of electrons/hydrogen by which the reduced co-enzyme, NAD, can be reoxidized.

The possibility of producing various products is especially high in a mixed culture because the presence of so many bacterial species offers the potential to induce a great variety of enzymes which are needed for various reactions. It is well known that heterotrophic bacteria degrade carbohydrate for energy and carbon which are necessary for their reproduction and life maintenance. The energy released from the chemical bonds of the substrate is stored in ATP, an energy-rich molecule. The more ATP a reaction pathway can yield, the more likely it is that it would predominate. The fact that only butyrate and acetate were the main products under the present conditions implied that their formation could give more energy to the bacteria than could the other pathways.

Thauer and co-workers [179] have extensively reviewed energy conservation in chemotrophic anaerobic bacteria. It seems that, in many anaerobic bacteria, the amount of ATP formed per mole of energy supplying substrate can be regulated, thus, permitting the organism to optimize the thermodynamic efficiency of energy transformation.

The formation of lactate can only give 4 moles of ATP per mole of lactose utilized, because no energy is available from the conversion of pyruvate to lactate even though it accepts the electrons/hydrogen produced. Conversion of pyruvate, however, to acetyl-CoA, the primary energy-rich intermediate, can offer more ATP, which is obtained during its further conversion to butyrate and acetate, and so the bacteria prefer the butyrate type fermentation. Furthermore, acetate, butyrate and ethanol have the same precursor, acetyl-CoA. That may be why they have the same type of production rate equation since acetyl-CoA is formed from pyruvate via pyruvate:ferredoxin oxidoreductase or pyruvate

formate lyase [179]. As with the formation of lactate, no extra ATP is produced during acetyl-CoA conversion to ethanol, and thus, the amount of ethanol, as a minor product, had the same level as lactate in the fermenter (Figures 4.27 4.29).

8 moles of ATP are produced per mole of lactose utilized via the pathway to acetate, 6 moles ATP to butyrate and 4 moles ATP to ethanol. The preference of bacteria on these pathways are also reflected in their affinity coefficients or half velocity concentrations, $K_{s,i}$. The first choice was the pathway to acetate ($K_s$ = 89 mg/l) and then to butyrate ($K_s$ = 532 mg/l) and finally to ethanol ($K_s$ = 929 mg/l).

There are two pathways for propionate formation; in the acrylate pathway lactate is reduced stepwise to propionate, in the succinate-propionate pathway pyruvate is converted to propionate via succinate [180]. The present experimental conditions may have been unfavorable to the bacterial species so that the necessary enzymes could not be induced to convert pyruvate to propionate via the succinate pathway even though the formation of propionate in this way also offers an extra production of ATP. In the next section it will be shown that changes in the environment had an effect on the production of propionate.

The thermodynamic efficiency of energy transfer from substrate to products explains why acetate and butyrate were the major products of lactose acidogenesis under the present conditions. It cannot, however, explain why the bacteria could not convert lactose solely to acetate which gives more ATP than do conversions to other products. The energy required for the synthesis of ATP from ADP and Pi is generally provided by reduction-oxidation (Redox) process. Anaerobic energy metabolism is often intramolecular, that is, electron-donating and electron-accepting steps are not only linked by the electron carrier (NAD) but also by the electron acceptor, which must be formed as a product from the substrate. During the formation of pyruvate from lactose the dehydrogenase required NAD as an electron/hydrogen acceptor and its reduced form, NADH, must be reoxidized

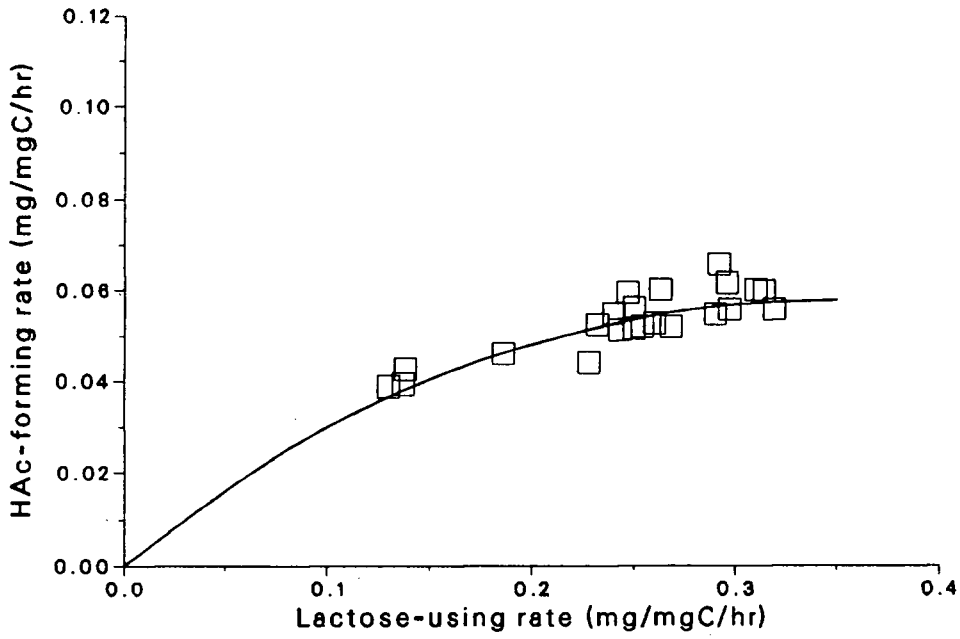


Figure 4.31: Production rate of acetate versus digestion rate of lactose

to NAD for the next redox cycle, otherwise digestion of lactose could not be carried on. In the acidogenic phase, the reoxidation of NADH is conducted by transferring the electron/H from NADH to products of fermentation.

Among the 5 products, only the formation of acetate cannot accept the electron from NADH. So, the bacteria must find other ways to compensate this enzyme cofactor. This may be the major reason why the formation of acetate remained constant with increase in the amount of lactose digested by unit weight of bacteria in one hour as shown in Figure 4.31, because the amount of NAD is a constant in unit weight of bacteria while conversion to acetate can not reoxidize the reduced NAD. However, formation of other products could transfer electrons from NADH to themselves, and thus, as shown in Figures 4.32, 4.34, 4.33, 4.35, their production rates increased dramatically with increase in lactose digestion rate on unit weight of biomass.

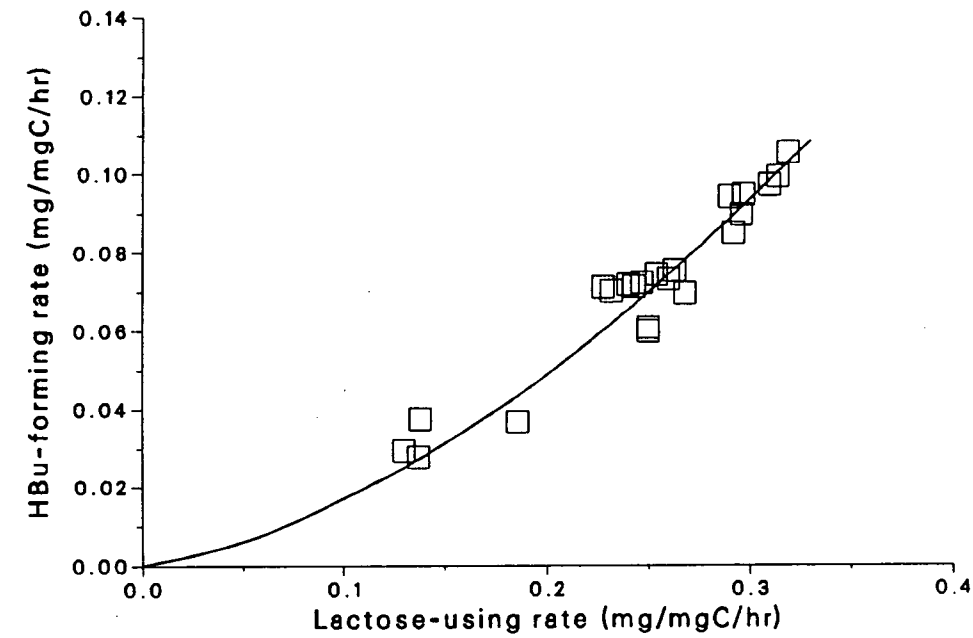


Figure 4.32: Production rate of butyrate versus digestion rate of lactose

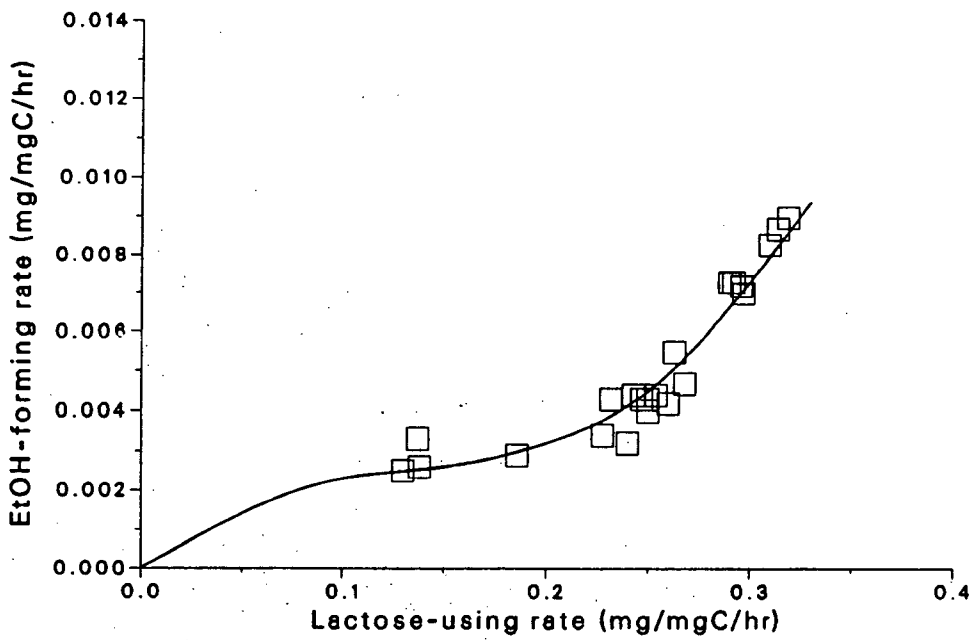


Figure 4.33: Production rate of ethanol versus digestion rate of lactose

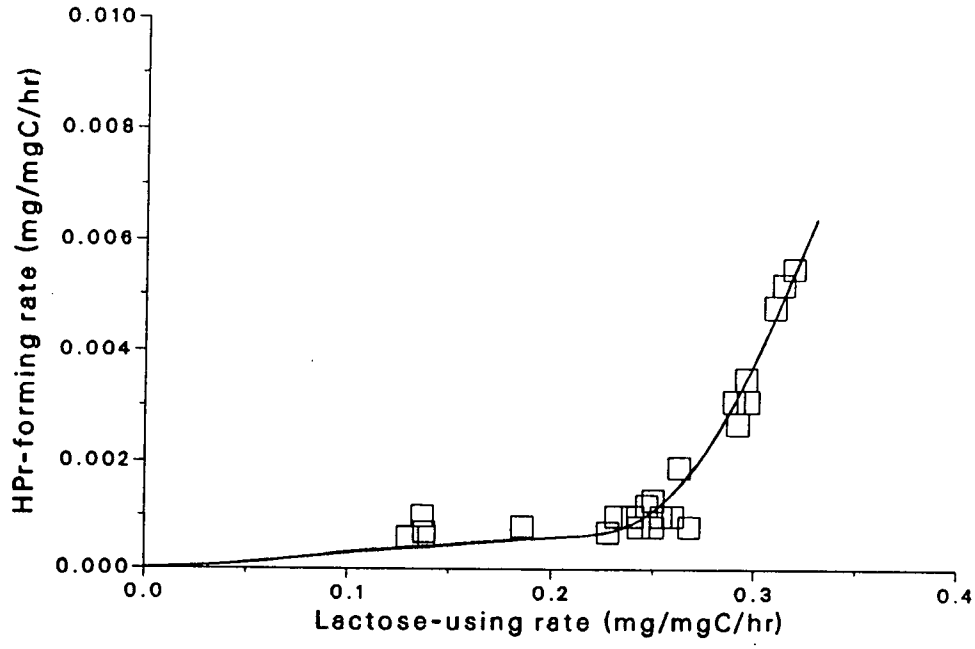


Figure 4.34: Production rate of propionate versus digestion rate of lactose

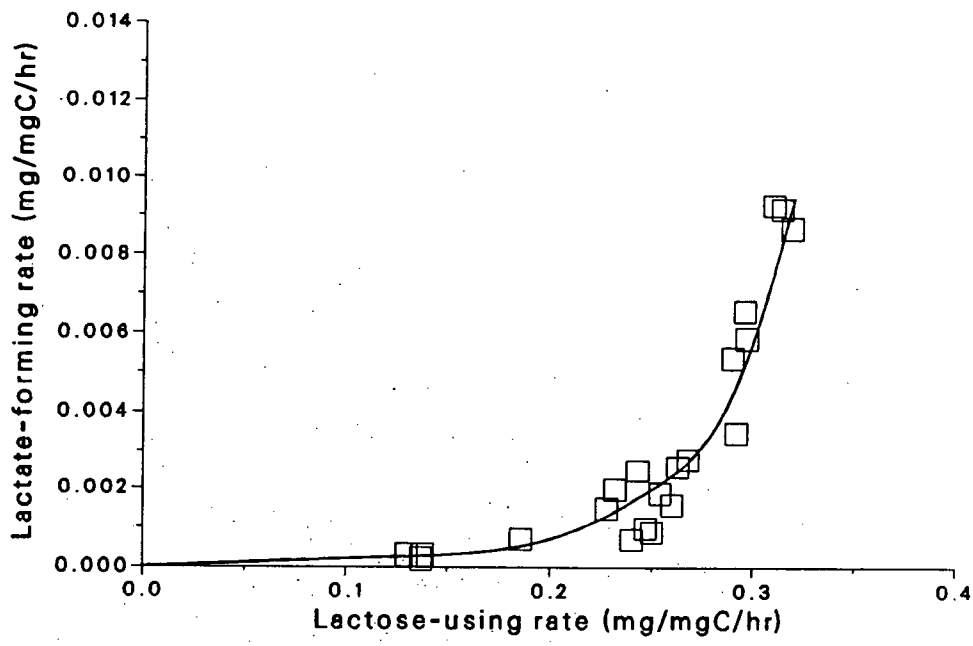


Figure 4.35: Production rate of lactate versus digestion rate of lactose

Table 4.16: Comparison of production rates of organic acids at two pH levels

| | Relative production rate | | | |
|---|---|---|---|---|
| pH | Acetate | Propionate | Butyrate | Lactate |
| 4.6 | 1 | 1 | 1 | 1 |
| 6.6 | 1.08 | 17.16 | 1.15 | 0.97 |

## 4.5 Responses of Acidogenic Biofilms to Disturbances

Immobilized bacterial communities are quite stable. A change in pH of the culture medium from 4.6 to 5.1 did not affect the lactose utilization rate nor its product distribution. However, when the pH of the culture medium jumped up to 6.5 and stayed at this level, it affected not only the product distribution but also the biofilm itself. The amount of biofilm attached on the support was reduced from a density of 4.1 $mgC/cm^2$ to 2.4 $mgC/cm^2$ and it was observed that the biomass on the bottom of the reactor increased and a lot of foam was produced on the medium surface. So, a dramatic change in pH could make the environment very unfavorable to some bacterial species. Unlike a suspended culture where a bacterial species will be washed out quickly if its growth rate is less than the dilution rate, these bacteria are trapped in the biofilm so that their death and lysis caused the biofilm thinning and the medium foaming. The change in the pH of culture medium gradually affected the distribution of the bacterial species and/or their fermentation mechanism, which was reflected in the change of the yield rates of organic acids, especially propionate formation. Table 4.16 compares the production rates of acetic, propionic, butyric and lactic acids at two pH levels, where the production rates at the pH of 4.6 are taken as one unit for the ease of comparison.

It is clear that the propionate production rate was increased considerably. Its concentration in the reactor effluent jumped from about 30 mg/l to 450 mg/l. This proves that low pH depresses the formation of propionate which is generally the least desirable

fermentative product for the following methane-producing bacteria.

An acidogenic reactor even under normal operation can become unstable because of load changes which are caused by fluctuations in feed concentration and/or flow rate. For a fixed film reactor these two factors produce the same results, a change in substrate concentration, because of negligible washout of cells. Figure 4.36 shows the response of the biofilm reactor after a change in flow rate, from 120 ml/hr to 280 ml/hr. The input concentration of lactose was constant at 5500 (mg/l). At the first steady state (flow rate 120 ml/hr), lactose was almost completely digested (100 mg/l) with very low lactate concentration (10–20 mg/l). The flow rate jump resulted in an increase in lactose and lactate concentrations in the fermenter. After reaching a peak value where its conversion was only about 24 per cent, the lactose concentration returned to a new low steady value (400 mg/l) corresponding to the new flow rate. In parallel, the lactate concentration returned to a new steady value (20 mg/l), too. This response may be due to some kind of temporary physiological slowdown of the bacteria at high concentrations of substrates or products because the bacteria could return to another stable state after a period of time for adaptation.

From the results of kinetic studies discussed in the previous sections it can be predicted that an increase in lactose concentration should result in higher production rates of butyrate, propionate, lactate etc., and thus an increase in their concentrations in the fermenter. Recently, van den Heuvel and co-workers investigated the effect of free butyric acid on the acidogenic dissimilation of glucose in anaerobic continuous cultures by adding extra acetate and butyrate to the culture medium and found that only free butyric acid inhibited bacterial activity and the inhibition was more obvious at lower pH values [181]. In the culture medium, butyrate is in equilibrium with its free molecule at steady state,

$$CH_3CH_2CH_2COOH \rightleftharpoons CH_3CH_2CH_2COO^- + H^+$$

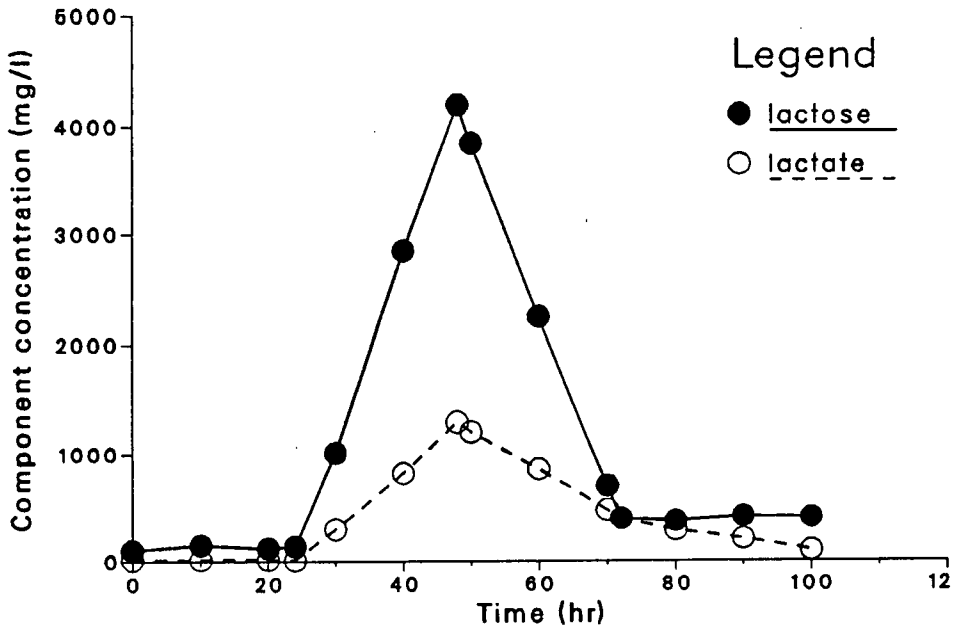


Figure 4.36: Responses of the acidogenic biofilm reactor to flow rate change. The solid line represents lactose concentration and the dash line lactate concentration.

The dissociation constant, K, is only a function of temperature,

$$K = \frac{[CH_3CH_2CH_2COO^-][H^+]}{[CH_3CH_2CH_2COOH]}$$

Lower pH values (higher $[H^+]$) and/or higher butyrate concentration can lead to more free butyric acid. It is widely accepted that free fatty acids will pass through the plasma membrane easily and may dissociate intracellularly, thereby abolishing the transmembrane pH-gradient which is a part of proton motive force necessary for bacterial functions [182].

# Chapter 5

## Start-up of Symbiotic Methanogenic Biofilms on Inert Surfaces

Compared with the start-up of acidogenic biofilms by which lactose is converted to organic acids, the build-up of methanogenic biofilms is more time consuming because of the much slower growth rate of methanogens and acetogens. Moreover, since methane- and acetate-producing bacteria form a symbiotic microbial community and collectively convert the fermentative products from the first acid-producing phase to methane, it would be valuable to know if support materials have some kind of selective function on the attachment of various bacterial species responsible for different substrate utilization. As discussed in Chapter 2, many properties of a support material may be able to influence the attachment of bacteria. One of them is wettability or hydrophobicity of the surface which has been shown by Verrier et al [112] to affect the attachment of different methanogenic bacteria.

### 5.1 Wettability of a Support Surface

Wettability measurement of a solid surface is an old technique. Compared with some new surface-sensitive techniques which probe the solid/vacuum interfaces like ESCA (electron spectroscopy for chemical analysis) and SEM (scanning electron microscopy), however, wettability measurements that probe the solid/liquid interface have some advantages such as great surface sensitivity (5–10 $\AA$), inexpensive, simple and compatible with most samples including organic materials and liquids [183].

When a liquid drop comes in contact with a solid, the liquid may wet the solid very

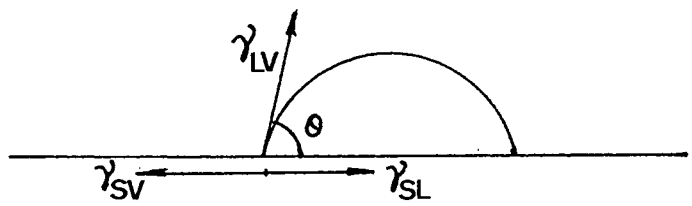


Figure 5.37: Schematic illustration of a spreading drop of liquid in contact with a solid surface, showing the relations between the contact angle, $\theta$, and three interfacial free energies.

well, and thus spread completely across the surface, or not so well, with a result that the drop edge expands to a maximum extent which is dependent on the strength of interaction between solid and liquid surfaces. The contact angle, $\theta$, as illustrated in Figure 5.37, is an important thermodynamic quantity that characterizes this interaction between a solid and a liquid surface at the interface with gas. It is generally agreed to give the name of contact angle to the angle within the liquid, i.e. $\theta$ as shown in Figure 5.37.

This angle is an experimental representation of an important thermodynamic relationship known as the Young equation, which relates the cosine of the angle, $\theta$, to the interfacial free energies of the three interfaces, solid-vapor (sv), solid-liquid (sl) and liquid-vapor (lv). At equilibrium,

$$\gamma_{lv} cos\theta = \gamma_{sv} - \gamma_{sl} \tag{5.26}$$

Obviously, the contact angle, $\theta$ can be interpreted only in terms of differences and ratios

of surface free energies rather than as a direct measure of interfacial tension or free energy between solid and liquid surface. However, with comparisons of measurements in similar systems rather than the interpretation of absolute values obtained from only one system, this technique of contact angle measurements is applicable to the characterization of solid-liquid interfaces.

Roughness of a surface also affects the "equilibrium" contact angles. Every groove, valley or scratch on a solid surface acts as a capillary tube in which the liquid rises if the contact angle is less than $90^0$ or descends if this angle is greater than $90^0$ [184]. Hence, a rough surface usually is better wetted than a smooth surface by a well-wetting liquid, while a poorly wetting liquid should spread on a smooth surface better than on a rough one. The liquid thus acts as a sensitive probe of the surface by interacting chemically with functional groups at the surface, or physically with surface asperities.

The contact angle formed by a drop on a horizontal solid surface can be computed from the dimensions of the drop. The computation is simple if the drop is so small that it can be treated as a spherical segment. As illustrated in Figure 5.38, the angle $\theta$ can be calculated from the volume, v, of the drop and the diameter, a, of its base.

If the drop is so small as to be nearly spherical, the relation between v and a is given by the equation [184],

$$\frac{a^3}{v} = \frac{24Sin^3\theta}{\pi(2 - 3Cos\theta + Cos^3\theta)} \tag{5.27}$$

Four types of material have been used in this study as the supports for symbiotic methanogenic biofilms (wood, ceramic, PVC and stainless steel) because they not only are widely used in industry but also give a quite wide range of hydrophobicity. The contact angle between a clean surface and a small water drop (1 $\mu$l) was measured with a 30 power microscope. For the base length, a, of a small drop, the average of the values

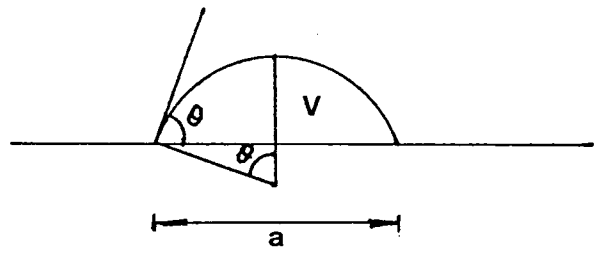


Figure 5.38: Illustration of calculating contact angle, assuming the drop being a spherical segment.

measured at 0, 45 and $90^0$ was used. The water contact angle on each material which is listed in Table 3.11 in Chapter 3, is an average of measurements on more than 10 drops.

## 5.2 Experimental Steps

The general setup has been illustrated in Chapter 3. The film attachment experiments were conducted in the continuous flow reactor as shown in Figure 3.10. The feed was a mixture of organic acids (acetate : propionate : butyrate = 6 : 3 : 3 g/l) plus growth stimulating inorganic salts as listed in Table 3.9. It was stored at 4 $^0C$ under an oxygen-free atmosphere provided by nitrogen bubbling. The inoculum was taken from a continuous flow methanogenic reactor which was fed with the same feed. Firstly, the reactor was filled with 500 ml of feed and 500 ml of tap water and the temperature of the medium solution was adjusted to 35 $^0C$ by the heat exchanger on the recycle line with nitrogen bubbling through the solution. After the temperature was constant at 35 $^0C$ and the pH of the medium was controlled at 7.1 by the automatic pH controller (with 0.2N

hydrochloric acid solution), the reactor was seeded with 400 ml of inoculum under a nitrogen atmosphere and operated in batch mode for 2 days with a recycle rate of 152 ml/min. The operation was then shifted to a continuous mode with a hydraulic retention time at 7 to 8 days controlled with the microvalve. Under this hydraulic retention time, the recycle ratio was greater than ten and hence, the reactor could be treated as a completely mixed continuous flow reactor with uniform nutrient concentration and temperature profiles being maintained in the reactor. Also this long retention time gave a considerable concentration of free bacterial cells suspended in the medium, which was essential for the investigation of attachment of free cells on support surfaces. At steady state, the concentrations of acetate, propionate and butyrate in the reactor were about 1,800, 1,000 and 100 mg/l, respectively. At this time, the four support materials mentioned above were inserted into the culture medium from the top of the reactor and the time was recorded as zero time for start-up of biofilms on the supports. A run started with a total of 32 samples which had been washed with detergent and distilled water before their being immersed into the medium. After some time (6 - 10 days) one of each type of surface was removed and the biomass accumulated on it was measured in a batch culture till all the samples were used.

A key, and also the most difficult, problem in this investigation was how to discriminate and describe quantitatively each bacterial group responsible for special substrate degradation in a mixed bacterial community. The usual methods such as by morphological difference, by protein content, or by special co-enzyme (e.g. $F_{420}$) content are not capable of discriminating the mixed bacterial species from each other. Based on a principal that the bacterial species responsible for a special substrate assimilation can be lumped into a group (such as acetate-degrading, propionate-degrading and butyrate-degrading bacteria), the slide samples with attached biomass were immersed in a "standard" medium which was prepared by diluting the feed to one fifth and the utilization

rates of each organic acid in the batch culture were measured. 50 ml of the standard medium which was used throughout this investigation was placed in a 150 ml Erlenmeyer flask immersed in a water bath at 35 $^0C$ and nitrogen gas bubbled through the medium to give good mixing and an oxygen free atmosphere. Each support slide with fixed biomass was placed in a flask and the concentrations of acetate, propionate and butyrate in the medium samples taken at regular intervals were measured by gas chromatography (see Appendix B). A sample of medium (1 - 5 ml) from the continuous flow reactor was treated in the same way in order to estimate the number of free cells in the fermenter. To be certain that the constant growth rate assumption would hold during the batch test, the run time of batch tests was controlled to maintain a high substrate concentration.

The mass of bacteria carrying out dissimilation of each of the three organic acids was monitored by following the degradation rates of the organic acids in the standard cultures. Substrate consumption is related to the growth and survival of the bacterial type using that particular substrate,

$$[dS/dt]_{total} = [dS/dt]_{growth} + [dS/dt]_{maintenance} \tag{5.28}$$

or,

$$V[dS/dt]_{total} = (\mu/Y + m)X \tag{5.29}$$

where,

$V$ = volume of batch culture medium (l)

$t$ = culture time (hr)

$S$ = concentration of a substrate in the batch culture (mg/l)

$\mu$ = specific growth rate of a bacterial group ($hr^{-1}$)

$Y$ = yield coefficient of a bacterial group (mg/mgS)

$m$ = maintenance coefficient (mgS/mg hr)

$X$ = total mass of bacteria which degrade that substrate (mg).

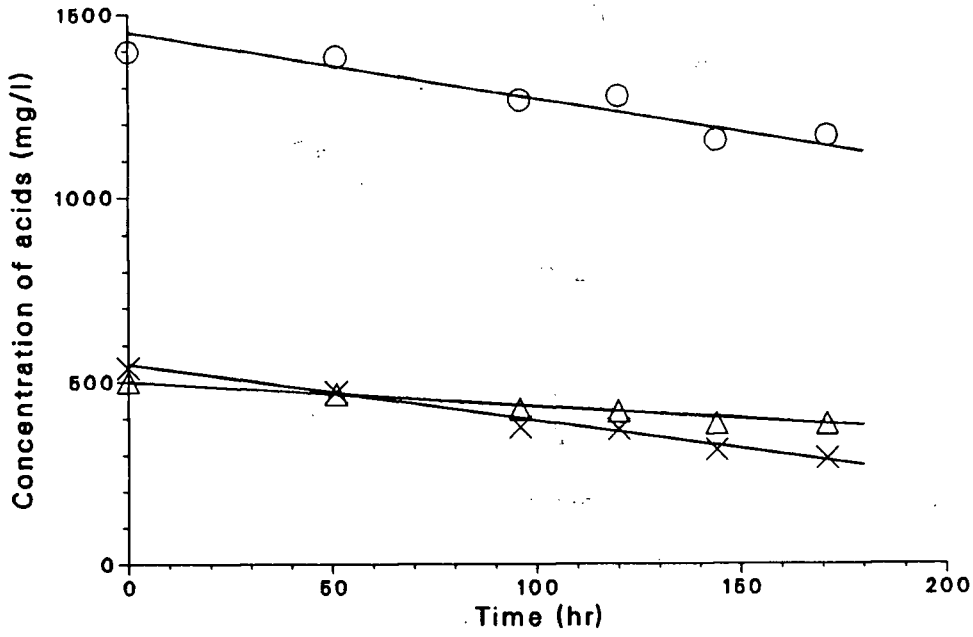


Figure 5.39: Organic acids degradation in a batch culture, o - acetate, △ - propionate, × - butyrate.

In a nutrient rich environment the microorganisms have sufficient food supply so that $\mu$ is a constant. Thus the total mass of a bacterial type is proportional to the utilization rate of that substrate.

$$X = \frac{V[dS/dt]_{total}}{\mu/Y + m} \tag{5.30}$$

Figure 5.39 shows that the concentrations of the three organic acids decreased linearly with culture time (i.e. $[dS/dt]_{total}$ = constant). The slopes are the utilization rates for each acid.

Therefore, it was assumed that the total number of bacteria remained constant during the tests. It was also assumed that the fixed bacteria had the same phsiological properties ($\mu$, $Y$ and $m$) as those of the free cells in the continuous flow reactor, which gives

$$\frac{X_{fixed}}{X_{free}} = \frac{[dS/dt]_{fixed}}{[dS/dt]_{free}} \tag{5.31}$$

where the subscripts "fixed" and "free" represent the biomass samples from fixed biofilms on the supports and from the medium of the continuous flow reactor.

## 5.3 A Kinetic Model of Biofilm Start-up

In general it can be deduced from the work which has been reported on bacterial attachment that the formation of a biofilm is the net result of several steps [81].

1. bacterial attachment on a clean surface
2. growth of fixed microorganisms
3. suspended cells attaching onto bacterial colonies/films
4. detachment of fixed cells into the aqueous environment

### 5.3.1 Attachment on Clean Surfaces

In the absence of external forces, bacterial cells dispersed in a fluid exhibit Brownian motion and touch the support surface randomly. In a flowing fluid they may be entrained in the fluid streamlines and be brought into contact with the surface as the fluid moves past it. If a cell contacts a surface for a long enough time for the cell to produce adhesive polymers [98] which bridge between the cell and the substratum, the cell is fixed to the support. Marshall et al [85] observed reversible and then irreversible attachment of bacteria at a surface. Thus two steps are involved; firstly, a bacterial cell approached the surface to form a reversible bacterium-substratum complex and secondly, the complex becomes a fixed cell.

$$x + A \overset{k_1/k_{-1}}{\rightleftharpoons} x\text{–}A \xrightarrow{k_2} xA$$

where,

$x$ = concentration of the suspended cells (cells/l)

$A$ = fractional clean surface area available to bacterial cells

$x-A$ = density of cell-substratum complex (cells/cm$^2$)

$xA$ = density of fixed cells (cells/cm$^2$)

The rate of complex formation is determined by the concentration of suspended cells [90] and the available clean area

$$\frac{d[x-A]}{dt} = k_1[x]A \tag{5.32}$$

It is assumed that the fixation of a cell-substratum comples is the rate limiting step since it involves some physiological activities for the cell to produce exopolymers. Therefore, the disappear rate of the complex is mainly due to the detachment of the complex into aqueous medium again.

$$-\frac{d[x-A]}{dt} = k_{-1}[x-A] \tag{5.33}$$

At equilibrium, the attachment and detachment rates will be equal

$$k_1[x]A = k_{-1}[x-A] \tag{5.34}$$

or,

$$[x-A] = (k_1/k_{-1})[x]A \tag{5.35}$$

$k_1$ and $k_{-1}$ are the specific attachment and detachment rate constants. The rate of bacterial cells attaching onto a clean surface (cells/cm$^2$.hr) is;

$$r_1 = k_2[x-A] = k[x]A \tag{5.36}$$

where

$$k = k_1k_2/k_{-1} \tag{5.37}$$

This overall rate constant, $k(\mathrm{l/cm^2.hr})$ indicates whether the rate of attachment is fast or slow. Thus, the value of k may be used as an indicator of the ease of bacterial attachment on a surface.

### 5.3.2 Growth of Attached Bacteria

Growth of the bacteria immobilized on a surface makes a major contribution to the development of biofilms [185]. The rate of growth may be expressed as

$$r_2 = \mu[xA] \tag{5.38}$$

The specific growth rate, $\mu$ ($\mathrm{hr^{-1}}$), is a constant if the fixed cells are able to get enough nutrients from their environment (thin biofilms at high substrate concentrations).

### 5.3.3 Attachment on Fixed Biomass

Attachment onto fixed biomass can be described by a similar set of steps to those of attachment on a clean surface,

$$x + A' \overset{k_3/k_{-3}}{\rightleftharpoons} x - A' \xrightarrow{k_4} xA$$

where $A'$ is the fractional area occupied by fixed colonies/films and

$$A + A' = 1 \tag{5.39}$$

Again assuming that the forward and backward rates easily reach equilibrium because of the very slow fixation of the complex, $x - A'$,

$$k_3[x]A' = k_{-3}[x - A'] \tag{5.40}$$

and so,

$$[x - A'] = (k_3/k_{-3})[x]A' \tag{5.41}$$

The rate of accumulation of fixed cells due to attachment of free cells on the biomass already fixed on the solid support is

$$r_3 = k_4[x - A'] = K[x]A' = K(1 - A)[x] \tag{5.42}$$

where $K = k_3k_4/k_{-3}$ (l/cm$^2$.hr), signifying the ease with which bacterial cells attach onto biomass already present. Obviously, in contrast to $k$, $K$ is not affected by the properties of support surfaces.

### 5.3.4 Detachment

The mechanisms of detachment of immobilized biomass previously has not been investigated throughly as was indicated in Chapter 2. The major possible reasons for detachment of fixed biofilms are sloughing (for thick biofilms) and shearing caused by fluid flow. In the latter case, the detachment may occur not only on the outer layer but also at some locations inside the biofilm depending on the bridging strength between the cells. The thicker the biofilm, the more connections there are between cells, and the greater is the probability that the connections may be broken. Therefore, the rate of detachment of fixed cells has been set proportional to the amount of biomass on the surface,

$$r_4 = K'[xA] \tag{5.43}$$

The parameter $K'$ (hr$^{-1}$) is influenced by the shear stress caused by culture medium flow, by the bacterial species, and by other factors which influence the structure and homogeneity of the biofilm, e.g. the concentration of cations such as $Ca^{2+}$, and $Mg^{2+}$.

The total rate of accumulation of one bacterial subgroup is the sum

$$r = r_1 + r_2 + r_3 - r_4$$

which gives,

$$\frac{d[xA]}{dt} = k[x]A + K[x](1 - A) + \mu[xA] - K'[xA] \tag{5.44}$$

or,

$$\frac{d[xA]}{dt} = (k - K)[x]A + K[x] + (\mu - K')[xA] \tag{5.45}$$

where A, the fractional area of clean surface, is a function of time,

$$\text{A} = 1 \qquad \text{at} \qquad \text{t=0}$$

and

$$\text{A} \rightarrow 0 \qquad \text{as} \qquad \text{t} \rightarrow \infty$$

It was observed during the experiments that the bacterial colonies, rather than a uniform biofilm with one- or two-cell thickness, were scattered on the surface and had different thickness. As the fixed microorganisms grew they spread slowly over the surface thus reducing the clean surface area left. Therefore, the clean surface area should be inversely proportional to the growth rate of the fixed bacteria which is an exponential function of time in a nutrient rich environment. This can be expressed as;

$$A = e^{-st} \tag{5.46}$$

The parameter $s$ ($\text{hr}^{-1}$) indicates the ease with which the colonies can spread over a surface and may be a function of rugosity of the surface. Substitute for $A$ in Equation 5.45,

$$\frac{d[xA]}{dt} = (k - K)[x]e^{-st} + K[x] + (\mu - K')[xA] \tag{5.47}$$

Integrating with the initial conditions,

$$[xA] = 0 \qquad \text{at} \qquad \text{t=0}$$

gives

$$\frac{[xA]}{[x]} = \frac{k - K}{s + \mu - K'}[e^{(\mu - K')t} - e^{-st}] + \frac{K}{\mu - K'}[e^{(\mu - K')t} - 1] \tag{5.48}$$

The density of fixed bacteria on a support slide, xA, and the concentration of free cells in the fermenter, x, were measured with the 'standard' batch cultures as discussed above. The left side of Equation 5.48 becomes,

$$\frac{[xA]}{[x]} = \frac{X_{fixed}}{X_{free}} \times \frac{volume\ of\ sample}{area\ of\ support} \tag{5.49}$$

where the volume of sample refers to the volume of medium taken from the continuous flow reactor (1–5 ml) and the area of support is the area of the removable support sample. Using Equation 5.31, Equation 5.48 becomes

$$\frac{[dS/dt]_{fixed} \times area}{[dS/dt]_{free} \times volume} == \frac{k-K}{s+\mu-K'}[e^{(\mu-K')t} - e^{-st}] + \frac{K}{\mu-K'}[e^{(\mu-K')t} - 1] \tag{5.50}$$

Now, the left side of Equation 5.50 can be experimentally determined with the data from the batch cultures as shown in Figure 5.39.

## 5.4 Estimation of Model Parameters

Equation 5.50 is a general equation which can be applied to each substratum; wood, ceramic, PVC and stainless steel, and also to each bacterial group; acetate-degrading, propionate-degrading and butyrate-degrading. Hence in all, 12 equations like Equation 5.50 can be written down with different parameters. Not all the parameters, however, in these 12 equations should be different since they may be independent of the surface type or the bacterial type. Since it was impossible, a priori, to determine which values were common to all equations, a direct search method [186] (see Appendix G) was used to search for a set of optimum parameters which would best fit one of the models with 13, 16, 21 and 22 parameters to the 12 curves (108 experimental data points as listed in Appendix D). The optimum parameters for each model were determined by comparision

of the local minimum fit errors obtained from different initial search points and by the significance of the values (e.g. the parameter values should be positive). Table 5.17 summarizes the results of screening the models by comparing the sum of absolute error between the experimental values and the values predicated by a model.

In the table, $K$ represents the attachment of free cells onto fixed biomass already on the support surfaces; $K'$ the detachment of immobilized cells into the medium; $\mu$ the specific growth rate of attached biomass; k the attachment of free cells onto clean surfaces and s the expansion of attached microbial colonies on support surfaces. The subscripts indicate the surfaces and the bacterial types

Since start-up of a biofilm is the net result of several steps like attachment, growth and detachment, a mechanistic model which describes these steps always contains more parameters than an empirical correlation. If the consideration is limited to one bacterial and one support type, 5 parameters and 4 freedoms (freedom = number of parameters - number of equations) are involved in Equation 5.48. In this case, some of the parameters may be highly correlated. However, when the number of types of bacteria and supports was increased, even though the total number of parametrs were increased, the freedom for each of bacterial and support type was decreased. Furthermore, since the steps described by the model always occur simultaneously during the build-up of a biofilm and could not be separated experimentally, changing one factor like support surface wettability which would affect one of the steps (free cells attaching onto clean surfaces), and thus, the value of the parameter ($k$) describing this step, may be the only practicable method to investigate this complicated process.

The simplest model, model 1, assumed that the surface characteristics had the same effect on the three bacterial groups, and thus there were only 13 parameters in the 12 equations. The sum of absolute errors for this model was 5.53 as compared to the experimental data. Model 2 tested whether the attachment-detachment of bacteria to

Table 5.17: Results of screening kinetic models of biofilm start-up

| Model | | 1 | 2 | 3 | 4 |
|---|---|---|---|---|---|
| Parameters | Unit | 13 | 16 | 21 | 22 |
| $K$ | cm/day | 0.001125 | 0.00225 | 0.000275 | 0.003194 |
| $K'_w$ | $day^{-1}$ | 0.02225 | 0.02225 | 0.02148 | 0.05192 |
| $K'_p$ | $day^{-1}$ | ,, | 0.02938 | ,, | ,, |
| $K'_s$ | $day^{-1}$ | ,, | 0.03062 | ,, | ,, |
| $K'_c$ | $day^{-1}$ | ,, | 0.02819 | ,, | ,, |
| $\mu_{wa}$ | $day^{-1}$ | 0.03444 | 0.03963 | 0.03581 | 0.06651 |
| $\mu_{pa}$ | $day^{-1}$ | ,, | ,, | ,, | 0.06364 |
| $\mu_{sa}$ | $day^{-1}$ | ,, | ,, | ,, | 0.06118 |
| $\mu_{ca}$ | $day^{-1}$ | ,, | ,, | ,, | 0.06151 |
| $\mu_{wp}$ | $day^{-1}$ | 0.02806 | 0.0330 | 0.03415 | 0.05481 |
| $\mu_{pp}$ | $day^{-1}$ | ,, | ,, | ,, | 0.06005 |
| $\mu_{sp}$ | $day^{-1}$ | ,, | ,, | ,, | 0.05788 |
| $\mu_{cp}$ | $day^{-1}$ | ,, | ,, | ,, | 0.05192 |
| $\mu_{wb}$ | $day^{-1}$ | 0.03875 | 0.0445 | 0.03504 | 0.07236 |
| $\mu_{pb}$ | $day^{-1}$ | ,, | ,, | ,, | 0.06632 |
| $\mu_{sb}$ | $day^{-1}$ | ,, | ,, | ,, | 0.07156 |
| $\mu_{cb}$ | $day^{-1}$ | ,, | ,, | ,, | 0.06757 |
| $k_{wa}$ | cm/day | 0.05319 | 0.04738 | 0.05596 | 0.06729 |
| $k_{wp}$ | cm/day | ,, | ,, | 0.03396 | ,, |
| $k_{wb}$ | cm/day | ,, | ,, | 0.082 | ,, |
| $k_{pa}$ | cm/day | 0.0245 | 0.02794 | 0.03356 | 0.02966 |
| $k_{pp}$ | cm/day | ,, | ,, | 0.02968 | ,, |
| $k_{pb}$ | cm/day | ,, | ,, | 0.04191 | ,, |
| $k_{sa}$ | cm/day | 0.0210 | 0.02844 | 0.02909 | 0.03119 |
| $k_{sp}$ | cm/day | ,, | ,, | 0.02628 | ,, |
| $k_{sb}$ | cm/day | ,, | ,, | 0.03786 | ,, |
| $k_{ca}$ | cm/day | 0.03481 | 0.03769 | 0.04202 | 0.03234 |
| $k_{cp}$ | cm/day | ,, | ,, | 0.03071 | ,, |
| $k_{cb}$ | cm/day | ,, | ,, | 0.06597 | ,, |
| $s_w$ | $day^{-1}$ | 0.04731 | 0.06306 | 0.05218 | 0.07837 |
| $s_p$ | $day^{-1}$ | 0.05675 | 0.06788 | 0.08931 | 0.09576 |
| $s_s$ | $day^{-1}$ | 0.05069 | 0.06638 | 0.0908 | 0.1082 |
| $s_c$ | $day^{-1}$ | 0.0595 | 0.06975 | 0.08536 | 0.05146 |
| sum of error | | 5.533 | 5.271 | 2.783 | 4.249 |

w,p,s,c: surfaces of wood, PVC, stainless steel and ceramic ring
a,p,b: bacteria degrading acetate, propionate and butyrate

the biomass was influenced by the substrata. This added 3 parameters and only reduced the sum of absolute error to 5.27. Model 4 tested the possibility that the specific growth rate of each species was influenced by the characteristics of the substrata. Although the number of parameters was increased to 22, the sum of absolute error was only reduced to 4.25. Model 3 which was used to describe the results was based on the assumption that each bacterial type attached differently to each surface, but their specific growth rates were independent of the surface properties because the support materials used in this study were inert (wood is not biodegradable to any extent in the short time period used) and fixed microbes could get enough nutrients from the culture medium with no help from the solid surfaces. Twenty one parameters in 12 equations gave a sum of absolute error of only 2.78 probably due to the reasonable assumptions which were made. Figures 5.40, 5.41 and 5.42 show how well this model fits the experimental points.

Mathamatically, although 22 parameters were estimated simultaneously and the total degree of freedom (22 - 12) of the search was 10, for each of the equations the degree of freedom was less than 1 (10/12) (a linear equation in general has one degree of freedom). Therefore, for each combination of bacterial and support type, the fit of the equation with the experimental data was made by adjusting less than one parameter, so, there was very low correlation between the parameters.

In addition to the assumption mentioned above that a special bacterial group (say, acetate- degrading bacteria) has the same specific growth rates on four different supports, the three bacterial groups have almost the same specific growth rates, 0.035 ($day^{-1}$). Lawrence and McCarty [142] obtained a similar result in their study on the kinetics of methanogenic cultures - that is, acetate-, propionate- and butyrate-degrading bacteria had the same specific growth rates. Moreover, a value of specific growth rate for methanogenic anaerobes was calculated from the data given by Verrier et al [111] as 0.027 ($day^{-1}$). This is good agreement considering that they used a different technique

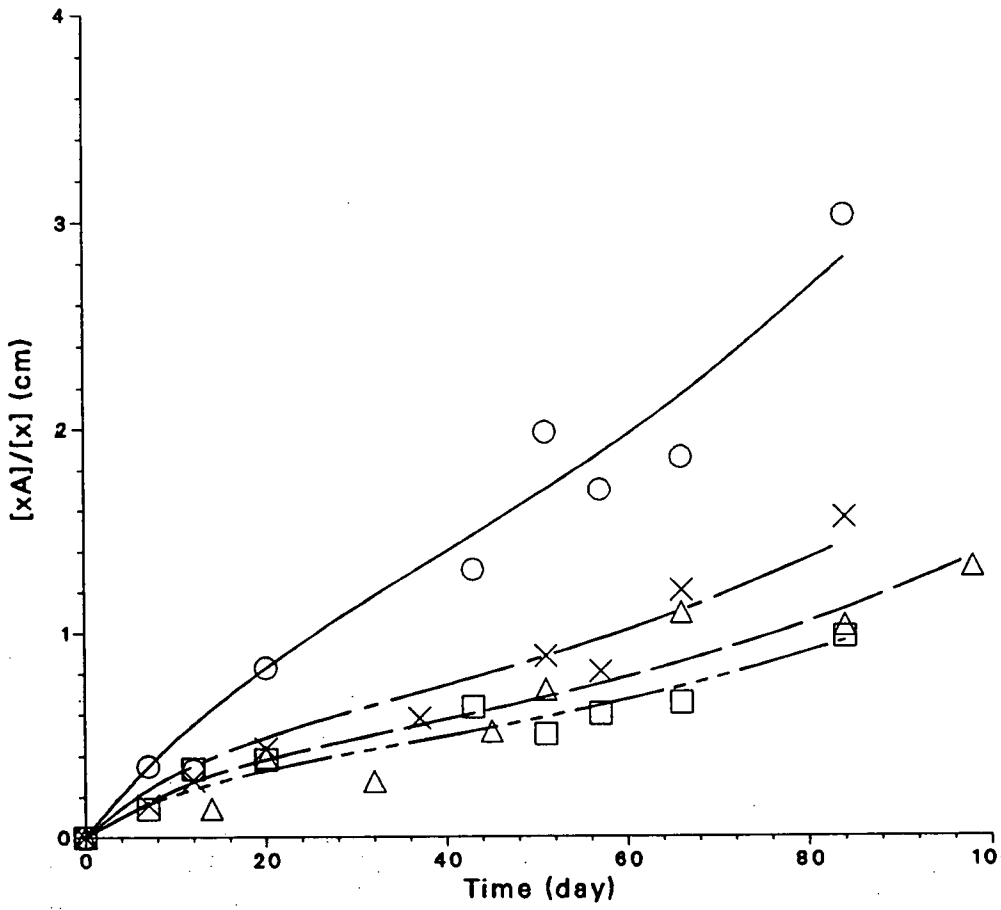


Figure 5.40: Build-up of acetate-degrading bacteria in the biofilms. The lines are calculated from the model. Surfaces: o - wood, × - ceramic, △ - PVC, □ - steel

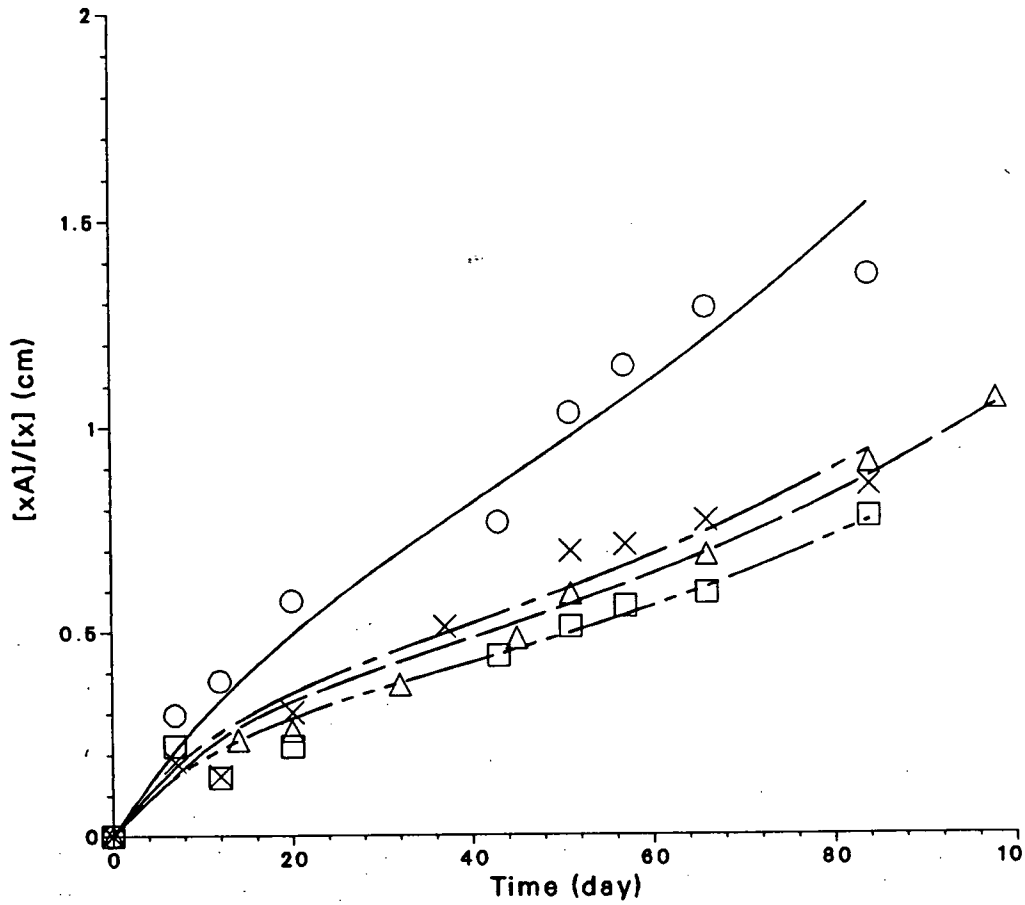


Figure 5.41: Build-up of propionate-degrading bacteria in the biofilms. The lines are calculated from the model. Surfaces: o - wood, × - ceramic, △ - PVC, □ - steel

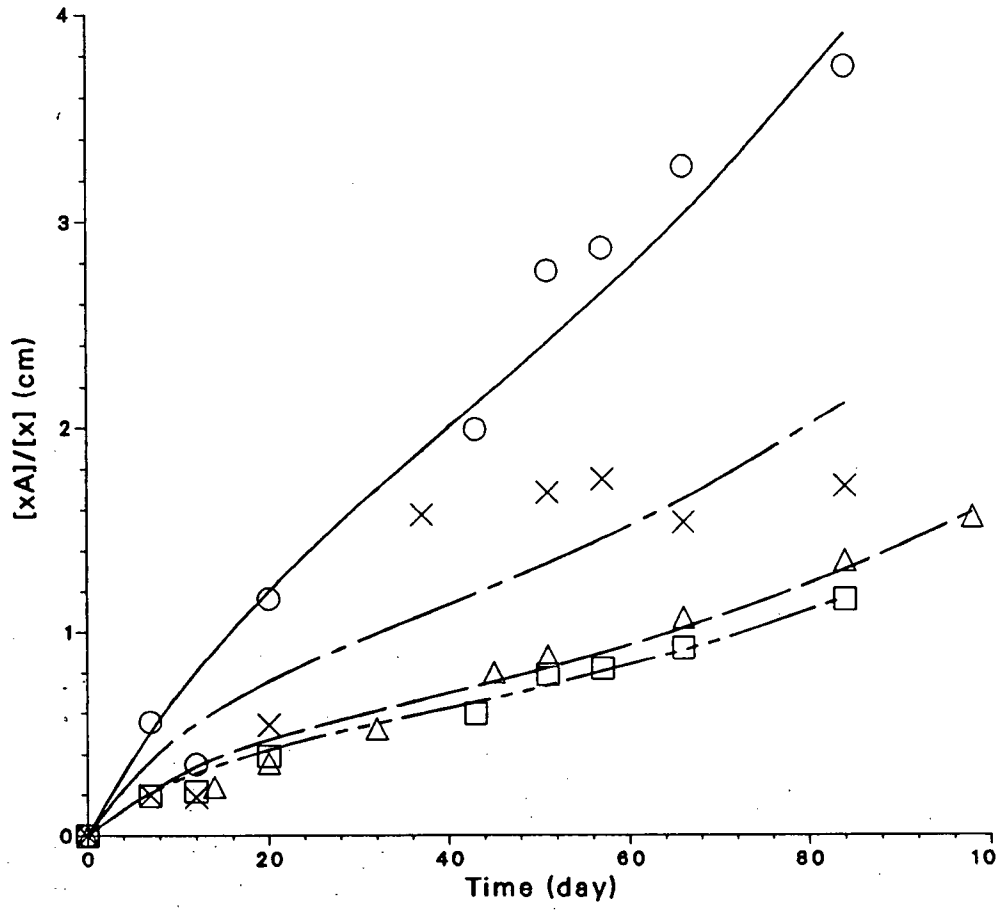


Figure 5.42: Build-up of butyrate-degrading bacteria in the biofilms The lines are calculated from the model. Surfaces: o - wood, × - ceramic, △ - PVC, □ - steel

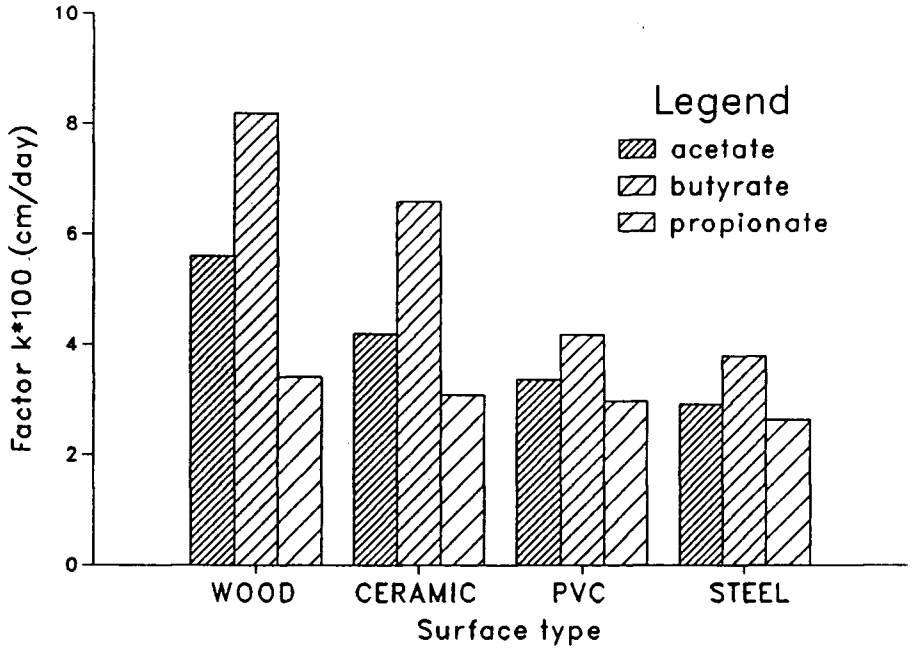


Figure 5.43: Ease of attachment of bacteria on substrata as shown by model parameter k.

to measure the growth rate on different substrates. The other two factors which were considered to be independent of surface type are K and K', the attachment and detachment to and from fixed biomass, respectively, since the surface involved was a biomass surface.

The parameter k, defined in Equation 5.36, is a proportionality factor which takes into account the ease with which bacteria can attach and remain on a surface. Figure 5.43 shows the same data graphically. It can be found that the acetate and butyrate degrading bacteria had obvious surface preferences of,

$$\text{wood} > \text{ceramic} > \text{PVC} > \text{stainless steel}$$

The propionate degrading bacteria, however, attached less easily and had almost no surface preference.

The spreading factor, s, was calculated for all the bacteria lumped together but for

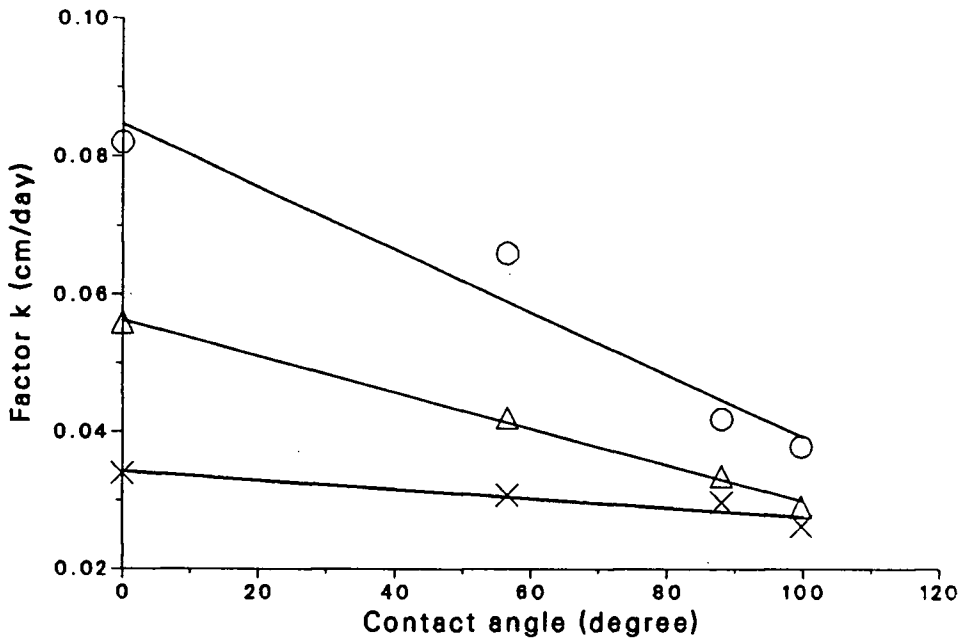


Figure 5.44: Attachment factor, k, as a function of water contact angle of surface. Line is the least square fit. o–butyrate degrading bacteria, △–acetate degrading bacteria, ×–propionate degrading bacteria

each support surface. Here it can be seen that, once attached, the ease with which the microorganisms spread on the surface by growth was in the order,

$$\text{stainless steel} > \text{PVC} > \text{ceramic} > \text{wood}$$

This is exactly the reverse of the ease of attachment order. Figure 5.44 is a plot of the attachment factor, k, against the water contact angles for the four surfaces tested. There appears to be a relationship between these two factors which can be fitted very well by a linear least square method. The fitting parameters are listed in Table 5.18. It was reported by van Loosdrecht et al [187] that on a single surface (sulfated polystyrene), attachment of 16 bacterial strains could be linearly correlated with the bacterial wall hydrophobicity (water contact angle between $15^0$ and $70^0$).

There have been some contradictory reports on the relationship between wettability and attachment as reported by Dexter et al [93], and by Pringle and Fletcher [188].

Table 5.18: Linear relations between specific attachment rates and water contact angles

| Bacteria | Intercept (cm/day) | Slope (cm/day.degree) | r-squared (%) |
|---|---|---|---|
| Acetate-degrading | 0.05632 | $-2.646\times10^{-4}$ | 99.6 |
| Propionate-degrading | 0.03422 | $-6.659\times10^{-5}$ | 88.1 |
| Butyrate-degrading | 0.0847 | $-4.546\times10^{-4}$ | 94.9 |

Bright and Fletcher [176] found that amino acid assimilation and respiration by attached and free-living marine *Pseudomonas spp* decreased with increasing water contact angle of the support surface while Fletcher and Leob [189] observed that lower hydrophobicity, i.e. smaller contact angles, promoted attachment of marine bacteria.

Absolom [190] has reported that bacterial attachment depends not only on the hydrophobicity of the substrata but also on the hydrophobicity of the bacterial wall [191]. The bacteria with hydrophilic surfaces have smaller contact angles and larger contact areas on hydrophilic support surfaces. Thus they are deformed more and may be able to remain on the surface for a longer time because more adhesive extracellular glycocalyces (capsules or s layers) are in contact with the substrate [192,100]. If bacterial cells can stay in contact with a substratum for a long time the physiological functions of the cells can produce more extracellular polysaccharide materials which bridge the cells and the substratum [85,189].

If it is assumed that the initial contact and attachment is a function of the relative hydrophobicity of the surface and the bacteria, the nature of the three bacterial types can be summarized as follows:

1. The butyrate degrading bacteria have the most hydrophilic wall surfaces since their specific attachment rate, k, decreases most rapidly with increasing hydrophobicity of the substrata.

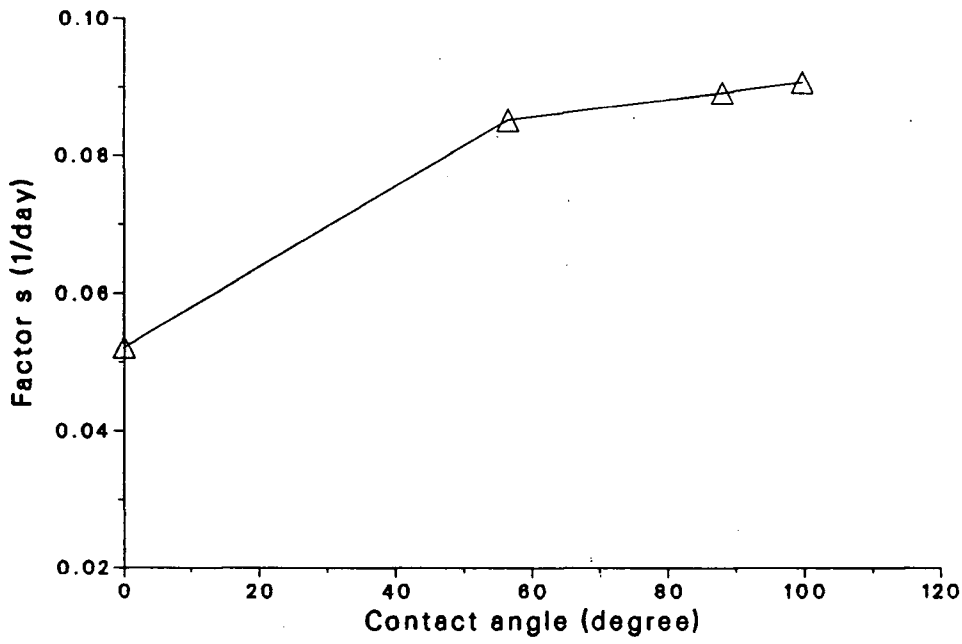


Figure 5.45: Spreading factor, s, as a function of the water contact angle of the surfaces for all bacteria.

2. The propionate degrading bacteria are least hydrophilic since the support surface wettability has only a small effect on their attachment.

3. The acetate degrading bacteria have somewhat hydrophilic wall surfaces.

Thus, since the surface of the three bacterial types have different hydrophobicities, it should be possible to some extent to influence the composition of a methanogenic biofilm by purposely choosing a substratum.

The coefficient of spread, s , defined by the film attachment model has also been shown to be affected by the substrata wettability. Figure 5.45 shows graphically this model parameter, which describes the rate of colony spreading on a surface, as a function of the wetting angle of surfaces.

Fixed cells divide within a hydrated exopolysaccharide matrix so that the daughter cells are trapped in a juxtaposition that results in the formation of microcolonies as

indicated in Chapter 2. In a fluid flow environment, as found in this study, solid supports offer shields for bacterial colonies fixed on them because the flow stagnates on the surface due to the fluid viscosity. However, on hydrophobic surfaces the solid surfaces do not strongly attract the water molecules and there is a greater possibility of slip. It is expected that this phenomenon will have an influence on the size of microcolonies. Flattening would result in a spreading of the microcolonies in the flow direction. Since the flow velocity approaches zero at a hydrophilic surface the microcolonies would be less flattened and the spreading would be slower than on a hydrophobic substratum. The more hydrophobic the surface, the more rapid is the spread of bacteria. Shimp and Pfaender [193] have also observed the spreading phenomena of microbial colonies as a function of flow rate.

# Chapter 6

## Intrinsic Kinetics of Methanogenesis of Organic Acids

Flow from the acidogenic phase reactor, where lactose was converted to organic acids by the acidogens, enters the second phase reactor where the symbiotic methanogenic bacteria convert these intermediates into gaseous products, methane and carbon dioxide. As discused in Chapter 2, many species of methane-producing bacteria have been identified and maintained in pure culture. All known species can utilize carbon dioxide and hydrogen as substrates for methane generation whereas a few of them can use acetate as their substrate to produce methane. Except for these two types of substrates ($CO_2/H_2$ and acetate), the methanogens must rely on the biological activities of acetogens, who can convert other substrates such as ethanol, propionic and butyric acids to acetate, carbon dioxide and hydrogen. Table 6.19 lists the four main reactions occurring in fatty acid methanogenesis reported by Thauer et al [179].

Table 6.19: Methanogenic reactions of organic acids

| Reactions | $\Delta$ G (kJ) |
|---|---|
| $CH_3COO^- + H_2O \rightarrow CH_4 + HCO_3^-$ | -31.0 |
| $CH_3CH_2COO^- + 3H_2O \rightarrow CH_3COO^- + HCO_3^- + H^+ + 3H_2$ | +76.1 |
| $CH_3CH_2CH_2COO^- + 2H_2O \rightarrow 2CH_3COO^- + H^+ + 2H_2$ | +48.1 |
| $4H_2 + HCO_3^- + H^+ \rightarrow CH_4 + 3H_2O$ | -135.6 |

Source is [179].

However, the acetogens cannot do this job at all at high hydrogen partial pressures,

Table 6.20: VFA distribution in anaerobic digestion process

| Substrate | HAc : HPr : HBu (w:w:w) | Reference |
|---|---|---|
| Sewage sludge | 1 : 0.6 : 0.2 | [201] |
| Raw sludge | 1 : 0.9 : 0.7 | [202] |
| Primary sludge | 1 : 0.8 : 0.4 | [203] |
| Sewage sludge | 1 : 0.3 : 0.3 | [204] |
| Sewage sludge | 1 : 0.3 : 0.3 | [26] |
| Lactose (D=0.25 1/hr) | 1 : 0.4 : 0.6 | [44] |
| Lactose (D=0.1 1/hr) | 1 : 0.1 : 0.2 | [44] |

and thus must rely on the methanogens to remove the produced hydrogen, too. In contrast to the case of lactose acidogenesis where all the bacterial species could be lumped as a single group from the point of view of lactose consumption, the methanogenic community includes at least four groups of bacteria classified by their substrates; butyrate-, propionate-, acetate-, and hydrogen-utilizing bacteria.

## 6.1 Experiments of Organic Acid Methanogenesis

The experimental setup was the same as for lactose acidogenesis; the general setup was as shown in Figure 3.10 and the biofilm support surface was made from PVC sheets as described in Chapter 3. The feed was a mixture of acetate, propionate and butyrate in a ratio of 1 : 0.5 : 0.5 by weight. This ratio was determined from the ratios of volatile fatty acids (VFA) concentrations produced in the conventional anaerobic digestion process and the two-phase digestion process as listed in Table 6.20.

The studies on lactose acidogenesis described in Chapter 4 revealed that under those experimental conditions the major products were acetate and butyrate with propionate being a minor product. However, propionate was still used in this study for more information about its rate of utilization, and its influence on the digestion of other components.

The necessary growth nutrients for the microorganisms were added as inorganic salts as shown in Table 3.9. The feed had an acetate concentration ranging from 2 to 5 g/l, and hence the acetate concentration in the fermenter could be controlled at different levels under the desired experimental dilution rates. Correspondingly, the concentrations of propionate and butyrate in the fermenter were also controlled at their own levels at the experimental dilution rates because the concentrations of propionate and butyrate in the feed had a fixed ratio to that of acetate (HAc : HPr : HBu = 1 : 0.5 : 0.5). The oxygen dissolved in the feed was stripped off with $N_2$. The feed was then kept under a $N_2$ atmosphere by bubbling $N_2$ through the feed because the methane-producing bacteria are obligate anaerobes. To avoid evaporating the volatile fatty acids the pH of the feed was adjusted to 7.0 – 7.2 by the addition of equimolar sodium hydroxide and potassium hydroxide. Every batch of feed was analyzed at least two times during the experiments to determine the feed concentrations.

The fermenter had a working volume of one liter. The flow rate, measured by collecting effluent during a period of time (3–4 hours), was controlled at above 30 ml/hr to maintain the dilution rate, D, greater than 0.72 $day^{-1}$. In their review of the anaerobic digestion literature, Henze and Harremoes [144] concluded that the maximum specific growth rate of methanogenic bacteria at 35 $^0$C was 0.4 $day^{-1}$. Under the chosen hydraulic conditions the bacterial cells suspended in the culture medium were washed out and this fraction of biomass retained in the reactor could be neglected in comparison with the biomass fixed on the supports. The negligible amount of free bacterial biomass was confirmed by analyzing the solid carbon content in the effluents as was done in the experiments of lactose acidogenesis.

The pH of the fermenter was controlled by an automatic pH controller at 7.1$\pm$0.2 with 0.3 to 1 N hydrochloric acid solutions. The HCl concentration was adjusted according to the strength of the methanogenic activity to have as low an influence on flow rate and

local pH in the fermenter as possible. The inoculum was obtained from the secondary phase reactor of a two-phase mini-plant which had been in continuous operation for two years.

The experiments on the methanogenesis of organic acids can be divided into four stages:

1. Adaptation; The feed used during this period was a mixture of acetate (3 g/l), propionate (1.5 g/l) and butyrate (1.5 g/l) so that the bacterial community would have a balanced population, containing acetate-, propionate-, butyrate-, and hydrogen-utilizing groups. The fermenter was filled with the feed (500 ml) and tap water (300 ml). Nitrogen was continuously bubbling through the medium for 2 hours to remove the dissolved oxygen. When the temperature reached 35 $^0$C, the fermenter was inoculated with 200 ml of inoculum and then operated in batch mode. After the three acids had been used up, half the volume of the culture (500 ml) was replaced by fresh feed and this was repeated 5 times.

2. Build-up of a symbiotic biofilm; Adaptation of the microorganisms to the mixture of fatty acids gave a balanced microorganism population which was suspended in the culture medium. At that time the supports made of PVC sheets were immersed in the medium under $N_2$ atmosphere. The operation, then, was shifted to continuous operation mode with the flow rate controlled below 6 ml/hr (dilution rate $D < 0.15$ $day^{-1}$) to avoid washout of the free cells. After about 60 days a uniform black biofilm could be observed on the grey PVC sheets.

3. Steady state operation; With build-up of the biofilm the flow rate was gradually increased to above 30 ml/hr to wash out the suspended cells. The temperature of the culture medium was kept at 35 $^0$C and the pH at 7.1. The fatty acid concentrations in the fermenter were controlled by adjusting the feed concentration and flow

rate. At each of the desired concentration levels, a steady state (effluent concentration fluctuation $< 10$ %) was maintained at least 3 days to get experimental data. Similar to the procedures for lactose acidogenesis, after a set of concentration levels had been investigated, the experiments were repeated on the same set of levels again and again. Therefore, the utilization rates of fatty acids could be obtained at each of the concentration levels but on different thickness of methanogenic biofilms. By comparing these data, the effect of internal mass transfer resistance could be estimated, and only those data not affected by the biofilm thickness were taken as the intrinsic data.

4. Interaction of fatty acids; Following the kinetic studies, the interaction of fatty acids was investigated in the "mature and balanced" methanogenic biofilms which contained all the bacterial types responsible for the utilization of three organic acids. In this stage, the concentration of one acid in the feed was adjusted at different levels while those of other two acids and other conditions were unchanged. Therefore, any change in the utilization rates of these two acids might be attributed to the effect of the acid with changed concentrations. The acetate concentration in the fermenter was adjusted from 800 to 1,100 mg/l, the propionate concentration from 0 to 2,000 mg/l, and the butyrate concentration from 100 to 1,500 mg/l. The culture temperature and pH were maintained at 35 $^0$C and 7.1, respectively.

The intrinsic kinetics of biofilms must be investigated under negligible external and internal mass transfer resistance. In this study the influence of external mass transfer was reduced as low as possible by increasing the recycle rate, and thus the linear velocity over the biofilm, which effectively reduced the external mass transfer resistance as indicated in the studies made on lactose digestion by acidogenic biofilms in Chapter 4. It should be easier to minimize the external and internal mass transfer resistance during

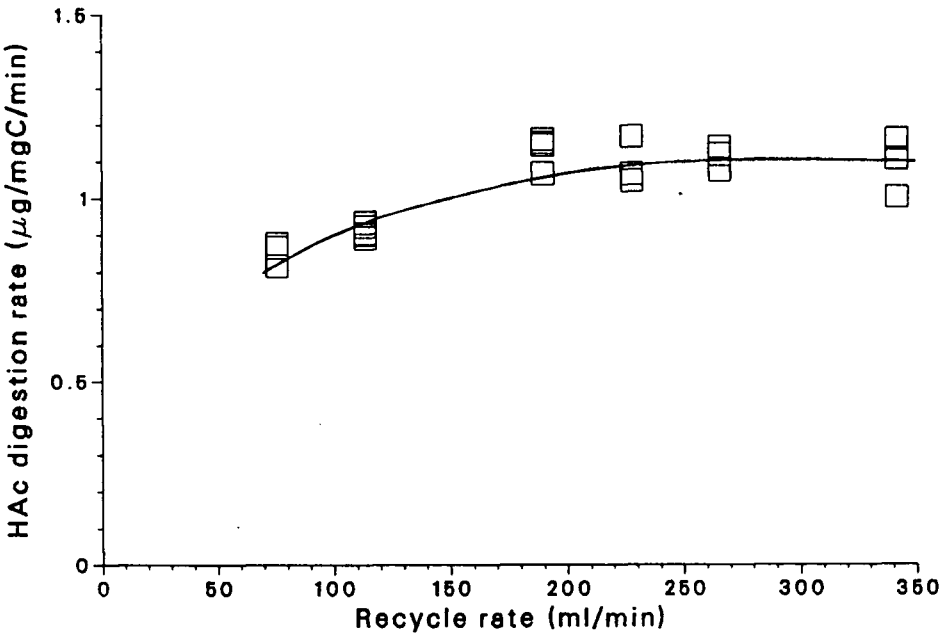


Figure 6.46: Influence of recycle rate on acetate utilization

the methanogenesis because the physiological activities of methanogens are much weaker than those of acidogens. Figure 6.46, Figure 6.47 and Figure 6.48 indicate that as long as the recycle rate was above 190 ml/min, i.e. a linear velocity of 2.8 cm/min over the biofilm, the utilization rates of acetate, propionate and butyrate should not be affected by external mass transfer. This conclusion was confirmed later by the relationship between these reaction rates and the bulk substrate concentrations. Grady and Lim [205] showed that the presence of external mass transfer resistance prevents the rate expression from exhibiting a Michaelis–Menten type of a dependence on the bulk substrate concentration even when the true kinetics were assumed to do so.

The influence of internal mass transfer resistance is always present if the mass transfer rate, based on the mechanism of molecular diffusion, is not much greater than the consumption rate, and if the bulk substrate concentration is taken as representative of the internal substrate concentrations within the biofilms. Obviously, the thinner the biofilm,

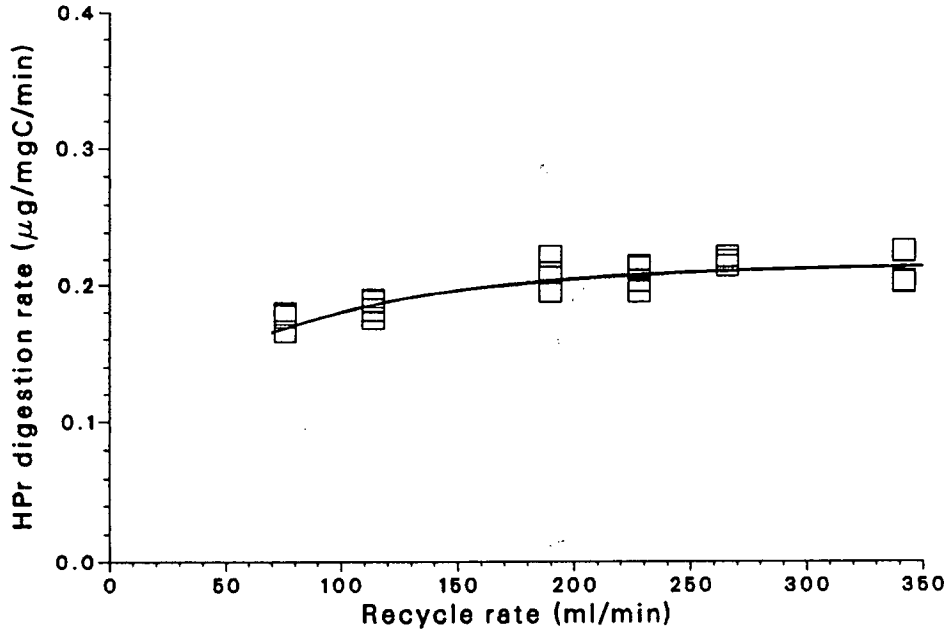


Figure 6.47: Influence of recycle rate on propionate utilization

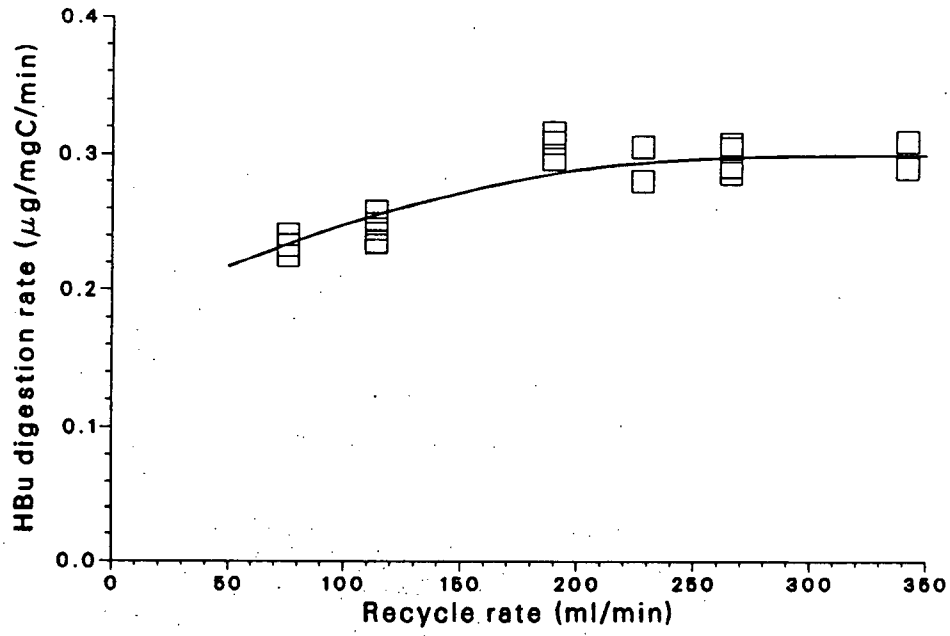


Figure 6.48: Influence of recycle rate on butyrate utilization

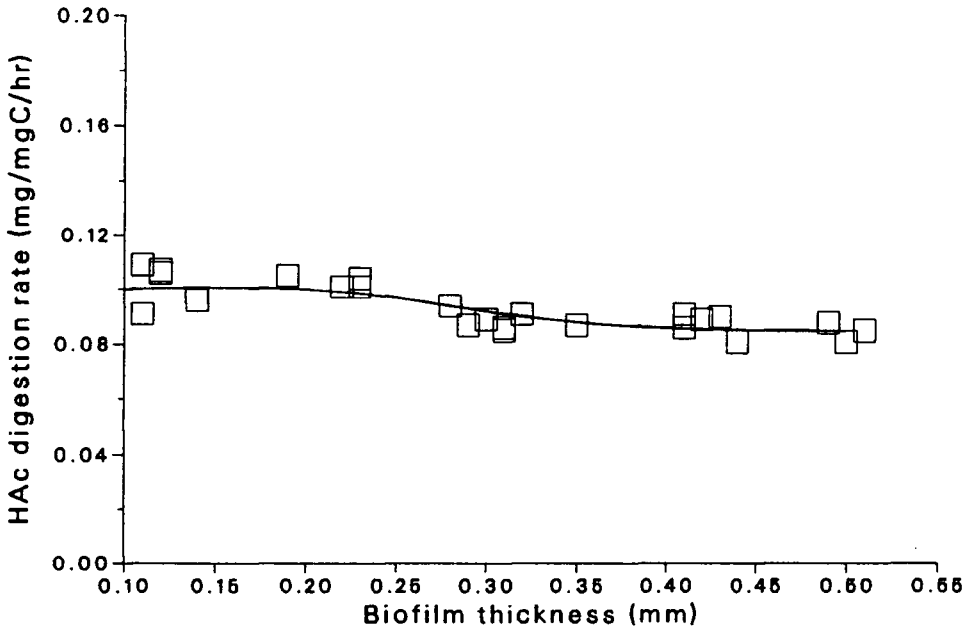


Figure 6.49: Influence of biofilm thickness on acetate digestion rate

the less the influence of internal mass transfer resistance. The kinetic data collected during the early stage of biofilm development are considered to be the result of pure bacterial reaction because a very thin biofilm had developed at that time.

Figure 6.49 shows that the acetate utilization rate per unit weight of biomass carbon gradually decreased with an increase of the methanogenic biofilm thickness because the bacterial cells embedded in the thicker biofilms saw lower substrate concentrations. Therefore, the experiments were arranged in such a way that the experiments at low substrate concentrations were conducted first and those at high concentrations later. Corresponding to higher bulk concentrations, the concentrations inside the biofilms were also higher, and hence, all the bacterial cells embedded in a thick biofilm might have their maximum utilization rates which was determined by the Michaelis-Menten type kinetics of the bacteria. Thereby, the effect of internal mass transfer resistance could be reduced. As shown in Figure 6.49, the internal mass transfer resistance in a biofilm

Table 6.21: Experimental conditions for organic acid methanogenesis

| Parameter | Unit | Condition |
|---|---|---|
| Temperature | $^0$C | 35 ± 2 |
| pH | | 7.1 ± 0.2 |
| Flow rate | ml/hr | > 30 |
| Dilution rate | day$^{-1}$ | 0.72 |
| Recycle rate | l/hr | 11.4 |
| Biomass | | methanogenic |
| Feed | g/l | HAc : HPr : HBu |
| for biofilm buildup | | 3 : 1.5 : 1.5 |
| for kinetics | | 2–5.5 : 1–2.7 : 1–2.7 |

having a thickness less than 0.3 mm could be considered to be minimal, and hence, the intrinsic kinetic data should be collected during this period (about 100 days).

Mixtures of acetate, propionate and butyrate in the ratio of 1 : 0.5 : 0.5 (weight) were used as the feeds for biofilm build-up and kinetic studies. However, investigations on the interaction between fatty acids were also conducted on the balanced biofilms with the feeds having different ratios of acetate, propionate and butyrate. The concentrations of each acid will be listed in the description of each test. Table 6.21 lists the experimental conditions for fatty acid methanogenesis. The recycle ratio, the ratio of recycle rate to flow rate, was up to 380, that is, much greater than 10. Therefore, the fermenter could be taken as a completely mixed continuous flow reactor (CSTR) and the effluent concentration was the same as that in the fermenter.

## 6.2 Development of Methanogenic Biofilms

The amount of biomass retained in a fermenter has a large effect on the performance of this reactor. In this study all the utilization rates of the organic acids were based on unit weight of active biomass. Therefore, the total amount of biomass in the reactor

must be known during the experiment. As was discussed in Chapter 4 for the acidogenic biomass, the methanogenic biomass also existed in three forms: biofilms, the major part of the retained biomass; free cells, a minor fraction under the experimental dilution rates; and the sludge on the reactor walls which was taken as biofilm on the walls as shown in Figure 4.20.

When the PVC biofilm supports as described in Figure 3.14 were immersed into the medium, about 30 removable PVC slides were also inserted into the fermenter. The biomass on these slides was measured at different times and was believed to be the same as those on the supports. Each time one or two slides were analyzed and it was observed that a uniform biofilm was forming on the supports because the two slides randomly taken from different locations in the reactor had almost the same amount of biomass. Figure 6.50 shows that the biomass on the slides increased gradually with the culture time. Correspondingly, the carbon content of the biomass on the slides also increased with the culture time as shown in Figure 6.51. The carbon content of the biofilms gave a very good linear relationship with their dry biomass as shown in Figure 6.52. The slope of the straight line in Figure 6.52 is 0.353 (mg carbon/mg dry biomass). From the carbon content of the biomass on a removable slide and the areas of the supports and the slide, the total carbon content of biofilms fixed on the supports at that time could be calculated.

The biomass on the reactor walls was not easily measured. The sludge which was introduced into the fermenter as seed and had reproduced during the period of biofilm development was removed by discharging the culture medium under a $N_2$ atmosphere after a visible black biofilm had formed and before the kinetic data were collected. Thus the biomass left on the reactor walls was taken to be the biofilm attached on the walls. Based on the same assumption used for acidogenic biomass, this part of biomass should have the same growth rate as the biomass on the supports. After the experiments were

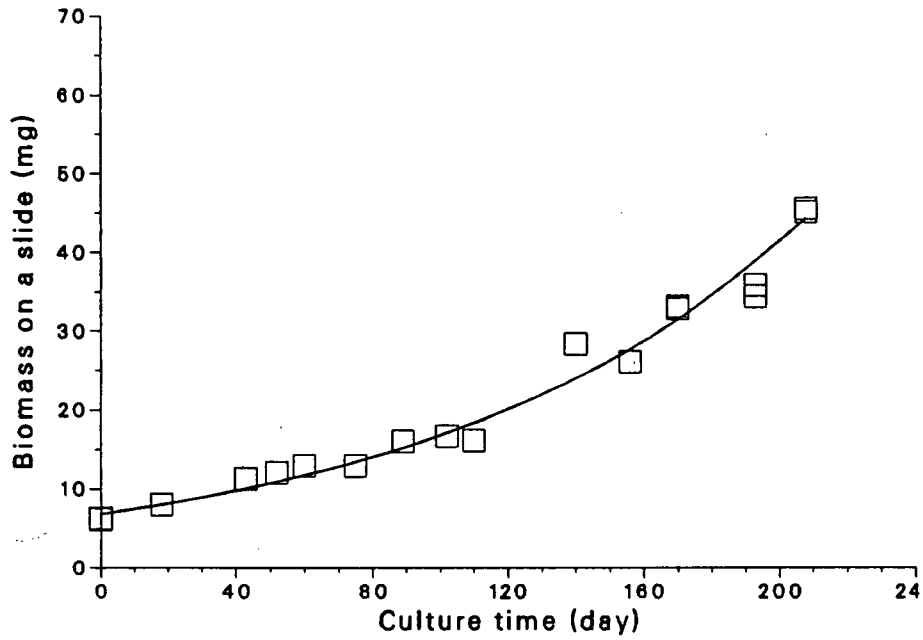


Figure 6.50: Biomass on slides increases with culture time

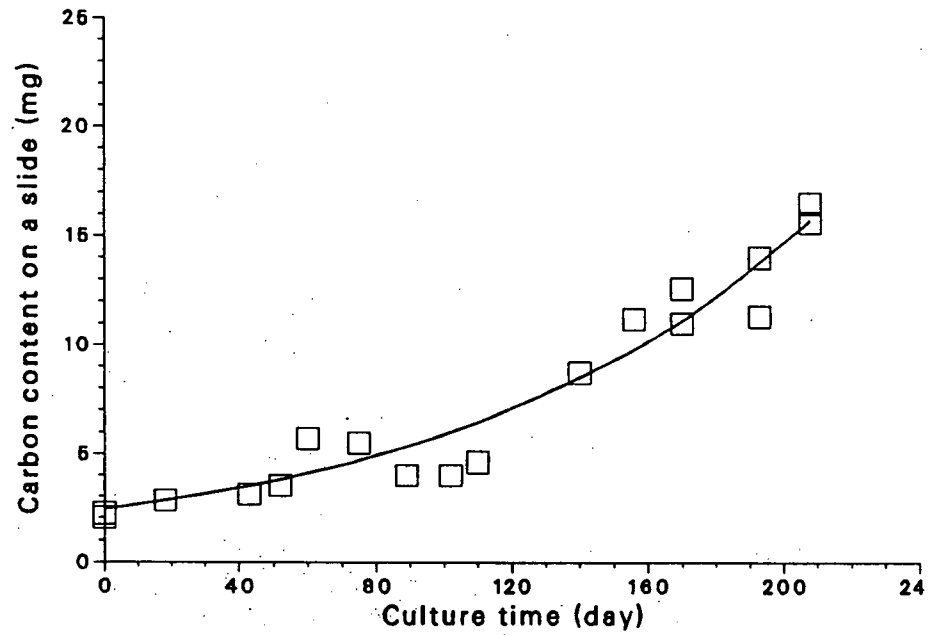


Figure 6.51: Total organic carbon on slides increases with culture time

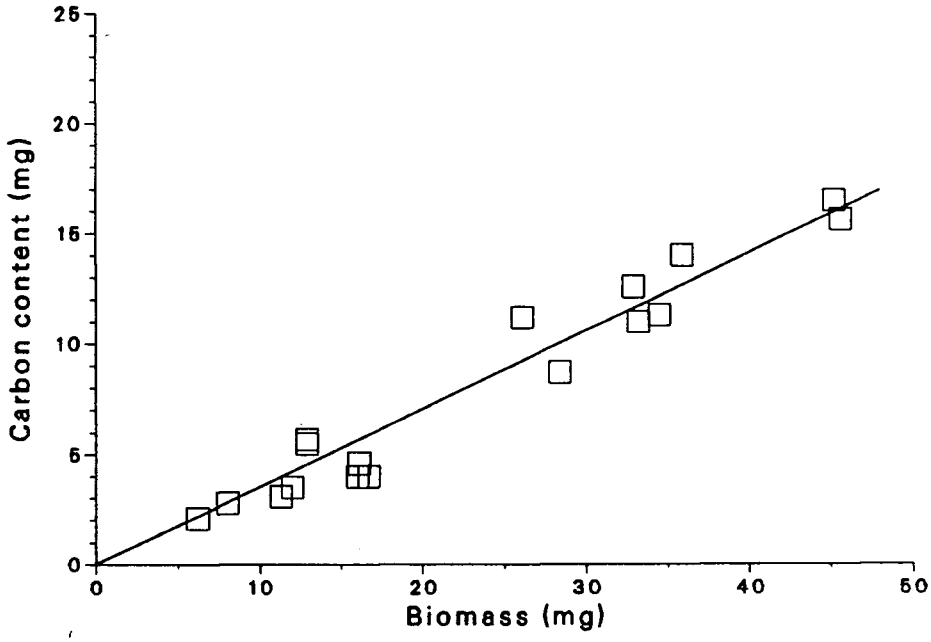


Figure 6.52: Relationship between organic carbon and dry biomass of biofilms

finished the biomass on the reactor walls was carefully collected and measured, and the initial amount of biomass was estimated by using this data and the growth rate of biofilms on the supports. The total biomass, in terms of total organic carbon, of the biofilms on the supports and reactor walls can be predicted by using the following equation.

$$TC = 1678.9e^{0.0090t} \tag{6.51}$$

Table 6.22 lists some analysis results of biomass samples taken from biofilms on the supports and 'sludges' on the reactor walls.

The 'biofilms' on the reactor walls contained more ash and less organic carbon because more inorganic salts (metal ions) were deposited on the bottom of the reactor. That is why the total carbon content of the biofilm, instead of the dry biomass, was used in this study.

Table 6.22: Properties of methanogenic biofilms

| Item | | Sample 1 | Sample 2 |
|---|---|---|---|
| Ash content (w%) | biofilm | 38.1 | 37.7 |
| | sludge | 58 | 59 |
| TOC content (w%) | biofilm | 34.4 | 35.2 |
| | sludge | 15.2 | 17.3 |

## 6.3 Interaction of Organic Acids

The methanogenesis of fatty acids depends on a symbiotic microorganism community which consists of at least four groups of bacteria. Each of them has its own substrate. Generally the substrate concentration affects the biological activity of the bacterial group responsible for the utilization of this substrate. One example is the dependence of lactose utilization rate on the lactose concentration as discussed in lactose acidogenesis. However, one substrate may also affect other groups of bacteria because of the symbiotic properties of the bacterial community. Scharer and Moo-Young [206] found that the kinetic information obtained using single substrates could not be used for predicting methane generation from a mixture of acids and when equimolar mixtures of acetate, propionate and butyrate were used, propionate was not consumed at all. This may be caused by the high substrate and/or product concentrations being toxic or beneficial to the bacterial activities, but may also be caused by inhibition or competition from other substrates in a feed of mixed organic acids. The following experiments were conducted by using the feeds with different concentrations of organic acids.

### 6.3.1 Influence of Acetate Concentration

Methanogenesis of organic acids was investigated in immobilized cell bioreactors by Scharer et al [114]. Their results indicated that acetic acid was consumed very rapidly

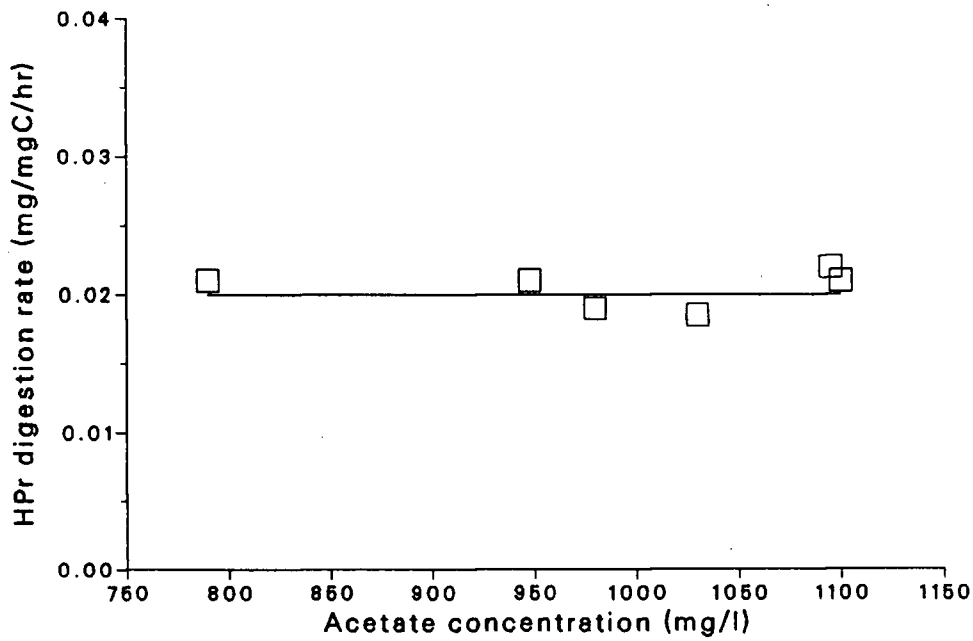


Figure 6.53: Effect of acetate concentration on propionate digestion (HPr=880–996 mg/l)

in comparison to propionic and butyric acids and the presence of acetic acid had an inhibiting effect on the utilization of either propionic or butyric acid. Therefore, it seems possible that acetogenesis of these two organic acids could be inhibited by their product, acetate. To test this hypothesis, the concentrations of propionate and butyrate were maintained in narrow ranges, 880–996 mg/l and 48–66 mg/l respectively, and only the acetate concentration was adjusted in the fermenter. Figure 6.53 and Figure 6.54 reveal that the digestion of neither propionate nor butyrate was inhibited by the presence of acetate. This means that in a balanced bacterial community the acetogens are not inhibited by the products of their metabolic activities.

### 6.3.2 Influence of Propionate Concentration

Propionate is the component most difficult for the bacteria to digest. Hence, it often appears in high concentrations in the effluent of an unstable digester. Its influence on

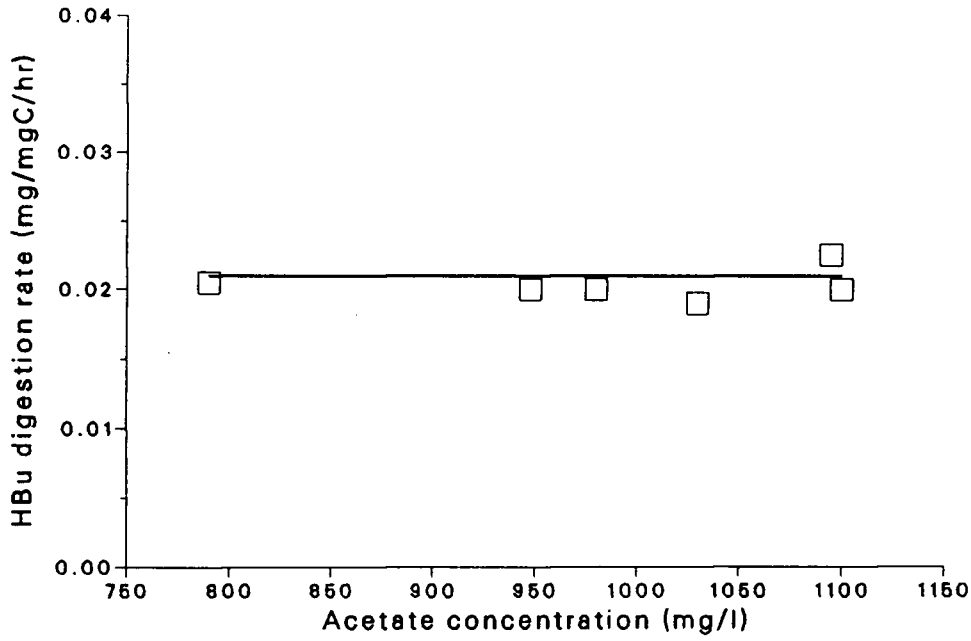


Figure 6.54: Effect of acetate concentration on butyrate digestion (HBu=48–66 mg/l)

the utilization rates of acetate and butyrate was investigated by maintaining acetate and butyrate concentrations in the fermenter in narrow ranges, 700–1000 mg/l and 50–80 mg/l respectively, while the propionate concentration was adjusted from 150–2300 mg/l. Any change observed in the utilization rates of acetate and butyrate would then be due to the changes in the propionate feed composition. Figure 6.55 shows no influence of propionate on acetate utilization. Figure 6.56, however, indicates that high propionate concentrations could inhibit the digestion of butyrate.

### 6.3.3 Influence of Butyrate Concentration

The bacteria responsible for the conversion to butyrate belong to the same group of microorganisms, acetogens, as do those which utilize propionate. The possible influence of butyrate concentration on acetate and propionate utilization was checked by adjusting butyrate concentrations in the fermenter while acetate and propionate concentrations

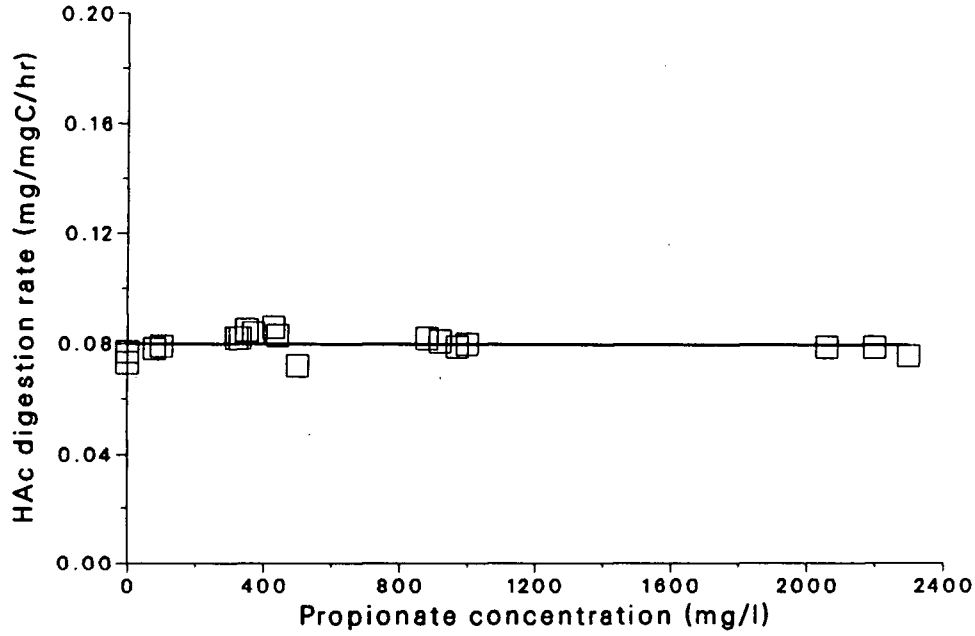


Figure 6.55: Effect of propionate concentration on acetate utilization (HAc=700–1000 mg/l)

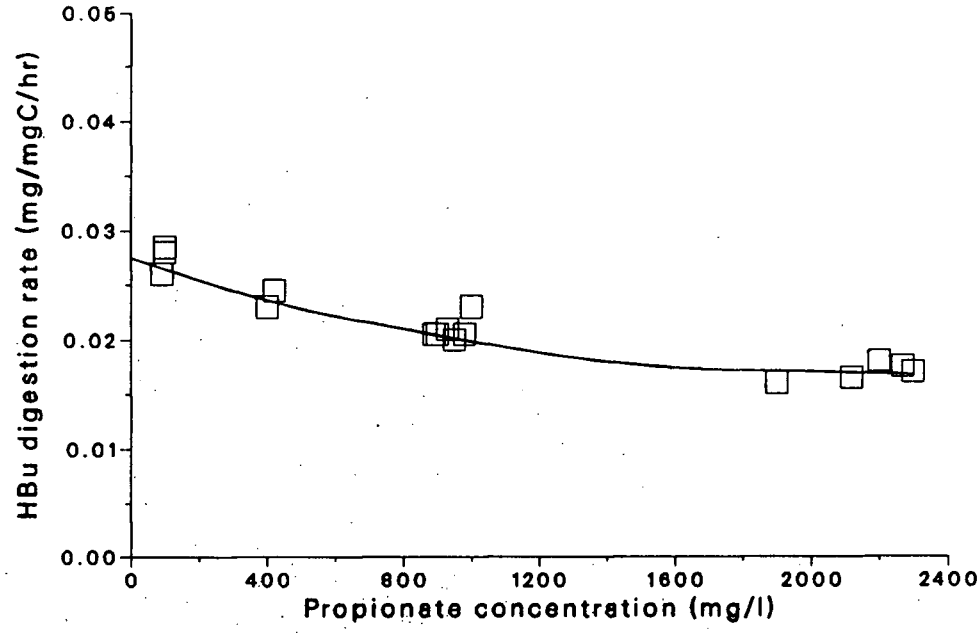


Figure 6.56: Effect of propionate concentration on butyrate utilization (HBu=50–80 mg/l)

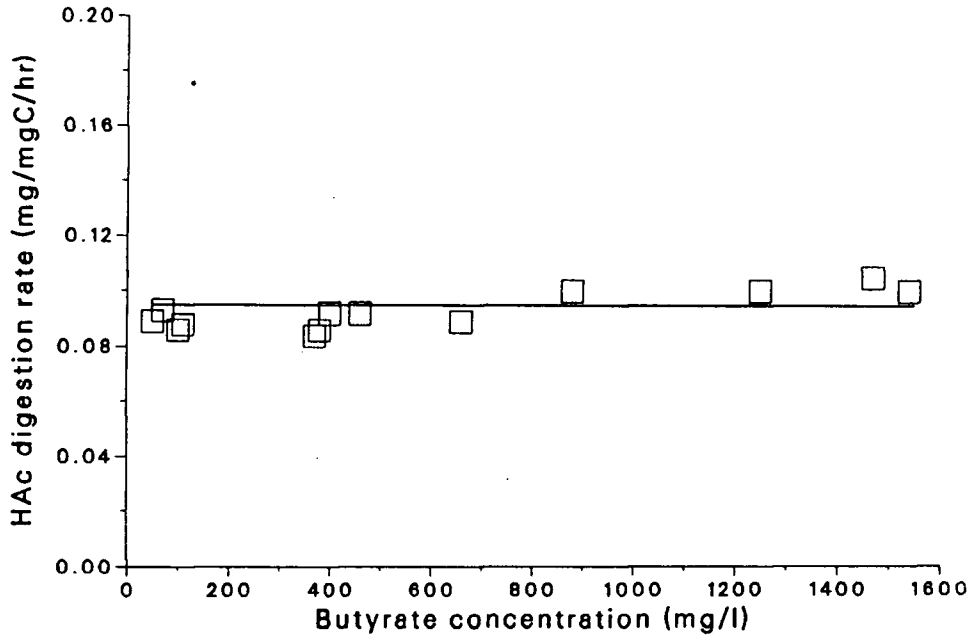


Figure 6.57: Effect of butyrate concentration on acetate digestion (HAc=1400–3000 mg/l)

were kept in a relatively narrow range, 1400–3000 mg/l and 700–900 mg/l respectively. Although the acetate concentrations changed from 1400 to 3000 mg/l no significant influence of butyrate concentration was observed on acetate digestion as shown in Figure 6.57. This was because at high substrate concentrations acetate-digesting bacteria had reached their maximum metabolism rate and hence further increase in acetate concentration had little effect on the utilization rate. Figure 6.58 shows no influence of butyrate concentration on propionate utilization even though the later inhibited the former's digestion. This may be an indirect evidence that conversion of these two fatty acids involves different bacterial species.

The interaction of substrates or bacterial groups of a balanced microorganism community can be summarized as follows:

- Acetate has no influence on the biological activities of acetogens which are responsible for the conversion of propionate and butyrate to acetate and $H_2$, and also,

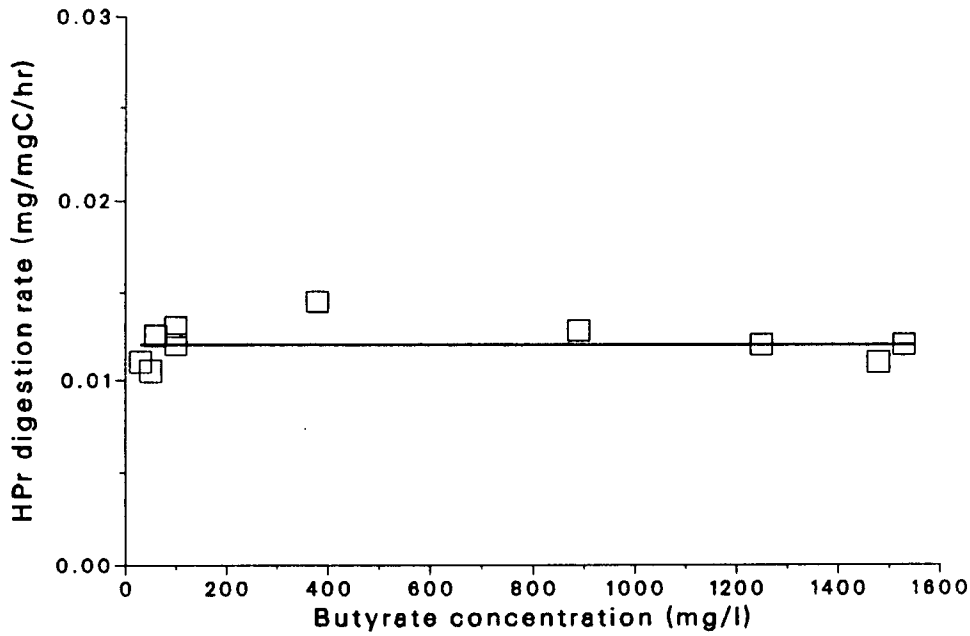


Figure 6.58: Effect of butyrate concentration on propionate digestion (HPr=700–900 mg/l)

neither propionate nor butyrate affects the methane-producing bacteria which can use acetate directly as substrate.

- Propionate-utilizing bacteria are not affected by acetate and butyrate, but propionate can inhibit the activity of butyrate-utilizing bacteria.
- Butyrate, like acetate, does not influence other fatty acids utilizing bacteria.

## 6.4 Utilization Rates of Organic Acids

The kinetics of organic acid digestion were investigated on feeds having a fixed ratio of acetate, propionate and butyrate. Therefore, each acid was always present in the fermenter so that a balanced bacterial community could be maintained. Various steady state levels of fatty acid concentration were obtained by changing

feed concentrations or residence time or both of them. A steady state which was judged from the concentration fluctuation in the effluent (< 10 was collected, such as the total amount of dry biomass, the total organic carbon, the gaseous production rate and composition, the culture medium flow rate and composition. The carbon recovery for these experiments ranged from 77 to 86 percent (see Appendix E) which included the gaseous carbon ($CH_4$ and $CO_2$) and carbon in the liquid phase (organic acids, $CO_2$). This balance is quite reasonable since the solid carbon contained in biomass either as free cells or as biofilms, was not calculated, nor were some minor fermentative products like valeric acid.

### 6.4.1 Propionate Utilization Rate

At steady state, a material balance of propionate around the fermenter gives

$$FS_{i,p} = FS_{e,p} + Wr_p \tag{6.52}$$

or,

$$r_p = \frac{F(S_{i,p} - S_{e,p})}{W} \tag{6.53}$$

where $r_p$ is the consumption rate of propionate (mg/mgC/hr), $S_{i,p}$, $S_{e,p}$ the propionate concentration in the feed and effluent (mg/l). For each steady state the right side on Equation 6.53 could be determined experimentally, and thus the propionate consumption rate. A Michaelis-Menten type equation was firstly used to describe the effect of propionate concentration on the propionate utilization rate.

$$r_p = \frac{r_{max,p} S_p}{K_p + S_p} \tag{6.54}$$

The two parameters, $r_{max,p}$ and $K_p$, were estimated by using the direct search method (see Appendix G) while the initial search point was determined from the least-square estimation of the linearized equation.

$$r_{max,p} = 0.021 \qquad \text{mg/mgC/hr}$$

$$K_p = 99 \qquad \text{mg/l}$$

However, a plot of $r_p$ against propionate concentration shows that a Michaelis-Menten type model, as represented by the dash line in Figure 6.59, can not describe the effect of propionate concentration on propionate utilization rate very well over the tested concentration range, especially from 200 to 800 mg/l.

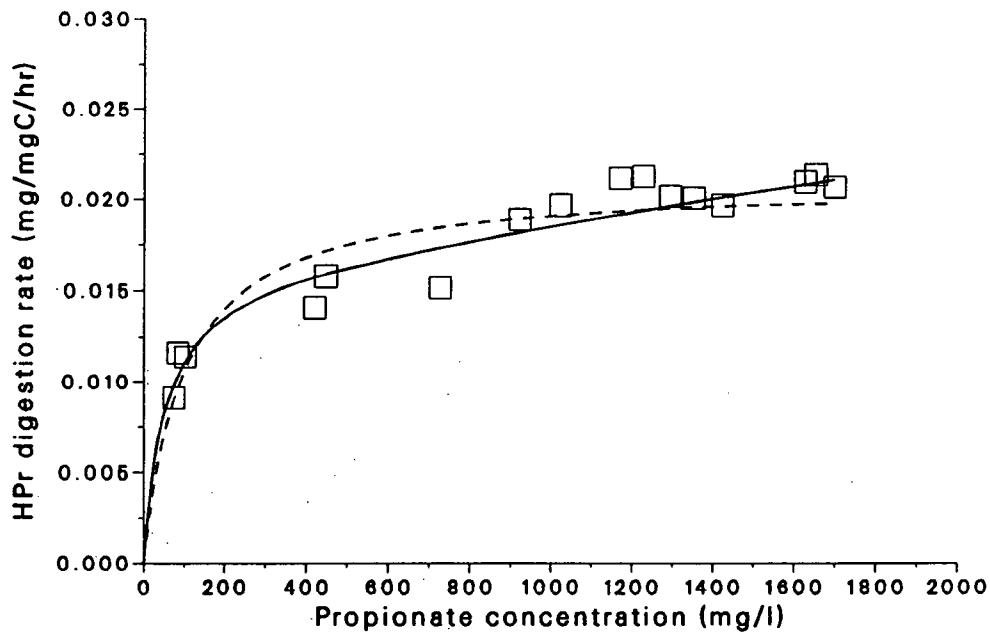


Figure 6.59: Dependence of propionate digestion rate on propionate concentration. The dash line represents Equation 6.54. The solid line is calculated from Equation 6.56

It may be proposed that the propionate utilization rate was promoted by higher

propionate concentration. Because acetate and butyrate have no influence on propionate-digesting bacteria as discussed before, the only possible influence is from propionate itself.

Digestion of propionate may involve many reactions promoted by various enzymes. It is generally assumed that there exists a slowest reaction step, or rate-limiting step, which is catalyzed by a key enzyme. The reaction mechanism can be assumed to be as follows:

$$E + S \underset{k_{-1}}{\overset{k_1}{\rightleftharpoons}} ES \xrightarrow{k_2} P + E \tag{1}$$

$$ES + S \xrightarrow{\beta k_2} P + ES \tag{2}$$

The first reaction is the well known Michaelis-Menten reaction. During the formation of the $ES$ complex, the enzyme molecule is twisted, which places some strain on the geometry of the substrate molecule. This strain renders it susceptible to attack by $H^+$ or $OH^-$ ions or by specific active groups of the enzyme. In this manner the substrate molecule is converted to its product. With increase in substrate concentration more and more enzyme will form the complex $ES$ and the rate of reaction will increase until, finally, virtually all the enzyme is in the form of $ES$. Introducing the second reaction is based on the assumption that $ES$ complex can still be attacked by another substrate molecule to form a product molecule. Therefore, the total substrate consumption rate is

$$r = \frac{k_2 S(1 + \beta S)}{(k_{-1} + k_2)/k_1 + S} \tag{6.55}$$

The detailed derivation of Equation 6.55 can be found in the Appendix F. Similar to the application of a Michaelis-Menten equation which describes the rate of

a key enzyme reaction to an overall substrate utilization rate, Equation 6.55 is transformed to give the overall propionate utilization rate by propionate-degrading microorganisms,

$$r_p = \frac{r_{max,p} S(1+\beta S)}{K_p + S} \tag{6.56}$$

This is a non-linear equation containing three unknown parameters, two of them, $r_{max,p}$ and $K_p$, having the same significance as those in a Michaelis–Menten type equation. These three parameters were estimated by using the direct search method to best fit the experimental data with Equation 6.56. The solid line in Figure 6.59 is calculated from the model with the following parameter values,

$r_{max,p} = 0.0162$ mg/mgC/hr

$K_p = 50$ mg/l

$\beta = 0.0002$ l/mg

The question of concern is whether it is worth adding another independent parameter, $\beta$, to the two–parameter model, Equation 6.54. Statistically, this can be answered by calculating the marginal effect of $\beta$ in reducing the variability in predicting the propionate utilization rates when the other two parameters are already in the model. The marginal effect is measured by a coefficient of partial determination which is defined as [207],

$$r^2_{1,2} = \frac{SSE_1 - SSE_2}{SSE_1} = 1 - \frac{SSE_2}{SSE_1} \tag{6.57}$$

Where $SSE_1$ and $SSE_2$ are the error sum of squares of the two models, respectively. The coefficient of partial determination was found to be 0.522, which means that, by adding the third parameter $\beta$, the error sum of squares of the modified

model could be reduced by 52.2 %, compared with the Michaelis-Menten model. Further statistial test can be made to determine whether or not there is a relation between the propionate utilization rate and the three paramenters in the modified Michaelis-Menten model. The F value was found to be 25.7 while $F_{0.95} = 5.79$ [207]. Hence, it can be concluded that all three parameters are significant in describing the propionate utilization rate.

### 6.4.2 Utilization Rate of Butyrate

At the same steady state a butyrate balance around the fermenter leads to the following equation,

$$FS_{i,b} = FS_{e,b} + r_b W \tag{6.58}$$

or,

$$r_b = \frac{F(S_{i,b} - S_{i,b})}{W} \tag{6.59}$$

Where $r_b$ is the butyrate utilization rate (mg/mgC/hr), $F$ the flow rate (l/hr), $W$ the total amount of biomass in terms of total organic carbon in the fermenter (mgC) and $S_{i,b}$, $S_{e,b}$ the butyrate concentrations (mg/l) in the feed and effluent, respectively. The rate, $r_b$, experimentally determined from the right side of Equation 6.59, is plotted vs the butyrate concentrations in the fermenter.

Firstly, the effect of butyrate concentration on butyrate utilization rate was modeled by a Michaelis-Menten model,

$$r_b = \frac{r_{max,b} S_b}{K_b + S_b} \tag{6.60}$$

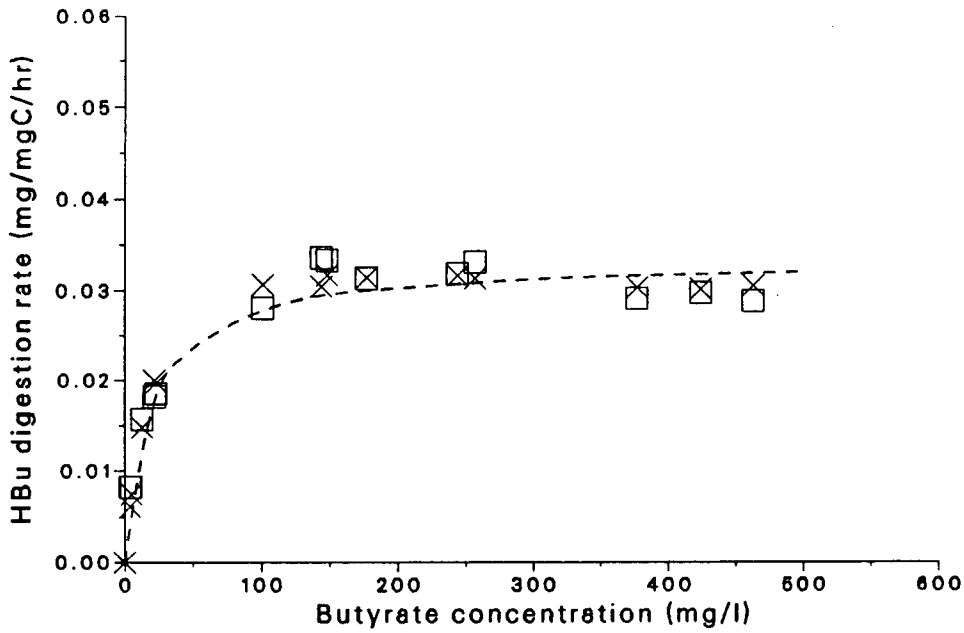


Figure 6.60: Dependence of butyrate digestion rate on butyrate concentration. The dash line is calculated from the Michaelis-Menten equation 6.60; The points (×) are calculated from Equation 6.62

Equation 6.60 was linearized to give an initial estimation of the two parameters, $r_{max,b}$ and $K_b$, and then, the direct search method was used, with the initial estimation as the start point, to further optimize the fitness of the model equation to the experimental data.

$$r_{max,b} = 0.0334 \qquad \text{mg/mgC/hr}$$

$$K_b = 20 \qquad \text{mg/l}$$

Figure 6.60 shows that the butyrate utilization rate is not predicted satisfactorily by the Michaelis-Menten type equation 6.60 represented by the dash line because the rate is depressed at higher butyrate (propionate) concentrations. There are two explanations for this phenomenon. One is that the rate is inhibited by propionate, as indicated earlier in the discussion about the interaction of substrates,

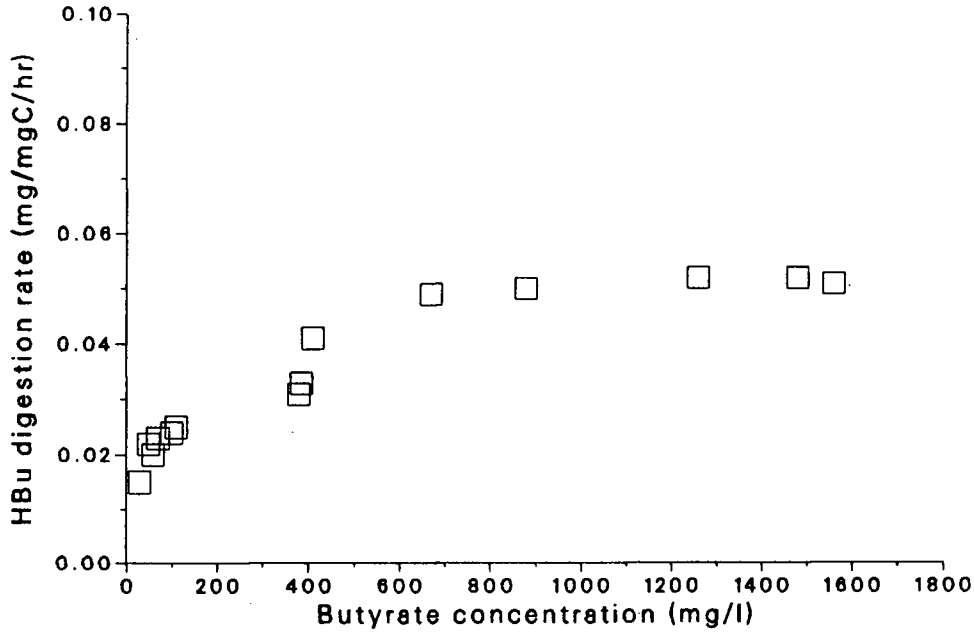


Figure 6.61: Influence of butyrate concentration on butyrate digestion (HPr = 690–900 mg/l)

since the feeds, having a fixed weight ratio of fatty acids, contained also a large amount of propionate at high butyrate concentrations. It may also, on the other hand, be attributed to high butyrate concentrations, i.e., a substrate inhibition. An experiment was designed to check the latter possible mechanism. The propionate concentration was controlled in a narrow range, 690–900 (mg/l), the butyrate concentration in the fermenter was adjusted from 100 to 1500 (mg/l).

As shown in Figure 6.61, the high butyrate concentration did not inhibit its utilization by the responsible bacteria, at least in the present experimental concentration range. Therefore, the only mechanism to explain why the butyrate digestion rate is inhibited is the effect of propionate. This result also indicates that the inhibition of butyric acid in anaerobic digestion processes, as reported by van den Heuvel [181], is caused by the effect of the acid on acidogenic microbes instead of methanogenic

bacteria. It appears that an increase in propionate concentration can promote its own utilization rate but will inhibit the butyrate digestion rate. The inhibition mechanism is assumed to be of the form:

$$E + S \underset{k_{-1}}{\overset{k_1}{\rightleftharpoons}} ES \xrightarrow{k_2} P + E \qquad (1)$$

$$ES_b + S_p \underset{k_{-3}}{\overset{k_3}{\rightleftharpoons}} S_pES_b \qquad \text{(deactivation)} \qquad (2)$$

In addition to the main reaction (1), a Michaelis-Menten reaction, the enzyme-butyrate complex, $ES_b$ may also be attacked by a propionate molecule, $S_p$, which results in a deactivated active enzyme center, $S_pES_b$. A reaction rate expression is derived from this mechanism (see Appendix F for detailed derivation).

$$r = \frac{k_2 S_b}{(k_{-1} + k_2)/k_1 + S_b + (k_3/k_{-3})S_b S_p} \qquad (6.61)$$

Correspondingly, the overall butyrate utilization rate, $r_b$, has a similar expression,

$$r_b = \frac{r_{max,b} S_b}{K_b + S_b + K_I S_b S_p} \qquad (6.62)$$

Where $r_{max,b}$ is the maximum butyrate digestion rate (mg/mgC/hr), $K_b$ the half velocity concentration (mg/l). $K_I$ is a equilibrium constant of the deactivation reaction and has a unit of reciprocal of concentration (l/mg). The direct search method was used to estimate the optimum parameter values to fit the experimental data with Equation 6.62.

$r_{max,b} = 0.0473$ mg/mgC/hr

$K_b = 27$ mg/l

$K_I = 0.000296$ l/mg

The points marked by the sign '×' in Figure 6.60 are predicted by Equation 6.62 with these parameters at different propionate concentrations (20–1700 mg/l).

Again, the addition of the third independent parameter, $K_I$, into the two-parameter model 6.60 was statistically tested by calculating the coefficient of partial determination, and its value was 0.53. Therefore, the introduction of $K_I$ into the model reduced the error sum of squares by 53 % compared with the two-parameter Michaelis-Menten equation 6.60. The F test shows that F = 241 > F(0.95: 2, 13) = 3.81, which means that the butyrate utilization rate is significantly related with all three parameters.

### 6.4.3 Acetate Utilization Rate

At steady state, the amount of acetate which was introduced into the reactor should be balanced by the amount consumed by the bacteria plus that in the effluent. The acetate introduced into the reactor could be divided into direct and indirect input. The direct input was the amount fed into the reactor as feed and the indirect part was the amount converted from propionate and butyrate by the acetogens. Generally one mole of propionate produces one mole of acetate and one mole of butyrate produces two moles of acetate as shown in Table 6.19. The material balance gives

$$FS_{i,a} + W(\frac{M_a}{M_p}r_p + \frac{2M_a}{M_b}r_b) = FS_{e,a} + r_aW \tag{6.63}$$

and it is re-arranged as

$$r_a = \frac{F(S_{i,a} - S_{e,a})}{W} + \frac{M_a}{M_p}r_p + \frac{2M_a}{M_b}r_b \tag{6.64}$$

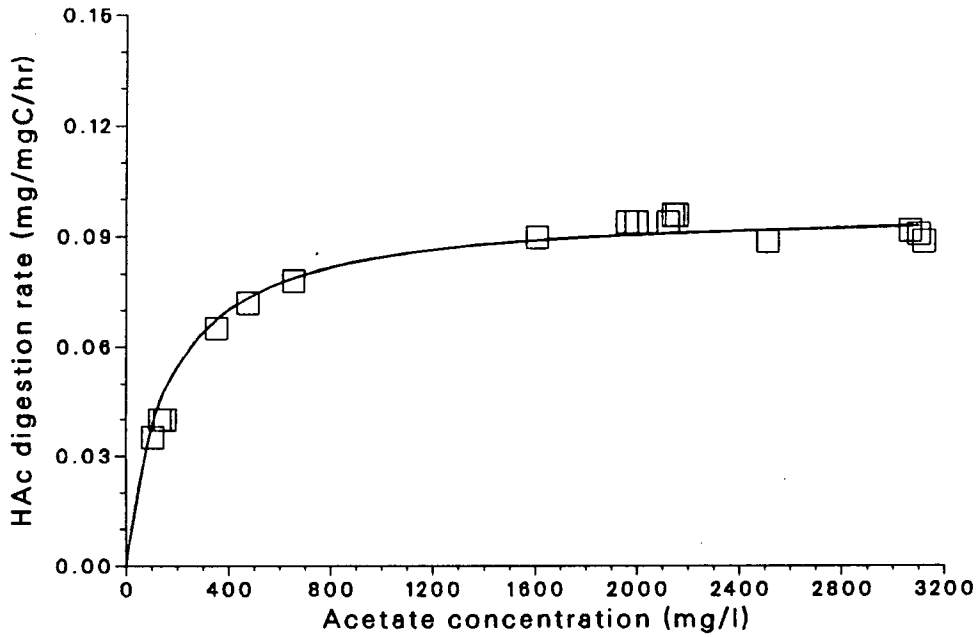


Figure 6.62: Dependence of acetate utilization rate on acetate concentration. The line is calculated from Equation 6.65

Where $F$ is the flow rate of medium (l/hr), $S_{i,a}$, $S_{e,a}$ the acetate concentrations (mg/l) in the feed and effluent, respectively, W the total amount of biomass retained in the fermenter in terms of total organic carbon (mgC), $M_a$, $M_p$, $M_b$ the molecular weight of acetate, propionate and butyrate, $r_a$, $r_p$, $r_b$ the utilization rates of acetate, propionate and butyrate (mg/mgC/hr), respectively. The items on the right side of Equation 6.64 can be determined experimentally. The rate, $r_a$, was plotted against the acetate concentrations in the fermenter, $S_{e,a}$, since in a completely mixed continuous flow reactor the effluent concentration equals the concentration within the reactor.

Figure 6.62 indicates that the dependence of acetate utilization rate on acetate concentration can be described quite well by a Michaelis–Menten type equation. Also it had previously been shown that the acetate utilization rate is affected by

neither propionate nor butyrate as discussed in the section on interaction between substrates.

$$r_a = \frac{r_{max,a} S}{K_a + S} \tag{6.65}$$

The two parameters are estimated by linearizing the non-linear Equation 6.65 as

$$\frac{S}{r_a} = \frac{S}{r_{max,a}} + \frac{K_a}{r_{max,a}} \tag{6.66}$$

and then by using the least square method to fit Equation 6.66 with the experimental data. The initial estimation of the parameters was then used as the first search point from which a direct search was conducted on Equation 6.65 to optimize its fitness to the experimental data. The results are

$$r_{max,a} = 0.098 \qquad \text{mg/mgC/hr}$$

$$K_a = 160 \qquad \text{mg/l.}$$

where $r_{max,a}$ is the maximum utilization rate of acetate and $K_a$ is the half velocity acetate concentration which characterizes the affinity of acetate-utilizing bacteria on acetate. In order to confirm the assumption of stoichiometry of propionate and butyrate conversion to acetate, a feed containing only acetate (14828 mg/l) was used. The acetate digestion rate at steady state was 0.093 (mg/mgC/hr) and acetate concentration in the fermenter was 5611 (mg/l). This rate was obviously the maximum rate since it was very close to the value of $r_{man,a}$. Therefore, it is further confirmed (1) that the presence of propionate and butyrate has no influence on acetate-utilizing bacteria; (2) that the stoichiometry of propionate and butyrate conversion to acetate was reasonable; (3) that the dependence of the acetate utilization rate on acetate concentrations follows the Michaelis–Menten equation up

to 5600 (mg/l).

Table 6.23 summarizes the utilization rates and half velocity constants for the methanogenesis of organic acids obtained in this study and reported in the literature. For the sake of comparison with other data, organic acids are converted to equivalent COD content using the ratios of 1.07 (mg COD/mg acetic acid), 1.51 (mg COD/mg propionic acid) and 1.86 (mg COD/mg butyric acid).

Table 6.23: Methanogenesis of organic acids

| Substrate | Culture | Temp. $C^0$ | pH | $r_{max}$ $\frac{mgCOD}{mgVSS.hr}$ | $K_s$ mgCOD/l | Reference |
|---|---|---|---|---|---|---|
| Acetate | HAc enrichment sludge | 35 | 7 | 0.36 | 165 | [142] |
| Propionate | HPr enrichment sludge | 35 | 7 | 0.6 | 34 | [142] |
| Butyrate | HBu enrichment sludge | 35 | 7 | 1.21 | 5 | [142] |
| Acetate | HAc enrichment biofilms | 35 | 7 | 0.11–0.21 | | [208] |
| Acetate | HAc enrichment sludge | 35 | 7 | 0.45–0.54 | | [144] |
| Acetate | HAc enrichment sludge | 38 | | 0.045 | | [144] |
| Propionate | mixed sludge | 33 | | 0.26 | 246 | [209] |
| Mixed acids | mixed biomass | 35 | 7.2 | 0.712 | 166 | [143] |
| Mixed acids | mixed biofilms | 37 | 7 | 0.02–0.24 | | [114] |
| Mixed acids | | | | | | |
| acetate | mixed biofilms | 35 | 7.1 | 0.3 | 171 | this study |
| propionate | mixed biofilms | 35 | 7.1 | 0.04 | 77 | this study |
| butyrate | mixed biofilms | 35 | 7.1 | 0.22 | 39 | this study |

It should be pointed out here that various measures of biomass have been used by researchers as a base for calculating the substrate utilization rates; suspended solid [143], suspended solid nitrogen [142], particulate protein content [114] and total

organic carbon (this study). Moreover, the cultures had different distributions of bacterial groups in the fermenter, some containing much more acetate-degrading bacteria due to acetate enrichment, some containing a distribution determined by substrate concentrations in the feed. And thus the substrate digestion rate would be different if the rate is based on whole biomass. The next section will discuss this problem further.

## 6.5 Distribution of Bacterial Groups in Balanced Biofilms

As indicated repeatedly, conversion of a mixture of acetate, propionate and butyrate to methane and carbon dioxide needs contributions from at least four distinct functional bacterial groups. This balanced microorganism community contains acetogens which convert propionate and butyrate to acetate and $H_2$, and methanogens which utilize acetate and $CO_2/H_2$ to produce methane and carbon dioxide. Whenever the biomass retained in a fermenter is referred to as the basis for the determination of the utilization rates of these organic acids, all four groups of bacteria are included. Obviously, the distribution of these bacterial species in biofilms has a great effect on the determination of digestion rates of each acid. It is almost impossible, experimentally, to measure this distribution because so many species are involved in the biological process and no convenient method exists to identify and count them. Even in a defined mixed culture the distribution of each species would change corresponding to changes in the environment, such as availability of substrates and nutrients, temperature, pH, alkalinity, dilution rate and toxic components. This may be one reason why the kinetic information obtained on a single acid could not be used to predict the digestion rates of mixtures of organic acids as found by Scharer and Moo-Young [206]. In the present study, a

mixture of three acids with a fixed ratio has been used in the adaptation of the inoculum, formation of biofilms and kinetic experiments with an attempt to have and maintain a balanced bacterial community by a sufficient supply of substrates. In this section, an effort will be made to estimate the distribution of the bacterial groups in a mixed and undefined biofilm.

Lawrence and McCarty [142] used a single acid as substrate to investigate the methanogenesis of fatty acids. In the case of acetic acid, the culture was quite simple and it was believed that only acetate utilizing methanogens existed. But for propionate or butyrate, at least three functional groups were involved, propionate- or butyrate-utilizing bacteria, hydrogen removing bacteria and acetate fermentation bacteria, even though they did not consider the fraction of microorganisms responsible for the generation of methane from $CO_2/H_2$. This approach might be explained by the fact that it is only recently that the important symbiotic function of this fraction of bacteria has been discovered. Their estimation of the bacteria distribution in the 'two-components' sludge was based on thermodynamic principles. The more free energy available as a result of biochemical transformations of substrate, the more bacteria growth responsible for this substrate dissimilation. More researchers, however, just took the mixed culture as a pure one, and so, their results were based on total volatile suspended solids [143,211,212], on adsorbed particulate organic nitrogen (PON) [114], or on volatile film solids [213]. Some of them only used the reactor volume as the basis for the evaluation of various types of fermenters such as upflow sludge bed reactors and fixed bed reactors [214] even though the retained biomass was the key parameter for these reactors.

In a nutrient-rich environment, all bacterial species get enough food supply and grow at their intrinsic maximum growth rate, correspondingly, each substrate is

consumed at its maximum dissimilation rate, $r_{max,i}$. Experimentally, this situation can be confirmed by using much higher concentrations of substrates in the fermenter than their half velocity concentrations, $K_i$. If this rate is based on 1 mg of biomass and only four major functional groups are considered, this one mg of biomass contains $m_a$, $m_p$, $m_b$, $m_h$ mgs of bacteria responsible for the utilization of acetate, propionate, butyrate and hydrogen, respectively.

$$m_a + m_p + m_b + m_h = 1 \quad (mgC) \tag{6.67}$$

that is,

$$m_a(1 + \frac{m_p}{m_a} + \frac{m_b}{m_a} + \frac{m_h}{m_a}) = 1 \tag{6.68}$$

or,

$$m_a = \frac{1}{1 + m_p/m_a + m_b/m_a + m_h/m_a} \tag{6.69}$$

The investigation on build-up of symbiotic methanogenic biofilms revealed that the acetate-, propionate- and butyrate-utilizing bacteria had the same intrinsic maximum growth rate, and this was also reported by Lawrence and McCarty [142] in their studies on single acid methanogenesis. Therefore, the distribution of these three specific bacterial groups in a biofilm mainly depends on their initial attachment on the biofilm supports because the initial attached cells simultaneously multiply, forming colonies and biofilms. The attachment of each specific bacterial group was expressed as $k_i[x]_i$, where $[x]_i$ is the free cell concentration in the culture medium and $k_i$ the specific attachment rate affected by the physicochemical properties of the supports.

$$\frac{m_p}{m_a} = \frac{k_p[x]_p}{k_a[x]_a} \tag{6.70}$$

and

$$\frac{m_b}{m_a} = \frac{k_b[x]_b}{k_a[x]_a} \tag{6.71}$$

If the number of bacterial cells in unit volume of medium was so high that the attachment rate became a quasi-0th order rate,

$$\frac{m_p}{m_a} = \frac{k_p}{k_a} \tag{6.72}$$

and

$$\frac{m_b}{m_a} = \frac{k_b}{k_a} \tag{6.73}$$

In the nutrient-rich environment, acetate, propionate and butyrate are being consumed at their maximum rates (mg/mgC/hr);

$$r_a = \frac{r_{max,a} S_a}{K_a + S_a} \simeq r_{max,a} \tag{6.74}$$

$$r_p = \frac{r_{max,p} S_p (1 + \beta S_p)}{K_p + S_p} \simeq r_{max,p}(1 + 0.0004 S_p) \tag{6.75}$$

$$r_b = \frac{r_{max,b} S_b}{K_b + S_b + K_I S_b S_b} \simeq \frac{r_{max,b}}{1 + 0.00015 S_p} \tag{6.76}$$

If propionate concentration in the environment is controlled under 1000 mg/l, but still much higher than 50 mg/l, the half velocity propionate concentration of the propionate dissimilation rate, Equations 6.75 and 6.76 simplify to,

$$r_p = r_{max,p} \tag{6.77}$$

and

$$r_b = r_{max,b} \tag{6.78}$$

When propionate and butyrate are digested by the bacteria at the above rates, hydrogen is produced as shown in Table 6.19, one mole of propionate to 3 moles of hydrogen and one mole of butyrate to 2 of moles hydrogen. In a mature balanced biofilm, these 5 moles of hydrogen must be removed by the $H_2$-utilizing bacteria to keep the $H_2$ concentration in the fermenter very low.

$$4H_2 + HCO_3^- + H^+ \rightarrow CH_4 + 3H_2O$$

Therefore, the hydrogen removal rate is

$$r_h = \frac{3}{M_p} r_{max,p} + \frac{2}{M_b} r_{max,b} \tag{6.79}$$

where $r_h$ is the hydrogen removal rate by symbiotic bacteria (mmol/mgC/hr), $M_p$, $M_b$ the molecular weight of propionate and butyrate. Correspondingly, according to the conversion of $CO_2/H_2$ to methane above, the methane production rate from $CO_2/H_2$ utilization, $r_{m,h}$ (mmol/mgC/hr), can be expressed as follows,

$$r_{m,h} = \frac{r_h}{4} = \frac{3}{4M_p} r_{max,p} + \frac{2}{4M_b} r_{max,b} \tag{6.80}$$

Another source of methane production is from acetate fermentation, one mole of acetate being converted to one mole of methane.

$$r_{m,a} = \frac{r_{max,a}}{M_a} \tag{6.81}$$

where $r_{m,a}$ is the methane production rate from acetate digestion (mmol/mgC/hr). Acetate conversion includes the reduction of the methyl group of acetic acid [142]. The dissimilation of acetic acid to methane requires the net transfer of one electron and the free energy decrement of the conversion is small. However, the formation of a methane molecule by carbon dioxide reduction requires a net transfer of eight electrons. Hence, the free energy decrement of the conversion of hydrogen and carbon dioxide to methane is approximately three times the free energy decrement of the dissimilation of acetic acid to methane and carbon dioxide as reported by Smith and Mah [64]. If formation of one mmole of methane from acetate gives $\Delta G$ (J) free energy, and then, the energy production rates (J/mgC/hr) for these two reactions are

$$r_{e,h} = 3r_{m,h}\Delta G \tag{6.82}$$

and

$$r_{e,a} = r_{m,a}\Delta G \tag{6.83}$$

The basic mechanism by which the free energy available from the two reactions may be utilized is by the trapping of this energy through the formation of the energy-rich intermediate, ATP. It has been shown that the yield of cells (cell mass mg) with respect to the amount of ATP (mmole) used is a constant, typically 10.5 (mg/mmol ATP) [210]. Assume these two groups of methane-producing bacteria having the same energy utilization efficiency, then the efficiency to store the free energy available from the reactions into ATP is $Y_{ATP}$ (mmol ATP/kJ free energy). The ratio of the bacterial biomass responsible for $CO_2/H_2$ utilization to that responsible for acetate conversion is proportional to their ATP yield rates from their own substrate utilization.

$$\frac{m_h}{m_a} = \frac{10.5 Y_{ATP} r_{e,h}}{10.5 Y_{ATP} r_{e,a}} = \frac{r_{e,h}}{r_{e,a}} \tag{6.84}$$

This equation implies that the group which can obtain more energy from its substrate utilization would predominate in the methanogenic sub-community. Replacing Equations 6.82, 6.83, 6.80 and 6.81 into Equation 6.84 gives

$$\frac{m_h}{m_a} = \frac{9/M_p r_{max,p} + 6/M_b r_{max,b}}{4/M_a r_{max,a}} \tag{6.85}$$

Put Equations 6.72, 6.73, 6.85 into Equation 6.69 and get Equation 6.86 for estimating the amount of biomass (mg organic carbon) responsible for acetate digestion within one mg organic carbon of biofilm in a nutrient-rich environment.

$$m_a = \frac{1}{1 + k_p/k_a + k_b/k_a + (\frac{9M_a}{M_p} r_{max,P} + \frac{6M_a}{M_b} r_{max,b})/4r_{max,a}} \tag{6.86}$$

Using Equations 6.72, 6.73, 6.85 and the estimated $m_a$ expression above gives the estimations for $m_p$, $m_b$ and $m_h$, respectively.

$$m_p = \frac{k_p/k_a}{1 + k_p/k_a + k_b/k_a + (\frac{9M_a}{M_p} r_{max,p} + \frac{6M_a}{M_b} r_{max,b})/4r_{max,a}} \tag{6.87}$$

$$m_b = \frac{k_b/k_a}{1 + k_p/k_a + k_b/k_a + (\frac{9M_a}{M_p} r_{max,p} + \frac{6M_a}{M_b} r_{max,b}/4r_{max,a}} \tag{6.88}$$

$$m_h = \frac{(\frac{9M_a}{M_p} r_{max,p} + \frac{6M_a}{M_b} r_{max,b})/4r_{max,a}}{1 + k_p/k_a + k_b/k_a + (\frac{9M_a}{M_p} r_{max,p} + \frac{6M_a}{M_b} r_{max,b})/4r_{max,a}} \tag{6.89}$$

Table 6.24 lists the maximum utilization rates of fatty acids, $r_{max,i}$, based on the integrated biomass of a methanogenic biofilm, the fractional biomass responsible

for each acid digestion in one mg of the integrated biomass and the recalculated maximum dissimilation rates of the organic acids, $r'_{max,i}$ based on only a fractional biomass being responsible for the specific dissimilation reaction. The hydrogen removing rate is estimated from the Equation 6.79.

Table 6.24: Fractional mass of bacterial groups and utilization rates of fatty acids

| Substrate | $r_{max}$ (mg/mgC/hr) | $m_i$ (mgC,i/mgC) | $r'_{max}$ (mg/mgC,i/hr) |
|---|---|---|---|
| Acetate | 0.098 | 0.26 | 0.38 |
| Propionate | 0.0162 | 0.22 | 0.074 |
| Butyrate | 0.0473 | 0.32 | 0.148 |
| $H_2$ | 0.0035 | 0.20 | 0.018 |

# Chapter 7

## Mass Transfer in Biofilms

Immobilization of microorganisms results in two distinctive phases in a fermenter, the liquid medium phase and the solid phase of biofilms or bioflocks. Different mechanisms of substrate transfer are involved in these two phases. The hydraulics, the macro-transport of water and substrates within the liquid phase, differs very much from one reactor type to another, just as the significance of a possible liquid film layer which is adjacent to the solid phase does. However, common to all types of reactors is the process of mass transfer within the solid phase which is a combination of bacterial cells, extracellular polysaccharides and some inorganic salts trapped in the biofilms. Fick's laws of diffusion form the basis for the current theoretical approaches to the mass transfer within the biofilms.

### 7.1 Diffusivities of Substrates in Water

Fick (1855) developed the laws of diffusion by analogy to Fourier's work and defined a one dimensional flux $J_A$ as:

$$J_A = D_{AB}\frac{dc}{dl} \tag{7.90}$$

Where $J_A$ is the flux of solute, A, through unit area across which diffusion is occurring, $c$ is the concentration of the solute and $l$ the distance in the solvent B. The quantity $D_{AB}$, which Fick called "the constant depending on the nature of the substance" is the diffusion coefficient of solute A in solvent B. To estimate the diffusivities of various solutes

in solvents, prediction methods have been developed based on a variety of theories, such as hydrodynamic theory, kinetic theory and statistical mechanics, as reported in several reviews [194,195,196]. Among them the Stokes-Einstein equation [197]

$$D_{AB} = \frac{RT}{6\pi\eta_B R_A} \tag{7.91}$$

has found wide application which considers the solute A as large spherical molecules diffusing in a dilute solution. Many researchers have used it as a starting point in developing their correlations [197]. In Equation 7.91 $\eta_B$ is the viscosity of the solvent and $R_A$ is the radius of the 'spherical' solute. In the present study an old but still widely used correlation for $D_{AB}$ in infinite dilution, the Wilke-Chang (1955) estimation method [198], was used to estimate the diffusivities of lactose, acetic, propionic and butyric acids in the culture mediums.

$$D^0_{AB} = \frac{7.4 * 10^{-8}(\phi M_B)^{1/2} T}{\eta_B V_A^{0.6}} \tag{7.92}$$

where

$D^0_{AB}$ = diffusivity of solute A at very low concentrations in solvent B, $cm^2/s$

$\phi$ = association factor of solvent B, dimensionless

$M_B$ = molecular weight of solvent B, g/mole

$T$ = temperature, K

$\eta_B$ =viscosity of solvent B, cp

$V_A$ = molar volume of solute A at its normal boiling temperature, $cm^3/mol$.

Table 7.25 lists the estimated diffusivities of the concerned solutes and experimental values if available. The values of $V_A$ were calculated from Le Bas' additive method [197]. The diffusivity of sucrose is also listed in the table since to this author's knowledge the experimental value of lactose diffusivity in water solutions is unavailable while sucrose has

Table 7.25: Diffusivities in water at 35 $^0C$

| Solute | $V_A$ ($cm^3/mol$) | $D \times 10^5$ ($cm^2/sec$) | $D_{exp} \times 10^5$ ($cm^2/sec$) | Reference |
|---|---|---|---|---|
| Lactose | 291.2 | 0.72 | | |
| Sucrose | 294.7 | 0.71 | 0.75 | [199] |
| Acetic acid | 68.4 | 1.71 | 1.74 | [199] |
| Propionic acid | 90.6 | 1.45 | | |
| Butyric acid | 112.8 | 1.27 | | |

the same molecular weight and equivalent molecular size as lactose. Equation 7.92 was also used to convert the experimental data measured at other temperatures to those at 35 $^0C$. Comparing the calculated diffusivities of acetate and sucrose with those measured experimentally indicates that Wilke-Chang equation 7.92 has a satisfying accuracy.

The diffusivity of a solute in infinite dilution implies that each solute molecule is in an environment of pure solvent. From an engineering viewpoint this value might be used to represent the diffusion coefficient for concentrations of solute up to 5 and perhaps 10 mole percent [197]. This reported finding may be due to the fact that the solute molecules in an aqueous solution are densely packed and strongly affected by the force fields of neighboring molecules and even in a dilute solution the major influence still comes from the water molecules. The concentrations of substrates in this study were not higher than 10 g/l. Although other components like nutrients and products exist in the culture medium, the substrate molecules are still mostly surrounded by the water molecules, and hence the medium can be thought of as a dilute solution.

## 7.2 Principle of Mass Transfer Measurement within Biofilms

As indicated in Chapter 2, the biofilms contain many irregular channels through which the substrates transport from outer to inner layers by molecular diffusion to replenish

the consumed substrates. The channels have very complicated structures, tortuous and even dead-ends. Therefore, it is almost impossible to describe them mathematically. It is common, analogous to reactions in a porous catalyst, to express the diffusion in the biofilm by a parameter, De, the effective diffusion coefficient. In this way, the transfer of substrate molecules in the biofilm can be imagined as proceeding in a homogeneous medium and still can be described by Fick's law,

$$J_A = De\frac{dc}{dl} \tag{7.93}$$

Compared with Equation 7.90, this modified Fick's law only replaced the diffusivity, $D_{AB}$, with the effective diffusivity, De.

When an active biofilm slab is immersed in a culture medium, the substrate molecules transport from the bulk solution to the outer face of the biofilm, and then, at the same time they penetrate into the biofilm, some of them are digested by the bacteria embedded in the biofilm. Finally a steady state is achieved and the substrate concentration has a distribution within the biofilm as shown in Figure 7.63.

Since in an active biofilm the substrate diffusion and digestion occur simultaneously, a diffusion–reaction model could be deduced by making a material balance around the elemental volume in Figure 7.63. Usually, biofilms are quite thin with the thickness ranging from tens to several hundreds of micrometers and thus the mass transfer from the side areas is negligible. A diffusion–reaction model with one dimensional diffusion is deduced as follows;

$$\text{Diffusion in} = \text{Diffusion out} + \text{Consumption by reaction}$$

$$-AD_e\frac{d}{dl}(S - \frac{dS}{dl}\Delta l) = -AD_e\frac{dS}{dl} + \Delta l A\rho_c r \tag{7.94}$$

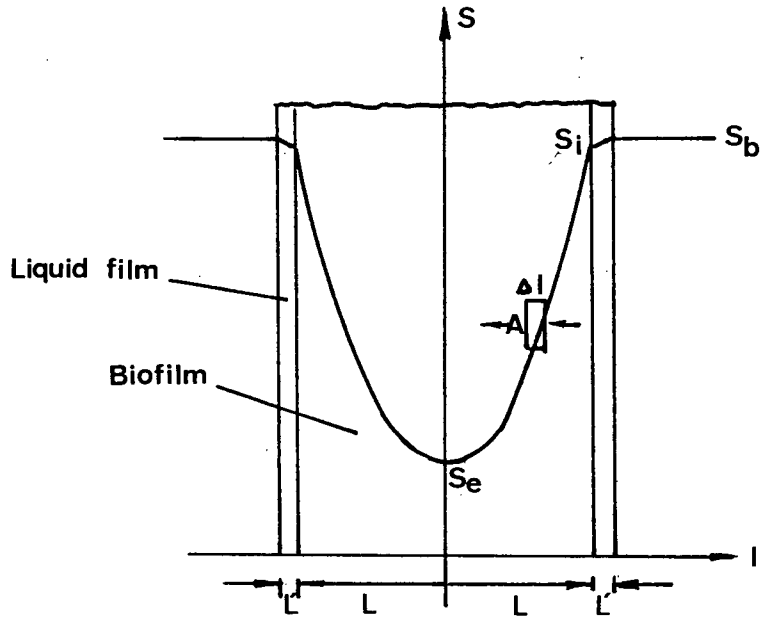


Figure 7.63: Substrate concentration distribution within a biofilm at steady state, The elemental volume has a thickness $\Delta l$ and an area A.

$$AD_e \frac{d^2S}{dl^2} \Delta l = \Delta l A \rho_c r \tag{7.95}$$

$$D_e \frac{d^2S}{dl^2} = \rho_c r \tag{7.96}$$

Where $D_e$ is the effective diffusion coefficient of substrate molecules in the biofilm ($cm^2/sec$), $S$ the substrate concentration ($mg/cm^3$), $\rho_c$ the density of the biofilm ($mgC/cm^3$), $r$ the substrate utilization rate based on unit weight of biofilm ($mg/mgC/sec$). $\Delta l$ and $A$ are the thickness and area of the elemental volume respectively. The left side of Equation 7.96 is the net amount of substrate transported into a unit volume of the biofilm and which should be digested by the bacteria embedded in this volume at steady state as represented by the right side of the equation. In situ measurement of substrate transport in active biofilms requires the knowledge of the intrinsic kinetics of substrate

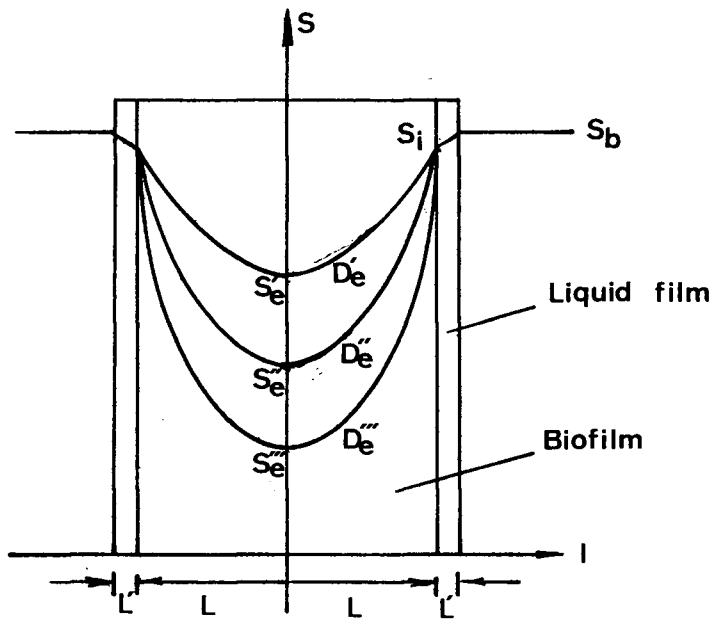


Figure 7.64: Influence of $D_e$ on substrate concentration distribution within a biofilm, $D'_e > D''_e > D'''_e$.

utilization by the target bacteria. The previous two chapters have described the intrinsic kinetics of lactose digestion in acidogenic biofilms and of organic acids degradation in methanogenic biofilms.

Mathematically, Equation 7.96 can be solved by a numeric method when two boundary conditions are determined.

$$S = S_i \qquad \text{at } l = \text{L} \qquad \text{(biofilm surface)}$$

$$dS/dl = 0 \qquad \text{at } l = 0 \qquad \text{(due to the symmetry of biofilms)}$$

Therefore, a family of curves can be obtained which describe the substrate concentration distribution depending on the values of effective diffusion coefficient as shown in Figure 7.64.

Theoretically, if another experimentally determined value can be found, for example,

$S_e$, the substrate concentration at the center of the biofilm slab, the substrate distribution within the biofilm can be determined uniquely, and thus, the effective diffusion coefficient. In this sense, the effective diffusion coefficient, $D_e$, becomes a model parameter of the reaction–diffusion model rather than a physical parameter determined only by the properties of the solute and the pseudo-homogeneous solvent (medium plus biofilms). However, as long as the assumption of one dimensional diffusion holds for the actual processes such as substrate diffusion in thin biofilms or bioflocks, the possible error caused by the assumption can be minimized or eliminated. Putting the utilization rate expressions for lactose and organic acids into the diffusion-reaction model, Equation 7.96, gives a second-order ordinary differential equation;

$$D_e \frac{d^2S}{dl^2} = \rho_c \frac{r_{max} S}{K_s + S} \tag{7.97}$$

A numerical method must be used to solve this equation. If the boundary conditions at $l = 0$ ($S_e$ and $dS/dl$) are known, the boundary condition problem can be solved as an initial value problem and the value of $D_e$ can be determined by fitting the experimental value of $S_i$, the substrate concentration on the biofilm surface, with the calculated value from Equation 7.97. In this study, the Runge-Kutta-Fehlberg (RKF) method, was selected from many available numerical methods [200] to solve this initial value problem. The RKF method (see Appendix G) has the advantages of requiring fewer calculations and having the ability to control local truncation error and its local error is less than $h^6$ (h is the step size).

So, the key point in the present work is how to measure the substrate concentration at the center of a biofilm, $S_e$, as well as the concentration on the biofilm surface, $S_i$, and also how to meet the boundary condition at the center of the biofilm, $dS/dl = 0$.

## 7.3 Experimental Setup

The general experimental setup has been described in Chapter 3, the same one as for the kinetic studies. The major difference is the support on which biofilms formed. In the kinetic experiments the support surface was made of many PVC sheets (1.5 mm thick) and thus the biomass on the supports was a major part of whole biomass retained in the reactor. In the measurement of substrate diffusivities within biofilms, however, a diffusion cell was used since the attention was focused on the biofilm growing on the membrane filters and other biomass was not very important. The device's structure has also been described in Chapter 3.

On the each side of the cell a cellulose nitrate membrane filter (pore size = 0.45 $\mu$m, Sartorius, W. Germany) was fixed by sandwiching it between two rubber gaskets, and hence, the bacteria (d = 1 $\mu$m) could not enter into the cell while the substrates could be transported into the cell through the layers of biofilm and the membrane filters. This was confirmed by the observation that there was no water leakage after replacing the membrane filters with plastic films. Biofilms (acidogenic or methanogenic ) formed uniformly on the filters and had the same thickness on each side of the cell as shown in Figure 7.65.

Because no bacteria was inside the cell due to the pore size of the filters, the substrates which moved into the cell would not be further digested, therefore, the substrate concentration within the cell, $S_e$, equals that on the other side of the membrane filter, $S'_e$, if a steady state was maintained. This condition could exist only at steady state because at unsteady states, mass transfer occurred across the filter, and thus, $S_e \neq S'_e$. The medium within the cell was recycled to promote a uniform concentration as well as the establishment of steady state. Moreover, because of the symmetry of both the cell's

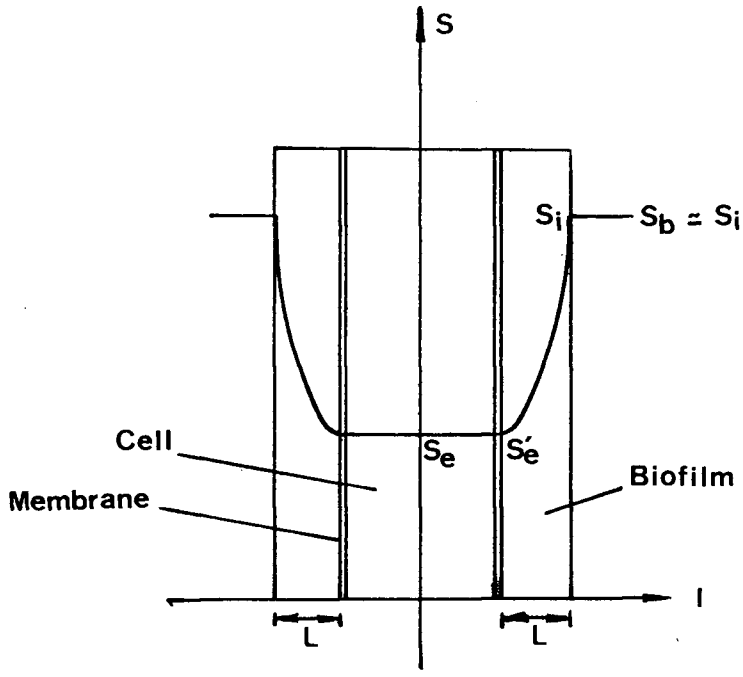


Figure 7.65: The biofilms symmetrically fixed on the two membrane filters of the diffusion-measuring cell

structure and the biofilms formed on the two membrane filters, the substrate concentration indice the divice, $S_e$, was the concentration at the biofilm center as mentioned in the last section if the two biofilms on the membranes were thought of as the two half biofilms shown in Figure 7.63. The symmetrical characteristics of the diffusion cell also gave another boundary condition at steady state, $dS/dl = 0$, at each membrane filter.

The two boundary conditions at $l$=0 are known or experimentally available from the discussion above. The third one, the substrate concentration on the biofilm surface, $S_i$, can be determined from the bulk concentration if the (imagined) liquid film thickness adjacent to the biofilm is known. Experimentally, the liquid velocity over the biofilm can be increased to such an extent that the liquid film or its effect is negligible and the substrate concentration on the biofilm surface approaches that of the bulk solution.

## 7.4 Diffusivity of Lactose in Acidogenic Biofilms

As in the experiments made to measure the kinetics of lactose utilization, the feed contains lactose as the limited organic substrate and inorganic salts as growth nutrients (listed in Table 3.9). The lactose concentration in the feed was 5–6 g/l. To prevent lactose from being digested in the feed tank, the same measures as mentioned in lactose acidogenesis kinetics were used, i.e. low temperature, low oxygen partial pressure and small amount of feed prepared each time. The pH of the culture was controlled at 4.6±0.2 with 0.5 N NaOH solution. The medium in the reactor was recycled to produce a uniform concentration and temperature distribution in the reactor, and also, to reduce the external mass transfer resistance by increasing the recycle flow rate. The temperature was maintained at 35±2 $^0C$.

In situ measurement of lactose diffusivity in acidogenic biofilms was carried out in two stages, formation of biofilms on the cell's membrane and measuring lactose concentrations outside and inside the cell at steady state.

The fermenter was first fed with a diluted feed (2 g lactose/l) and $N_2$ was introduced to strip off the oxygen dissolved in the medium. After the temperature and pH of the medium were adjusted to 35 $^0C$ and 4.6, respectively, the diffusion device which had a capacity of 30 $cm^3$ was immersed in the medium. Gradually the medium penetrated into the device through the membranes. When the liquid outside and inside the cell reached the same level, recycle of the liquid within the cell was started. Analyses for lactose showed the same concentrations outside and inside the cell. Under a $N_2$ atmosphere the fermenter was seeded with 50 ml of inoculum collected from the effluent of lactose acidogenesis. The fermenter was then operated in batch mode. To obtain qualitative information on the formation of the biofilms, when the cell was immersed in the reactor some PVC slides, used as in the kinetic studies, were also immersed into the medium

since it was believed that biofilm formation was easier on the membranes than on PVC sheets. After the lactose had been used up, half the volume of the culture (500 ml) was replaced by a fresh feed (5 g lactose/l) and this was repeated until a biofilm had formed on the membranes. After biofilms were observed on the removable PVC slides the reactor operation was shifted to continuous mode. Every seven days the biofilm on a removable PVC slide was measured and the second stage started when a thick biofilm (ca. 1 mm) had formed.

The second stage was to measure the steady-state lactose concentrations outside and inside the cell. To ensure that a steady-state concentration was being measured, a disturbance was given to the concentration inside the cell while the outside concentration was maintained as stable as possible. This was done by replacing 20 ml of the liquid within the cell with the same volume of distilled water which had been stripped of dissolved $O_2$ by $N_2$, and then the lactose concentration within the cell was monitored until there was no further change in the concentration.

Figure 7.66 shows that the lactose concentration inside the device, after dilution with oxygen-free distilled water, approached a constant value, which means that a steady state was reached. To confirm this, the dynamic behavior of the device was further investigated.

When the lactose concentrations inside and outside the cell were at a steady state, the feed flow rate, and thus the outside concentration was gradually reduced to a new level, and then returned to the original flow rate as shown in Figure 7.67. It was found that the inside lactose concentration, corresponding to the change in the lactose concentration of the bulk solution, also decreased to a lower value of 30 mg/l from a steady-state of 46 mg/l and then it returned to the original level of 45 mg/l as shown in Figure 7.68. This indicated that the dynamic response of the cell was quite good and that as long as

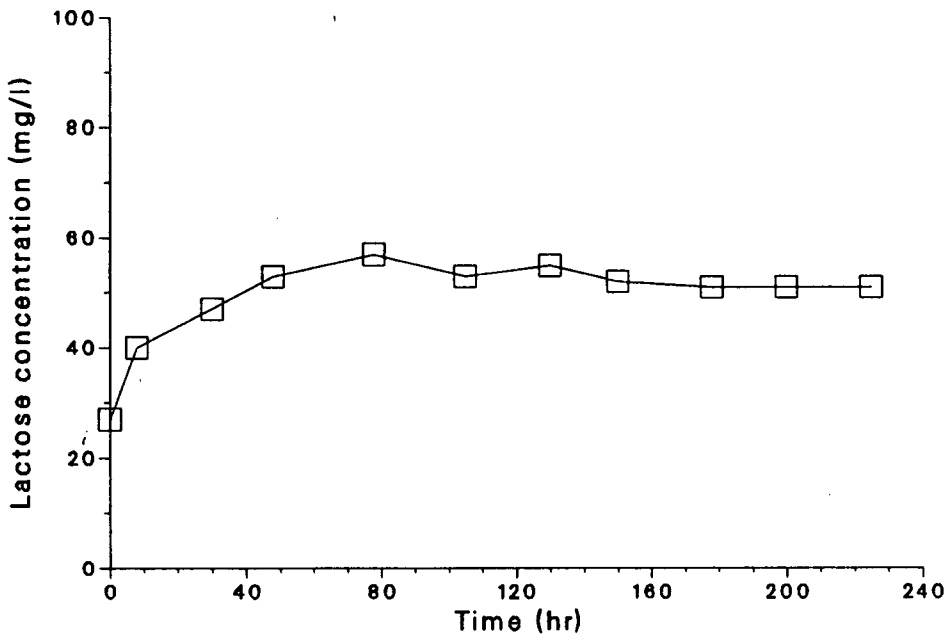


Figure 7.66: A steady-state lactose concentration inside the cell was established after a dilution. The lactose concentration outside the cell ranged from 1750 to 1900 mg/l.

a steady-state outside concentration was maintained longer than 5 hours, a corresponding steady-state inside lactose concentration could be obtained because under normal operating conditions the inside lactose concentration fluctuation was not more than 15 mg/l.

This dynamic behavior also made it possible to use reliable operating conditions since fluctuations in the outside lactose concentration was unavoidable, however it was relatively easy to keep it at a steady state for 5 – 8 hours. Moreover, during this short period of time the biofilm thickness (see Chapter 4) would not increase markedly and a quasi-steady state biofilm thickness could be assumed.

As shown in the experimental results of the kinetic studies in Chapter 4, the external mass transfer could be reduced to a negligible extent by increasing the recycle velocity, and thus the velocity over the biofilms. Under this condition the lactose concentration

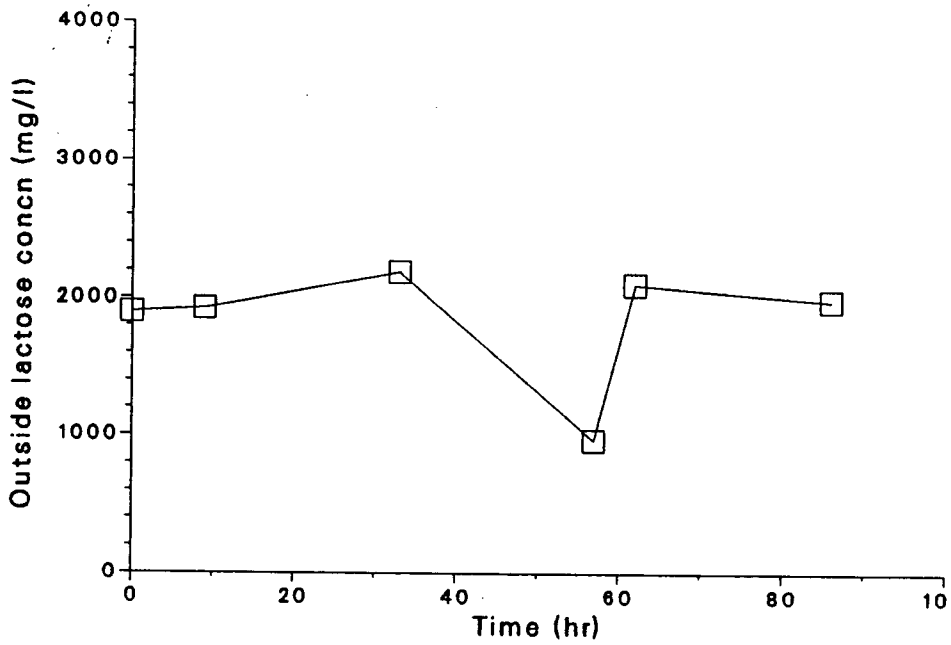


Figure 7.67: A controlled change in the lactose concentration of bulk culture solution

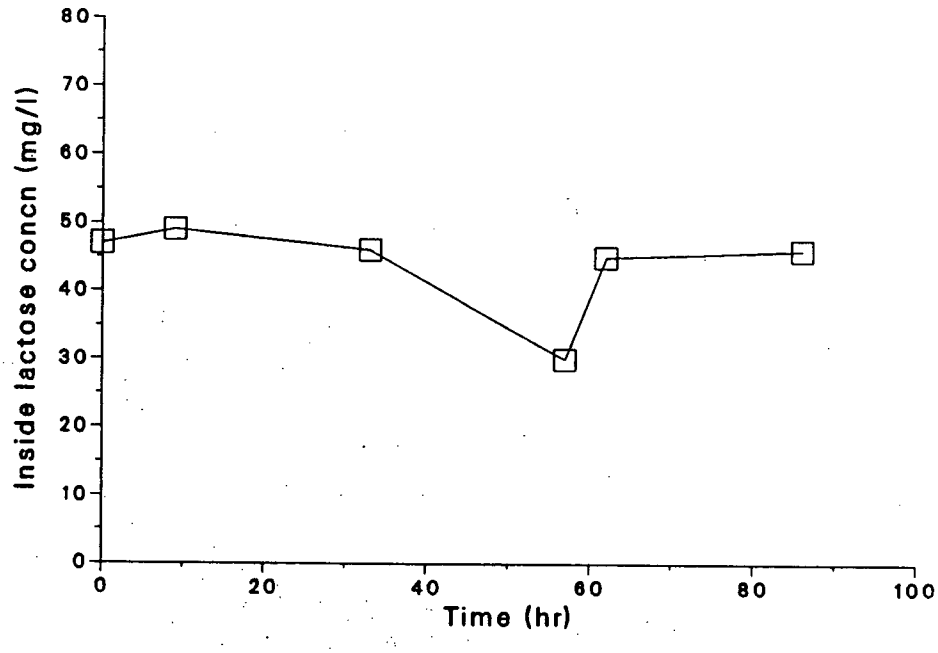


Figure 7.68: Dynamic response of lactose concentration inside the cell to the controlled change in the outside lactose concentration

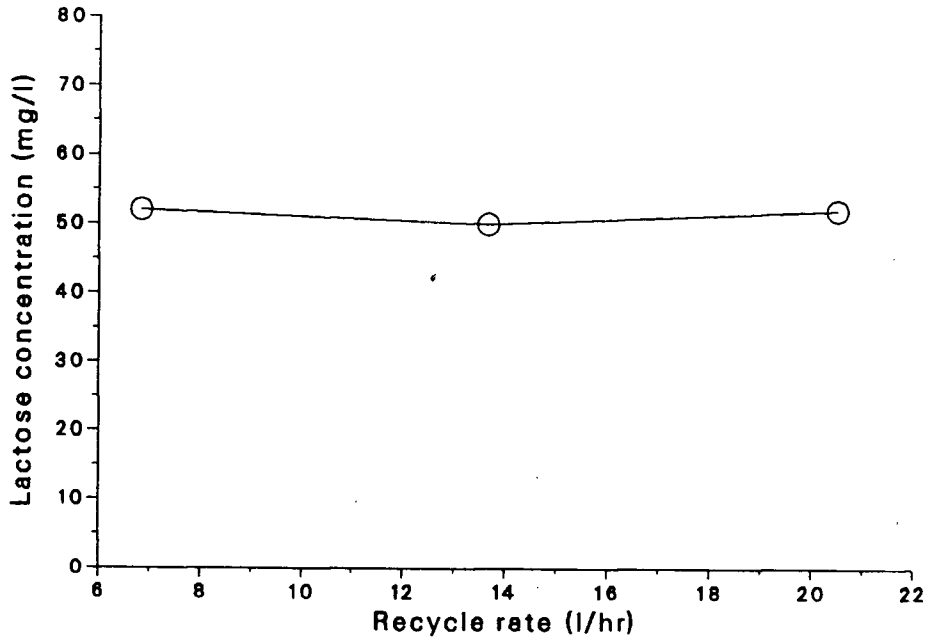


Figure 7.69: Effect of recycle rate on the lactose concentration inside the cell. The lactose concentration in the bulk solution ranged from 1857 to 1750 mg/l

on the biofilms, $S_i$, was very close to the concentration, $S_b$, in the bulk solution which was measurable. Figure 7.69 indicates that under different recycle rates the steady-state lactose concentration inside the cell did not change markedly when the outside concentration was kept within a narrow range. This fact implies: (1) that the major resistance to lactose transfer from the bulk solution to the cell was in the biofilm and (2) that the mass transfer resistance between the bulk solution and the biofilm surface was negligible. Therefore, with a recycle rate of 220 ml/min the bulk solution, $S_b$, was a reasonable approximation of $S_i$.

Finally after steady-state lactose concentrations outside and inside the cell had been measured and judged to be satisfactory, the diffusion cell was taken out of the fermenter and the biofilms on the membrane filters were carefully collected and analyzed according to the procedures described in Chapter 3. The biofilms on the two membrane filters had

Table 7.26: Effective diffusivity of lactose within acidogenic biofilms at 35 $^0C$

| Parameter | Unit | Value |
|---|---|---|
| $S_b$ | mg/l | 2114 |
| $S_e$ | mg/l | 45 |
| $L$ | mm | 1.3 |
| $\rho_c$ | mgC/ml | 29.7 |
| $r_{max}$ | mg/mgC/hr | 0.3144 |
| $K_s$ | mg/l | 201 |
| $D_e$ | $\times 10^{-5}$ cm$^2$/sec | 0.47 |
| $De/D$ | | 0.653 |

almost the same thickness, 1.32 mm and 1.29 mm respectively, which means that the biofilms were symmetrical. Therefore, the prerequisite on the boundary conditions at $l$ = 0 as discussed in the last section was satisfied and the conditions were reliable. By using these data and the numerical solution method, the diffusivity of lactose within the acidogenic biofilms was estimated and the results are listed in Table 7.26.

Obviously, the value of lactose effective diffusivity in acidogenic biofilms estimated in this way depended on many factors even if the calculating error of the numerical method was controlled to within a reasonable range ($< 10^{-4}$). It was affected not only by the calculated values of the intrinsic lactose utilization rate in biofilms, $K_s$ and $r_{max}$, but also by the biofilm thickness and density, $L$ and $\rho_c$, as well as the lactose concentrations inside and outside the diffusion cell, $S_e$ and $S_b$. Table 7.27 compares the influence of these data on the effective diffusivity, De, (the sensitivity of De to the possible error of these data) by giving one of them a 10 % fluctuation while the rest are unchanged. The most sensitive parameter was the biofilm thickness which could give a 15 % error and the least sensitive ones were concentration inside the device, $S_e$ and the kinetic parameter $K_s$ since they gave a corresponding error less than 5 %. The error caused in the other parameters was not amplified or reduced. Therefore, experimentally, more attention was

Table 7.27: Sensitivity of lactose effective diffusivity to experimental error

| Parameter | $S_e$ | $S_b$ | $L$ | $\rho_c$ | $r_{max}$ | $K_s$ |
|---|---|---|---|---|---|---|
| Unit | mg/l | mg/l | mm | mgC/ml | mg/mgC/hr | mg/l |
| Value | 45 | 2114 | 1.3 | 29.7 | 0.314 | 201 |
| Error (%) | +10 | +10 | +10 | +10 | +10 | +10 |
| De error (%) | +2.9 | -7.1 | +15.9 | +10 | +10 | -4.8 |
| Error (%) | -10 | -10 | -10 | -10 | -10 | -10 |
| De error (%) | -3.1 | +8.4 | -14.9 | -10 | -10 | +5.2 |

given to the measurement of the sensitive parameters like the biofilm thickness, density, and the maximum utilization rate to reduce the possible error.

## 7.5 Effective Diffusivities of Organic Acids in Methanogenic Biofilms

Using the same diffusion–measuring device and the fermenter as described before, the process for measuring the effective diffusivities of organic acids in methanogenic biofilms could also be divided into two stages, formation of the biofilms on the two membrane filters of the cell and then measuring the organic acids concentrations inside and outside the cell.

### 7.5.1 Formation of Symbiotic Methanogenic Biofilms

In order to build up balanced methanogenic biofilms which comprised acetate-, propionate- and butyrate-utilizing bacteria, on the membranes of the device, an inoculum was collected from a methanogenic phase reactor which was being fed with a mixture of organic acids. Also, the feed was a mixture of acetate, propionate and butyrate at concentrations of 5, 2.5, 2.5 (g/l), respectively, which could supply enough substrates to each bacterial group in the fermenter. The inorganic salts listed in Table 3.9 were used as growth nutrients.

The reactor was firstly filled with 500 ml of tap water and 500 ml of culture medium and nitrogen was introduced to strip out the dissolved oxygen. The cell was immersed into the solution, and the liquid penetrated into the cell through the membrane filters. After the liquid surface inside the cell reached the same level as that of the culture medium outside the cell, recycling was started. The pH and temperature in the reactor were adjusted to $7.1 \pm 0.2$, $35 \pm 2^0 C$, respectively. Under a nitrogen atmosphere the reactor was seeded with 50 ml of the inoculum then operated in a batch mode. After the organic acids had been used up by the bacteria, 500 ml of culture medium was replaced by 500 ml of fresh feed, which was repeated till black bacterial colonies were observed on a removable PVC slide which was inserted into the reactor at the same time as the cell was immersed into the medium. Afterwards, the reactor was shifted to continuous flow mode. The flow rate was gradually changed to and maintained at 40 ml/hr (dilution rate $\simeq 0.04$ $hr^{-1}$). At this rate the organic acids concentrations in the fermenter were kept high enough, 3 g/l, 1.5 g/l and 0.5 g/l for acetate, propionate and butyrate respectively, to support the bacterial growth at their maximum rates.

### 7.5.2 Effective Diffusivities of Propionate and Butyrate in the Biofilms

As indicated previously the diffusion–reaction model, Equation 7.96, which describes a substrate concentration distribution within a biofilm can be solved numerically or analytically and the model parameter, $D_e$, can be determined if three boundary conditions are measured experimentally; the substrate concentration on the biofilm surface, $S_i$, and the substrate concentration inside the device, $S_e$, and the concentration gradient, $dS/dl$, at the membrane filters. The last one ($dS/dl = 0$) can be assumed confidently as long as the biofilms on the two membrane filters have the same thickness, which was to a great extent dependent on the symmetrical structures of the device and the fermenter. Thickness measurements of the biofilms on the two membrane filters at the end of the

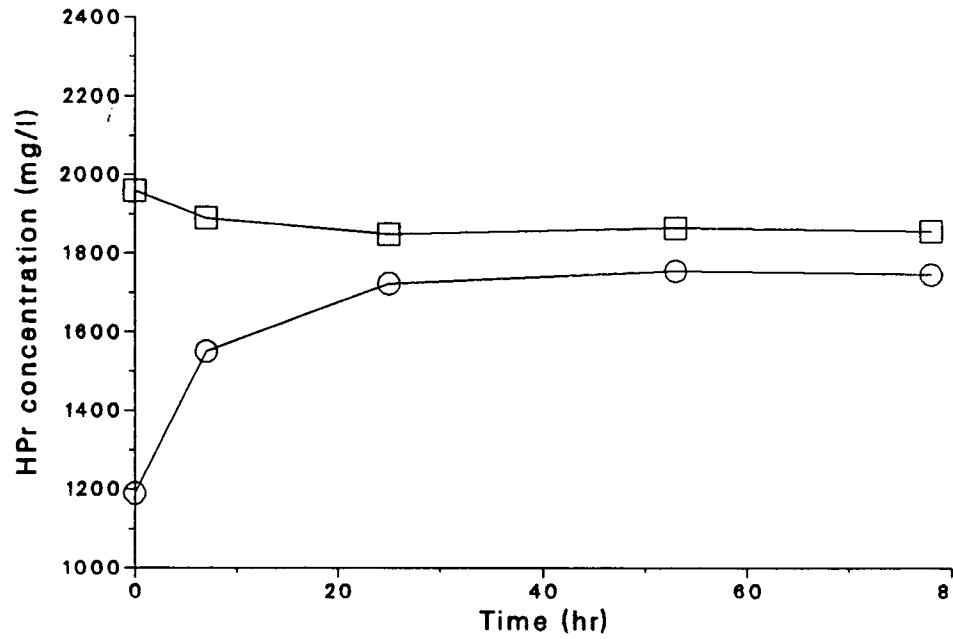


Figure 7.70: Establishment of a steady state propionate concentration inside the cell (o) after a dilution. □ – propionate concentration outside the cell

experiments confirmed the accuracy of this assumption.

Using the substrate concentration inside the cell as the value at the interface between the biofilm and the membrane filter would be reliable only when a steady state throughout the biofilm was established and no microbes existed inside the cell. Establishment of a steady state was checked by displacing 20 ml of the medium inside the cell with the same volume of oxygen-free distilled water and then monitoring the concentration change while the outside concentration was kept as constant as possible. That the concentrations of propionate and butyrate inside the cell, after dilution with the oxygen-free distilled water, gradually approached a constant as shown in Figure 7.70 and Figure 7.71 implied that a steady state was established.

This dilution operation was repeated eight times both to confirm the establishment of a steady state in the films and to minimize the biological activity inside the cell. It

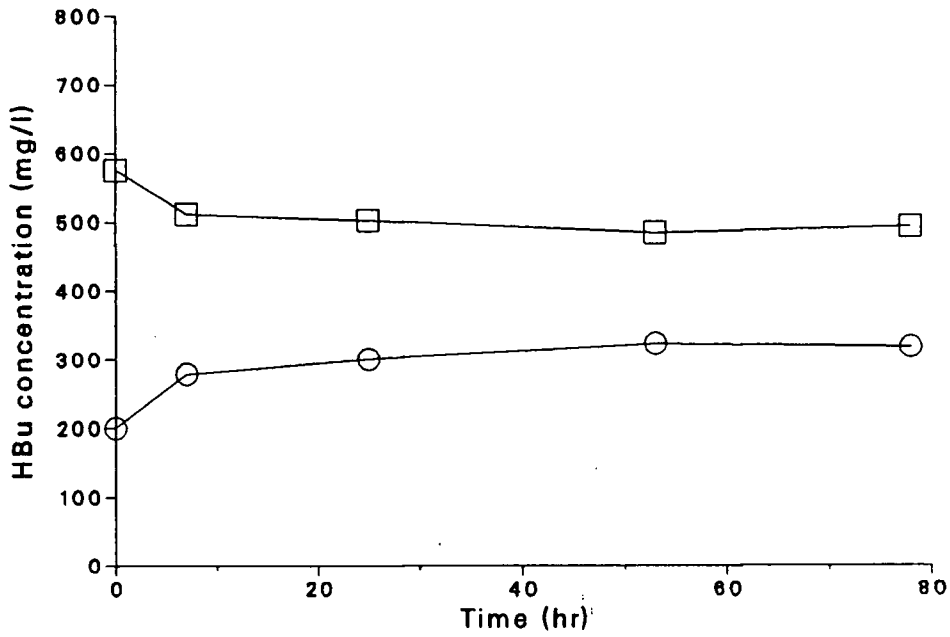


Figure 7.71: Establishment of a steady state butyrate concentration inside the cell (o) after a dilution. □ – butyrate concentration outside the cell

was believed that the number of microbes inside the cell could be neglected because of the filtering action of the membrane filters (pore size 0.45 $\mu$m) and the dilution of the medium inside the dive with oxygen-free water.

The bulk substrate concentrations were taken as those on the biofilm surface. This assumption, however, was reliable only when the external mass transfer resistance was small. The effect of external mass transfer resistance was to reduce the substrate concentration on the biofilm surface and thus the substrate concentration inside the cell. If this resistance is minimized or the external mass transfer is far faster than the rates of substrate digestion and internal mass transfer within the biofilms, the substrate concentration on the biofilm surface would be very close to the bulk concentration, and correspondingly the inside concentration would reach its maximum value. Experimentally this was checked by increasing the recycle rate to a value above which the inside

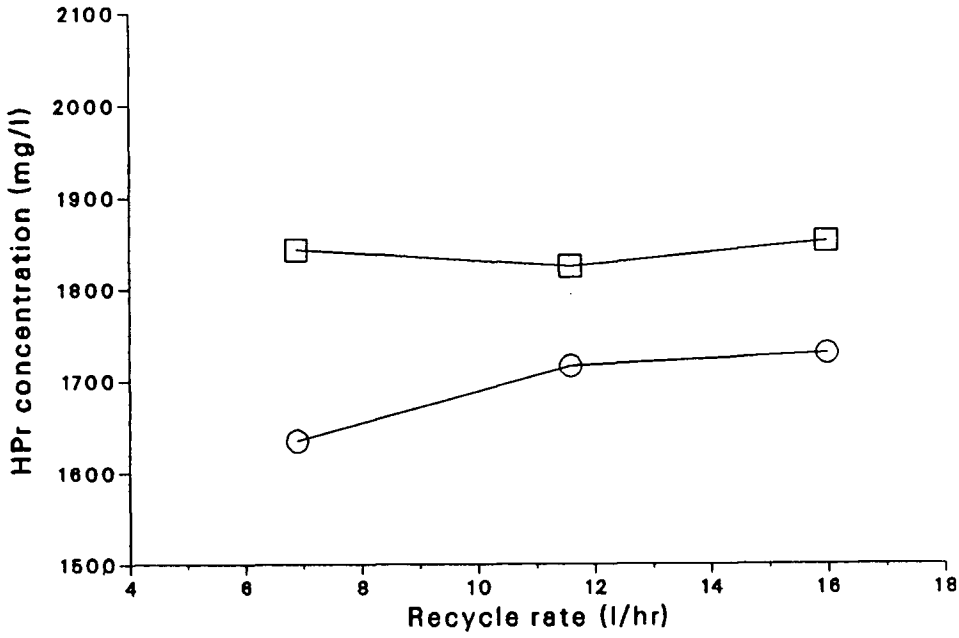


Figure 7.72: Effect of recycle rate on propionate concentration inside the cell (o), □ – porpionate concentration outside the cell.

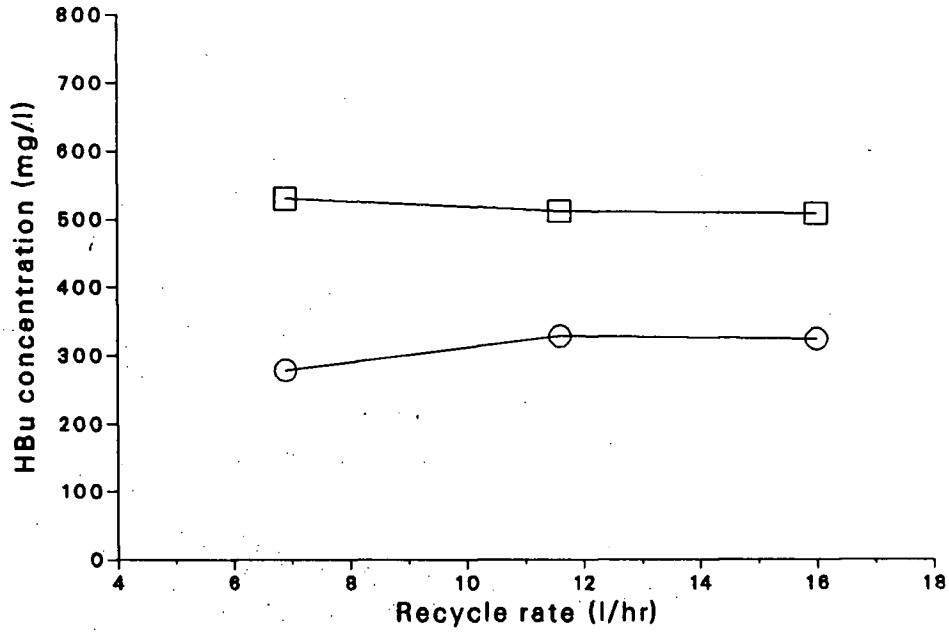


Figure 7.73: Effect of recycle rate on butyrate concentration inside the cell (o), □ – butyrate concentration outside the cell.

concentrations leveled off. Figure 7.72 and Figure 7.73 show that when the recycle rate was raised above 11.4 l/hr, (superficial velocity = 3 cm/min), the concentrations of propionate and butyrate inside the cell approached their constant values, which indicated that the external mass transfer resistance had been minimized and was not a rate limiting step. Thereby, the bulk substrate concentrations could be reasonably taken as those on the biofilm surface.

Steady state concentrations of propionate and butyrate inside and outside the cell were averaged for four measurements which were conducted at a recycle rate of 16 l/hr. Substituting the intrinsic utilization rates of propionate and butyrate, Equations 6.75 and 6.76, for the reaction rate on the right side of the diffusion-reaction model (Equation 7.96) gives the following equations which describe diffusion and dissimilation of these two acids in the methanogenic biofilm,

$$D_{e,p}\frac{d^2S_p}{dl^2} = \rho_c\frac{r_{max,p}S_p(1+\beta S_p)}{K_p+S_p} \tag{7.98}$$

$$D_{e,b}\frac{d^2S_b}{dl^2} = \rho_c\frac{r_{max,b}S_b}{K_b+S_b+K_IS_pS_b}. \tag{7.99}$$

Where the subscripts, $p$ and $b$, refer to propionate and butyrate. The reaction rates for each of the acids are based on an integrated biomass (mg/mgC/hr), i.e., a biomass containing a mixture of bacterial groups responsible for the utilization of various substrates, as discussed in Chapter 6. Correspondingly the density of the biomass, $\rho_c$, has units of carbon content in unit volume of the integrated biomass (mgC/ml). The density and thickness of the biofilms on the membrane filters were measured according to the steps described in Chapter 3. For each of the equations above, three boundary conditions were known;

$$S_p = S_{e,p} \text{ and } dS_p/dl = 0, \qquad \text{at } l = 0,$$

Table 7.28: Effective diffusivities of propionate and butyrate

| Item | Unit | Propionate | Butyrate |
|---|---|---|---|
| $S_b$ | mg/l | 1805 | 515 |
| $S_e$ | mg/l | 1725 | 326 |
| $\rho_c$ | mgC/ml | 26.8 | 26.8 |
| $L$ | mm | 0.78 | 0.78 |
| $r_{max}$ | mg/mgC/hr | 0.0162 | 0.0473 |
| $K_s$ | mg/l | 50 | 27 |
| $D_e$ | $\times 10^5 cm^2/sec$ | 0.60 | 0.357 |
| $D_e/D$ | | 0.41 | 0.281 |

$$S_b = S_{e,b} \text{ and } dS_b/dl = 0, \qquad \text{at } l = 0,$$

$$S_p = S_{b,p} \text{ and } S_b = S_{b,b}, \qquad \text{at } l = L.$$

Where $L$ is the biofilm thickness, $S_{e,p}$ and $S_{b,p}$ are the propionate concentrations inside and outside the device, $S_{e,b}$ and $S_{b,b}$ the butyrate concentrations inside and outside the cell. The same programs as were used for lactose diffusion were used for solving the differential Equations 7.98, 7.99 and searching for optimum values of effective diffusion coefficients of propionate and butyrate in the biofilms by fitting the calculated values from the model with the experimental values of the concentrations of propionate and butyrate on the biofilm surface, $S_{b,p}$ and $S_{b,b}$. The outcome is summarized in Table 7.28.

### 7.5.3 Effective Diffusivity of Acetate in Methanogenic Biofilms

Acetate, as discussed in the kinetic studies of organic acids digestion, is an intermediate product of propionic and butyric acids dissimilation by the acetogens. To develop a balanced bacterial community, the kinetic investigation used a feed mixture of acetate, propionate and butyrate in a weight ratio of 1 : 0.5 : 0.5. In situ measurement of diffusivities of fatty acids in an active biofilm needs a knowledge of the intrinsic kinetics of the dissimilation of these acids in the biofilm. It was, therefore, necessary to use

the same feed composition as was used for the kinetic studies to develop methanogenic biofilms on the two membrane filters so that the bacterial community had the same distribution of bacterial species in the two cases. When the measurement of effective diffusivities of propionate and butyrate was made, the concentration of acetate was also analyzed. The data, however, could not be used to calculate the effective diffusivity of acetate in the biofilm because the two longer chain acids were converted to acetate and thus their diffusion would affect the acetate concentration inside the cell. Instead, a feed which contained only acetate was used to measure the effective diffusivity of acetate. The time of this feed shift was made short so that it could be assumed that this shift did not cause a considerable change in the distribution of bacterial species in the biofilm. The input of acetate into the elemental volume of biofilm as shown in Figure 7.63 was only by diffusion, and Equation 7.96 is still valid for acetate diffusion and reaction.

$$D_{e,a}\frac{dS_a}{dl} = \rho_c \frac{r_{max,a} S_a}{K_a + S_a} \tag{7.100}$$

Figure 7.74 indicates that the external mass transfer resistance could be neglected as long as the recycle rate was above 12 l/hr. Figure 7.75 shows the establishment of steady–state acetate concentration throughout the biofilm after a disturbance to the acetate concentration inside the cell was made by diluting it with oxygen–free distilled water.

For the above differential equation (Equation 7.100), three boundary conditions are;

$$S_a = S_{e,a} \text{ and } dS_a/dl = 0 \qquad \text{at } l = 0,$$

$$S_a = S_{b,a} \qquad \text{at } l = L.$$

The effective diffusivity of acetate in the methanogenic biofilm is estimated by solving Equation 7.100 with the three boundary conditions. Table 7.29 summarizes the results of the numerical solution.

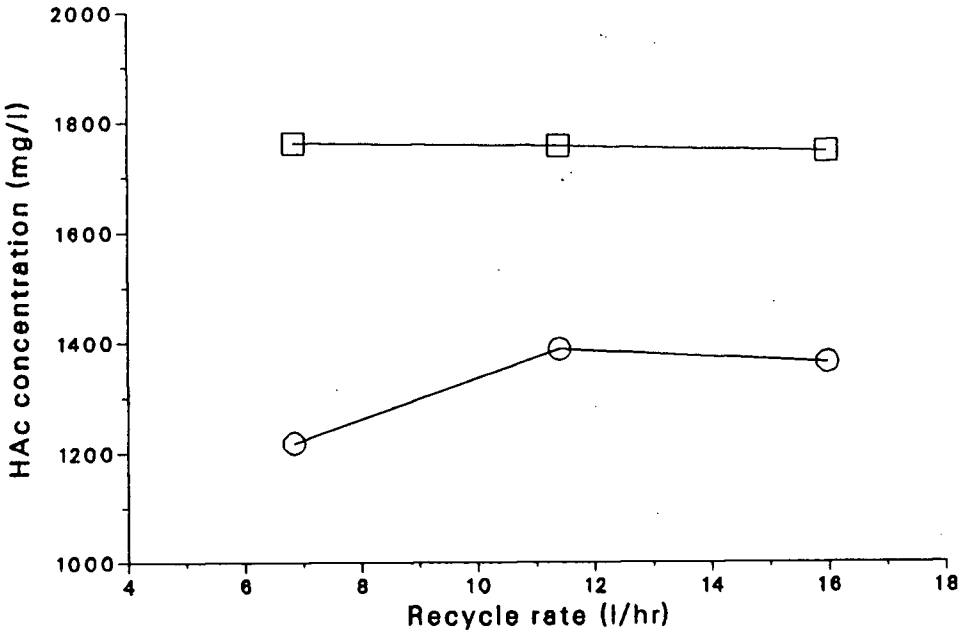


Figure 7.74: Effect of recycle rate on the acetate concentration inside the cell (o), □ – acetate concentration outside the cell

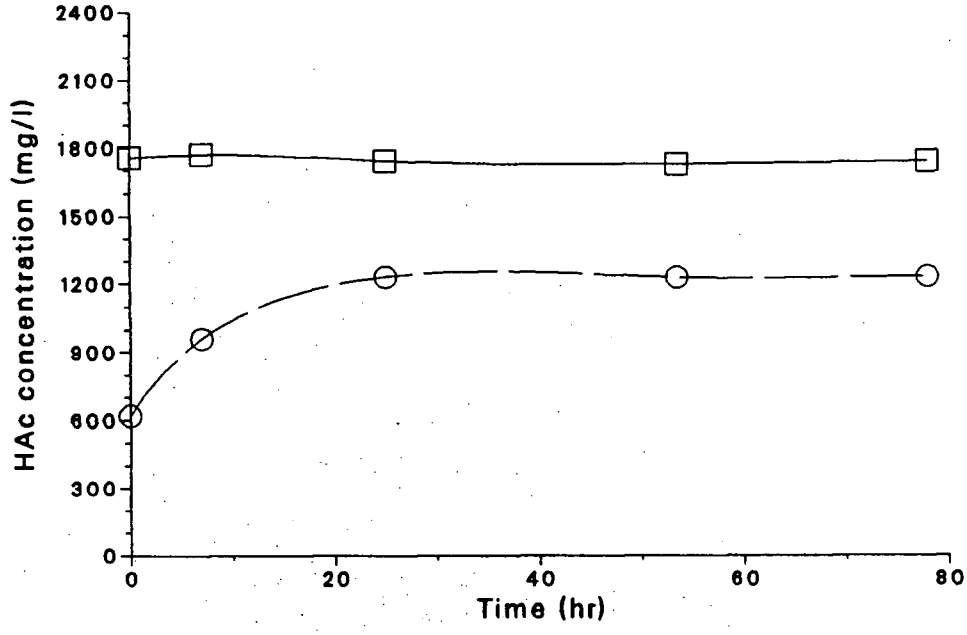


Figure 7.75: Establishment of a steady state acetate concentration inside the device (o) after a dilution, □ – acetate concentration outside the cell.

Table 7.29: Effective diffusivity of acetate in methanogenic biofilms

| Item | Unit | Value |
|---|---|---|
| $S_b$ | mg/l | 1760 |
| $S_e$ | mg/l | 1390 |
| $\rho_c$ | mgC/ml | 26.8 |
| $L$ | mm | 0.78 |
| $r_{max}$ | mg/mgC/hr | 0.098 |
| $K_s$ | mg/l | 160 |
| $D_e$ | $\times 10^5 cm^2/sec$ | 0.54 |
| $D_e/D$ | | 0.31 |

During the period of this measurement, it was assumed that the bacterial components in the biofilm had not changed considerably even though an acetate-only feed was used, because the experimental time was held short and bacterial growth was very slow. Experimentally, in order to check this assumption, a repeat experiment was conducted by using the previous feed mixture of three acids again (5, 2.5, 2.5 g/l for acetate, propionate and butyrate respectively). The propionate and butyrate concentrations inside the cell were analyzed at steady state and no significant change was found in the inside concentrations while the outside concentrations were very close to the values shown in Figures 7.70 and 7.71. And also, the steady states were achieved in an equivalently short period of time after a disturbance was given to the concentrations inside the device. These facts implied that the bacterial components in the biofilm had not changed significantly during the acetate-only feed test.

As is well known, the bacterial species distribution in a mixed culture is to a great extent dependent on their environment, especially the substrate concentrations if other conditions such as pH, temperature and inorganic salt growth nutrients are unchanged. At the beginning of this subsection it was explained that to produce a bacterial community as similar as possible to the one used in the kinetic studies, the same feed composition

was used in the measurement of effective diffusivities. It is assumed that as long as all the bacteria can obtain enough food from their environment they will grow at their own maximum rate and thus the fraction of each species in a mixed culture would be determined uniquely. This idea was proposed and used when the distribution of bacterial species in a biofilm was estimated in the last chapter even though high propionate concentrations had some influences on the utilization rates of propionate and butyrate, and thus may affect the growth rates of bacteria responsible for these two reactions (see sections "Interaction of organic acids" and "Distribution of bacterial groups in balanced biofilms" in Chapter 6). For bacterial biofilms which are built up in situ, however, the effect of the properties of the support materials should be considered, too. This will be discussed in next subsection.

### 7.5.4 Effect of Support Properties on the Measurement of Diffusivities

In the previous subsections, measurement of the effective diffusivities of acetate, propionate and butyrate in biofilms was discussed. The measurement was conducted in situ on active methanogenic biofilms which formed on two nitrocellulose membrane filters using as substrate a mixture of acetate, propionate and butyrate. The intrinsic kinetics used in the diffusion-reaction model were obtained on active methanogenic biofilms which formed with a feed of the same fatty acids composition and ratio. Therefore the effect of substrates on the distribution of bacterial species could be eliminated. The influence of the properties of the biofilm support, however, had been ignored when the utilization rates of organic acids obtained in the biofilms forming on PVC supports were used for the biofilms forming on the nitrocellulose membrane. This assumes that the composition of bacterial species in the biofilms forming on PVC supports was the same as that in the biofilms forming on nitrocellulose membranes.

The change in composition of bacterial species in a biofilm may have no great physical

effect on the structure of biofilm channels through which the substrates transfer into the inner part of the biofilm. However, it may have considerable effect on the consumption rate of a special substrate in a unit volume of the biofilm because the content of the bacterial species responsible for this reaction may change. The influence of support properties on the composition of bacterial species in a biofilm is mainly due to the influence of the support surfaces on the attachment of bacterial species when the supports are immersed in a nutrient-rich culture medium. This is because acetate-, propionate- and butyrate-utilizing bacteria have almost the same growth rate in a nutrient-rich medium as indicated in Chapter 5 as well as in the kinetic studies conducted by Lawrence and McCarty [142].

Many properties of support surfaces may affect the attachment of free microbes onto the support. It was found that the wettability of the surface was an important parameter and that a significant relationship existed between this parameter and the attachment rates of acetate-, propionate- and butyrate- utilizing bacteria in the formation of symbiotic biofilms on different inert surfaces as discussed in Chapter 5. For example, the butyrate- utilizing microbes prefer surfaces with high wettability such as wood. The membrane filters used as biofilm support in the measurement of diffusivities is made of quite pure cellulose nitrate, a derivative of cellulose. Surfaces made of cellulose have very high wettability because the wettability of a surface depends mainly on its interaction with water at the surface. The celluloses, especially the amorphous ones, contain a great number of "free-hydroxyls" available for site adsorption of water molecules, and thus strong interaction occurs through the formation of hydrogen bonds between water molecules and the surface. Therefore, the nitrocellulose surface has a wettability similar to a wood surface because it is made of the same macro-molecules, cellulose, and thus the water contact angle on the nitrocellulose surface is taken as zero.

As proposed in Chapter 6, on the distribution of bacterial groups in a balanced

symbiotic methanogenic biofilm, Equations 6.86, 6.87 and 6.88 could be used to estimate, in one mg of organic carbon of the biofilms on the nitrocellulose membrane filters, the fractions of biomass, $m_a$, $m_p$, $m_b$, responsible for dissimilation of acetate, propionate and butyrate.

$$m_a = \frac{1}{1 + k_p/k_a + k_b/k_a + (\frac{9M_a}{M_p} r_p + \frac{6M_a}{M_b} r_b)/(4r_{max,a})} \tag{7.101}$$

$$m_p = \frac{k_p/k_a}{1 + k_p/k_a + k_b/k_a + (\frac{9M_a}{M_p} r_p + \frac{6M_a}{M_b} r_b)/(4r_{max,a})} \tag{7.102}$$

$$m_b = \frac{k_b/k_a}{1 + k_p/k_a + k_b/k_a + (\frac{9M_a}{M_p} r_p + \frac{6M_a}{M_b} r_b)/(4r_{max,a})} \tag{7.103}$$

The propionate concentrations inside and outside the cell were above 1000 mg/l (Table 7.28) and so its effect on the utilization rates of propionate and butyrate should not be neglected.

$$r_p = r_{max,p}(1 + 0.0002S_p) \tag{7.104}$$

and

$$r_b = \frac{r_{max,b}}{1 + 0.000296S_p} \tag{7.105}$$

An average propionate concentration inside and outside the cell was taken as its representative concentration within the biofilm, since the difference between the concentrations on the two sides was small. The specific attachment rates of acetate-, propionate- and butyrate-degrading bacterial species on wood surface, $k_{w,i}$, are used as those on a hydrophilic nitrocellulose surface. Table 7.30 lists the results of calculations using Equations 6.86, 6.87 and 6.88.

Rewriting the diffusion-reaction model (Equation 7.96) gives

Table 7.30: Distribution of bacterial species in biofilms forming on nitrocellulose membranes

| Item | Unit | Values |
|---|---|---|
| $k_a$ | cm/day | 5.596 |
| $k_p$ | cm/day | 3.396 |
| $k_b$ | cm/day | 8.20 |
| $r_p$ | mg/mgC/hr | 0.0219 |
| $r_b$ | mg/mgC/hr | 0.0311 |
| $m_a$ | mgC/mgC | 0.263 |
| $m_p$ | mgC/mgC | 0.160 |
| $m_b$ | mgC/mgC | 0.375 |
| $r_{max,a}$ | mg/mgC/hr | 0.098 |
| $r_{max,p}$ | mg/mgC/hr | 0.0162 |
| $r_{max,b}$ | mg/mgC/hr | 0.0473 |
| $r'_{max,a}$ | mg/mgC,a/hr | 0.373 |
| $r'_{max,p}$ | mg/mgC,p/hr | 0.101 |
| $r'_{max,b}$ | mg/mgC,b/hr | 0.126 |

$$D_e \frac{d^2 S_j}{dl^2} = \rho_c m_j r'_j \tag{7.106}$$

where the subscription, $j$, refers to acetate, propionate and butyrate respectively, $\rho_c$ is the density of an integrated biomass which contains the four types of bacteria responsible for utilization of acetate, propionate, butyrate and $CO_2/H_2$ (mgC/ml), $m_j$ the fraction of the biomass which is responsible only for the degradation of the jth substrate, $r'_j$ is the dissimilation rate of the jth substrate based on the biomass only responsible for the utilization of the jth components (mg/mgC$_j$/hr). The maximum values of $r'_j$ are also listed in Table 7.30. The dependency of reaction rates on the substrate concentrations would generally not be affected by the distribution of bacterial species in the biofilms. Therefore, for each one of the organic acids, a diffusion-reaction equation can be established similar to those discussed in the previous subsections.

Table 7.31: Effect of bacterial species distribution on the measurement of diffusivities

| | Biofilm on PVC supports | | | Biofilm on membrane supports | | |
|---|---|---|---|---|---|---|
| Substrate | m | $D_e$ | $D_e$/D | m | $D_e$ | $D_e$/D |
| | $mgC_j/mgC$ | $\times 10^5 cm^2/sec$ | | $mgC_j/mgC$ | $\times 10^5 cm^2/sec$ | |
| Acetate | 0.255 | 0.541 | 0.31 | 0.263 | 0.558 | 0.32 |
| Propionate | 0.220 | 0.601 | 0.41 | 0.160 | 0.437 | 0.30 |
| Butyrate | 0.318 | 0.357 | 0.28 | 0.375 | 0.421 | 0.33 |

$$D_{e,a}\frac{d^2S_a}{dl^2} = \rho_c m_a \frac{r'_{max,a}S_a}{K_a + S_a} \tag{7.107}$$

$$D_{e,p}\frac{d^2S_p}{dl^2} = \rho_c m_p \frac{r'_{max,p}S_p(1+\beta S_p)}{K_p + S_p} \tag{7.108}$$

$$D_{e,b}\frac{d^2S_b}{dl^2} = \rho_r m_b \frac{r'_{max,b}S_b}{K_b + S_b + K_I S_b S_p} \tag{7.109}$$

Using the three boundary conditions for each acid and the programs for solving the differential equations as well as for searching optimum parameter values gives the effective diffusivity of each acid in the methanogenic biofilms. The results are summarized in Table 7.31 and compared with the diffusivity values calculated under the assumption that there was no difference in the bacterial distribution in the biofilms forming on the PVC support or on the nitrocellulose membranes.

In Table 7.31, 'biofilm on PVC supports' refers to the methanogenic biofilms which formed on PVC support, and correspondingly the effective diffusivities are obtained by using the utilization rates of organic acids in these biofilms while 'biofilm on membrane supports' means that the bacterial components in the biofilms forming on the membranes have been corrected according to the hydrophilic properties of the nitrocellulose filter, and also the effective diffusivities. As indicated in the study of build-up of symbiotic

methanogenic biofilms on various inert supports, the physiochemical properties of the support surface affect the attachment of free microbes, especially the propionate- and butyrate-utilizing bacteria. The former is most insensitive to the wettability of the support surface while the latter prefers hydrophilic surfaces. The PVC supports on which the kinetic investigation of organic acids digestion was conducted was very weakly wettable (88 $^0$ water contact angle), but the nitrocellulose membranes are very hydrophilic (0 $^0$ water contact angle). Therefore, the fractional biomass of propionate-utilizing bacteria on the membrane was less than that on the PVC support because of the increase in fractional biomass responsible for conversion of butyrate. If this difference of bacterial components in the biofilms forming on various supports is ignored, the influence of solute size on effective diffusivities calculated from the diffusion-reaction model as shown in Table 7.31 can not be explained. The bigger propionate molecule has a faster molecular diffusion rate than the smaller acetate molecules. This error, however, can be corrected by considering the change in bacterial compositions in the biofilms forming on different support surfaces.

## 7.6 Influence of Biofilm Structure on Diffusivities

Figure 7.76 shows a top view of a methanogenic biofilm magnified 400 times with a microscope (NIKON) after a water layer on the biofilm was carefully absorbed by a filter paper.

When such a porous biofilm composed of irregular channels of various sizes is immersed in an aqueous solution, the channels are filled with water and solute molecules are transported in these channels just as they are in free solution. However, the presence of solid biomass would certainly affect the motion of a solute molecule. There are two mechanisms by which a solute molecule may lose momentum in the axial direction.

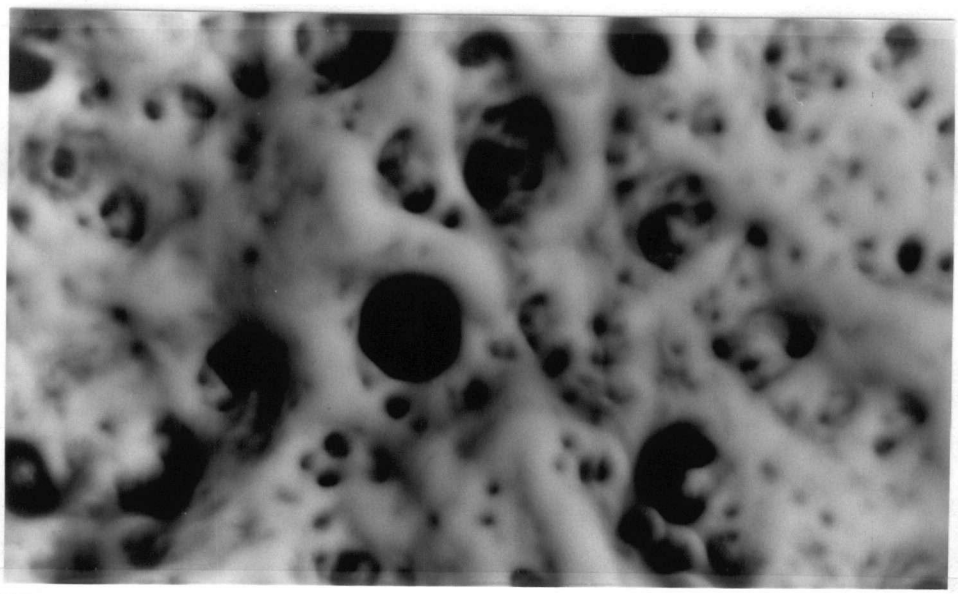

Figure 7.76: Top view of a methanogenic biofilm, (× 400)

1. By direct transfer to the wall as a result of molecule-wall collisions

2. By transfer to water molecules as a consequence of collisions between solute and solvent molecules

The first mechanism, Knudsen diffusion, will predominate when the diameter of a channel is small compared with the molecular mean free path lengths (the distance between two molecular collisions). In this situation, molecule-wall collisions are much more frequent than molecule- molecule collisions. This is true, especially for gas mixtures at low pressures and high temperatures. Unlike the diffusion in gases a solute molecule is surrounded by water molecules in a diluted solution and even in a channel of micropore size the collisions between solute and water molecules are more frequent than those between solute molecules and wall. Hence, it is reasonable to suggest that the fluxes, just as in the bulk diffusion, are described by the second mechanism, and will still be described

by Fick's law since inter-molecular collisions still dominate over molecule-wall collisions. But, the diffusion coefficient must be replaced by an effective diffusion coefficient, $D_e$.

$$D_e = K_l D \tag{7.110}$$

Where $K_l$ is a factor determined by the geometry of the pore structure only. $K_l$ should be independent of the pore size, provided this is large compared with the mean free path lengths, but it should be proportional to the void fraction, and should reflect the fact that the available directions for molecular drift are constrained by the orientation of the pores. Thus it is common to find $K_l$ expressed in the form

$$K_l = \frac{\varepsilon}{\tau} \tag{7.111}$$

and so,

$$D_e = \frac{\varepsilon}{\tau} D \tag{7.112}$$

or,

$$\frac{\varepsilon}{\tau} = \frac{D_e}{D} \tag{7.113}$$

Where $\tau$ is a tortuosity factor determined by the statistics of pore orientations, and $\varepsilon$ is the biofilm void fraction occupied by the channels or fractional area through which solute molecules can enter into the biofilms by diffusion.

The value of $\varepsilon$ can be determined experimentally provided the biofilm can be assumed to have a uniform void fraction. Some biomass collected from intact biofilms was filled into a small Kimax tube (diameter = 4 mm) and then centrifuged at 4000 rpm until the dense biomass volume became a constant as shown in Figure 7.77.

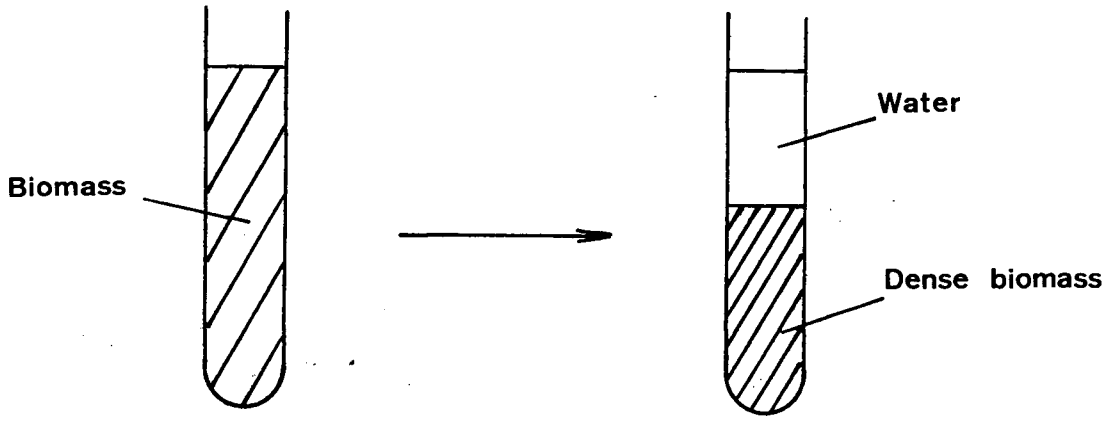


Figure 7.77: Experimental determination of biofilm void fraction

The water volume is thought of as the total volume of channels, because they were full of water and collapsed into solid biomass under the centrifugal force, while the water is left. The void fraction of the biofilm is calculated by the following equation.

$$\varepsilon = \frac{V_w}{V_w + V_{mass}} \tag{7.114}$$

where $V_w$ is the water volume and $V_{mass}$ the solid biomass volume. For the acidogenic biofilms, $\varepsilon = 0.66 \pm 0.04$, on the basis of 4 samples.

From Equation 7.113 the tortuosity of acidogenic biofilms

$$\tau = \varepsilon \frac{D}{D_e} = 0.66 \times \frac{0.72}{0.47} = 1.03 \tag{7.115}$$

This value of $\tau$ means that the influence of acidogenic biofilm structure on lactose effective diffusivity is mainly from the fractional area occupied by the solid biomass which reduced the area available to lactose diffusion into the biofilm, and also that the biofilms

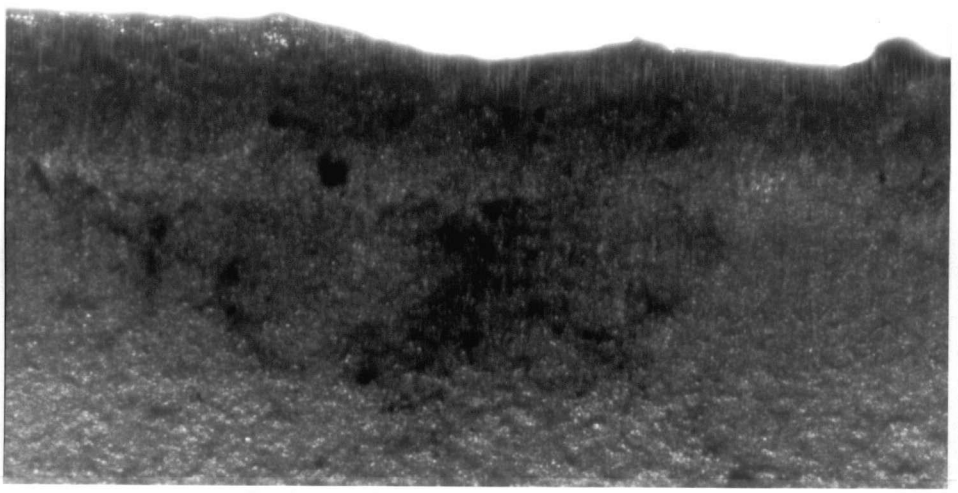

Figure 7.78: Straight vertical channels (along the black and white boundary) in a section of an acidogenic biofilm ($\times$ 100). The down black part is biofilm and PVC support.

had almost straight channels. Observation of biofilms on a PVC slide with a microscope revealed that some vertical channels existed in the biofilms as shown in Figure 7.78

The channels shown in this picture are the macro-channels which were formed during the development of the biofilm, and so might be affected by the production and release of gaseous fermentation products, such as $CO_2$. More numerous are the micro-channels through which the substrate molecules are transported to microbial cells embedded in the exopolysaccharide matrix.

The same measurements were made on methanogenic biofilms. The fractional area available for organic acid transfer in the methanogenic biofilms, $\varepsilon$, is calculated from Equation 7.114, $\varepsilon = 0.54 \pm 0.03$. Another structure parameter of the biofilms, tortuosity factor, can be obtained from the values of $\varepsilon$, $D_e$ and $D$ with Equation 7.113. For each acid, the parameter $\tau$ is calculated from the ratio of its effective diffusivity to free diffusivity.

Table 7.32: Comparison of acidogenic and methanogenic biofilms

| Parameter | Unit | Acidogenic | Methanogenic |
|---|---|---|---|
| $\rho$ | g dry mass/ml | 0.087 | 0.076 |
| Carbon content | mgC/mg.dry mass | 0.342 | 0.348 |
| $\rho_c$ | g carbon/ml | 0.030 | 0.027 |
| $\varepsilon$ | | 0.66 | 0.54 |
| $\tau$ | | 1.03 | 1.69 |
| Color | | milk white | black |
| Growth rate | mgC/mgC.day | 0.0259 | 0.0090 |

$$\tau_a = \varepsilon(D/D_e)_a = 0.54/0.32 = 1.69 \tag{7.116}$$

$$\tau_p = \varepsilon(D/D_e)_p = 0.54/0.30 = 1.80 \tag{7.117}$$

$$\tau_b = \varepsilon(D/D_e)_b = 0.54/0.34 = 1.59 \tag{7.118}$$

The subscripts mean that the tortuosity is estimated from the diffusivity ratios of acetate, propionate and butyrate, respectively. Because the organic acids are transported in the same methanogenic biofilms the difference in the values of tortuosity is due to experimental and calculation errors. An average value of 1.69 is taken as representative. The relative error is less than 7 percent.

Table 7.32 summarizes some parameters describing the acidogenic and methanogenic biofilms. Comparisons between these two types of biofilms gives some interesting properties of the biofilms. In the experiments it was observed that the methanogenic biofilms were obviously different from the acidogenic biofilms. The former was black and the latter milk white since the sulfate-reducing bacteria in the methanogenic biofilms reduced $S^{+6}$ to $S^{-2}$ some of which formed insoluble black FeS while the sulfate-reducing bacteria

could not survive in the acidogenic environment even though the acidogenic biofilms were also fed with the same sulfate solution. The methanogenic biofilms, however, have almost the same carbon content as the acidogenic biofilms per unit weight of dry biomass. This means that the bacterial species composing these two functionally distinctive bacterial groups have almost the same carbon content. The differences in the values of $\varepsilon$ and $\tau$ obtained from the methanogenic and acidogenic biofilms reflect the difference in the structure of these two kind of biofilms, the methanogenic biofilms having more tortuous channels and less void area for internal mass transfer than those of acidogenic biofilms. The difference in the void fractional volume, $\varepsilon$, of the biofilms may be attributed both to biofilms' growth rates, the net accumulation rate of acigogenic biofilms being 3 times faster than that of methanogenic biofilms, and to biofilms' appearance since it could be observed that the acidogenic biofilms had numerous stringy filaments extending outward into the liquid while the methanogenic biofilms had soomther surface. When the biofilms were taken out from the medium, the filaments collapsed to hold up some water. In methanogenic biofilms, the release of great amount of methane which is sparingly soluble in water produced lots of tiny bubbles which arised at the direction almost perpendicular to the direction of substrate transport, which gave higher mass transfer resistance and thus, more tortuous channels than those in acidogenic biofilms.

# Chapter 8

## Conclusions and Recommendations

### 8.1 Conclusions

1. After it was confirmed that the external and internal mass transfer resistance had no significant influences on lactose fermentation in acidogenic biofilms under the conditions of these experiments, the intrinsic kinetics of lactose degradation and production of acetate, propionate, butyrate, lactate and ethanol were investigated in a continuous flow reactor (CSTR) at 35 $^0C$ and pH of 4.6. The culture medium was chemically defined. The major fermentative products of lactose under these conditions were acetate and butyrate while the minor products were propionate, ethanol and lactate. The utilization rate of lactose, as a function of lactose concentration, $S$ (mg lactose/l), can be described by a Michaelis–Menten type equation as can the formation rates of acetate, butyrate and ethanol;

$$r_{lactose} = \frac{0.3144 S_{lac}}{201 + S_{lac}} \qquad \text{(mg Lactose/mgC/hr)}$$

$$r_{acetate} = \frac{0.0599 S_{lac}}{89 + S_{lac}} \qquad \text{(mg HAc/mgC/hr)}$$

$$r_{butyrate} = \frac{0.115 S_{lac}}{532 + S_{lac}} \qquad \text{(mg HBu/mgC/hr)}$$

$$r_{ethanol} = \frac{0.0101 S_{lac}}{929 + S_{lac}} \qquad \text{(mg Eth/mgC/hr)}$$

The formation rates of two other minor products, propionate and lactate, have linear relationships with lactose concentration under the experimental conditions;

$$r_{propionate} = 1.25 \times 10^{-6} S_{lac} \qquad \text{(mg HPr/mgC/hr)}$$

$$r_{lactate} = 2.18 \times 10^{-6} S_{lac} \qquad \text{(mg HLa/mgC/hr)}$$

All these rates are based on a milligram of carbon of attached biomass. The low pH value (4.6) of the culture medium could depress the formation of propionate, an intermediate the following methanogenic bacteria cannot digest easily. A dramatic change in pH (5 to 6.5) caused lysis of some embedded bacteria with the acidogenic biofilm thinning and the fermenter foaming.

2. The rate of formation of a methanogenic biofilm is slower than that of an acidogenic biofilm. A study on build-up of symbiotic methanogenic biofilms on different inert supports was conducted by culturing a mixture of methane–producing bacteria in a nutrient rich medium in the presence of four types of supports; wood, ceramic ring, PVC and stainless steel. The three groups of bacteria, acetate-degrading, propionate-degrading and butyrate-degrading, were found to attach at different rates to different substrata. A semi-theoretical kinetic model has been proposed to depict the process of bacterial attachment. For attachment of each of three bacterial types onto each of four support surfaces, the accumulation of fixed biomass on unit area of support surface, $[xA]$, with time can be expressed as following;

$$\frac{[xA]}{[x]} = \frac{k-K}{s+\mu-K'}[e^{(\mu-K')t} - e^{-st}] + \frac{K}{\mu-K'}[e^{(\mu-K')t} - 1]$$

A model with 21 parameters has been found to be able to fit 12 equations like the equation above. For each type of bacteria, a linear relationship is found between

the model parameter, k, which is a specific attachment rate of free bacterial cells onto clean surfaces, and the wettability of the surfaces. If it is explained that the bacteria with more hydrophilic surfaces attach more easily to more hydrophilic supports, then the order of decreasing hydrophobicity of bacterial wall surfaces is;

butyrate degraders > acetate degraders > propionate degraders

The rate of spread of bacterial microcolonies on support surfaces was also found to be influenced by the wettability of the substrata. In this case, the spreading factor, s, that is, the ease with which the microcolonies spread on surfaces, was found to increase with the hydrophobicity of the surfaces. Compared with the rate of attachment of bacteria onto a clean surface and that of fixed bacterial growth, the attachment of free cells onto immobilized biomass already on the surface was negligible. The specific growth rates of the three types of bacteria were found to be the same, and therefore, the composition of a fixed biomass, i.e., the distribution of each group of bacteria in the fixed bacterial community, is to a great extent dependent on the initial attachment rate of each type of bacteria which is affected by the wettability of the supports.

3. Again after external and internal mass transfer resistance had been experimentally minimized and/or eliminated, biomethanation kinetics of organic acids in methanogenic biofilms were investigated at a pH of 7.1 and 35 $^0C$. The substrate was a mixture of organic acids containing acetic, propionic and butyric acids at a weight ratio of 1 : 0.5 : 0.5 (mg/l). The degradation rate of acetate can be expressed by a Michaelis–Menten equation,

$$r_{HAc} = \frac{0.098 S_{HAc}}{160 + S_{HAc}} \qquad \text{(mg HAc/mgC/hr)}$$

However, the degradation of propionate and butyrate are affected by the concentration of propionic acid in the medium, and so, two modified Michaelis–Menten equations are used for the assimilation rates of propionic and butyric acids. For propionic acid utilization, higher propionic acid concentration promotes its degradation,

$$r_{HPr} = \frac{0.0162 S_{HPr}(1 + 0.0002 S_{HPr})}{50 + S_{HPr}} \qquad \text{(mg HPr/mgC/hr)}$$

On the other hand, the utilization of butyric acid is inhibited by high concentrations of propionate,

$$r_{HBu} = \frac{0.0473 S_{HBu}}{27 + S_{HBu} + 0.000296 S_{HBu} S_{HPr}} \qquad \text{(mg HBu/mgC/hr)}$$

In the three equations above, the rates are based on unit weight of carbon in the methanogenic biofilms and the concentrations of fatty acids in mg/l. To check the interaction between the three organic acids, feeds having various ratios of the three organic acids were also used and it was found that only propionic acid concentration had promotional and inhibitory influences as described above.

4. A methanogenic biofilm is a symbiotic bacterial community including four fundamental types of bacteria, acetate degraders, propionate degraders, butyrate degraders and hydrogen-utilizing bacteria. A method has been proposed to estimate the distribution of each bacterial group in a methanogenic biofilm from the knowledge of the attachment rate of methanogens and acetogens on clean surfaces, the kinetics of utilization of the organic acids, and the hydrogen and the energy balance in mature methanogenic biofilms. The compositions (mg carbon of the ith bacterial type per mg carbon of total biomass) of mature symbiotic methanogenic biofilms

Table 8.33: Organic carbon fraction of each bacterial group in methanogenic biofilms on PVC and nitrocellulose membrane filter supports

| Substrate degraders | Acetate wt% | Propionate wt% | Butyrate wt% | Hydrogen wt% |
|---|---|---|---|---|
| on PVC | 25.5 | 22.0 | 31.8 | 20.7 |
| on membrane | 26.3 | 16.0 | 37.5 | 20.2 |

on PVC supports and nitrocellose membrane filters were estimated and listed in Table 8.33.

5. Based on the intrinsic kinetics of lactose fermentation in acidogenic biofilms and organic acids digestion in methanogenic biofilms, in situ measurements of mass transfer of lactose and organic acids were conducted in active biofilms. Effective diffusivities of lactose and organic acids, defined by a modified Fick's law and a diffusion-reaction model, were estimated from steady state concentration drops through an active biofilm by numerically solving a diffusion-reaction model. The effective diffusivity of lactose in an acidogenic biofilm is $0.47\times10^{-5}$ cm$^2$/sec that is 65.3% of its diffusivity in pure water. After a correction was made to allow for the fact that the composition of bacterial types might be somewhat different in methanogenic biofilms fixed on both PVC and nitrocellulose filter supports, the effective diffusivities of acetate, propionate and butyrate were found to be $0.558\times10^{-5}$, $0.4374\times10^{-5}$ and $0.421\times10^{-5}$ cm$^2$/sec, respectively, which means that diffusivities of acetate, propionate and butyrate in methanogenic biofilms have been reduced to about 30.2 % of the values in pure water. By using these data and the experimentally measured fractional void volume of biofilms, tortuosity factor $\tau$, a parameter describing the structure of channels formed in biofilms, was estimated for acidogenic biofilms ($\tau = 1.03$) and methanogenic biofilms ($\tau = 1.69$) respectively.

A comparison was also made between other properties of these two kind of biofilms.

## 8.2 Recommendations

Going back to the questions put froward in Chapter 1, two problems have been tentatively solved in this study, i.e. the measurement of the intrinsic kinetics and mass transfer of lactose and organic acids in the corresponding biofilms, and so it may be possible to calculate an optimum biofilm thickness. Further studies are, however, needed on how to control a growing biofilm at a steady state thickness so as to maintain an optimum operation for a long time.

### 8.2.1 Concentration Effect

Obviously, an optimum biofilm thickness with which a fermenter can hold up the largest amount of active biomass without dead volume caused by excess biomass is dependent on substrate concentrations in the bulk medium and at the interface between a biofilm and a support. The former mainly depends on the flow pattern in a reactor while the latter would be determined mainly by the process designer, e.g, a concentration which gives a half maximum reaction rate, ($K_s$). From the effect of concentration on optimum biofilm thickness, a biofilm should have a thickness which gradually decreases with the reduced substrate concentration from the inlet to the outlet. Therefore, a plug flow of medium over a biofilm with decreasing thickness as shown in Figure 8.79 may be an ideal for optimum operation.

### 8.2.2 Controlling Biofilm Thickness

To this author's knowledge, few studies have been conducted on how to control a growing biofilm at a constant film thickness though some investigations have been conducted

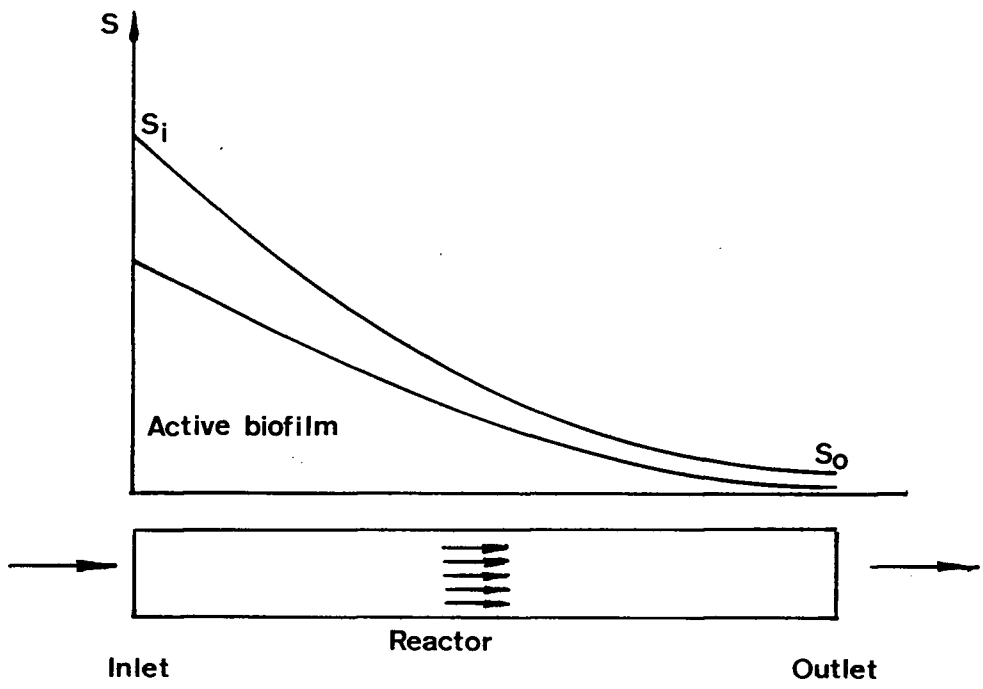


Figure 8.79: Illustration of an optimum operation of biofilm reactors. No back- mixing of medium is assumed.

on the influence of shear stress of fluid flow on biofilms. Most of investigations were concentrated on the formation of biofilms or on the possibility of biofilm technology being applied to a special wastewater. It may be thought that a steady state biofilm would be established automatically by the action of fluid flow stress and sloughing. However, in most cases of present industrial applications, the fluid flow rates are quite low due to the long residence time required for the slow utilization rate of substrates and so it can not be used purposely to control the biofilm thickness. In some fluidized bed reactors the biofilm on sand carriers are very thin due to strong turbulent flow, and hence, the thickness is controlled, but not kept at an optimum value. Sloughing is not a good method, either, because it occurs randomly with a result that block biomass would be lost and a bare support left. Moreover, it has been observed in this investigation that an over thick acidogenic biofilm (3–4 mm) could hold quite strongly on a membrane filter even though

the substrate concentration within the biofilm had fallen to zero at a thickness of about 2 mm. Another experimental observation which shows that sloughing does not occur easily was that anaerobic biofilms, especially the acidogenic biofilms, could stand in a pure water for a very long time (up to 7 days) without falling off.

Although there are many factors which can influence attachment and formation of biofilms (genetic, physiological, environmental, chemical factors) as discussed in Chapter 2, those which can be used to control the size of microbial aggregations (thickness of biofilms, size of granules) are generally limited to chemical or physical methods.

The chemical methods utilize some chemicals such as pH, chelating agents (like EDTA), to redisperse the fixed biomass into the medium, or, a decrease in the amount of chemicals in a medium which are beneficial for the formation of the extracellular polymer matrix such as $Ca^{++}$ could also reduce film thickness. The most striking advantage of a chemical method is that it would not cause extra back-mixing in a fermenter and thus an approach to the ideal flow pattern shown in Figure 8.79 can be attained. However, it may not be easy for an operator to use chemicals to control biofilm thickness by redispersing immobilized biomass, and also, the lysis of bacteria which have been damaged by the chemicals may introduce extra operational difficulties such as foaming in a fermenter as observed in this study.

Another method is by physical means as have been utilized in fluidized bed fermenters. As indicated above, the active biofilm on supports (usually sand) can be kept very thin due to the interactions among particles and/or between particles and liquids, but it is difficult to control the biofilm thickness at a desirable value by this method. Moreover, with this method the turbulence of fluid flow and thus the back–mixing in the fermenter must be increased, which greatly decreases the thickness of an active biofilm and the hold-up of active biomass in the fermenter while the bulk medium concentration approaches the outlet concentration due to the back-mixing.

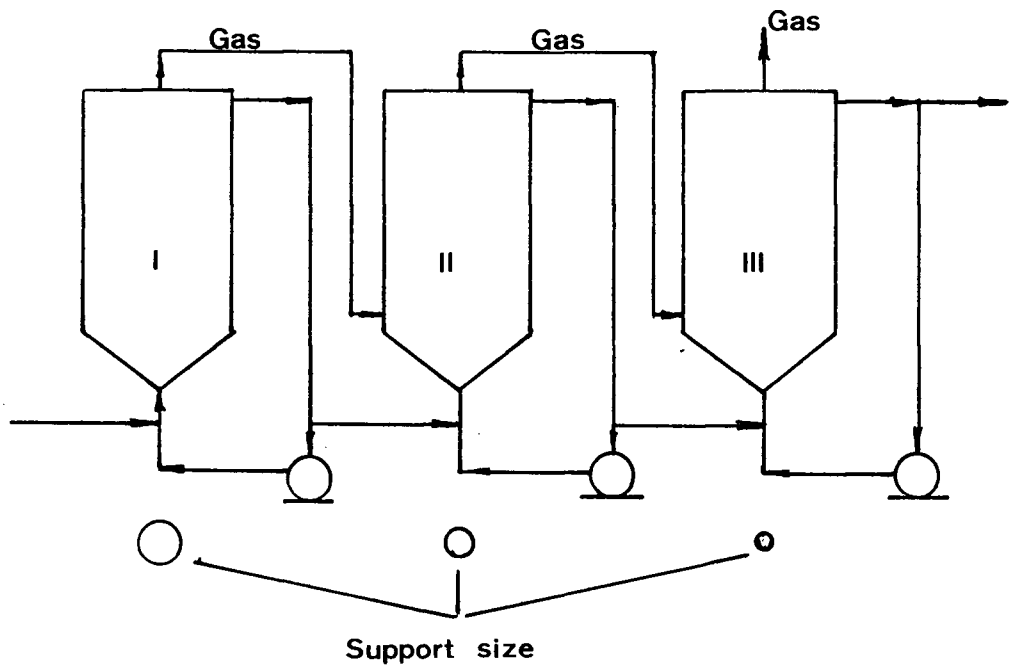


Figure 8.80: Illustration of a process of three stages of cheese whey treatment

### 8.2.3 A Compromised Physical Method

With a physical method to control the biofilm thickness, the excess biomass can be easily removed from the fermenter, thus, a long term stable operation can be established. First of all, considering the concentration effect on biofilm thickness and the complete back-mixing caused by fluid flow, it is suggested that the process of cheese whey treatment be divided into several stages connected in series, not only two stages (or two phases) and each stage can be operated with a small amount of back-mixing. Figure 8.80 shows a process of three stages. The distribution of acidogens and methanogens (with acetogens) is flexible. It may be possible for the first stage to act as the acidogenic phase and the following two stages as the methanogenic phase.

One recommended support is balls of porous materials such as natural sponge or polyurethane foam which can entrap the active biomass within their pores. The size

of the balls, however, should be controlled according to the optimum biofilm thickness calculated for the special conditions in a stage. In general, the first stage has the balls with the biggest diameter, with gradually decreased ball size in the following stages. The last stage may use sand as its support if the desirable biofilm thickness is very thin. The excess biomass produced by the growing biofilms can be removed from the surface of the balls by fluidizing the reactors as with sand fluidized beds while the biomass within the balls will always be active throughout the balls because of their controlled sizes.

As is well known, the microbial growth in the first one or two stages will be the fastest because of the faster intrinsic growth rate of acid-producing bacteria and the higher substrate concentrations. Therefore most of the excess biomass should be removed in these stages. Another arrangement is recommended in which the first two stages are operated in a fluidized bed mode having supports as suggested above, while the last stage is operated in a plug flow mode with stationary supports such as needle-punched PVC. The removal of excess biomass from the stationary supports may be performed periodically by recycling the medium which would add a stress on the biofilm or by adding stripping chemicals.

In conclusion, a long term optimal and stable operation of fermenters using immobilized microorganisms depends to great extent on whether the excess biomass due to microbial growth can be removed from the reactors smoothly and continuouly to maintain the size of microbial aggregates at an optimum value. The results of this study have offered some basic data for calculating the optimum size of the microbial aggregates, but more investigations are needed on how to control a growing biofilm at this desirable thickness.

## Bibliography


[1] F. Kosikowski, "Cheese and fermental milk foods", F.V. Kosikowski and Associates, Brooktindale, New York, p455 (1977)

[2] OCDE, "Milk and milk products balances in OCDE contries 1979-1987", Head of Publication Service, OECD, France, (1989)

[3] Beak Engineering Ltd, "Anaerobic treatment of dairy effluent", Report EPS3/FP/1, Environmental Canada, Ontario, Canada, (1986)

[4] S.W. Watson, A.E. Peterson and R.D. Powell, "Benefits of spreading whey on agricultural land", Journal of Water Pollution Control Federation, 49:24-34 (1977)

[5] P.G. Muller, "Economic evaluation of feeding whey to livestocks, part 2 ", Project Report for Food Research Institute, Research Branch, Agriculture Canada, (1979)

[6] R. Hirschl and F.V. Kosikowski, "A new type of acid whey concentrate product derived from ultrafiltration", Journal of Dairy Science, 58:793 (1975)

[7] E.H. Marth, "Fermetation products from whey" in "Byproducts from milk", edited by B.H. Webb, The Avi Publishing Company, Inc. , Westport, Connecticut, (1970)

[8] I. Galsmar and A. Bergmann, "Spray drying of whey", Journal of the Society of Dairy Technology, 20:106-110 (1967)

[9] T.A. Nickerson, "Lactose" in "Byproducts from milk", edited by B.H. Webb, The Avi Publishing Company, Inc., Westport, Connecticut, (1970)

[10] S. Knight, W. Smith and J.B. Mickle, "Cheese whey disposal using *Saccharomyces fragilis* yeast", Cultural Dairy Products Journal, 7(2):17-22 (1972)

[11] A. Gomez and F.J. Castillo, "Production of biomass and $\beta$-D-galactosidase by *Candida pseudotropicalis* grown in continuous culture on whey", Biotechnology and Bioengineering, 25:1341-1357 (1983)

[12] G.J. Moulin, M. Guillaume and P. Galzy, "Alcohol production by yeast in whey ultrafiltrate", Biotechnology and Bioengineering, 22:1277-81 (1980)

[13] E.R. Hall and G.P. Adams, "Anaerobic treatment of cheese whey", Proc. Seminar on Anaerobic Fixed-Film Digestion, Ontario Ministry of Environment/Pollution Control Association of Ontario, Toronto, pp65-76 (1986)

[14] J.C. Young and P.L. McCarty, "Anaerobic filter for waste treatment", Journal of Water Pollution Control Federation, 41:R160 (1969)

[15] M.S. Switzenbaum, "A comparison of the anaerobic filter and the anaerobic expanded/fluidized bed processes", Water Science and Technology, 15:345-358 (1983)

[16] G. Lettinga, A.F.M. van Velsen, S.W. Hobna, W. de Zeeuw and A. Klapwijk, "Use of upflow sludge blanket (USB) reactor concept for biological wastewater treatment, especially for anaerobic treatment", Biotechnology and Bioengineering, 22:699-734 (1980)

[17] M.S. Switzenbaum and S.G. Danskin, "Anaerobic expanded bed treatment of whey", Proceedings (36th) of Industrial Waste Conference, Purdue University, Ann Arbor Science, Michigan, 1982

[18] P.H. Boeing and V.F. Larsen, "Anaerobic fluidized bed whey treatment", Biotechnology and Bioengineering, 24:2539-56 (1982)

[19] J. Dehaast, T.J. Britz, J.C. Novello and P.M. Lategan, "Anaerobic digestion of cheese whey using a stationary fixed-bed reactor", New Zeland Journal of Dairy Science and Technology, 18:261-71 (1983)

[20] L. van den Berg and K.J. Kennedy, "Dairy waste treatment with anaerobic stationary fixed-bed film reactors", Water Science and Technology, 15:359(1983)

[21] F.X. Wildenauer and J. Winter, "Anaerobic degestion of high-strength acidic whey in pH-controlled upflow fixed film loop reactor", Applied Microbiology and Biotechnology, 22:367 (1985)

[22] P.J. Reynolds and E. Colleran, "Comparison of start-up and operation of anaerobic fixed bed and hybrid sludge-bed/fixed-bed reactors treating whey wastewater", Proceedings of EWPCA Conference Anaerobic Treatment, Amsterdam, p515 1986

[23] F.G. Pohland and S. Ghosh, "Developments in anaerobic stabilization of organic wastes—the two-phase concept", Environmental Letters, 1(14):255 (1971)

[24] F.E. Mosey, "Methamatical modeling of the anaerobic digestion process: regulatory mechanisms for the formation of short-chain volatile acids from glucose", Water Science and Technology, 15:209-32 (1983)

[25] M.J. Hammer et al, "Dialysis separation of sewage sludge digestion", Journal of the American Society of Civil Engineers, SA5, 907(1969)

[26] S. Ghosh, J.R. Conrad and D.L. Klass, "Anaerobic acidogenesis of waste water sludge" Journal of Water Pollution Control Federation, 47:31-45 (1975)

[27] S. Ghosh and M.D. Henry, "Stabilization and gasification of soft drink manufacturing waste by conventional and two-phase anaerobic digestion", Proceedings of the 36th Purdue Industrial Wasts Conference, Lafayette, IN. p292, 1981

[28] S. Ghosh et al, "Two-phase upflow anaerobic digestion of concentrated sludge", Proceedings of the 5th Symposium on Biotechnology for Fuels and Chemicals", Gattinburg, TN, 1983

[29] J.D. Keenan, "Multiple staged methane recovery from solid wastes", Journal of Environmental Science and Health, A11(8/9):525 (1976)

[30] S. Ghosh, J.P. Ombregt and P. Pipyn, "Methane production from industrial wastes by two-phase anaerobic digestion", Water Research 19(9):1083-88 (1985)

[31] I. Berkovitch, "The treatment plant that gives more than just clean water", Process Engineering, April p77 (1986)

[32] R.F. Hickey and R.W. Owens, "Methane generation from high- strength industrial wastes with the anaerobic biological fluidized bed", Biotechnology and Bioengineering Symposium, No.11 1981

[33] S.-T. Yang, I.-C. Tang and M.R. Okos, "Defined bacterial culture development for methane generation from lactose" Biotechnology and Bioengineering, 32:28-37 (1988)

[34] I.J. Callander and J.P. Barford, "Cheese whey anaerobic digestion — effect of chemical flocculant addition" Biotechnology Letters, 5:153-58 (1983)

[35] J. Dehaast, T.J. Britz, J.C. Novello, and E.W. Veywey, "Anaerobic digestion of deproteined cheese whey", Journal of Dairy Research, 52:457-67 (1985)

[36] S.R. Harper and F.G. Pohland, "Recent developments in hydrogen management during anaerobic biological waste water", Biotechnology and Bioengineering, 28:558-602 (1985)

[37] F. Ehlinger, J.M. Audic, D. Verrier and G.M. Faup, "The influence of the carbon source on microbiological clogging in an anaerobic filter", Water Science and Technology, 19:261-273 (1987)

[38] J.C. Young and M.F. Dahob, "Effect of media design on the performence of fixed bed anaerobic reactors", Water Science and Technology, 15(8/9):369 (1983)

[39] E.R. Hall, "Improving hydraulic efficiency in high rate anaerobic systems", Proc. of Seminar Bridging the Gap between Research and Full Scale Operation in Wastewater Treatment, Ontario Ministry of Environment/Pollution Control Association of Ontario, pp55-57 (1984)

[40] Kuroda Masao et al, "Methanogenic bacteria attached to solid supports", Water Research, 25(5):653-656 (1988)

[41] A. Bhadra, J.M. Scharer and M. Moo-Young, "Methanogenesis from volatic fatty acids in down flow stationary fixed-bed reactor", Biotechnology and Bioengineering, 30:314-319 (1986)

[42] R. Wollersheim, "Adhesion and biofilm development of acetate- and butyrate-degrading microorganisms on glass surfaces", Biotechnology Letters, 11(10):749-752 (1989)

[43] W.D. Murray and L. van den Berg, "Effects of support material on the development of microbial fixed films converting acetic acid to methane", Journal of Applied Bacteriology, 51:257-265 (1981)

[44] W.S. Kisaalita, K.V. Lo and K.L. Pinder, "Acidogenic fermentation of lactose", Biotechnology and Bioengineering, 30:88-95 (1987)

[45] W.S. Kisaalita, K.V. Lo and K.L. Pinder, "Influence of dilution rate on the acidogenic phase products distribution during two-phase lactose anaerobiosis", Biotechnology and Bioengineering, 34:1235-1250 (1989)

[46] W.S. Kisaalita, "Anaerobic fermentation of whey: acidogenises ", PhD thesis, University of British Columbia, British Columbia, Canada, 1987

[47] P. Harremoes, "Biofilm kinetics" in "Water pollution microbiology", ed. by R. Mitchell, John Wiley & Sons, New York, N.Y. Vol.2, pp71-109 (1978)

[48] L.G. Scheve, "Elements of biochemistry", Allyn and Bacon, Inc. Newton, Massachusetts, p355 (1984)

[49] D.F. Toerien and W.H.Journal Hattingh, "Anaerobic digestion I. the microbiology of anaerobic digestion", Water Research, 3:385-416 (1969)

[50] R.E. McKinney, "Microbiology for sanitary engineers", McGraw–Hill, New York, (1962)

[51] D.F. Toerien, M.L. Siebert and W.H.Journal Hattingh, "The bacterial nature of the acid–forming phase of anaerobic digestion", Water Research, 1:497 (1967)

[52] F.Journal Post, A.D. Allen and T.C. Reid, "Simple medium for the selective isolation of Bacteroids and related organisms and their occurence in sludge", Applied Microbiology, 15:213 (1967)

[53] H.W. Doelle, "Basic metabolic processes" in "Biotechnology, a comprehensive treatise in 8 volumes: vol.1 microbial fundamentals", ed. by H.-Journal Rehm and G. Reed, p113 (1981)

[54] P.C. McCarty, J.S. Jeris, R.E. McKinney, K. Reed and C.A. Vath, "Microbiology of anaerobic digestion" Report No. R62-29 Sedgwick Lab. of Sanitary Science, MIT Cambridge, (1962)

[55] G. Gottschalk "Bacterial metabolism", Springer Verlag (1986)

[56] R.E. Hungate, "Hydrogen as an intermediate in the rumen fermentation", Archives of Microbiology, 59:158-164 (1967)

[57] J.G. Zeikus, "The biology of methanogenic bacteria", Bacteriological Reviews, 41(1):514-541 (1977)

[58] M.C. Siebert, D.F. Toerien and W.H.Journal Hattingh, "Bacterial nature of the acid–forming phase of anaerobic digestion", Water Research, 2:545-554 (1968)

[59] A. Kiener and T. Leisinger, "Oxygen sensitivity of methanogenic bacteria", Systematic and Applied Microbiology, 4:305-312 (1983)

[60] B.C. McBride and R.S. Wolfe, "A new coenzyme of methyl transfer, coenzyme M", Biochemistry, 10:2317-2324 (1971)

[61] C.D. Taylor and R.S. Wolfe, "Structure and Methylation of coenzyme M ($HSCH_2CH_2SO_3$)", Journal Biological Chemistry, 249:4879-4885 (1974)

[62] S.F. Tzeng, R.S. Wolfe and M.P. Bryant, "Factor 420– dependent pyridine nucleotide–linked formate metabolism of Methanobacterium ruminantium", Journal of Bacteriology, 121:184-191 (1975)

[63] J.S. Jeris and P.C. McCarty, "Biochemistry of $CH_4$ fermentation using $^{14}C$ tracers", Journal Water Pollution Control Federation, 37:178 (1966)

[64] P.H. Smith and R.A. Mah, "Kinetics of Acetate Metabolism During Sludge Digestion", Applied Microbiology, 14:368-371 (1966)

[65] M.Journal Pine and H.A. Barker, "Studies on the methane fermentation XII The pathway of hydrogen in acetate fermentation", Journal of Bacteriology, 71:644-648 (1956)

[66] M.Journal Pine and W. Vishniae, "The methane fermentation of acetate and methanol", Journal of Bacteriology, 73:736-742 (1957)

[67] K. Decker, K. Jungermann and R.K. Thauer, "Energy production in anaerobic organisms", Angewandte Chemie, International Edition in English, 9:138-158 (1970)

[68] T.C. Stadtman and H.A. Barker, "Studies on methane fermentation IX The origen of methane in the acetate and methanol fermentations by Methanosarcina", Journal of Bacteriology, 61:81-86 (1951)

[69] J.G. Zeikus, P.Journal Weimez, D.R. Nelson and L. Paniels, "Bacterial methanogenesis: acetate as a methane prosursor in pure culture", Archives of Microbiology, 104:129-134 (1975)

[70] T.E. Cappenberg, " A study of mixed continus culture of sulfate-reducing and methane-producing bacteria", Microbial Ecology, 2:60-72 (1975)

[71] L. van den Berg, G.B. Patel, P.S. Clack and C.P. Lentz, "Factors affecting rate of methane fermentation from acetic acid by enriched methanogenic cultures", Canadian Journal of Microbiology, 22:1312-1319 (1976)

[72] M.Journal Wolin, "Hydrogen transfer in microbial communities" in "Microbial interactions and communities", ed. by A.T. Bull and J.H. Slater Academic Press, London (1982)

[73] M.P. Bryant, E.A. Wolin, M.Journal Wolin and R.S. Wolfe, "Methanobacillus omelianskii, a symbiotic association of species of bacteria", Archives of Microbiology, 59:20-31 (1967)

[74] Journal Dolfing, "Acetogenesis" in "Biology of anaerobic microorganisms", ed. by A.J.B. Zehnder, New York, Wiley, pp417-468 (1988)

[75] M.Journal McInerney, M.P. Bryant, R.B. Hespell and J.W. Costertar, "Syntrophomonas wolfei gen. nov. sp. nov., an anaerobic, syntrophic fatty acid-oxidizing bacterium", Applied and Environmental Microbiology, 41:1029-1039 (1981)

[76] P.R. Boone and M.P. Bryant, "Propionate-degrading bacterium, Syntrophobacter wolinii sp. nov. gen. nov., from methaogenic ecosystems", Applied and Environmental Microbiology, 40:626-632 (1981)

[77] D.O. Mountfort, W.Journal Brulla, L.R. Krumholz and M.P. Bryant, "Isolation and Characterization of an anaerobic syntrophic benzoate-degrading bacterium from sewage sludge", Archives of Microbiology, 133:249-256 (1982)

[78] N.G. Wofford, P.S. Beaty and M.Journal McInerney, "Prepartion of cell-free extracts and enzymes involved in fatty acid metabolism in Syntrophomonas wolfei", Journal of Bacteriology, 167:179-185 (1986)

[79] M. Koch, Journal Dolfing, K. Wuhrman and A.J.B. Zehnder, "Pathways of propionate degradation by enriched methanogenic cultures", Applied and Environmental Microbiology, 45:1411-1414 (1983)

[80] M.S. Salkinoja-Salonen, E.-Journal Nyns, P.M. Sutton, L. van den Berg and A.D. Wheatley, "Start-up of an anaerobic fixed-film reactor", Water Science and Technology, 15:305-308 (1983)

[81] J.D. Bryers, "Biologically active surfaces: processes governing the formation and persistence of biofilms", Biotechnology Progress, 3(2):57-68 (1987)

[82] M.S. Powell and N.K.H. Slater, "The deposition of bacterial cells from laminar flows onto solid surfaces", Biotechnology and Bioengineering, 25:891 (1983)

[83] J.E. Duddridge, C.A. Kent and J.F. Laws, "Effects of surface shear stress on the attachment of *Pseudomonas fluorescens* to stainless steel under defined flow conditions", Biotechnology and Bioengineering 24:153 (1982)

[84] C.E. Zobell, "Influence of bacterial activity on source sediment", Journal of Bacteriology, 46:39-56 (1943)

[85] K.C. Marshall, R. Stout and R. Mitchell, "Mechanism of the initial enents in the sorption of marine bacteria to surfaces", Journal of General Microbiology, 68:337-348 (1971)

[86] J.D. Bryers and W.G. Characklis, "Processes governing biofilm formation", Biotechnology and Bioengineering, 24:2451 (1982)

[87] Y.K. Park and B.C. Rivera "The effect of shear stress on biofilm loss rate", Biotechnology and Bioengineering, 24:501-506 (1982)

[88] C.M. Brown, D.C. Ellwood and J.R. Hunter, "Growth of bacteria at surfaces: influence of nutrient limitation", FEMS Microbiology Letters, 1:163-166 (1977)

[89] D.C. Ellwood, J.R. Hunter and V.M.C. Longyear, "Growth of Stretococcus mutants in a chemostat", Archives of Oral Biology, 19:659-664 (1974)

[90] M. Fletcher, "The effects of culture concentration and age, time and temperature on bacterial attachment to polystyrene", Canadian Journal of Microbiology, 23:1-6 (1977)

[91] R.E. Baier, "Influence of the initial surface condition of materials on bioadhession" in Proceedings of 3rd Inter. Congress. on Marine Corrosion and Fouling, ed. by R.F. Acker, B.F. Brown, J.R. Depalma and W.P. Iverson, Northwestern Univ. Press., pp 633-639 (1973)

[92] S. Takakuwa, T. Fujimori and H. Iwasaki, "Some properties of cell–sulfur adhesion in Thiobacillus thioxidans", Journal of General and Applied Microbiology, 25:21-29 (1979)

[93] S.C. Dexter, "Influence of substratum critical surface tension on bacterial adhesion–in situ studies", Journal of Colloid and Interface Science, 70:346-453 (1979)

[94] M. Fletcher and G.I. Loeb, "The influence of substratum characteristics on the attachment of a marine pseudomonad to solid surfaces", Applied and Environmental Microbiology, 37:67-72 (1979)

[95] M.C.M. van Loosdrencht, Journal Lyklema, W. Worde, G. Schraa and A.J.B. Zehnde, "The role of bacterial cell wall hydrophobicity in adhesion", Applied and Environmental Microbiology, 53:1893-1897 (1987)

[96] M.C.M. van Loosdrencht, Journal Lyklema, W. Worde, G. Schraa and A.J.B. Zehnde "Elecrophoretic mobility and hydrophobicity in adhesion", Applied and Environmental Microbiology, 53:1898-1901 (1987)

[97] T.A. Stenstrom, "Bacterial hydrophobicity, an overall parameter for the measurement of adhesion potential to soil particles", Applied and Environmental Microbiology, 55(1):142-147 (1989)

[98] M. Fletcher, "Adherence of marine micro-organisms to soomth surfaces" in "Bacterial adherence", ed. by E.H. Beachey, London and New York, Chapman and Hall, pp 347-371 (1980)

[99] P.R. Rutter, "The physical chemistry of the adhesion of of bacteria and other cells" in "Cell adhesion and motility–3rd symposium of the British Socity for cell biology", ed. by A.S.G. Curtis and J.D. Pitts, Cambridge University Press., pp103-135 (1980)

[100] Th.F. Tadros, "Particle-surface adhesion" in "Microbioal adhesion to surfaces", ed. by R.C.W. Berkiley et al, Ellis Horwood, Chichester, England, pp93-116 (1980)

[101] K.C. Marshall, "Interfaces in Microbial Ecology", Haward University Press. Cambridge Mass, (1976)

[102] S.C. Dexter, J.D. Sullivan Jr., Journal Willians III and S.W. Watson, "Influence of substrate wetability on the attachment of marine bacteria to various surfaces", Applied and Environmental Microbiology, 30(2):298-308 (1975)

[103] M. Fletcher and G.D. Floodgate, "An electron microscopic demonstration of an acidic polysaccharide involved in the adhesion of a marine bacterium to solid surface", Journal of General Microbiology, 74:325-334 (1973)

[104] W.A. Corpe and H. Winters, "The biology of microfouling of solid surfaces with special reference to power plant heat exchangers", Condenser Biofouling Control Symposium Proceedings, Electric Power Research Institute, ed. by J.F. Garey et al, Ann Arbor, Mich. pp29-42 (1980)

[105] I.W. Sutherland, "Surface carbohydrates of the prokaryote cell", Academic Press. London and New York, p472 (1977)

[106] W.F. Dudman and J.F. Wilkinson, "The composition of extracellular polysaccharides of Aerobacter–Klebsiell strains", Biochemical Journal, 62:289-295 (1959)

[107] M. Shapiro and M.S. Switzenbaum, "Initial anaerobic biofilm development", Proceedings of 2nd Inter. Conference on Fixed-film Biological Processes, ed. by J.T. Bandy et al, Vol. 1, Arlington, Virginia, July 10-12 (1984)

[108] W.D. Murray and L. van den Berg, "Effects of support material on the development of microbial fixed films converting acetic acid to methane", Journal of Applied Bacteriology, 51:257-265 (1981)

[109] L. van den Berg and K.Journal Kennedy, "Support materials for stationary fixed film reactors for high-rate methanogenic fermentations", Biotechnology Letters, 3(4):165-170 (1981)

[110] P. Huysman, P. van Meenen, P. van Assche and W. Verstraete, "Fators affecting the colonization of non porous and porous packing materials in model upflow methane reactors", Biotechnology Letters, 5(9):643- 648 (1983)

[111] D. Verrier and G. Albagnac, "Adhesion of anaerobic bacteria from methanogenic sludge onto inert solid surfaces", EUR report # 10024 pp537-541 (1985)

[112] D. Verrier, B. Mortier, H.C. Dubourguier and G. Albagnac, "Adhesion of anaerobic bacteria to inert supports and development of methanogenic biofilms", Proc. 5th Inter. Symposium on Anaerobic Digestion, ed. by E.R. Hall and P.N. Hobson, Pergamou Press, Oxford, Bologna, Italy, pp61-79 (1988)

[113] M.S. Switzenbaum, K.C. Scheuer and K.E. Kallmeyer "Influence of materials and precoating on initial anaerobic biofilm development", Biotechnology Letters, 7(8):585-588 (1985)

[114] J.M. Scharer, A. Bhadra and M. Moo-Young, "Methane production in immmobilized cell bioreactor" in "Bioreator immobilized enzymes and cells: fundamentals and application", ed. by M. Moo-Young, Elsevier Applied Science Publications Ltd., (1988)

[115] G. Astarita, "Mass transfer with chemical reaction", Elsevier, Amsterdam, (1967)

[116] V.G. Levich, "Physicochemical hydrodynamicas", New York, Prentice Hall, (1962)

[117] M. Moo-Young and H.W. Blanch, "Design of biochemical reactors, mass transfer criteria for simple and complex systems", Advances in Biochemical Engineering, 19:1-57 (1981)

[118] J.C. Kissel, "Modeling mass transfer in biological wastewater treatment processes", Water Science and Technology, 18:35-45 (1986)

[119] E.Journal LaMotta, "External mass transfer in a biological film reactor", Biotechnology and Bioengineering, 18:1359-1370 (1976)

[120] R.W. Robinson, D.E. Akin, R.A. Nordstedt, M.V. Thomas and H.C. Aldrich, "Lingt and electron microscopic examinations of methae- producing biofilms from anaerobic fixed-bed reactors", Applied and Environmental Microbiology, 48(1):127-136 (1984)

[121] T.T. Eighmy, D. Maratea and P.L. Bishop, "Electron microscopic examination of wastewater biofilm formation and structural components", Applied and Environmental Microbiology, 45(6):1921-1931 (1983)

[122] M. Harvey, C.W. Forsberg, T.Journal Beveridge, Journal Pos and J.R. Ogilvie, "Methanogenic activity and strustural characteristics of the microbial biofilm on a needle-punched polyester support", Applied and Environmental Microbiology, 48(3):633-638 (1984)

[123] S.B. Libicki, P.M. Salmon and C.R. Robertson, "The effective diffusive permeability of a nonreacting solute in microbial cell aggregates", Biotechnology and Bioengineering, 32:68-85 (1988)

[124] E.Journal LaMotta, "Internal diffusion and reaction in biological films", Environmental Science and Technology, 10(8):765-769 (1976)

[125] H.R. Bungay and D.M. Harold, "Simulation of oxygen transfer in mcirobial slimes", Biotechnology and Bioengineering, 13:569-579 (1971)

[126] Y.S. Chen and H.R. Bungay, "Microelectorde studies of oxygen transfer in trickling filter slimes", Biotechnology and Bioengineering, 23:781-792 (1981)

[127] K. Williamson and P.L. McCarty, "Verification studies of the biofilm model for bacterial substrate utilization", Journal of Water Pollution Control Federation, 48(2):281-296 (1976)

[128] J.V. Matson and W.G. Characklis, "Diffusion into microbial aggregates", Water Research, 10:877-885 (1976)

[129] M. Onuma and T. Omura, "Mass-transfer characteristics within microbial systems", Water Science and Technology, 14:553-568 (1982)

[130] H.H. Siegrist and W. Gujer, "Mass transfer mechanisms in a heterotrophic biofilm", Water Research, 19(11): 1369-1378 (1985)

[131] P.G. Smith and P. Coackley, "Diffusivity, tortuousity and pore structrue of activated sludge", Water Research, 18(1): 117-122 (1984)

[132] A.D. Meunier and K.Journal Williamson, "Packed bed biofilm reactors: design", Journal of Environmental Engineering Division, ASCE, 107:319-337 (1981)

[133] B.E. Rittmann and P.L. McCarty, "Variable-order Model of bacterial-film kinetics", Journal of Environmental Engineering Division, ASCE, 104:889-900 (1978)

[134] Y.-T Wang, M.T. Suidan and B.E. Rittmann, "Kinetics of methanogens in an expanded-bed reactor", Journal of Environmental Engineering Division, ASCE, 112:155-170 (1986)

[135] N.P. Harris and G.S. Hansford, "A study of substrate removal in a microbial film reactor", Water Research, 10:935-943 (1976)

[136] B. Atkinson and I.S. Daoud, "Diffusion effects with microbial films", Transactions, Institute of Chemical Engineers, 48:245-254 (1970)

[137] V.H. Edwards, "The influence of high substrate concentraions on microbial kinetics", Biotechnology and Bioengineering, 12:679-712 (1970)

[138] C.P.L. Grady, Jr, "Modeling of biological fixed films – A state-of-the-art review" in "Fixed-film, biological processes for wastewater treatment", ed. by Y.C. Wu and E.D. Smith, Noyes Data Corporation pp75-134 (1983)

[139] W.K. Shieh and L.T. Mulcahy, "Experimental determination of intrinsic kinetic coefficients for biological wastewater treatment systems", Water Science and Technology, 18:1-10 (1986)

[140] I.Journal Callander and J.P. Barford, "Cheese whey anaerobic digestion–effect of chemical flowclant addition", Biotechnology Letters, 5:153-158 (1983)

[141] R.F. Hickey, "Methane generation from high-strengh industrial wastes with the anaerobic biological fluidised bed", Biotechnology and Bioengineering Symposium, Number 11, John Wiley and Sons, New York, NY, (1981)

[142] A.W. Lawrence and P.L. McCarty, "Kinetics of methane fermentation in anaerobic treatment", Journal of Water Pollution Control Federation, 41(2):R1-R17 (1969)

[143] Chiu-Yue Lin, Kazuaki Sato, Tatsuya Noike and Junichiro Matsumoto, "Methanogenic digestion using mixed substrate of acetate, propionic and butyric acids", Water Research, 20(3):385-394 (1986)

[144] M. Henze and P. Harremoes, "Anaerobic treatment of wastewater in fixed film reactors — a literature review", Water Science and Technology, 15:1-101 (1983)

[145] R.Journal Zoetemyer, J.C. Heuvel, and A. Cohen, "pH influence on acidogenic dissimilation of glucose in an anaerobic digester", Water Research, 16(3):303-311 (1982)

[146] R.S. Oremland, L. Marsh, and D.Journal DesMarais, "Methanogenesis in big soda lake nevada: an alkaline, moderately hypersaline desert lake", Applied and Environmental Microbiology, 43:462-468 (1982)

[147] R.C. Harriss, E. Gorham, D.I. Sebacher, K.B. Bartlett and P.A. Flebbe, "Methane flux from northern peatlands", Nature, 315:652-654 (1985)

[148] A.J.B. Zehnder, K. Ingvorsen and T. Marti, "Microbiology of methane bacteria", The Second International Symposium on Anaerobic Digestion, 6–11 Sept. Travemunde, Germany, (1981)

[149] R.A. Mah and M.R. Smith, "The Methanogenic bacteria" in "The prokaryotes, vol. 1", ed. by M.P. Starr, H. Stolp, H.G. Truper, A. Balows and H.G. Schlegel, Springer, Berlin, pp948-977 (1981)

[150] L. Bhatnagar, M.K. Jain, J.P. Aubert and J.G. Zeikus, "Comparison of assimilatory organic nitrogen, sulfur, and carbon sources for growth of *Methanobacterium* species", Applied and Environmental Microbiology, 48:785-790 (1984)

[151] L. van den Berg and C.P. Lentz, "Food processing waste treatment by anaerobic digestion", Proceedings of the 32nd Industrial Waste Conference, Purdue University, Lafayette, Indiana, Ann Arbor Science, Ann Arbor, Mich., 1978, pp252-258 (1977)

[152] R.E. Speece and P.L. McCarty, "Nutrient requirements and biological accumulation in anaerobic digestion" in " Advances in Water Pollution Research", ed. by W.W. Eckenfelder, Perganon Press, Oxford, UK, (1964)

[153] P. Scherer and H. Sahm, "Influence of sulphur-containing compounds on the growth of Methanosarcina barkeri in a defined medium", European Journal of Applied Microbiology and Biotechnology, 12:28-35 (1981)

[154] L. Daniels, N. Belay and B.S. Rajagopal, "Assimilatory reduction of sulfate and sulfite by methanogenic bacteria", Applied and Environmental Microbiology, 51:703-709 (1986)

[155] D.Journal Hill, "Effects of carbon: nitrogen ratio on anaerobic digestion of dairy manure", Agricultural Wastes, 1:267-278 (1979)

[156] P. Pipyn and W. Verstraete, "Lactate and Ethanol as Intermediates in Two-Phase Anaerobic Digestion", Biotechnology and Bioengineering, 23:1145-1154 (1981)

[157] P.L. McCarty, "The methane fermentation" in " Principles and applications in aquatic microbiology", ed. by H. Heukelekian and N.C. Dondero, John Wiley and Sons, New York, NY, (1964)

[158] R.E. Speece, G.F. Parkin and D. Gallagher, "Nickel stimulation of anaerobic digestion", Water Research, 17:677-683 (1983)

[159] K.Journal Kennedy and R.L. Droste, "Startup of anaerobic downflow stationary fixed film (DSFF) reactors", Biotechnoloty and Bioengineering, 27:1152-1165 (1985)

[160] J.A. Howell and B. Atkinson, "Sloughing of microbial film in trickling filters", Water Research, 10:307-315 (1976)

[161] M.H. Turakhia and W.G. Characklis, "Activity of *Pseudomonas aeraginosa* in biofilms: effect of calcium", Biotechnology and Bioengineering, 33:406-414 (1989)

[162] S. Ghosh and D.L. Klass, "Two-phase anaerobic digestion", Process Biochemistry, 13(4):15-24 (1978)

[163] P.L. McCarty, "Energetics and kinetics of anaerobic treatment" in "Anaerobic biological treatment processes", Advances in biochemistry series 105 ACS, Washington D.C., pp91-107 (1971)

[164] J.F. Andrews, "Kinetics and characteristics of volatile acid production in anaerobic fermentation processes", International Journal of Air and Water Pollution Controll, 9:439-461 (1965)

[165] J.A. Mueller and J.L. Mancini, "Anaerobic filter kinetics and applications", Proceedings of the 30th industrial waste conference 1975 Purdue University, Lafayette, Indiana, Ann Arbor Science, Ann Arbor, Mich 1977 pp423-447 (1975)

[166] M. Lindgren, "Mathematical modeling of the anaerobic filter process", Water Science and Technology, 15(8-9):197-207 (1983)

[167] R.W. Harvey and L.Y. Young, "Enumeration of particle- bound and unattached respiring bactria in th salt mash enviroment", Applied and Environmental Microbiology, 40:156-160 (1980)

[168] C.W. Hendricks, "Sorpotion of hetreotrophic and euteric bactria to glass surfaces in the continuous culture of river water", Applied Microbiology, 28:572-578 (1974)

[169] W.H. Jeffrey and J.H. Paul, "Activity measurements of planktomic microbial and microfouling communities in an eutrophic estnary", Applied and Environmental Microbiology, 46:157-162 (1986)

[170] M.C.M. van Loosdrecht, Journal Kyklema, Journal Morde and A.J.B. Zehnder, "Influence of interfaces on microbial activity", Microbiological Reviews, 54(1):5-87 (1990)

[171] W.H. Jeffrey and J.H. Paul, "Activity of an attached and free-living *Vibrio sp.* as measured by thrymidine incorporation, p-indonitrotetrazolium reduction, and ATP/ADP Ratios", Applied and Environmental Microbiology, 51:150-156 (1986)

[172] T.C. Kieft and D.E. Caldwell, "Chemostat and in-situ colonization kinetics of *Thermotrix Thiopara* on caldite and pyrite surfaces", Geomicrobiology Journal, 3:217-229 (1984)

[173] D.E. Caldwell and J.R. Lawrence, "Growth kinetics of *Pseudomonas fluorescens* microcolonies within the hydrodynamic boundary layers of surface microenvironments", Microbial Ecology, 12:299-312 (1986)

[174] A.S. Gordon ans F.Journal Millero, "Adsorption-mediated decrease in the biodegradation rate of organic compounds", Microbial Ecology, 11:289-298 (1985)

[175] G. Stucki and M. Alexander, "Role of dissolution rate and solubility in biodegradation of aromatic compounds", Applied and Environmental Microbiology, 53:292-297 (1987)

[176] J.Journal Bright and M. Fletcher, "Amino assimilation and electron transport system activity in attached and free-living marine bacteria", Applied and Environmental Microbiology, 45:818-825 (1983)

[177] R. Hattori and T. Hattori, "Growth rate and molar growth yield of *E. coli* adsorbed on an anion exchange resin", Journal of General and Applied Microbiology, 27:287-298 (1981)

[178] A. Cohen, J.M. van Germert, R.Journal Zoetemeyer, A.M. Breure, "Main characteristics and stoichiometric aspects of acidogenesis of soluble carbohydrate containing wastewaters", Process biochemistry, 19(6):228-232 (1984)

[179] R.K. Thauer, K. Jungermann and K. Decker, "Energy conservation in chemotrophic anaerobic bacteria", Bacteriological Reviews, 41(1)100-180 (1977)

[180] G. Gottschalk, "Bacterial Metabolism" Springer-Verlag New York Inc. New York, pp167-121 (1979)

[181] J.C. van den Heuvel, H.H. Beeftink and P.G. Verschuren, "Inhibition of the acidogenic dissimilation of glucose in anaerobic continuous cultures by free butyric acid", Applied Microbiology and Biotechnology, 29:89-24 (1988)

[182] P.J.F. Henderson, "Iron transport by energy-conserving biological membranes", Annual Review of Microbiology, 25:393-428 (1971)

[183] Journal Domingue, "Probing the chemistry of the solid/liquid interface", American Laboratory, pp50-55, Oct. (1990)

[184] J.Journal Bikerman, "Surface chemistry - theory and applications", Academic Prss Inc. New York, (1958)

[185] D.C. Ellwood, C.W. Keevil, P.D. Marsh, C.M. Brown and J.N. Wardell, "Surface-associated growth", Philosophical Transations of the Royal Society of London, Ser. B, 297:517-532 (1982)

[186] A.C. Bajpaj, L.R. Mustoe, and D. Walker, "Advanced engineering mathematics", John Wiley & Sons, Ltd., p110 (1977)

[187] M.C.M. van Loosdrecht, Journal Lyklema, N. Norde, G. Schraa and A.J.B. Zehnder, "The role of bacterial cell wall hydrophobicity in adhesion", Applied and Environmental Microbiology, 53(8):1893-1897 (1987)

[188] J.H. Pringle and M. Fletcher, "Influence of substratum wettability on attachment of freshwater bacteria to solid surfaces", Applied and Environmental Microbiology, 45:811-817 (1983)

[189] M. Fletcher and G.D. Floodgate, "The adhesion of bacteria to solid surfaces" in "Microbial ultrastructure: the use of the electron microscope", ed. by R. Fuller and D.W. Lovelock, Academic Press, London, pp101-107 (1976)

[190] D.R. Absolom, "The role of bacterial hydrophobicity in infection", Canadian Journal of Microbiology 34(3):287-298 (1988)

[191] N. Mozes, D.E. Amorg, A.Journal Leoñard and P.G. Rouxhet, "Surface properties of microbial cells and their role in adhesion and flocculation", Colloids and Surfaces, 42(3-4):313 (1989)

[192] B. Dahneke, "The influence of flatting on the adhesion of particles", Journal of Colloid and Interface Science, 40:1-13 (1972)

[193] R.Journal Shimp and F. Pfaender, "Effects of surface area and flow rate on marine bacterial growth in activated carbon columns", Applied and Environmental Microbiology 44(2):471-477 (1982)

[194] F.A.L. Dullien, "New relation between viscocity and the diffusion coefficients based on Lamm's theory of diffusion", Transactions of the Fraraday Society, 59:856-68 (1963)

[195] R.K. Ghai, H. Ertt and F.A.L. Dullien, "Liquid diffusion of nonelectrolytes I", AIChE Journal, 19:881-900 (1973)

[196] T. Lofin and E. McLaughlin, "Diffusion in binary liquid mixtures", Journal of Physical Chemistry, 73:186(1969)

[197] R.C. Reid, J.M. Prausnitz and B.E. Poling, "The Properties of Gases ans Liquids", McGraw-Hill Book Company, New York, pp577-624 (1987)

[198] C.R. Wilke and P. Chang, "Correlation of diffusion coefficients in diluted solutions", AIChE Journal, 1:264 (1955)

[199] D.R. Lide, "Handbook of chemistry and physics", 71th Edition, CRS Press 1990/1991

[200] M.E. Davis "Numerical methods and modeling for chemical engineers", John Wiley and Sons, Inc., p18 (1984)

[201] L.E. Muller, E. Hindin, J.V. Lunsford and G.H. Dunstan, "Some characteristics of anaerobic sludge digestion I. effects of loading", Journal of Water Pollution Control Federation, 31:669-676 (1959)

[202] E. Hindin and G.H. Dunstan, "Effect of detention time on anaerobic digestion" Journal of Water Pollution Control Federation, 32:930-938 (1960)

[203] J.A. Eastman and J.F. Ferguson, "Solubilization of organic carbon during the acid phase of anaerobic digestion", Journal of Water Pollution Control Federation, 53:352-366 (1981)

[204] M.L. Massey and F.G. Pohland, "Phase separation of anaerobic stabilization by kinetic controls", Journal of Water Pollution Control Federation, 50:2204-2222 (1978)

[205] C.P.L. Grady Jr. and H.C. Lim, "Biological wastewater treatment: theory and applications", Marcel Dekher, New York, NY (1980)

[206] J.M. Scharer and M. Moo-Young, "Methane generation by anaerobic digestion of cellulose-containing waste", Advances in Biochemical Engineering, 11:85 (1979)

[207] Journal Neter, W. Wasserman and G.A. Whitmore, "Applied Statistics", Allyn and Bacon, Inc. Boston, pp518-521 (1982)

[208] L. van den Berg, "Effect of temperature on growth and activity of a methanogenic culture utilizing acetate", Canadian Journal of Microbiology, 23:898-902 (1977)

[209] W. Gujer and A.J.B. Zehnder, "Conversion processes in anaerobic digestion", Water Science and Technologh, 15:127-167 (1983)

[210] C.L. Cooney, "Growth of microorganisms" in "Biotechnology: a conprehensive treaties in 8 vol. Volume 1. microbial fundamentals", ed. by H.Journal Rehm and G. Reed, Verlag Chemie Gmbh, D-6940 Weinheim (1981)

[211] L.G.M. Gorris, J.M.A. van Deursen, C. van der Drift and G.D Vogels, "Biofilm development in laboratory methanogenic fluidized bed reactors", Biotechnology and Bioengineering, 33:687-693 (1989)

[212] W.L. Bolle, Journal van Breugel, G.C. van Eybergen, N.W.F. Kossen and W. van Gils, "Kinetics of anaerobic purification of industrial wastewater", Biotechnology and Bioengineering, 28:542-548 (1986)

[213] R.L. Droste and K.Journal Kennedy, "Steady state kinetics of anaerobic downflow stationary fixed film reactors", Water Science and Technology, 19:275-285 (1987)

[214] M. Dohanyos, B. Dosova, Journal Zabranska and P. Grau, "Production and utilization of volatile fatty acids in various types of anaerobic reactors", Water Science and Technology, 17:191-205 (1985)

[215] M. Dubios, K.A. Gilles, J.K. Hamilton, P.A. Rebers and F. Smith "Colorimetric method for determination of surgars and related substrances", Analytical Chemistry, 28(3):350-356

[216] R.L. Markus, "Colorimetric determination of lactic acid in body fluids utilising cation exchange of deproteinization", Archives of Biochemistry, 29:159-165

# Appendix A

## Fermentation Pathways

### A.1 Four Fermentation Pathways of Glucose to Pyruvate

1. Embden–Meyerhof–Parnas (EMP) pathway of glucose utilization is considered to be widely used among fungi, yeasts and bacteria and has the overall reaction

$$\text{Glucose} + 2\text{ATP} + 2\text{NAD}^+ \rightarrow 2\text{Pyruvate} + 4\text{ATP} + 2(\text{NADH} + \text{H}^+).$$

Figure A.81 shows the reaction intermediates and the enzymes which catalyses the formation of these intermediates.

2. Hexose monophosphate (HMP) pathway is largely concerned with biosynthetic metabolism because of its provision of pentoses which are needed for the synthesis of nucleic acids and nucleotide-containing prosthetic groups. The HMP pathway can be operated in two different variations. The first variation is referred to as the em pentose shunt or pentose cycle which does not lead directly to pyruvate as shown in Figure A.82 [53]. The overall reaction is

$$\text{Glucose} + 12\text{NADP}^+ + 7\text{H}_2\text{O} + \text{ATP} \longrightarrow$$
$$6\text{CO}_2 + 12(\text{NADPH} + \text{H}^+) + \text{H}_3\text{PO}_4 + \text{ADP}.$$

Another variation is used by oxidative microorganisms, the partly complete cycle to produce pyruvate from glyceraldehyde 3–phosphate, catalyzed by the same enzymes as the EMP pathway. The sum of reactions for this second variation is

$$3\text{Glucose} + 6\text{NADP}^+ + \text{ATP} \longrightarrow 2\text{Ffructose 6-P} + \text{Glyceraldehyde 3-P} + 3\text{CO}_2$$
$$+\text{ADP} + 6(\text{NADPH} + \text{H}^+) + \text{H}_3\text{PO}_4.$$

and the pathway is shown in Figure A.83.

3. The Entner–Doudoroff (ED) pathway was discovered by Entner and Doudoroff during metabolic studies of *Pseudomonas saccharophila* as shown in Figure A.84.

4. In addition to the well known EMP, HMP and ED pathways, there is another pathway, phosphoketolase (PK) pathway as shown in Figure A.85. It is, however, possessed by only a small group of bacteria, the heterofermentative *Lactobacilli*.

## A.2 Formation of Organic Acids from Pyruvate

The following figures show the mechanisms of the formation of acetate (Figure A.86), butyrate (Figure A.87), mixed products (Figure A.88) and propionate (Figure A.89) from glucose via the common intermediate, pyruvate.

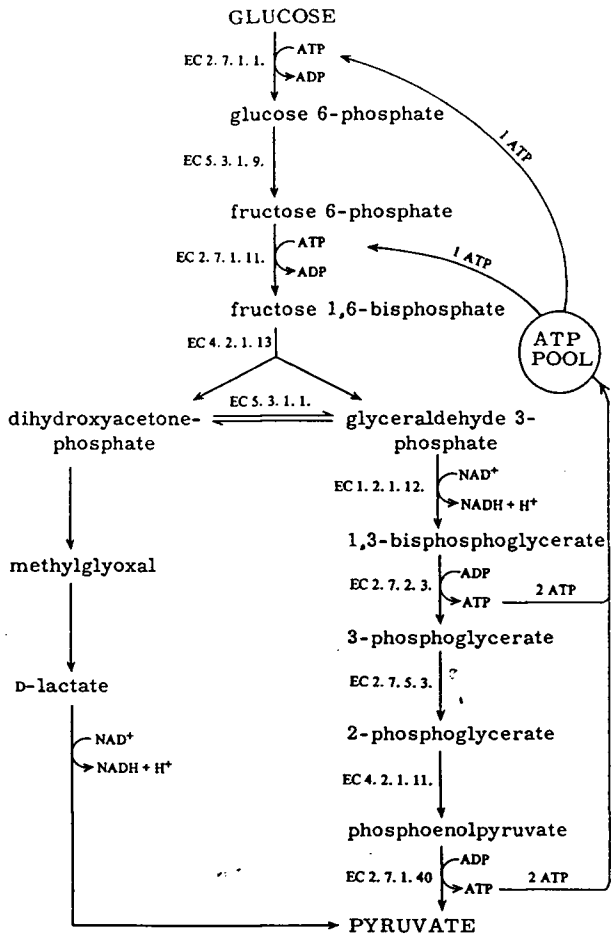


Figure A.81: EMP pathway of glucose conversion to pyruvate. Key to the enzymes: EC 2.7.1.1: hexokinase; EC 5.3.1.9: glucosephosphate isomerase; EC 2.7.1.11: phosphofructokinase; EC 4.2.1.13: fructosebisphosphate aldolase; EC 5.3.1.1: triosephosphate isomerase; EC 1.2.1.12: glyceraldehyde 3-phosphate dehydrogenase; EC 2.7.2.3: phosphoglycerate kinase; EC 2.7.5.3: phosphoglyceromutase; EC 4.2.1.11: Enolase; EC 2.7.1.40: pyruvate kinase. Source is [52].

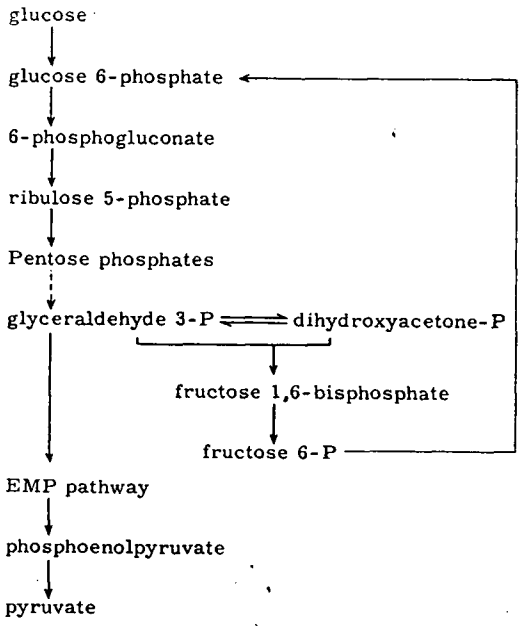


Figure A.82: Schematic representation of the cyclic (pentose shunt) and non-cyclic nature of the HMP pathway. Source is [52].

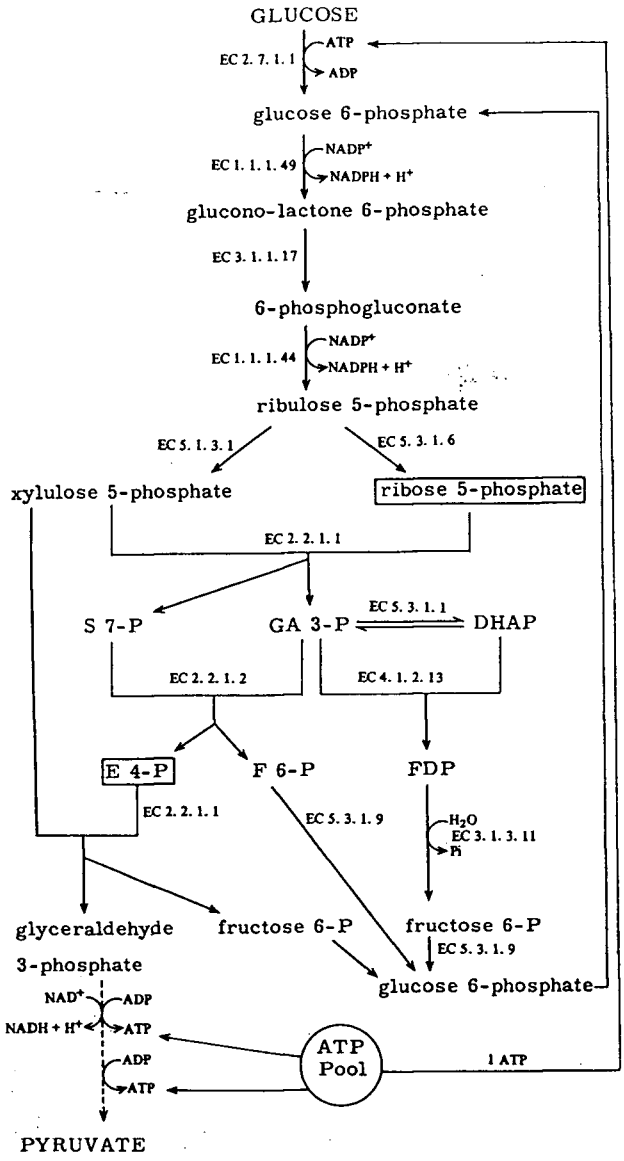


Figure A.83: HMP pathway of glucose utilization. S 7-P: sedoheptulose 7-phosphate; GA 3-P: glyceraldehyde 3-phosphate; DHAP: dihydroxy-acetonephosphate; E 4-P: erythrose 4-phosphate; F 6-P: fructose 6-phosphate; FDP: fructose 1,6-bisphosphate. Key to the enzymes: EC2.7.1.1: hexkoinase; EC 1.1.1.49: glucose 6-phosphate dehydrogenase; EC 3.1.1.17: gluconolactonase; EC 1.1.1.44: 6-phosphogluconate dehydrogenase; EC 5.1.3.1: ribulosephosphate 3-epimerase: EC 5.3.1.6: ribose 5-phosphate isomerase; EC 2.2.1.1: transketolase; EC 4.1.2.13: fructose bisphosphate aldolase; EC 3.1.3.11: hexose diphosphatase; EC 5.3.1.9: glucose 6-phosphate isomerase. Source is [52].

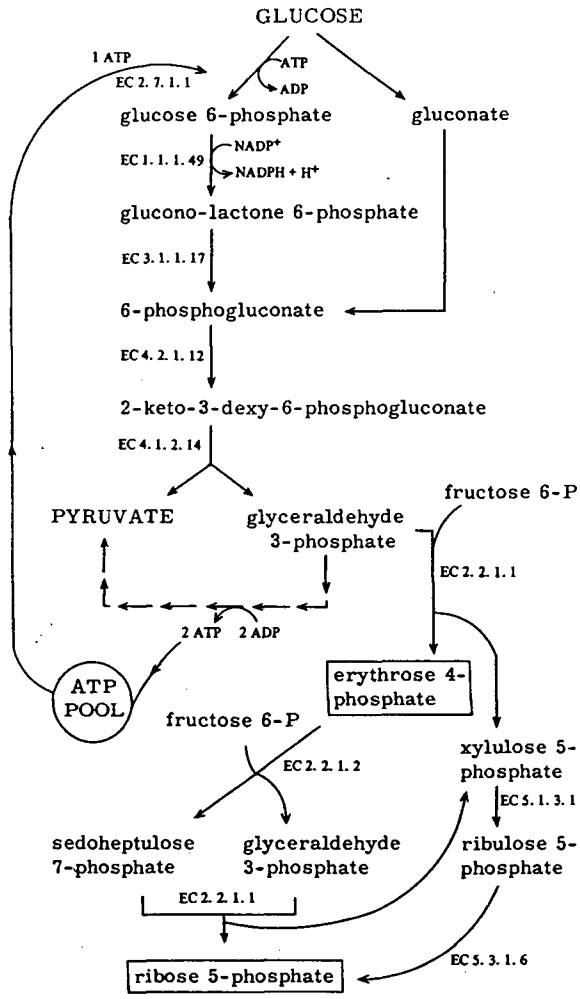


Figure A.84: ED pathway of glucose utilization. The abbreviations as in HMP pathway. Key to the enzymes: EC 2.7.1.1: hexokinase; EC 1.1.1.49: glucose 6-phosphate dehydrogenase; EC 3.1.1.17: gluconolactonase; EC 4.2.1.12: phosphogluconate dehydratase; EC 4.1.2.14: phospho-2- keto-3-deoxygluconate aldolase; EC 2.2.1.1: transketolase; EC 2.2.1.2: transaldolase; EC 5.1.3.1: ribulosephosphate 5- phosphate isomerase. Source is [52].

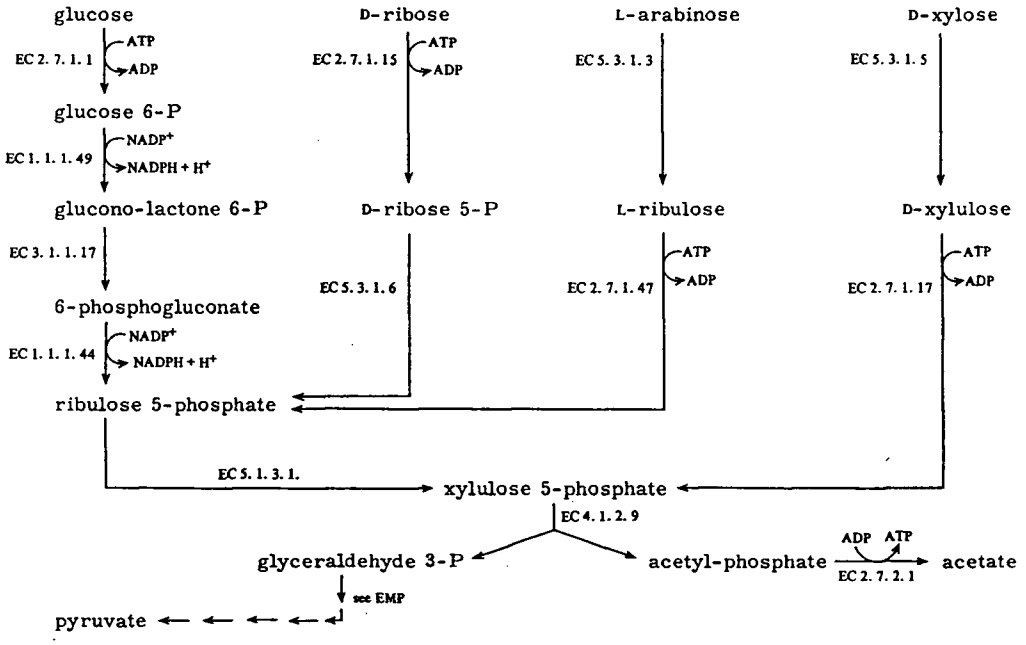


Figure A.85: PK pathway of hexose and pentose utilization. Key to the enzymes: EC 2.7.1.1: hexokinase; EC 1.1.1.49: glucose 6-phosphate dehydrogenase; EC 3.1.1.17: gluconolactonase; EC 1.1.1.44: phosphogluconate dehydrogenase; EC 5.1.3.1: ribulose phosphate 3-epimerase; EC 2.7.1.15: ribokinase; EC 5.3.16: ribosephosphate isomerase; EC 5.3.1.3: arabinose isomerase; EC 2.7.1.47: ribulokinase; EC 5.3.1.5: xylose isomerase; EC 2.7.1.17: xylulokinase; EC 4.1.2.9: phosphokeitolase; EC 2.7.2.1: acetokinase. Source is [52].

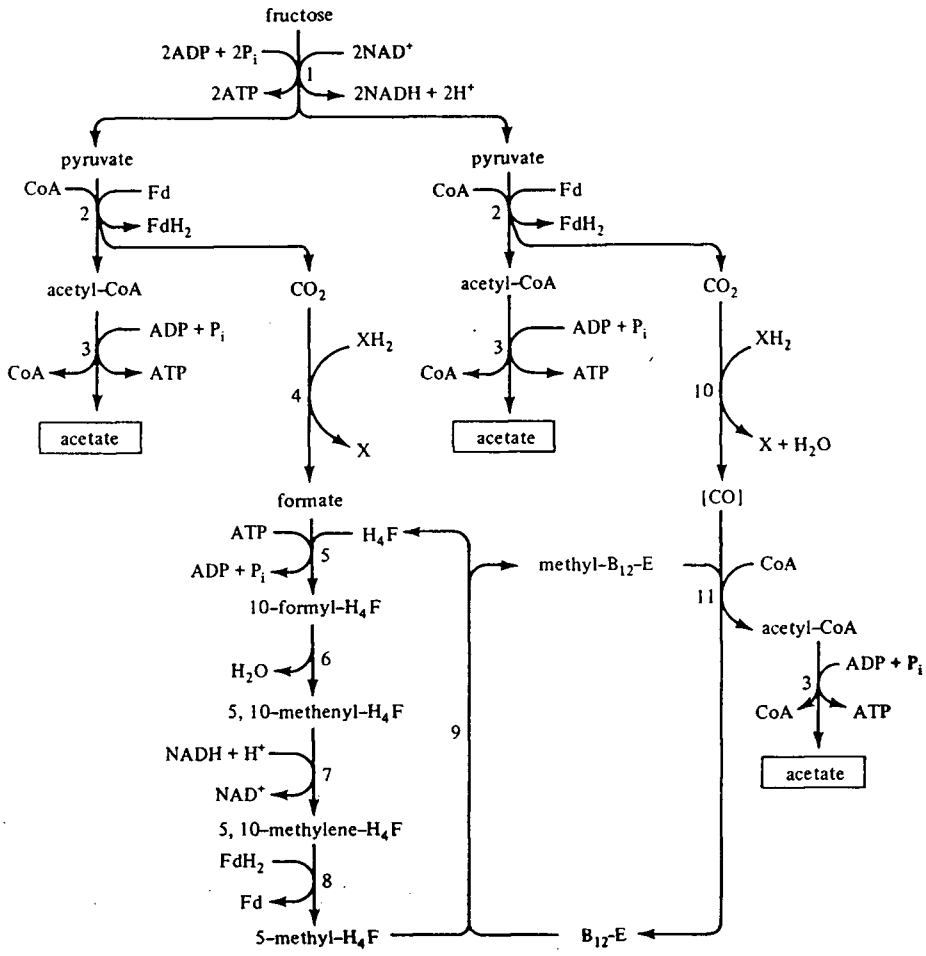


Figure A.86: Formation of acetate from pyruvate. 1, Degradation of fructose via the Embden-Meyerhof-Parnas pathway; 2, pyruvate-ferredoxin oxidoreductase; 3, phosphotransacetylase plus acetate kinase; 4, formate dehydrogenase; 5, formyl-tetrahydrofolate synthetase; 6, methenyl-tetrahydrofolate cyclohydrolase; 7, methylene- tetrahydrofolate dehydrogenase; 8, methylene-tetrahydrofolate reductase; 9, tetrahydrofolate: $B_{12}$ methyltransferase; 10, CO dehydrogenase; 11, acetyl-CoA-symthesizing enzyme; [CO], enzyme-bond. Source is [54].

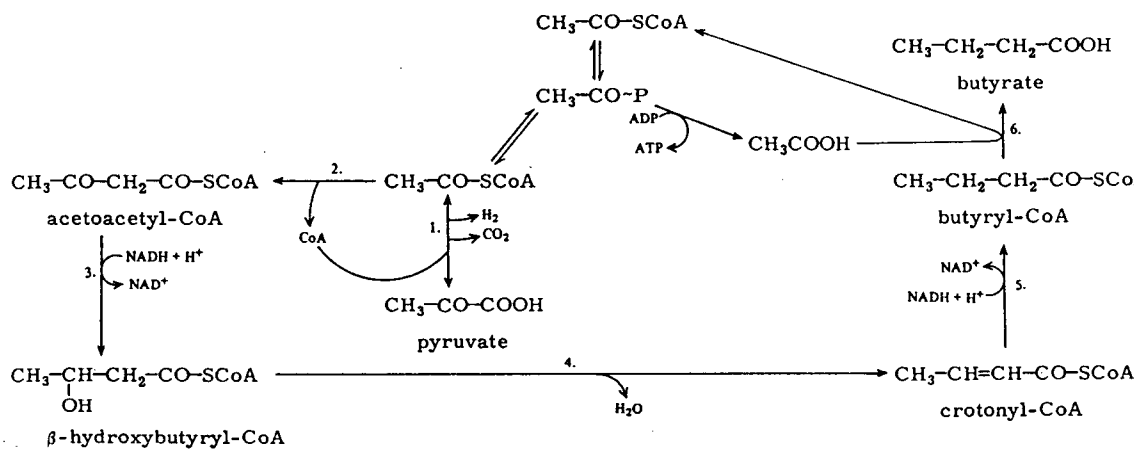


Figure A.87: Butyrate formation from pyruvate by *Clostridia*. Key to the enzymes: 1, pyruvate-ferrodoxin oxidoreductase; 2, acetyl-CoA-acetyl transferase; 3, 3-hydroxybutyryl-CoA dehydrogenase; 4, 3-hydroxyacyl-CoA hydrolyase; 5, butyryl-CoA dehydrogenase; 6, fatty acid CoA transferase. Source is [52].

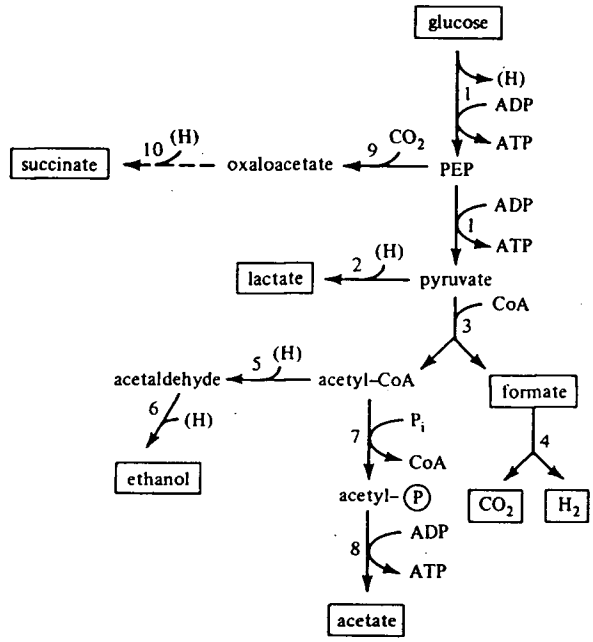


Figure A.88: Formation of mixed products (ethanol, lactate, etc.). 1, enzymes for the EMP pathways; 2, lactate dehydrogenase; 3, pyruvate- formate lyase; 4, formate-hydrogen lyase; 5, acetaldehyde dehydrogenase; 6, alcohol dehydrogenase; 7, phosphotransacetylase; 8, acetate kinase; 9, PEP carboxylase; 10, malate dehydrogenase, fumarase and fumarate reductase. Source is [54].

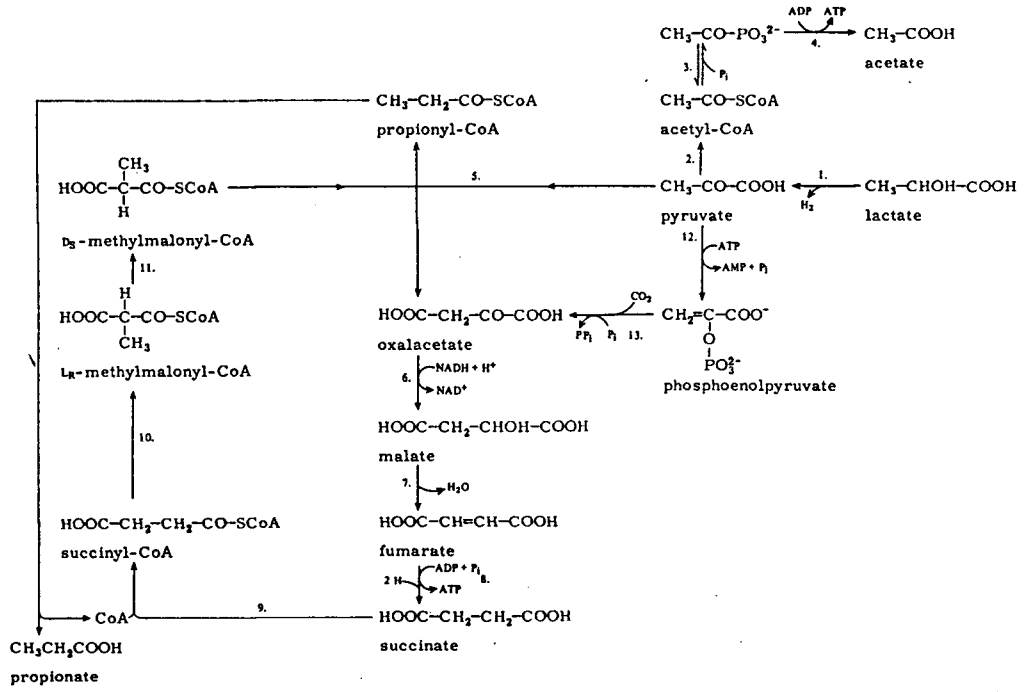


Figure A.89: Formation of propionate from pyruvate or lactate. 1, lactate dehydrogenase; 2, pyruvate-ferredoxin oxidorecuctase; 3, phosphoacetyl transfrase; 4, acetate kinase; 5, Ds-methylmalonyl- CoA-pyruvate transcarboxylase; 6, malate dehydrogenase; 7, fumarase; 8, fumarate reductase; 9, succinyl-CoA transferase; 10, $L_R$- methylmalonyl-CoA mutase; 11, methylmalonyl-CoA racemase; 12, pyruvate-phosphate dikinase; 13, PEP-carboxytransphosphorylase. Source is [52].

# Appendix B

## Analysis Methods

The first two sections describe the analysis of a liquid sample for lactose, lactate, acetate, propionate, butyrate, and ethanol. The third section covers the measurement of the production rate and compositions of the gaseous products. The last one explains the analysis of solid samples including total organic carbon (TOC), dry weight and ash content of a biomass, etc.

### B.1 Determination of Lactose

The lactose concentration in the feed mixtures or the fermenter effluents was assayed with a colorimetric method. Simple sugars, oligosaccharides, polysaccharides, and their derivatives, including the methyl ethers with free or potentially free reducing groups, give an orange-yellow color when treated with phenol and concentrated sulfuric acid. The method is simple, rapid, and sensitive, and gives reproducible results because the color produced is permanent. Therefore, it is unnecessary to pay special attention to the control of the analytical conditions [215].

#### B.1.1 Reagents and Apparatus

- Phenol solution, 5 % by weight, prepared by adding 20 grams of reagent grade phenol (BDH) to 380 grams of distilled water, which was used throughout the experiments.

- Sulfuric acid, reagent grade 95.5 % (BDH), specific gravity 1.84.

### B.1.2 Procedure

1. Five mL of filtrate of the liquid sample filtrated with a membrane filter (d = 0.45 $\mu$, Sartorius, W. Germany) were diluted to such that it contained between 10–100 mg lactose/l.

2. After one mL of the phenol solution and one mL of the diluted solution was pipetted into a test tube (15 mL), five mL of sulfuric acid were added rapidly, the stream of acid being directed against the liquid surface to obtain good mixing.

3. The tube was allowed to stand 10 minutes in air, and then, was shaken in a water bath to be maintained at 20–30 $^0$C for 10 minutes.

4. In parallel, two such samples were prepared for one sugar solution. A blank was prepared by substituting distilled water for the sugar solution.

5. Put the samples and the blank in three colorimeter tubes and read the absorbance of the samples at a wave length of 480 nm after the meter's zero point was adjusted on the blank.

6. The concentration of lactose was then determined from the readings by reference to the standard curve in Figure B.90 which had been obtained by analyzing a few lactose solutions with known concentration.

## B.2 Determination of Lactate

When a very dilute solute solution of lactic acid is heated in the presence of a high concentration of sulfuric acid, it is converted to acetaldehyde. The acetaldehyde can

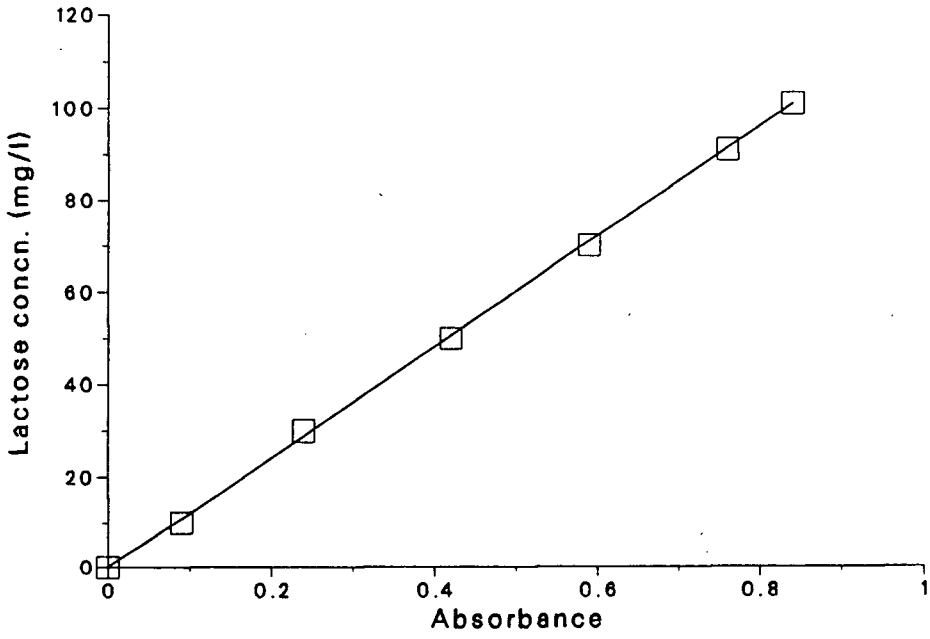


Figure B.90: Standard curve of lactose concentration vs absorbance at 480 nm, The line is calculated from the equation: $S_{lactose}$ = 120.3369 'absorbance' - 0.07461.

then be assayed by a sensitive color test employing p–hydroxydiphenyl which gives the sample a purple color [216]. This method was modified by adding of sulfuric acid to the aqueous samples so rapidly that a large amount of reaction heat released could be used to supply sufficient heat for the conversion of lactate to acetaldehyde.

### B.2.1 Reagents and Apparatus

- $CuSO_4$ solution; 4 grams of $CuSO_4.5H_2O$ (BDH) were dissolved in 100 mL of distilled water.
- Hydroxydiphenyl solution; 1 gram of p–hydroxydiphenyl (BDH) was dissolved in 100 mL of 0.08N NaOH solution and stored in a brown bottle in a refrigerator till needed.
- Sulfuric acid; reagent grade 95.5 % (BDH).

- Spetronic 70 (BAUSH & LOMB) spectrophotometer.

### B.2.2 procedure

1. Five mL of filtrate of reactor effluent filtered through a membrane filter (d = 0.45 $\mu$) were diluted to give 1–9 mg lactate pre mL.

2. After one mL of the diluted solution and 50 $\mu$L $CuSO_4$ were added into a test tube (15mL), 5 mL of sulfuric acid was added rapidly into the sample by directing the stream of the acid onto the liquid surface.

3. The sample was allowed to stand in air for 20 minutes and then cooled below 20 $^0$C in tap water.

4. 50 $\mu$L of hydroxydiphenyl solution were added without touching the tube's wall, mixed thoroughly, and the sample was allowed to stand for 6 hours.

5. In parallel, two such samples were prepared for each effluent solution. A blank was also prepared by replacing the effluent solution with distilled water.

6. Put the two samples and the blank in three colorimetric tubes of the spectrophotometer. The lactate concentration was then determined from the readings at a wave length of 570 nm, after the meter's zero point had been adjusted using the blank, by reference to the standard line of lactate concentration vs absorbance as shown in Figure B.91.

## B.3 Determination of Volatile Fatty Acids and Ethanol

Acetic acid, propionic acid, butyric acid and ethanol are easily vaporized. Therefore, they can be assayed with a gas chromatograph.

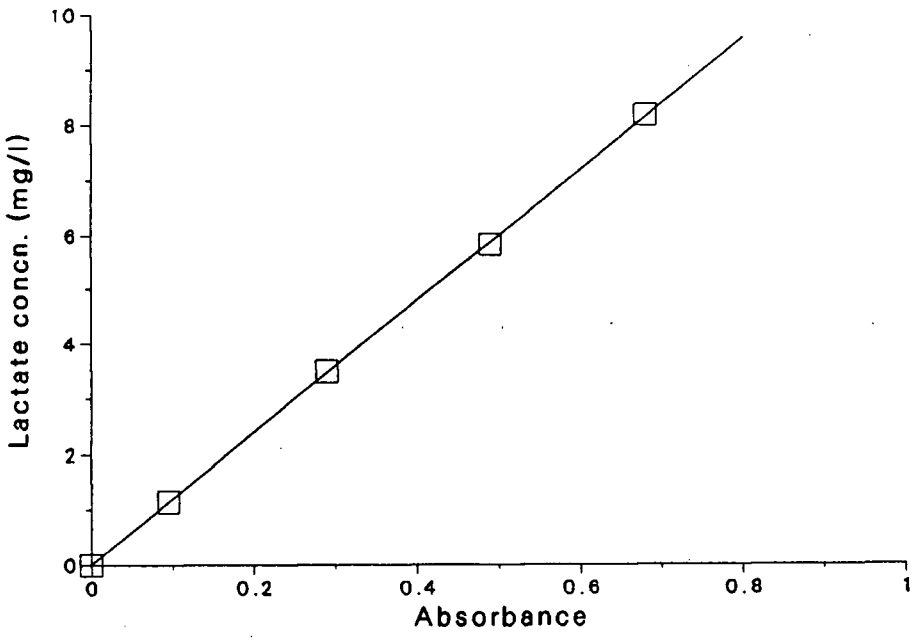


Figure B.91: Standard curve of lactate concentration vs absorbance. The line is calculated from the equation: $S_{lactate} = 12.0048$ 'absorbance + 0.005522.

### B.3.1 Reagents and Apparatus

- 0.2N Phosphoric acid solution.
- 9 standard samples having known concentrations of ethanol (8–600 mg/l), acetic acid (500–7200 mg/l), propionic acid (200–1300 mg/l), butyric acid (600–1800 mg/l), iso-butyric acid (7–20 mg/l) and valeric acid (0–2000 mg/l).
- Analytical gas chromatograph (GC)–Model 311 (CARLE), equipped with both a TCD and a FID.
- Gas cylinders of air, hydrogen and He (UNION CARBIDE).
- A 60/80 Carbopack C/0.3 Carbowax 20 M/0.1 % $H_3PO_4$ column, 30" × 1/8" stainless steel (SUPELCO).

- A computing intergrator–SP 4100 (SPECTRA–PHYSICS).

### B.3.2 Procedure

1. Five mL of filtrate of the reactor effluent, filtered through a membrane filter (d = 0.45 $\mu$), was titrated with 0.2N phosphoric acid solution until the pH value of the sample was below 2. It was calculated by Kisaalita [46] that the pH value of a sample must be acidified below 2.73 if the strongest acid in the sample, acetic acid, could be in free form. The amount of added acid solution was recorded to calculated the dilution factor.

2. The air, hydrogen and He regulators were set at 12, 20, and 23 psig respectively since it is advised by the GC manufacture that these pressures would give an optimal ratio of air to hydrogen and a suitable residence time of the components. The oven temperature was set at 120 $^0$C.

3. After the GC was maintained at the desired state, the FID was turned on and 5–10 minutes were allowed for stabilizing the baseline of the computing integrator.

4. 0.5 $\mu$L of the acidified sample was injected for each run. Each sample was analyzed at least three times and then an average was reported.

5. For each sample, 0.5 $\mu$L of a standard sample which had the nearest composition to the unknown sample, was also injected. Therefore, the composition of the unknown sample was determined from the concentration factors calculated from the standard sample, $f_i$, (the concentrations, $S_{standard,i}$ devided by the peak areas, $A_{standard,i}$ ) and the peak areas of the components in the sample, $A_{unknown,i}$.

$$S_{unknown,i} = A_{unknown,i} \times f_i = A_{unknown,i} \times \frac{S_{standard,i}}{A_{standard,i}}$$

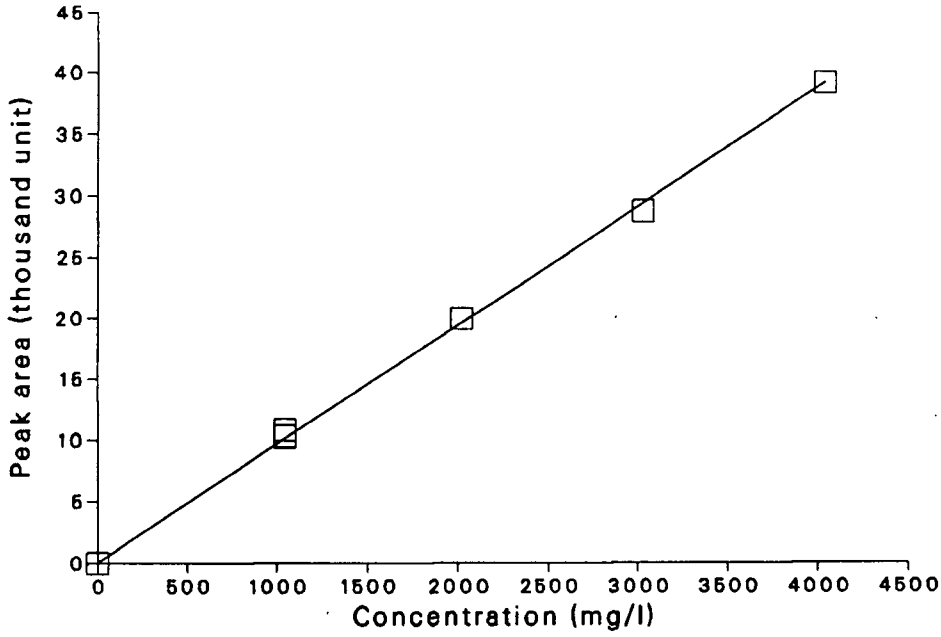


Figure B.92: A typical calibration curve of acetate.

As shown in Figures B.92, B.93 and B.94, the concentrations of acetate, propionate and butyrate have a linear relationship with their peak area at a steady operation state of the GC. In order to avoid the possible effect on the concentration factors caused by change in the operation state of the GC, a standard sample was injected at each time of the analysis.

Figure B.95 is a typical volatile fatty acid chromatogram.

## B.4 Gas Composition

### B.4.1 Apparatus

- Analytical gas chromatograph (GC) - Model 311 (CARLE), equipped with both a TCD and a FID.
- Helium as the carrier gas.

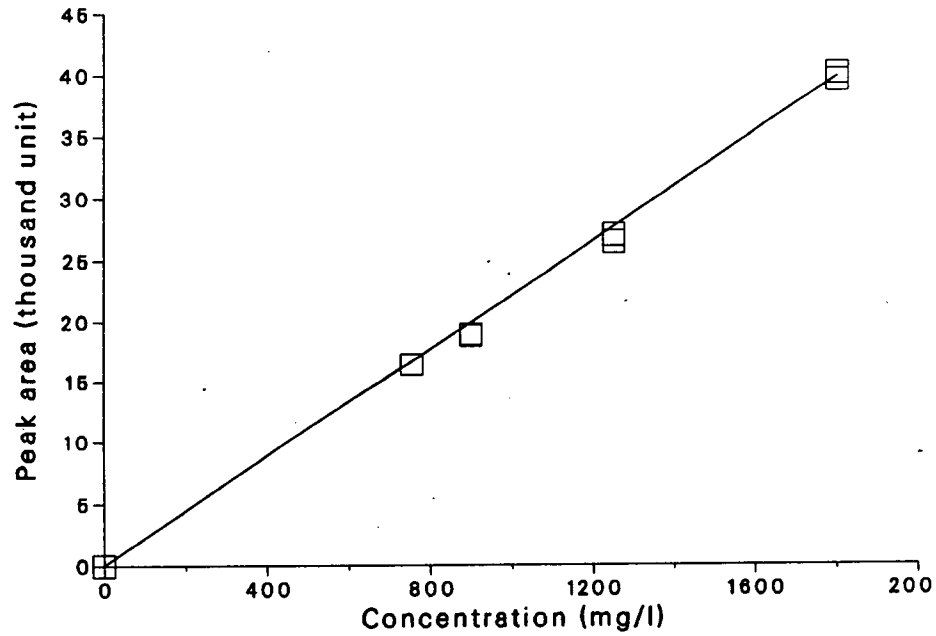


Figure B.93: A typical calibration curve of propionate.

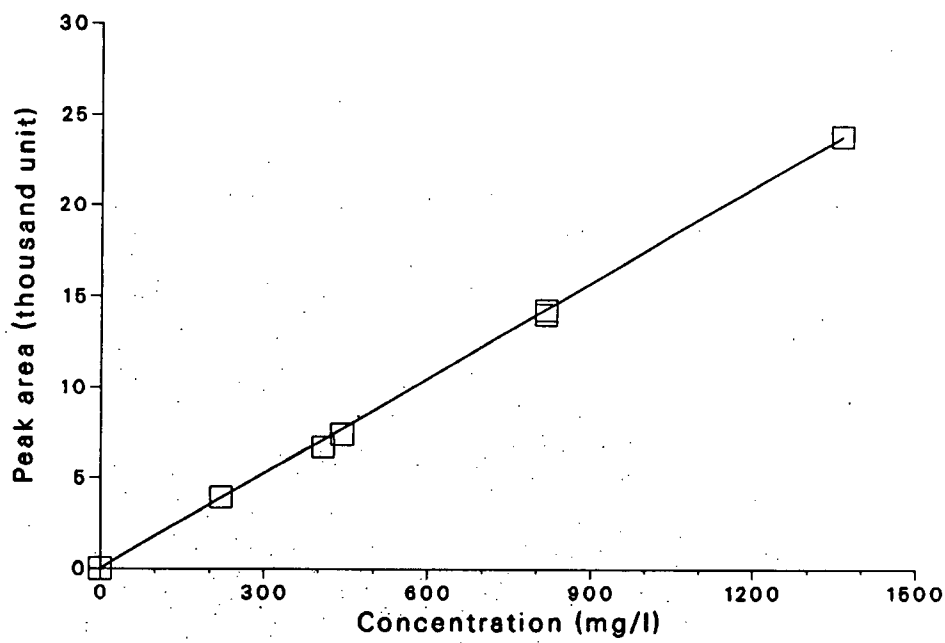


Figure B.94: A typical calibration curve of butyrate.

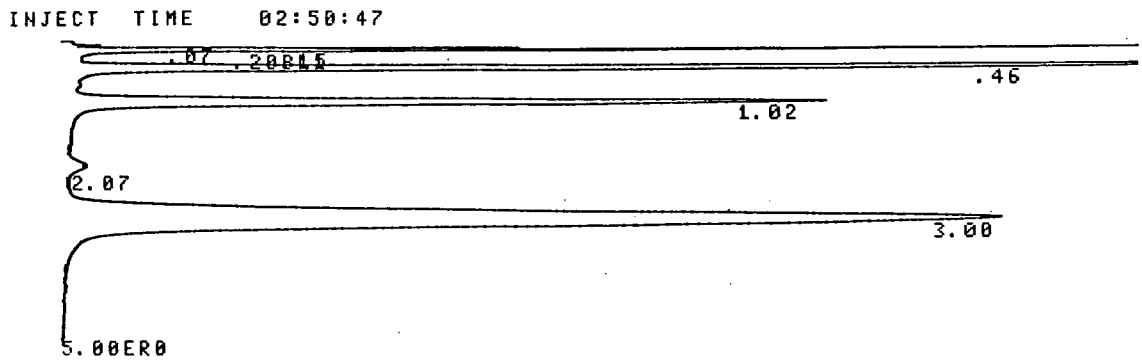


Figure B.95: A typical volatile fatty acid chromatogram. Residence time (min): ethanol (0.20); acetic acid (0.47); propionic acid (1.03); iso–butyric acid (2.10); butyric acid (3.01).

- A 10 % carbowax 20 M on chromosorb W–HF 80/100 mesh column, 8' × 1/8" stainless steel (CHROMTOGRAPHIC SPCIALITIES).
- A computing integrator – SP 4100 (SPECTRA PHYSICS).
- Standard gas sample (UNION CARBIDE); $CH_4$ = 59.97 %, $CO_2$ = 30.0 %, others = 10.03 %.
- A gas tight syringe (1 ml, GASTIGHT, #1001).

### B.4.2 Procedure

1. The carrier gas, He, was set at 12 psig and the oven temperature was controlled at 35 $^0$C. After the GC had reached a steady state, the thermal conductivity detector (TCD) was turned on, and then, 10 minutes were allowed to let the base line of the integrator stabilized.

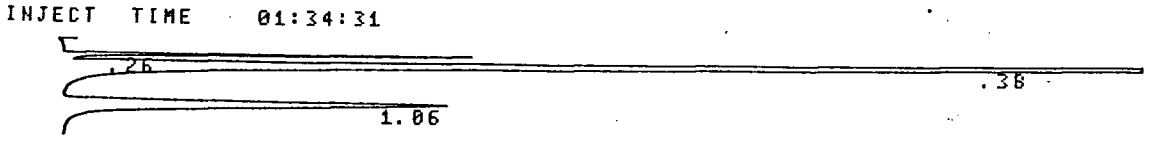


Figure B.96: A typical chromotogram of gaseous samples. Residence time (min): air (0.26); methane (0.38); carbon dioxide (1.86).

2. Repeat injecting 1 ml of the standard gas with the gas tight syringe three times, an average concentration factor (a ratio of the concentration and the peak area of a component) was obtained for each component. This single point method to calculate the concentration factor was reliable in this study because the standard gas composition was very close to the compositions of the reactor gaseous effluents which showed no markedly change in the compositions (see Appendix E).

3. Repeat injection of 1 ml, for three times, of the gaseous sample which was directly collected with the same syringe from the gas collector as shown in Figure 3.10 in Chapter 3. The composition of the gas sample was determined from the peak areas of the components ($CO_2$, $CH_4$) as shown in Figure B.96 as well as the concentration factors obtained from the standard gas as depicted in step 2.

## B.5 Determination of Carbon Content in a Liquid Sample

The carbon content in a liquid sample was assayed by a total carbon analyzer which can convert the organic carbon dissolved or suspended as small particles in the aqueous solution to $CO_2$ with a strong oxidizing agent like sodium persulfate (1M). The produced carbon dioxide is then carried by a stream of oxygen to an infrared analyzer which is specially designed to measure the concentration of the carbon dioxide. This analysis was used for determining both the concentration of free bacterial cells in the culture medium and the total carbon content of a biofilm, by preparing these two types of samples differently.

### B.5.1 Sample Preparation

- Concentration of free bacterial cells in the culture medium: Two samples were needed for analyzing the concentration of free cells in a culture medium. Sample 1 was obtained directly from the effluent of the fermenter and sample 2 was a filtrate prepared by filtering the same effluent solution through a membrane filter (pore size 0.45 $\mu$). The concentration of free bacterial cells was determined from the difference in the carbon contents of these two samples because the free cells in the sample 2 had been removed before the carbon analysis.

- Carbon content of a biofilm: A mass of wet biofilm was dried at 70 $^0$C to a constant weight. The dried biomass, after weighing, was dissolved in 50 mL of distilled water. To promote the dissolution of the biomass and removal of inorganic carbon, the solution was first adjusted to a pH below 1 with sulphuric acid and then, heated and mixed on a hot plate (THERMIX, FISHER) at about 80 $^0$C for 5 hours. Finally, the solution was cooled to room temperature and distilled water was added into the solution to a volume of 100 ml for carbon content analysis.

### B.5.2 Reagents and Apparatus

- Total carbon analyzer (ASTRO).
- Sodium persulfate solution; 238 grams of ultra-pure reagent grade sodium persulfate (BDH) was dissolved in one liter of distilled water.
- Standard solutions; (1) 2360 mg carbon/l – 5.5 mL of ethylene glycol (BDH) was dissolved in one liter of distilled water, (2) 429 mg carbon/l – 1 mL of ethylene glycol was dissolved in one liter of distilled water, (3) 86 mg carbon/l – 0.2 mL of ethylene glycol was dissolved in one liter of distilled water.
- Oxygen cylinder (UNION CARBIDE)

### B.5.3 Procedure

1. The total carbon analyzer was operated in the total carbon and manual mode and an analysis range was chosen (100 ppm, 500 ppm or 2500 ppm), depending on the strength of a sample. A standard solution mentioned above was chosen so that its concentration was about 70 % of the full range.
2. The analyzer was stabilized for 4 hours with an oxygen flow rate of 300 ml/min and distilled water as a liquid carrier.
3. After the sodium persulfate solution was used as the liquid carrier, 30 minutes were allowed to stabilize the machine, and then 20 ml of the standard solution was injected. At least three injections of the standard solution were needed to let the analyzer determine an average concentration factor.
4. After following the startup instructions, 20 mL of a sample prepared by the methods discussed above was injected. An average carbon content of the sample was reported

from three injections.

## B.6 Analysis of a Biofilm

The analysis of a biofilm consisted of (1) dry biomass, (2) carbon content, (3) ash content, (4) water volume of a wet biomass, (5) density and (6) biofilm thickness.

### B.6.1 Dry Biomass and Carbon Content of a Biofilm

A wet biofilm attached on a removable PVC slide was dried in a oven at 70 $^0$ to a constant weight. This low temperature was used to avoid any influence from the plastic which might decompose at a high temperature. After cooling to room temperature in a desiccator and weighing, the dry biomass with the PVC slide was put in a flask to be dissolved in distilled water as explained in the last section. The cleaned PVC slide was then dried again, cooled to room temperature in the desiccator and weighed. The difference between the two weights was the dry biomass of the biofilm. The carbon content of the biofilm was calculated from the carbon content of the biomass solution (100 mL) which was determined with the carbon analyzer as described in the last section.

### B.6.2 Ash Content of a Biomass

A weighed dry biomass was ignited in a oven at 550 $^0$C for 5 hours. After cooled to 200 $^0C$ in the oven and then to room temperature in a desiccator, the ash was weighted.

### B.6.3 Water Volume, Density and Thickness of a Biofilm

An intact biomass of a wet biofilm which was taken out of the fermenter was carefully and immediately scraped into a small Kimax test tube ($\phi$ = 4 mm) and then was centrifuged at 4000 rpm to a constant volume of dense biomass at the bottom of the tube.

After the water volume and the total volume were measured, the dense biomass was assayed as described before for the dry biomass and carbon content. The densities of the biofilm sample , dry biomass or carbon content per unit volume of the biofilm, were then calculated from the total volume of the biofilm sample and the dry biomass or carbon content.

When the thickness of a biofilm was concerned, two methods were employed. For a thick biofilm, the biomass sample was collected from an exactly known area of a support. Following the same steps as above, the total volume was measured and the thickness was determined by dividing the total volume by the area. However, for a thin biofilm, to minimize the error caused by the operation, the dry biomass and carbon content of a biofilm sample which was collected from on an exactly known support area was determined, and then by using the densities of the biomass which were determined from a large amount of biomass, the volume of the biofilm sample as well as the thickness of the biofilm were calculated.

# Appendix C

## Results of Lactose Acidogenesis

Table C.34: Accumulation of acidogenic biofilms on removable PVC slides

| Time (day) | Dry Biomass (mg) | Carbon Content (mg) |
|---|---|---|
| 0 | 18.8 | 5.33 |
| 9 | 25.3 | 6.69 |
| 16 | 25.8 | 8.60 |
| 16 | 23.5 | 6.48 |
| 23 | 37.2 | 14.50 |
| 23 | 25.9 | 6.87 |
| 30 | 48 | 13.42 |
| 30 | 43.3 | 15.54 |
| 38 | 42.6 | 13.54 |
| 38 | 49.1 | 18.33 |
| 46 | 60.2 | 22.50 |
| 51 | 58.8 | 18.30 |
| 51 | 70.8 | 27.89 |
| 61 | 70.3 | 30.5 |
| 65 | 64.6 | 24.3 |
| 65 | 70.9 | 27.80 |
| 76 | 103.1 | 43.00 |
| 76 | 110.8 | 47.60 |
| 84 | 116 | 46.60 |
| 84 | 117 | 39.40 |

Table C.35: Results of lactose acidogenesis

| No. | Biofilm mg C | Flow rate mL/hr | $S_{in}$ mg/l | $S_{out}$ mg/l | HLa mg/l | Ethol mg/l | HAc mg/l | HPr mg/l | HBu mg/l | $C_{recov}$ % |
|---|---|---|---|---|---|---|---|---|---|---|
| A001 | 1931.6 | 100 | 9992 | 4000 | 180 | 160 | 1165 | 93 | 1887 | 67.2 |
| A002 | 1982.3 | 102 | 9992 | 3783 | 169 | 175 | 1088 | 107 | 2060 | 67.7 |
| A004 | 2198.7 | 113 | 9992 | 3883 | 178 | 170 | 1170 | 102 | 1944 | 67.6 |
| A006 | 2256.4 | 111 | 9108 | 2935 | 137 | 150 | 1289 | 73 | 1882 | 65.8 |
| A007 | 2315.6 | 94 | 9108 | 1725 | 89 | 184 | 1668 | 68 | 2158 | 64.6 |
| A101 | 2635.7 | 90 | 8957 | 1249 | 75 | 160 | 1767 | 55 | 2221 | 63.4 |
| A103 | 2775.9 | 103 | 7329 | 600 | 25 | 107 | 1391 | 134 | 1650 | 56.0 |
| A203 | 3787.7 | 168 | 4591 | 402 | 16 | 66 | 1038 | 18 | 833 | 52.1 |
| A301 | 3989.1 | 115 | 5004 | 201 | 10 | 91 | 1476 | 25 | 1308 | 67.6 |
| A302 | 4093.8 | 112 | 5004 | 261 | 11 | 92 | 1422 | 23 | 1081 | 61.2 |
| A303 | 4201.2 | 121 | 5004 | 250 | 8 | 115 | 1369 | 35 | 971 | 57.8 |
| A305 | 4782.0 | 236 | 5004 | 390 | 30 | 68 | 891 | 14 | 1450 | 61.9 |
| A403 | 5168.4 | 273 | 5053 | 514 | 14 | 60 | 1042 | 18 | 1367 | 63.2 |
| A405 | 5586.0 | 308 | 5053 | 582 | 18 | 78 | 1080 | 22 | 1318 | 64.2 |
| A501 | 5732.6 | 313 | 8384 | 3080 | 99 | 134 | 1006 | 57 | 1734 | 66.5 |
| A502 | 5883.0 | 329 | 8384 | 3073 | 105 | 125 | 1001 | 55 | 1704 | 65.5 |
| A601 | 6525.2 | 230 | 7807 | 706 | 25 | 121 | 1598 | 23 | 1712 | 55.4 |
| A603 | 7052.4 | 279 | 7807 | 1040 | 70 | 118 | 1315 | 21 | 1771 | 55.9 |
| A803 | 8238.1 | 275 | 7752 | 809 | 65 | 128 | 1574 | 30 | 2116 | 64.7 |
| A804 | 8238.1 | 288 | 7752 | 797 | 71 | 126 | 1468 | 23 | 2052 | 61.9 |
| A805 | 8454.2 | 318 | 7752 | 830 | 43 | 112 | 1402 | 26 | 1957 | 58.9 |
| A806 | 8454.2 | 313 | 7752 | 888 | 52 | 118 | 1404 | 27 | 2020 | 60.9 |

# Appendix D

## Results of Buildup of Methanogenic Biofilms

The experimental data of buildup of symbiotic methanogenic biofilms on the four types of supports (wood, ceramic, PVC and stainless steel) are listed, as a ratio of the concentration of bacterial cells fixed on the supports to the concentration of free cells suspended in the medium ($[xs]/[x]$ cm), in the following three tables.

Table D.36: Accumulation of acetate-degrading bacteria on inert supports

| Time day | Wood cm | Ceramic cm | PVC cm | Steel cm |
|---|---|---|---|---|
| 0 | 0 | 0 | 0 | 0 |
| 7 | 0.348 | 0.159 | - | 0.139 |
| 12 | 0.330 | 0.279 | - | 0.336 |
| 14 | - | - | 0.140 | - |
| 20 | 0.830 | 0.433 | 0.392 | 0.381 |
| 32 | - | - | 0.274 | - |
| 37 | - | 0.707 | - | - |
| 43 | 1.310 | - | - | 0.635 |
| 45 | - | - | 0.517 | - |
| 51 | 1.982 | 0.884 | 0.721 | 0.502 |
| 57 | 1.700 | 0.810 | - | 0.603 |
| 66 | 1.860 | 1.207 | 1.098 | 0.656 |
| 84 | 3.032 | 1.563 | 1.035 | 0.978 |
| 98 | - | - | 1.322 | - |

Table D.37: Accumulation of propionate-degrading bacteria on inert supports

| Time day | Wood cm | Ceramic cm | PVC cm | Steel cm |
|---|---|---|---|---|
| 0 | 0 | 0 | 0 | 0 |
| 7 | 0.297 | 0.182 | - | 0.221 |
| 12 | 0.38 | 0.147 | - | 0.143 |
| 14 | - | - | 0.236 | - |
| 20 | 0.576 | 0.303 | 0.259 | 0.219 |
| 32 | - | - | 0.427 | - |
| 37 | - | 0.512 | - | - |
| 43 | 0.768 | - | - | 0.441 |
| 45 | - | - | 0.484 | - |
| 51 | 1.033 | 0.697 | 0.593 | 0.511 |
| 57 | 1.148 | 0.712 | - | 0.561 |
| 66 | 1.288 | 0.771 | 0.687 | 0.594 |
| 84 | 1.368 | 0.856 | 0.913 | 0.780 |
| 98 | - | - | 1.065 | - |

Table D.38: Accumulation of butyrate-degrading bacteria on inert supports

| Time day | Wood cm | Ceramic cm | PVC cm | Steel cm |
|---|---|---|---|---|
| 0 | 0 | 0 | 0 | 0 |
| 7 | 0.558 | 0.197 | - | 0.193 |
| 12 | 0.35 | 0.187 | - | 0.214 |
| 14 | - | - | 0.236 | - |
| 20 | 1.164 | 0.543 | 0.354 | 0.39 |
| 32 | - | - | 0.524 | - |
| 37 | - | 1.575 | - | - |
| 43 | 1.992 | - | - | 0.597 |
| 45 | - | - | 0.800 | - |
| 51 | 2.764 | 1.684 | 0.881 | 0.790 |
| 57 | 2.874 | 1.750 | - | 0.819 |
| 66 | 3.270 | 1.538 | 1.070 | 0.921 |
| 84 | 3.751 | 1.716 | 1.350 | 1.158 |
| 98 | - | - | 1.564 | - |

# Appendix E

## Results of Organic Acid Methanogenesis

Table E.39: Accumulation of methanogenic biofilms on removable PVC slides

| Time day | Number | Dry Biomass mg | Carbon Content mg |
|---|---|---|---|
| 0 | B02 | 6.0 | 1.95 |
| 0 | B18 | 6.4 | 2.27 |
| 18 | B29 | 8.0 | 2.8 |
| 43 | B32 | 11.3 | 3.1 |
| 52 | B26 | 12.0 | 3.5 |
| 60 | B21 | 12.9 | 5.7 |
| 75 | B12 | 12.9 | 5.5 |
| 89 | B09 | 16.0 | 4.0 |
| 102 | B14 | 16.7 | 4.0 |
| 110 | B36 | 16.1 | 4.6 |
| 140 | B27 | 28.4 | 8.7 |
| 156 | B35 | 26.1 | 11.2 |
| 170 | B31 | 32.9 | 12.6 |
| 170 | B07 | 33.2 | 11.0 |
| 193 | B37 | 35.9 | 14.0 |
| 193 | B25 | 34.5 | 11.3 |
| 208 | B17 | 45.2 | 16.5 |
| 208 | B24 | 45.6 | 15.6 |

Table E.40: Methanogenesis of acetate, propionate and butyrate

| No. | Biofilm mg C | Flow rate ml/hr | $HAc_{in}$ mg/l | $HAc_{out}$ mg/l | $HPr_{in}$ mg/l | $HPr_{out}$ mg/l | $HBu_{in}$ mg/l | $HBu_{out}$ mg/l | $C_{recov}$ % |
|---|---|---|---|---|---|---|---|---|---|
| B21 | 1887.3 | 35.6 | 2791 | 654 | 1531 | 728 | 1004 | 23 | 82 |
| B23 | 1921.6 | 59.9 | 2791 | 1608 | 1531 | 924 | 1004 | 101 | |
| B24 | 1939.0 | 75.6 | 2791 | 1962 | 1531 | 1026 | 1004 | 148 | 78 |
| B31 | 2342.4 | 69.0 | 1646 | 476 | 985 | 449 | 640 | 22 | |
| B32 | 2363.6 | 59.0 | 1646 | 353 | 985 | 422 | 640 | 13 | 77 |
| B42 | 2563.0 | 33.2 | 1646 | 133 | 985 | 104 | 640 | 4 | |
| B45 | 2633.1 | 34.0 | 1646 | 154 | 985 | 85 | 640 | 5 | |
| B57 | 2933.4 | 63.0 | 900 | 105 | 500 | 75 | 360 | 5 | |
| B65 | 3180.9 | 59.7 | 4094 | 2511 | 2474 | 1425 | 2109 | 419 | 78 |
| B67 | 3297.5 | 53.6 | 4094 | 1999 | 2474 | 1173 | 2109 | 177 | 79 |
| B68 | 3327.3 | 57.0 | 4094 | 2156 | 2474 | 1230 | 2109 | 144 | |
| B69 | 3357.4 | 57.5 | 4094 | 2123 | 2474 | 1295 | 2109 | 244 | |
| B72 | 3480.5 | 62.4 | 4094 | 2142 | 2474 | 1354 | 2109 | 257 | |
| B75 | 3575.7 | 68.6 | 4925 | 3102 | 2719 | 1655 | 1969 | 463 | |
| B77 | 3740.3 | 68.6 | 4925 | 3122 | 2719 | 1629 | 1969 | 377 | |
| B78 | 3774.1 | 72.9 | 4925 | 3068 | 2719 | 1701 | 1969 | 424 | 86 |

The carbon recovery includes the carbon of $CH_4$ and $CO_2$ in gas and $CO_2$ in the effluent. The $CO_2$ in the effluent is calculated from the gas composition as a saturated solution.

Table E.41: Gas production rate and composition of organic acid methanation

| Rate | Temperature | Pressure | Composition | | |
|---|---|---|---|---|---|
| | | | $CH_4$ | $CO_2$ | Others |
| ml/hr | $^0C$ | mmHg | % | % | % |
| 133.3 | 24.5 | 767.6 | 72.1 | 18.6 | 10.2 |
| 106.4 | 23.3 | 743.0 | 70.9 | 15.2 | 14.4 |
| 80.1 | 22.7 | 750.0 | 73.6 | 16.2 | 10.2 |
| 51.0 | 22.9 | 750.0 | 81.5 | 13.8 | 5.3 |
| 144.4 | 23.2 | 765.0 | 74.1 | 17.6 | 7.8 |
| 189.6 | 23.4 | 762.0 | 71.7 | 22.8 | 3.5 |
| 201.9 | 20.6 | 748 | 74.7 | 25.0 | 3.0 |

# Appendix F

## Derivation of Utilization Rate Models of Propionate and Butyrate

### F.1 Utilization Rate Model of Propionate

The utilization of propionate in a symbiotic methanogenic biofilm is assumed to have a mechanism as follows:

$$E + S \overset{k_1/k_{-1}}{\rightleftharpoons} ES \xrightarrow{k_2} P + E \tag{1}$$

$$ES + S \xrightarrow{\beta k_2} P + ES \tag{2}$$

The sum of the fractions of active enzyme centers, $[E]$, and of the substrate-enzyme complex centers, $[ES]$, should equal one because the total amount of enzyme active centers is a constant in a given amount of biomass,

$$[E] + [ES] = 1 \tag{F.119}$$

By using the Michaelis–Menten assumption that the concentration of the substrate–enzyme complex is unchanged at steady state, i.e.,

$$\frac{d[ES]}{dt} = k_1[E][S] - k_{-1}[ES] - k_2[ES] = 0 \tag{F.120}$$

or,

$$k_1[E][S] = (k_{-1} + k_2)[ES] \tag{F.121}$$

Hence, the fraction of the empty active enzyme centers can be expressed by

$$[E] = \frac{k_{-1} + k_2}{k_1[S]}[ES] \tag{F.122}$$

Substituting Equation F.122 for the fraction of active enzyme centers in Equation F.119 gives

$$[ES] = \frac{k_1[S]}{k_1[S] + k_{-1} + k_2} \tag{F.123}$$

From reactions (1) and (2), the consumption rate of the substrate can be written as follows:

$$r = -\frac{dS}{dt} = k_1[E][S] - k_{-1}[ES] + \beta k_2[ES][S] \tag{F.124}$$

Put Equation F.121 into Equation F.124 to give

$$r = k_2[ES](1 + \beta[S]) \tag{F.125}$$

Finally, replacing the fraction of the substrate-enzyme complex in Equation F.125 by its expression,Equation F.123, the substrate (propionate) utilization rate can be expressed as a function of substrate concentration, S,

$$r = \frac{k_2 S(1 + \beta S)}{(k_{-1} + k_2)/k_1 + S} \tag{F.126}$$

## F.2 Utilization Rate Model of Butyrate

The utilization of butyrate by acetogens in the methanogenic biofilms is affected by the presence of propionate, especially at the high concentrations of the latter. The reaction mechanism is assumed as follows:

$$E + S_b \overset{k_1/k_{-1}}{\rightleftharpoons} ES_b \xrightarrow{k_2} P + E \tag{1}$$

$$ES_b + S_p \overset{k_3/k_{-3}}{\rightleftharpoons} S_pES_b \qquad \text{(deactivation)} \tag{2}$$

With the assumptions that the sum of the fractions of the three types of active centers (E, $ES_b$ and $S_pES_b$) should equals one, and that the fraction of deactivated centers is a constant at steady state,

$$[E] + [ES_b] + [S_pES_b] = 1 \tag{F.127}$$

and,

$$\frac{d[S_pES_b]}{dt} = k_3[ES_b][S_p] - k_{-3}[S_pES_b] = 0 \tag{F.128}$$

or,

$$[S_pES_b] = \frac{k_3}{k_{-3}}[ES_b][S_p] \tag{F.129}$$

The Michaelis–Menten assumption that the substrate–enzyme complex is a constant at steady state gives

$$\frac{d[ES]}{dt} = k_1[E][S_b] - k_{-1}[ES_b] - k_2[ES_b] - k_3[ES_b][S_p] + k_{-3}[S_pES_b] = 0$$

or,

$$k_1[E][S_b] = (k_{-1} + k_2)[ES_b] \tag{F.130}$$

The fraction of active empty enzyme centers, $[E]$, can be expressed by

$$[E] = \frac{k_{-1} + k_2}{k_1[S_b]}[ES_b] \tag{F.131}$$

Put the expressions for $[E]$ and $[S_pES_b]$, Equations F.129 and F.131 into Equation F.127 to give the expression of $[ES_b]$ as the following,

$$[ES_b] = \frac{[S_b]}{[S_b + (k_3/k_{-3})[S_b][S_p] + (k_1 + k_2)/k_1} \tag{F.132}$$

The substrate b is consumed by the reaction (1) only, and its utilization rate is

$$r_b = -\frac{dS}{dt} = k_1[E][S_b] - k_{-1}[ES_b] \tag{F.133}$$

By using Equation F.130, the rate expression becomes

$$r_b = k_2[ES_b] \tag{F.134}$$

Substituting Equation F.132 for $[ES_b]$ in Equation F.134, the digestion rate of butyrate is expressed as a function of the concentrations of butyrate and propionate, $S_b$ and $S_p$,

$$r_b = \frac{k_2 S_b}{(k_{-1} + k_2)/k_1 + S_b + (k_3/k_{-3})S_p S_b} \tag{F.135}$$

# Appendix G

## Numerical Methods

The numerical methods used in this study include a direct search method for the estimation of parameters in a non-linear function and the Runge–Kutta–Fehlberg (RKF) method for the numerical solution of a differential equation.

### G.1 Direct Search Method

The estimation of several parameters in a non-linear function is generally converted to an optimization problem, minimizing the difference between the experimental results and the data predicted by the model (a non-linear function) by changing the values of the parameters. For a non-linear function of several variables, it is common that a direct search method is used because of the complexity of the differentiations of the function. There have been several methods devised which comprise two major stages in a direct search, an exploratory stage and a pattern stage. One of the simplest methods is due to Hooke and Jeeves [186] which has been used in this study. The algorithm is designed to seek the best direction of search and move fast in that direction as shown in Figure G.97. First of all, a base camp is established at $\mathbf{x}^0$. For this first stage of the expedition, this point is also the advanced camp $\mathbf{x}^1$, from which explorations are made. A step of a given length, d, is taken in each of the coordinate directions in turn. If a success is encountered in a direction insofar as a lower objective function value is achieved, progress has been made. If it is not, the step in this direction is decreased by d from the start point and tested again; if it still produces no decrease, stay at the start point. When all

variables are thus dealt with, the exploratory state is complete. It is deemed a success if the value of the function at the latest point, $x'$, is less than f($x^0$). Otherwise it is a failure. If successful, the base camp is moved to $x'$ and the advanced camp is moved to $x^1 = x' + (x' - x_0)$; A new search is carried out from the new advanced camp and the process repeated. A computer program in Pascal language is attached here which has been successfully used in a personal computer with Turbo Parscal.

## G.2 Runge-Kutta-Fehlberg Method

Since there are relatively few differential equations arising from practical problems like the reaction–diffusion model for which analytical solutions are known, one must resort to numerical methods. In general, an mth-order differential equation,

$$y^{(m)} = f(x, y, y', y'', \ldots, y^{(m-1)})$$

with initial conditions

$$y(x_0) = y_0$$

$$y'(x_0) = y_0'$$

$$\vdots$$

$$y^{(m-1)}(x_0) = y_0^{(m-1)}$$

can be rewritten as an equivalent system of m first-order equations. To do so, a new set of dependent variables $y_1(x)$, $y_2(x)$, ..., $y_m(x)$ are defined by

$$y_1 = y$$

$$y_2 = y'$$

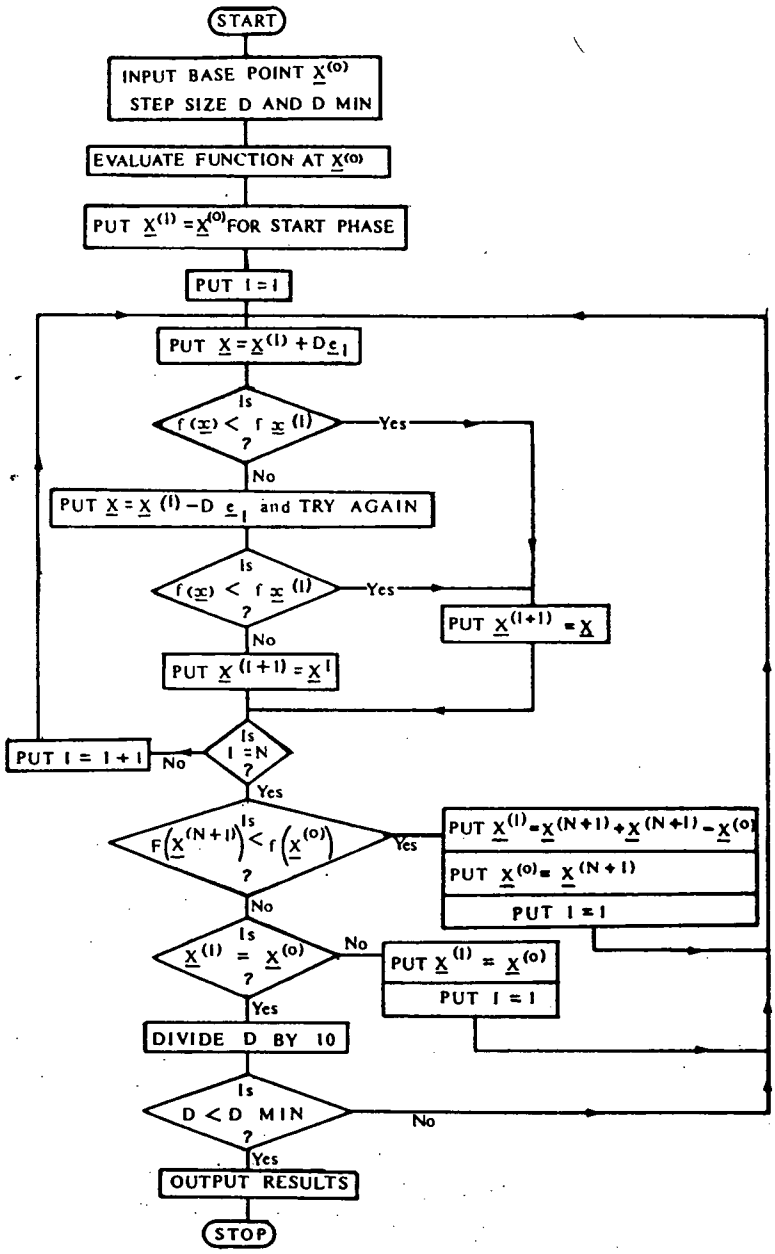


Figure G.97: Flow chart of the direct search method

$$y_3 = y''$$

$$\vdots$$

$$y_m = y^{(m-1)}$$

Therefore, a mth-order differential equation (e.g. the reaction-diffusion model is a 2nd–order differential equation) can be numerically solved like m first-order differential equations.

Runge–Kutta methods are explicit algorithms that involve evaluation of the function f at points in a small interval, between $x_i$ and $x_{i+1}$. In order to estimate the errors occurring during computation, a local error would be calculated from the difference between $u^*_{i+1}$ and $u_{i+1}$ where $u_{i+1}$ is calculated using a step–size of h and $u^*_{i+1}$ using a step–size of h/2. Since the accuracy of the numerical method depends upon the step–size to a certain power, $u^*_{i+1}$ will be a better estimate for $y(x_{i+1})$ than $u_{i+1}$. Therefore,

$$|z_{i+1} - u*_{i+1}| < |z_{i+1} - u_{i+1}|$$

and so,

$$e_{i+1} = z_{i+1} - u_{i+1} \simeq u*_{i+1} - u_{i+1}$$

Runge–Kutta formulas, if two half–step procedure is used, would need many computations. A better procedure is Runge–Kutta–Fehlberg's method [200], which uses a Runge–Kutta formula of higher-order accuracy than used for $u_{i+1}$ to compute $u^*_{i+1}$. In this study, the Runge–Kutta–Fehlberg fourth-order method was used and the pari of formulas is

$$u_{i+1} = u_i + [\frac{25}{216}k_1 + \frac{1408}{2565}k_3 + \frac{2197}{4104}k_4 - \frac{1}{5}k_5] \qquad e_{i+1} = 0(h^5)$$

$$u*_{i+1} = u_i + [\frac{16}{135}k_1 + \frac{6656}{12825}k_3 + \frac{28561}{56430}k_4 - \frac{9}{50}k_5 + \frac{2}{55}k_6] \qquad e_{i+1} = 0(h^6)$$

,

where

$k_1 = hf(x_i, u_i)$

$k_2 = hf(x_i + \frac{1}{4}h, u_i + \frac{1}{4}k_1)$

$k_3 = hf(x_i + \frac{3}{8}h, u_i + \frac{3}{32}k_1 + \frac{9}{32}k_2)$

$k_4 = hf(x_i + \frac{12}{13}h, u_i + \frac{1932}{2197}k_1 - \frac{7200}{2197}k_2 + \frac{7296}{2197}k_3)$

$k_5 = hf(x_i + h, u_i + \frac{439}{216}k_1 - 8k_2 + \frac{3680}{513}k_3 - \frac{845}{4104}k_4)$

$k_6 = hf(x_i + \frac{1}{2}h, u_i - \frac{82}{27}k_1 + 2k_2 - \frac{3544}{2565}k_3 + \frac{1859}{4104}k_4 - \frac{11}{40}k_5)$

Notice that the formula for $u_{i+1}$ is fourth–order accurate but requires five function evaluations as compared with the four of the Rung–Kutta–Gill method, which is of the same order accuracy. However, if $e_{i+1}$ is to be estimated, the half-step method using the Runge–Kutta–Gill method requires eleven function evaluations while the RKF method requires only six. The following computer program , written in Pascal language, was used to solve numerically the reaction-diffusion model which has been described in Chapter 7 on mass transfer in active biofilms.

## G.3 The Computer Programs in Pascal Language

The direct search program (Procedure MULTIVAR) and the RKF program (Procedure RungeKutta) are called by a main program (Program SEARCH). The main program reads the experimental data from a DOS file 'Data' (Procedure GETDATA), calculates the value of the objective function at a set of estimated parameters (Procedure SUM), determines if a search is successful by comparing the values of the objective function at two search points (Procedure TESTARRY) and completes the search for a set of parameters which give the minimum value of the objective function (Procedure MULTIVAR).

The objective function used in this study was a sum of square errors between the experimental data and the values predicted by a model at a set of estimated parameters. For the model of build-up of symbiotic methanogenic biofilms, the predicted values could be directly calculated from the model. However, for the reaction–diffusion model, the program (Procedure RungeKutta) of Runge–Kutta–Fehlber's method must be called in by the procedure SUM to calculate the substrate concentrations on the biofilm surface with the model, and then, by comparing the calculated values with the experimentally measured values, a set of optimal parameters (diffusion coefficients) were determined.

```
PROGRAM SEARCH;
{The main program}

CONST dimen = 1;{dimensions of parameter set }
      nequatn = 1;{number of equations }
      ntime = 1;{number of experimental data of}
                {independent variable x}
      nmax = 2;{number of dependent variables y plus 1}

TYPE {type of variables; real, integr, etc}
  arry2 = ARRAY[1..ntime, 1..nmax] OF  real;
  paramet = ARRAY[1..dimen] OF real;
  arry1 = ARRAY[1..nequatn] OF real;

VAR {names of the variables}
  data : arry2;
  para0 : paramet;
  step, stepm: real;
  i: integer;
  filvar : text;

PROCEDURE GETDATA(VAR data:arry2);
{read data from a disk file}

VAR i,j : integer;
```

```
BEGIN { read data from the DOS file 'Data'}
  assign(filvar, 'Data');
  {$i-} {turn off error checking}
  reset(filvar);
  {$i+} {turn it back on}
  FOR i := 1 TO ntime DO BEGIN     {Data file}
    FOR j := 1 TO nmax DO          {x, y}
      read(filvar,data[i,j]);      {x, y}
      readln(filvar)               {....}
  END                              {x, y}
END;


PROCEDURE SUM(x:paramet;VAR yvalue: REAL);
{calculate the values of the objective function}
{x gives the parameters}
{yvalue sends out the calculation result}

VAR
  equatn : arry1;
  i, j : integer;
  y: real;

{$i RungKuta.pas}
{Runge-Kutta method to solve a differential equation}
{It should be removed if differential equations not involved}

BEGIN
  RungeKutta (y); {solution of a differential equation}
      yvalue := sqr(y - data[1,1]) {sum of error}
END;

PROCEDURE TESTARRY(x1ary,x2ary:paramet;VAR r1,r2:INTEGER);
{compare the values of the objective function at two points}
{and determine if a search is success}

VAR i: INTEGER;

BEGIN
  r1 := 1;
  r2 := 1;
  FOR i := 1 TO dimen DO
    BEGIN
      IF x1ary[i] = x2ary[i] THEN
        result1 := 1
      ELSE
        result2 := 0
    END
END;
```

```
{$i multivar.pas}
{the direct search program}

BEGIN {main program}
  writeln('input your initial guess of parameters');
  FOR I := 1 TO dimen DO
    BEGIN
      WRITE('p',i, '=');
      readln(para0[i])
    END;
  write('step length =');
  readln(step);
  write('minimum step length =');
  readln(stepm);
  getdata(data);
  multivar;
  writeln('a perfect exit')
END.
```

```
PROCEDURE MULTIVAR;
{the direct search method}

VAR para,para1,para2: paramet;
    i, x1ex0,x1nex0: integer;
    fvalue, fvalue0, fvalue1, fvalue2, f: real;

BEGIN{procedure multivar}
  FOR i := 1 TO dimen DO
   begin
     para[i] := para0[i];
     para1[i] := para0[i]
   end;
  REPEAT {reduce step length loop}
    for i := 1 to dimen do
    para[i] := para0[i];
    FOR i := 1 TO dimen DO
      BEGIN {N parameters' exploration}
        para[i] := para1[i] + step;
        SUM(para,f);
        fvalue := f;
        SUM(para1,f);
        fvalue1 := f;
        IF fvalue >= fvalue1 THEN
          BEGIN {backward one step}
            para[i] := para1[i] - step;
            IF para[i] < 0 THEN
              para[i] := 0;
            SUM(para,f);
            fvalue := f;
            SUM(para1,f);
            fvalue1 := f;
            IF fvalue >= fvalue1 THEN
              para2[i] := para1[i]
            ELSE
              para2[i] := para[i]
          END {end badkward one step}
        ELSE
          para2[i] := para[i]
    END; {end n prameters' exploration}
    SUM(para2,f);
    fvalue2 := f;
    SUM(para0,f);
    fvalue0 := f;
    writeln('function value fvalue0=',fvalue0);
    IF fvalue2 >= fvalue0 THEN
      BEGIN
```

```
        TESTARRY(para1,para0,x1ex0,x1nex0);
        IF x1ex0 = x1nex0 THEN
          step := step / 2
        ELSE
          FOR i := 1 TO dimen DO
            para1[i] := para0[i]
      END
    ELSE
      FOR i := 1 TO dimen DO
       BEGIN
         para1[i] := para2[i] + para2[i] - para0[i];
         para0[i] := para2[i]
       END;
   IF (2*step) < stepm THEN
      BEGIN
        WRITELN('THE MINIMUM FUNCTION =',fvalue0);
        writeln('N parameters');
        FOR i := 1 TO dimen DO
        writeln('para[',i,']=',para0[i])
      END;
   FOR i := 1 TO dimen DO
   WRITE('  ',para0[i]);
   writeln
 UNTIL (2*step) < stepm
END;
```

```
PROCEDURE RungeKutta (VAR Sinitial : real);
{Runge-Kutta-Fehlberg's method}

label start;
const
  a11 = 25/216;
  a13 = 1408/2565;
  a14 = 2197/4104;
  a21 = 16/135;
  a23 = 6656/12825;
  a24 = 28561/56430;
  a25 = 9/50;
  a26 = 2/55;
  b31 = 3/32;
  b32 = 9/32;
  b41 = 1932/2197;
  b42 = 7200/2197;
  b43 = 7296/2197;
  b51 = 439/216;
  b53 = 3680/513;
  b54 = 845/4104;
  b61 = 8/27;
  b63 = 3544/2565;
  b64 = 1859/4104;
  b65 = 11/40;
  m = 4; {2 times the number of differential equations}
  elt = 0.00001; {error of lacal trunction}
  ex = 0.001; {error of final length}
  division = 1000; {division of a biofilm thickness}
  thickness = 0.078; {biofilm thickness (cm)}
Var
  y0, y, z, u: array[1..m] of real;
  step, lmark: real;
  k: array[1..6,1..m] of real;
  i: integer;
  {y0,u: HBu, dHBu/dx, HPr, dHPr/dx}

{Four functions are defined as following}

FUNCTION F1(a,b,c,d: real): real;
{a,b,c,d are false variables}
  begin
    F1 := b;
  end;
```

```
FUNCTION F2(a,b,c,d: real): real;
{a,b,c,d are false variables}
  begin
    F2 :=x[1]*a/(0.027+a+0.296*a*c);
    {the utilization rate of butyrate}
  end;

FUNCTION F3(a,b,c,d: real): real;
  begin
    F3 := d;
  end;

FUNCTION F4(a,b,c,d: real): real;
  begin
    F4 :=27.1*c*(1+0.2*c)/(0.05+c);
    {the utilization rate of propionate}
  end;

Begin
    step := thickness/division;
    lmark := 0;
    y0[1] := 0.326; {HBu concen. (mg/ml) inside the cell}
    y0[2] := 0; {ds/dx of HBu inside the cell}
    y0[3] := 1.715; {HPr concen. (mg/ml) inside the cell}
    y0[4] := 0; {ds/dx of HPr inside the cell}
    {Four initial conditions}

    start: for i := 1 to m do
       u[i] := y0[i];
       k[1,1] := step*F1(u[1],u[2],u[3],u[4]);
       k[1,2] := step*F2(u[1],u[2],u[3],u[4]);
       k[1,3] := step*F3(u[1],u[2],u[3],u[4]);
       k[1,4] := step*F4(u[1],u[2],u[3],u[4]);
       for i := 1 to m do
       u[i] := y0[i] + k[1,i]/4;
       k[2,1] := step*F1(u[1],u[2],u[3],u[4]);
       k[2,2] := step*F2(u[1],u[2],u[3],u[4]);
       k[2,3] := step*F3(u[1],u[2],u[3],u[4]);
       k[2,4] := step*F4(u[1],u[2],u[3],u[4]);
       for i := 1 to m do
       u[i] := y0[i]+b31*k[1,i]+b32*k[2,i];
       k[3,1] := step*F1(u[1],u[2],u[3],u[4]);
       k[3,2] := step*F2(u[1],u[2],u[3],u[4]);
       k[3,3] := step*F3(u[1],u[2],u[3],u[4]);
       k[3,4] := step*F4(u[1],u[2],u[3],u[4]);
       for i := 1 to m do
```

```
        u[i] := y0[i]+b41*k[1,i]-b42*k[2,i]+b43*k[3,i];
        k[4,1] := step*F1(u[1],u[2],u[3],u[4]);
        k[4,2] := step*F2(u[1],u[2],u[3],u[4]);
        k[4,3] := step*F3(u[1],u[2],u[3],u[4]);
        k[4,4] := step*F4(u[1],u[2],u[3],u[4]);
        for i := 1 to m do
        u[i] := y0[i]+b51*k[1,i]-8*k[2,i]+b53*
                k[3,i]-b54*k[4,i];
        k[5,1] := step*F1(u[1],u[2],u[3],u[4]);
        k[5,2] := step*F2(u[1],u[2],u[3],u[4]);
        k[5,3] := step*F3(u[1],u[2],u[3],u[4]);
        k[5,4] := step*F4(u[1],u[2],u[3],u[4]);
        for i := 1 to m do
        u[i] := y0[i]-b61*k[1,i]+2*k[2,i]-b63
                *k[3,i]+b64*k[4,i]-b65*k[5,i];
        k[6,1] := step*F1(u[1],u[2],u[3],u[4]);
        k[6,2] := step*F2(u[1],u[2],u[3],u[4]);
        k[6,3] := step*F3(u[1],u[2],u[3],u[4]);
        k[6,4] := step*F4(u[1],u[2],u[3],u[4]);
        for i := 1 to m do begin
        y[i]:=y0[i]+a11*k[1,i]+a13*k[3,i]+a14*
              k[4,i]-k[5,i]/5;
        z[i]:=y0[i]+a21*k[1,i]+a23*k[3,i]+a24
              *k[4,i]-a25*k[5,i]+a26*k[6,i];
        end;
          if abs(y[1]-z[1]) > elt then begin
            step := step/2;
            goto start;
            end;
          if abs(y[2]-z[2]) > elt then begin
            step := step/2;
            goto start;
            end;
          lmark := lmark + step;
          if abs(thickness - lmark) > ex then
            begin
              for i := 1 to m do y0[i] := z[i];
              if (lmark+2*step) <= thickness then
              begin
                step := 2*step;
                goto start;
              end;
              step := thickness - lmark;
              goto start;
            end;
          writeln('concn = ', z[1]);
          writeln('ds/dx =', z[2]);
          Sinitial := z[1];
end;
```